COMMUNICATIONS QUARTERLY

THE JOURNAL OF COMMUNICATIONS TECHNOLOGY

Fall 1997

$9.95

The Laser Diode as an Optical Source

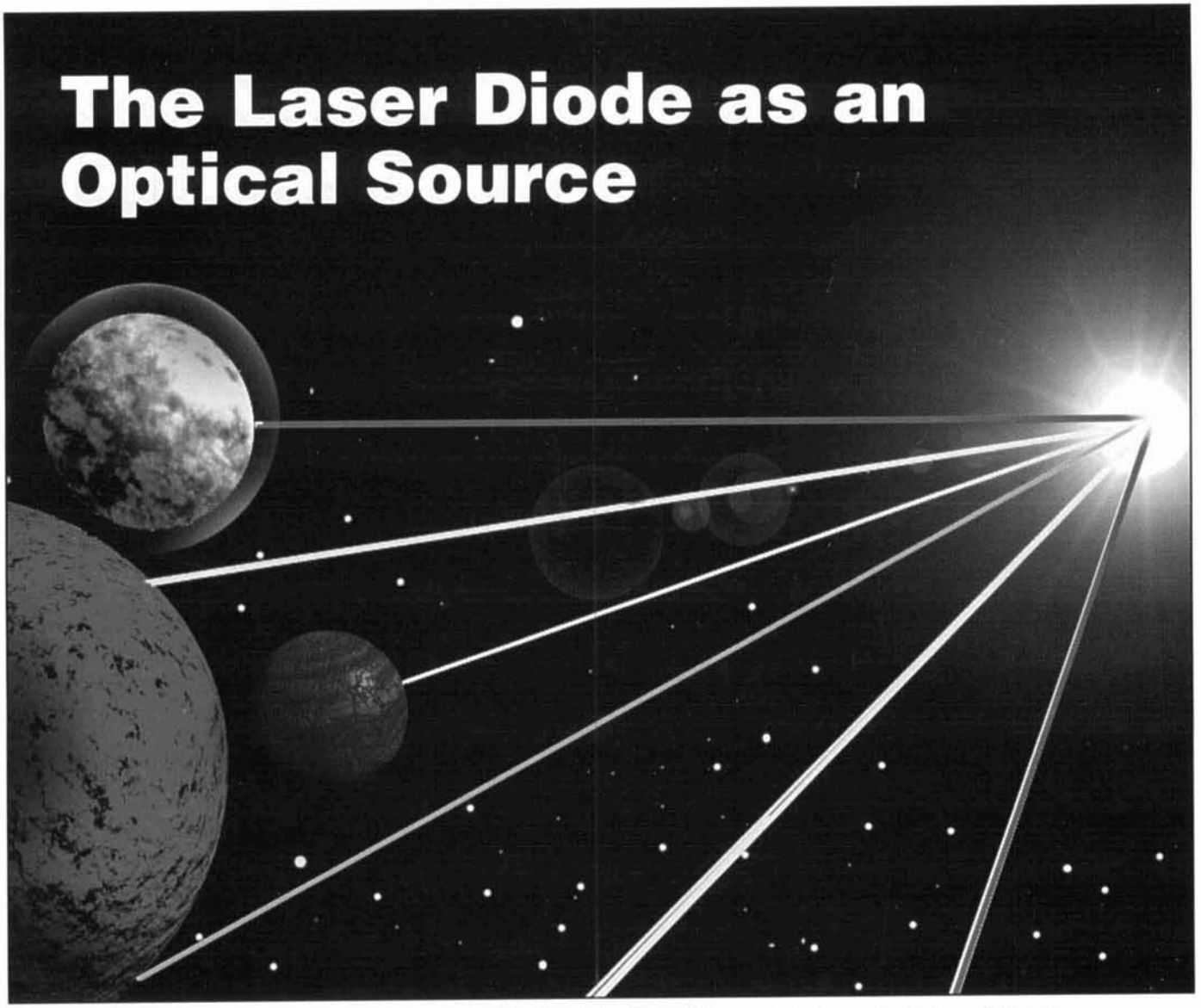

U.S. $9.95

73>

0 73361 64880 8

- Ferreting Out the Truth in Scientific Studies
- Practical Applications for Diplexers
- Source Impedance of HF Tuned PAs and the Conjugate Match
- Demystifying JFET Self-biasing
- A Trip to Heard Island
- Capacity Hats and Yagis
- Nikola Tesla: The Unsung Inventor
- Solving the Classic Cube Problem with Kirchoff's Laws
- A Reference Dipole for 2 Meters
- *Communications Quarterly*'s 5-year Article Index

.... POWER ON WITH ASTRON
SWITCHING POWER SUPPLIES ....

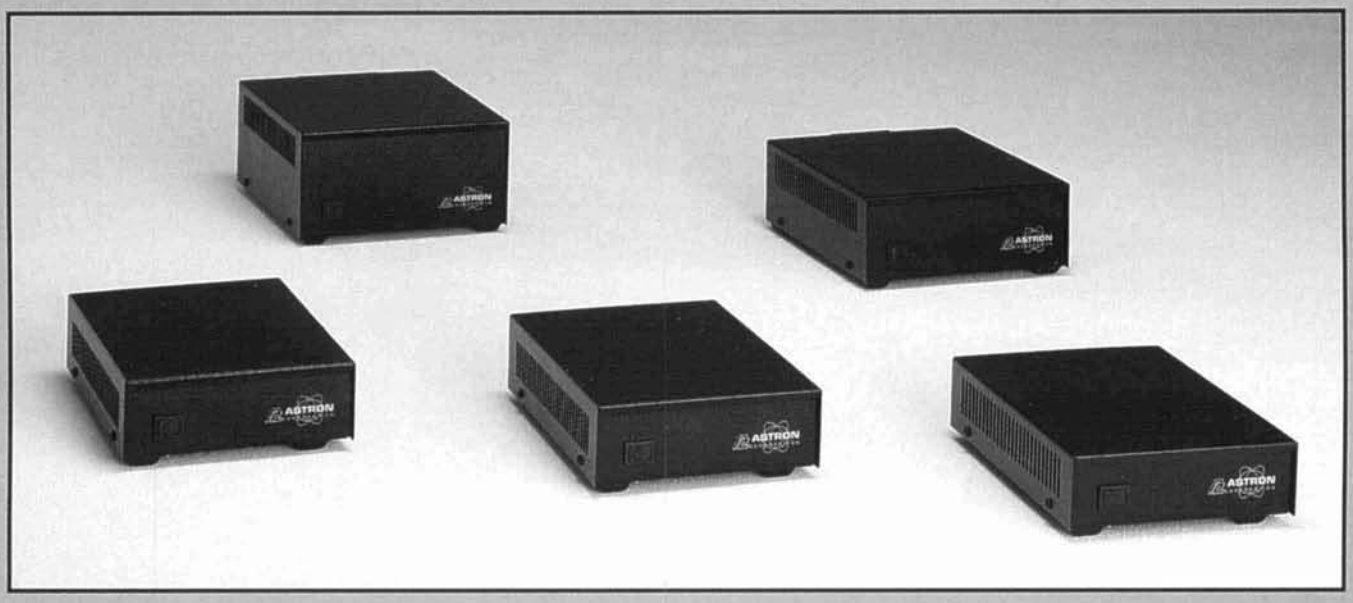

SPECIAL FEATURES:

- HIGH EFFICIENCY SWITCHING TECHNOLOGY SPECIFICALLY FILTERED FOR USE WITH COMMUNICATIONS EQUIPMENT, FOR ALL FREQUENCIES INCLUDING **HF**.
- HEAVY DUTY DESIGN
- LOW PROFILE, LIGHT WEIGHT PACKAGE.
- EMI FILTER
- MEETS FCC CLASS B

PROTECTION FEATURES:

- CURRENT LIMITING
- OVERVOLTAGE PROTECTION
- FUSE PROTECTION
- OVER TEMPERATURE SHUTDOWN

SPECIFICATIONS:

INPUT VOLTAGE: 90-132 VAC 50/60Hz
OR 180-264 VAC 50/60Hz
SWITCH SELECTABLE

OUTPUT VOLTAGE: 13.8 VDC

MODEL	CONT. AMP	ICS	SIZE	WT.(LBS)
SS-10	7	10	1 1/8 x 6 x 9	3.2
SS-12	10	12	1 3/8 x 6 x 9	3.4
SS-18	15	18	1 3/8 x 6 x 9	3.6
SS-25	20	25	2 7/8 x 7 x 9 3/8	4.2
SS-30	25	30	3 3/4 x 7 x 9 5/8	5

ASTRON CORPORATION

9 AUTRY, IRVINE, CALIFORNIA 92618
714-458-7277 FAX 714-458-0826
www.astroncorp.com

COMMUNICATIONS QUARTERLY

THE JOURNAL OF COMMUNICATIONS TECHNOLOGY

CONTENTS

Volume 7, Number 4 Fall 1997

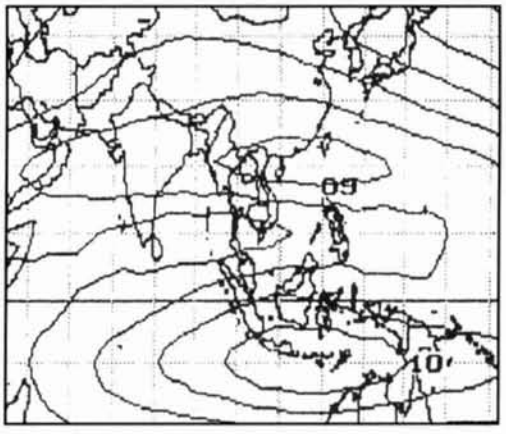

page 45

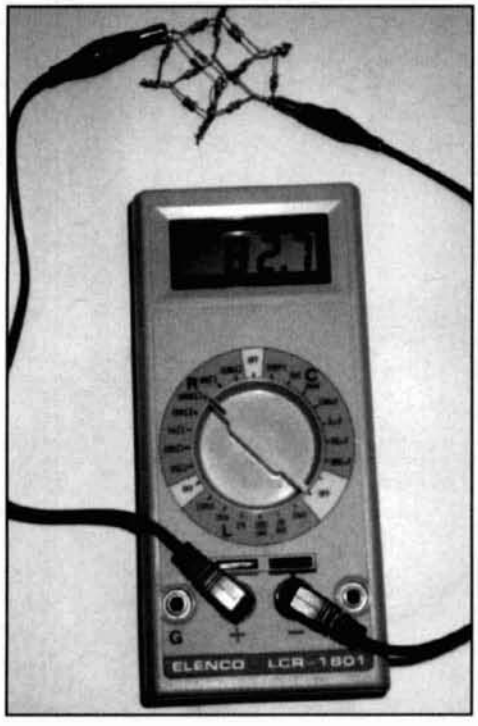

page 87

On the Cover: Will interplanetary travelers use optical communications to relay messages between the planets? To get a jump on the future, read about optical communications today in "The Laser Diode," by Richard Bitzer, WB2ZKW, on page 6. Cover design by Bryan Bergeron, NU1N.

EDITORIAL

The Debate Over the Conjugate Match

Disagreements between the players in the world of amateur radio aren't uncommon. In years past, we've seen controversies erupt over different types of baluns, wars over the best kinds of antenna, and arguments about the elimination of parasitics from amplifiers. Some arguments are based on fact, others on happenstance. But persons involved on either side of any of these disagreements often hold strong opinions (just read the threads on any of the amateur radio user groups on the Internet). These conflicts are a part of our amateur radio endeavors, and probably serve to keep us all honest.

For many years, there has been just such a disagreement regarding the conjugate match. In this issue of *Communications Quarterly*, Walter Maxwell,W2DU, Jack Belrose, VE2CV, and Tom Rauch, W8JI, look at the conjugate match and arguments against it made by others in the amateur radio community. But, before you turn to the article in question (see page 25), a little background information might be helpful.

A controversy is born

The beginnings of what would later become the conjugate match controversy first took root in the 1970s. It was then that Walter Maxwell, W2DU, wrote several articles on the conjugate match for various ARRL publications. He first prepared a series of stories for *QST* called "Another Look at Reflections" and later contributed pieces on the conjugate match to *The ARRL Handbook* and *Antenna Book*. His articles "The Conjugate Match and the Zo Match" and "The Conjugate Match and the Pi-Network Tank" appeared in editions of these handbooks from 1986 to 1994. The material was later included in Maxwell's *Reflections—Transmission Lines and Antennas*.

Years later, in November 1991, Warren Bruene, W5OLY, published a piece on RF amplifiers and the conjugate match in *QST*. A universally renowned expert on the design and operation of RF amplifiers, Bruene presented measurements which he felt supported his long-held view that the correct loading for vacuum tube-tuned RF power amplifiers does not provide a conjugate match. To make his measurements, Bruene devised a test setup that provided a means to "look back" into an operating amplifier. Publication of this article sparked the controversy between Maxwell and Bruene.

After reading the November 1991 *QST* article, Maxwell expressed concerns that there were serious flaws in Bruene's work. At the same time, Bruene pushed forward with his point of view—urging that ARRL publications be revised and references to the conjugate match be deleted. Then, much to Maxwell's dismay, beginning with *The 1995 ARRL Handbook*, text regarding the conjugate match was changed to reflect a view contradictory to Maxwell's and more like Bruene's. According to Maxwell, his plea for a rebuttal was refused by *QST*.

To professionalism

It's not my place to take positions in such controversies; but it is my place as the editor of a technical publication to present as much information as possible, so *Communications Quarterly* readers can determine the facts for themselves. Here's an opportunity for all who wish to dig into the story of the conjugate match, recreate the experiments detailed by both parties, and share your findings with each other. Remember, empirical study and observation are the tools that will bring us ever closer to scientific truth.

In the interest of science

To start us on our way, we have the article by Maxwell, Belrose, and Rauch, rebutting criticism of Maxwell's conjugate match theory. We present it here so parties on either side of this dispute will be able to learn what the authors have to say regarding this subject. My challenge to you is to read this article, and those that have gone before, and make your own determinations about the conjugate match.

Your opinions on the conjugate match controversy (and other topics, of course) are welcome. Write to me at P.O. Box 465, Barrington, New Hampshire, 03825 or send e-mail to: <ka1stc@aol.com>.

Terry Littlefield, KA1STC
Editor

Editorial Offices: P.O. Box 465, Barrington, NH 03825. Telephone/FAX: (603) 664-2515. **Business Offices:** 76 North Broadway, Hicksville, NY 11801. Telephone: (516) 681-2922. FAX: (516) 681-2926.

Periodical postage paid at Hicksville, NY and additional mailing offices.Statement of Ownership, Management and Circulation,10-1-97, Communications Quarterly, 76 North Broadway, Hicksville, NY 11801. Publication # 10539433. Issued 4 times a year, subscription price $33.00 per year. Publisher Richard A. Ross, Editor Terry Littlefield, Managing Editor Edith Lennon owned by CQ Communications, Inc. Stockholders Richard A. Ross, Alan M. Dorhoffer. Circulation (Average of 12 Preceding Months): Net Press Run 8,259. Sales Through Dealers and News Agents 2,870. Mail Subscriptions 3,535. Total Paid 6,405. Free Distribution 60, Total Distribution 6,465, Copies Not Distributed 1,084. Returns from News Agents 710. Total 8,259. Circulation (Single Issue Nearest Filing): Net Press Run 7,239. Sales Through Dealers and News Agents 2,548. Mail Subscriptions 3,455. Total Paid 6,003, Free Distribution 60, Total Distribution 6,063, Copies Not Distributed 547, Returns from News Agents 629, Total 7,239. s./Richard A. Ross, Publisher.

Postmaster: Please send change of address to Communications Quarterly, CQ Communications, Inc., 76 North Broadway, Hicksville, NY 11801. ISSN 1053-9344.

Printed in U.S.A.

PRODUCT LINEUP

MILITARY AND COMMERCIAL PRODUCTS

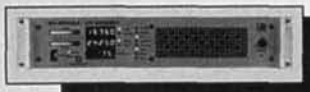

ST8000A **- Ruggedized HF Modem, MIL connectors, high MTBF, touch panel controls**

ST8000 **- HF Modem, Tuneable Mark/Space tones, memories, space tuning indicator, up to 1200 baud FSK**

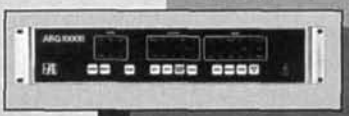

ARQ1000B **- Error Correction Terminal, CCIR-476/625 TOR ARQ/FEC**

HFCS1000 **- High Frequency Communications Simulator, Training device simulates HF receiver operation, .5 to 30 Mhz**

LP1210 **- Ten Channel ruggedized Loop Power Supply, 10 channels, MIL 188 to neutral loop, 100K hrs MTBF**

LP1200A **- Loop Power Supply, 1 channel, polar or neutral, 20/60 ma, RS232/MIL188, motor control**

DS3486 **- Radio Data Communications Terminal, Rack mount, 486, VGA, Floppy drive, 420 Mb Hard Drive**

DSP PRODUCTS

DSP4100 **- DSP Modem, Stand-alone DSP modem for CLOVER, Clover 2000, TOR, Pactor, RTTY and ASCII. + 12 VDC.**

PCI4000+ **- HF DSP MODEM, PC plug-in card. Operates CLOVER, CLOVER2000, TOR, RTTY and ASCII**

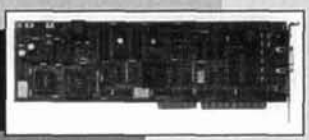

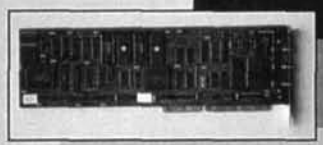

P38 **- HF DSP MODEM, PC Plug-in card. Designed with the Amateur in mind. Operates CLOVER, Pactor, AMTOR, RTTY and ASCII**

FAX4100 **- FAX-OVER-RADIO Interface, Interfaces a G3 FAX machine to the DSP4100/CLOVER2000 Modem.**

L14100 **- Line Interface for FAX4100, Share G3 Fax machine between phgone lines and FAX4100.**

CLOVER2K **- Voice Bandwidth CLOVER software, for PCI4000 and DSP2000, TOR, Pactor, RTTY and ASCII. +12 VDC.**

HAL COMMUNICATIONS CORP.

1201 WEST KENYON ROAD

URBANA, IL 61801

PHONE 217 367-7373 FAX 217 367-1701

Web Page www.halcomm.com E-mail halcomm@halcomm.com

TECHNICAL CONVERSATIONS

Information wanted

Dear Editor:

Being retired and earning a rather small pension, I cannot afford to subscribe to your outstanding quarterly. Nevertheless, I am a fervent reader of this high-class publication. I am lucky to have a very good relation with ON7PC, Pierre Cornelis, who subscribed to the magazine and who passes it on to me every quarter.

Although economically speaking, I do not support the magazine, morally I am a good friend of it. I wonder if someone could help me.

For our national amateur magazine, I prepared an article on the theorems of Thévenin and Norton. During my many contacts with amateurs, I found out that practically nobody understands these theorems, so I decided to do something about it. I want to introduce the articles with a few biographic notes on both these gentlemen. Unfortunately, all my efforts to find something about them are without any result to this day. I asked information of technical high schools and universities in Belgium, France, and the United States. Nobody can give me any historical details about either of these gentlemen. Somebody even told me that the names may be nicknames.

I wonder if somebody on your staff, or perhaps a reader, may know anything interesting about them. I am looking for: given name, birth date, place of birth, country, curriculum vitae, when and how they came to the theorems, where they worked, were they professors, what kind of work did they do, when did they die, and so on.

There are two ways to send me your findings. You can write to me at: Fleurbacy Fernand, ON4ZA, Asterlaan 20, B2550 KONTICH, BELGIUM. You can also send a reply by Internet to one of my friends, indicating clearly that a reply is desired for ON4ZA. Here is his Internet address: <dries.decadt@innet.be>.

Since *Communications Quarterly* publishes very interesting historical articles regularly, I thought that you or your readers may be in a position to find something about the biographies of both Thévenin and Norton (not to be confounded with Norton of the computer program). You are more or less my last hope!

I thank you very much in anticipation and send you my very best regards.

Fleurbacy Fernand, ON4ZA
Kontich, Belgium

Reply to Rudy Severns, N6LF

Dear Editor:

Rudy's comments ("Technical Conversations," Summer 1997, page 5) bring out important issues regarding the use of elevated radials to create a vertical antenna with two resonant frequencies. To illustrate this point, let's consider a quarter-wave vertical with two unequal length elevated radials where the lengths are set to produce resonance at two desired frequencies. At the first resonate frequency, one radial will take most of the radial system current while, at the second resonant frequency, the other radial will take most of the radial system current. As a result, the radiation pattern will be different at each frequency. This may be acceptable for some uses, but will not produce an omnidirectional pattern at either frequency.

A potential way around this problem is to use two pairs of in-line radials that are either shortened or lengthened following the rule that radial lengths should be less than 60 bounded by 45 degrees or longer than 120 degrees bounded by 150 degrees. Each in-line pair would have its own inductor or capacitor to produce resonance as shown in **Figure 1**. One in-line pair and its reactive component (inductor or capacitor) would set one resonant frequency, and the second in-line pair and its reactive component would set the second resonant frequency. This would have the potential to provide an almost omnidirectional pattern at both frequencies with acceptable VSWRs. I hope someone interested in this type of antenna will try this design approach and let us know how it works.

Thanks to all for your interest and comments, especially W5OLY

Dick Weber, K5IU
Prosper, Texas

Dear Editor:

During the two years I spent investigating elevated radials, I gave several presentations on my

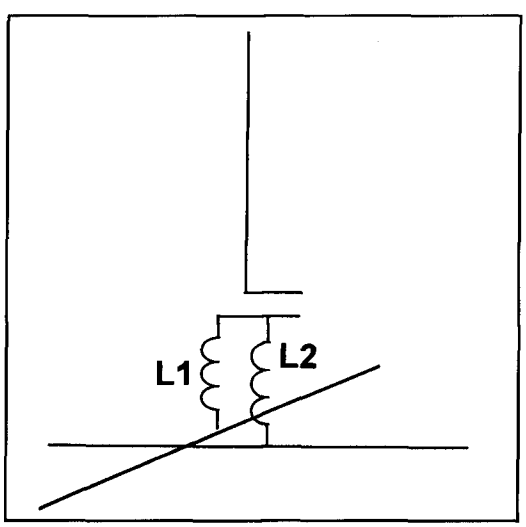

Figure 1. Two independent sets of in-line, shortened radials.

work—although not complete at those times. These presentations included talks at the 1995 and 1996 W5 DX BASH, a talk at the North Texas Contest Club, and one at the Rockwell Ham Radio Club in Richardson, Texas. During these talks, I was asked many excellent questions that challenged my efforts and helped identify important issues. To those who attended these presentations, I wish to thank you for your interest and comments. I would especially like to thank Warren Bruene, W5OLY. After my talk at the Rockwell Ham Radio Club, Warren took the time to write me, in detail, about several issues. Because of his comments and suggestions, I made changes which I believe improved my article ("Optimal Elevated Radio Vertical Antennas, Spring 1997, page 9).

Dick Weber, K5IU
Prosper, Texas

A few problems...

Dear Editor:

Just received the summer 1997 issue of *Communications Quarterly*. The artistic portion of the cover is really great. CQ sure has a good staff in that department. But why didn't they reverse portions of the photos so that the maximum spot activity matched maximum T-index and so forth? And...where did they get the "incorrect" max/min dates (should be Min September 1986 and Max July 1989)? Moreover, the dates don't coincide with the graph dates. Max July 1989 and Min May 1996 would have been appropriate, don't you think? I believe I mentioned in a fax just after I mailed the photo that the photos should probably be reversed. It is too bad to see such errors. I'll always be happy to advise in appropriate situations. Regards,

Peter O. Taylor
Spring Green, Wisconsin

Mea culpa—Ed.

Try this graph instead

Dear Editor:

Thanks for the e-mail a few days ago on the revised graph for my article "An Analytical Look at HF Path Losses" (Summer 1997, page 9). Enclosed is the graph (**Figure 1**) I should have sent you in the first place! Same data, though you could never tell by looking, and this way it does make a lot more sense.

Glad you could use the article

Crawford MacKeand, WA3ZKZ, WP8CMY

Dear Editor:

The current issue arrived in today's mail, and I am delighted you were able to use the loading profile article ("Loading Profiles for Wideband Antennas, Summer 1997, page 27). There are

(Continued on page 105)

Richard Bitzer, *WB2ZKW*
7 Oaktree Road
Monmouth Junction, New Jersey 08852

THE LASER DIODE

Try using one as an optical transmitter source

The visible output HeNe laser has been the choice for amateur communications systems for quite some time. It was the first mass-produced laser available on the commercial market priced within the financial reach of radio amateurs interested in pursuing optical communications. The device's main drawbacks were the high-voltage power supply required to operate the laser and the limited ability to be directly current modulated beyond 12 to 14 percent. However, a number of amateurs have used these lasers with success.

Recently, another visible output laser called the double heterostructure semiconductor diode laser or more simply, the diode laser, has appeared on the market. The purchase price of these optical double heterostructure diode lasers in small quantities has become affordable.

These lasers have a number of advantages over the bulkier HeNe gas type: They operate with only a few volts applied, are more efficient for the same optical output power as the HeNe laser, are physically smaller, are directly compatible with pc board construction, and can

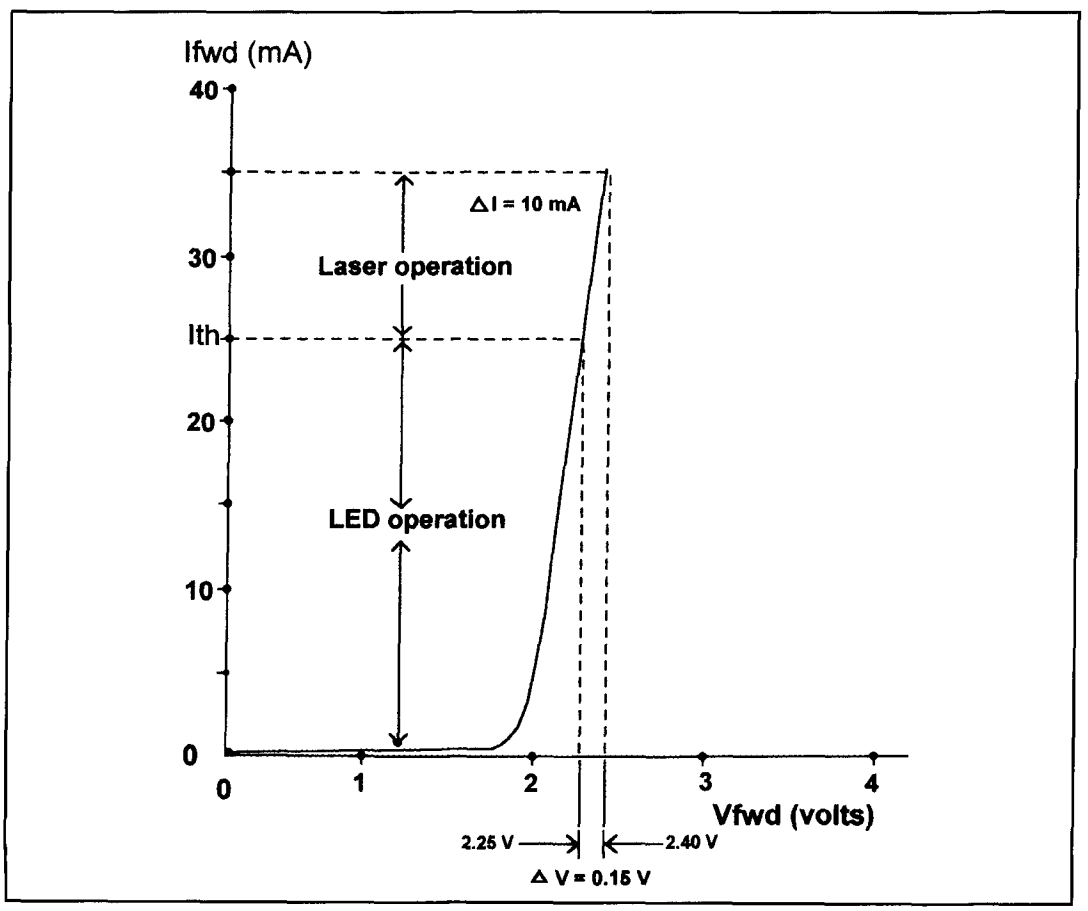

Figure 1. Diode laser I-V characteristics.

PROFESSIONAL DESOLDERING with the New & Improved

DEN-ON SC7000Z

More Vacuum

Lane Norman - Normans Electronics Inc. Atlanta GA 404-451-5057
A cost effective solution to desoldering equipment at less than half the price of most equipment. It's performance is ASTOUNDING.

Mike Murphy - Service Center -Van Nuys CA 818-785-7805
The single best investment of repair equipment we've made. It outperforms all other desoldering tools we've used. Easier to use and least expensive.

Quicker Vacuum

Bob Monroe - M.A.R.C. Electronics - Virginia Beach VA 804-468-3932
Best investment we've made. Saves time, especially with multi-sided PCB's. Extremely pleased with warranty. Failed within 6 months and replaced by DEN-ON overnight.

Dick Manning - Dicks Electronics - Hartland WI 414-367-8339
The ease & speed of component removal greatly increases productive time. The SMD kit makes SMD removal a breeze, even for inexperienced Techs.

George Hefner - Hefner Electronics - Coleridge NE 402-283-4333
Being a one-men service center, I hesitated to spend the money on a desoldering tool , however all that changed when I nearly ruined a $400 computer logic board. It has cut my desoldering time by 50%.

Higher Temperature

Don Cressin - Certified Electronics Service - Ellicott City MD 301-461-8008
We have obtained excellent results with the SC7000 including repairing high density U/V tuners. It is one of the best purchases we have made.

Doug Pettit - LuRay Electronics - LuRay VA 703-743-5400
We found that the SC7000 not only saves money vs. wick, but saves valuable time in troubleshooting. It allows you to be more accurate in removing SMD's.

Randy Whitehead - Service West - Salt Lake City UT 801-262-4069
My techs thought it would be a waste. I bought one anyway after a demo. My techs then fought over it. Now we have three. It is the Best desoldering tool we have ever used.

Timothy Kraft Monikraft, Inc. Cherry Hill , NJ 609-751-3252
We replaced all our existing desoldering stations with the SC7000. Our technicians are very pleased with the improved performance, portability, and reliability over our previous higher priced equipment.

FREE TRIAL
Available on Request

Sale Price $395.00

Price includes stand worth $25.00 one extra filter, and two tip cleaners.

Bill Warren CET/ CSM - Warrens Audio & Video Knoxville TN - 234-546- 1128
We have been extremely satisfied with the quality and durability of the DEN-ON SC7000 as well as with after the sale support.

Keith Sahs - J & M Electronics - Omaha NE 402-291-7100
It's a must tool for my bench. I can desolder multiple pin IC's quickly and clean. It will even take up large solder amounts on tuner and case grounds.

Don Scott - LAV Electronics Healeah-Miami Lakes FL
I am a constant user of the SC7000 Desoldering Tool and for quick component removal, this unit has no equal. It also comes with excellent company support. I am very satisfied and highly recommend it to anyone in the servicing field.

Evaluated in the Summer Issue of Communications Quarterly.

Check us out on the WEB → http://www.heinc.com

New Features

- Totally Self Contained diaphragm vacuum pump and AC motor for high vacuum suction or reversible hot air blow for SMD removal.
- 100Watt Ceramic heater with zero-crossover switching heater control circuit which prevents spikes and leakage currents.
- Unique patented long lasting filter cartridge design. Solder builds up on easily cleaned baffle, while air flows around the outside of baffle.
- Totally ESD Safe. The housing contains carbon and the tip is at ground potential for complete ESD Protection.
- Maximum vacuum of **650mmHg** is attained in **100 milliseconds**.
- Temperature adjustable from 300°C - **500°C** (572°F - **932°F**).
- More suction power and hotter temperature if needed.

New Specifications

- **Voltage**——AC100v,120V,230V,50/60HZ
- **Power Consumption**——120W
- **Pump**——Diaphragm Type
- **Motor Output**——12W
- **Vacuum Attained**——**650mmHg**
- **Temperature Range**——300°C—**500°C** (572°F—**932°F**)
- **Air Flow Rate**——15 Liter/Minute (Open)
- **Heater**——100W (Ceramic)
- **Control System**——Feed Back Zero Cross-over Type
- **Net Weight**——420Grams
- **Max.Temp. of Hot Blow**——400°C

Visa - M/C - Discover - American Express - Terms to Qualifying Companys
30 Day Money Back Total Satisfaction Guarantee - One Year Parts and Labor Warranty

HOWARD ELECTRONIC INSTRUMENTS INC
Your Desoldering Specialists

Toll Free U.S. and Canada
1-800-394-1984

Web Site www.heinc.com
E-Mail sales@heinc.com
International (316) 744-1993
or Fax (316) 744-1994

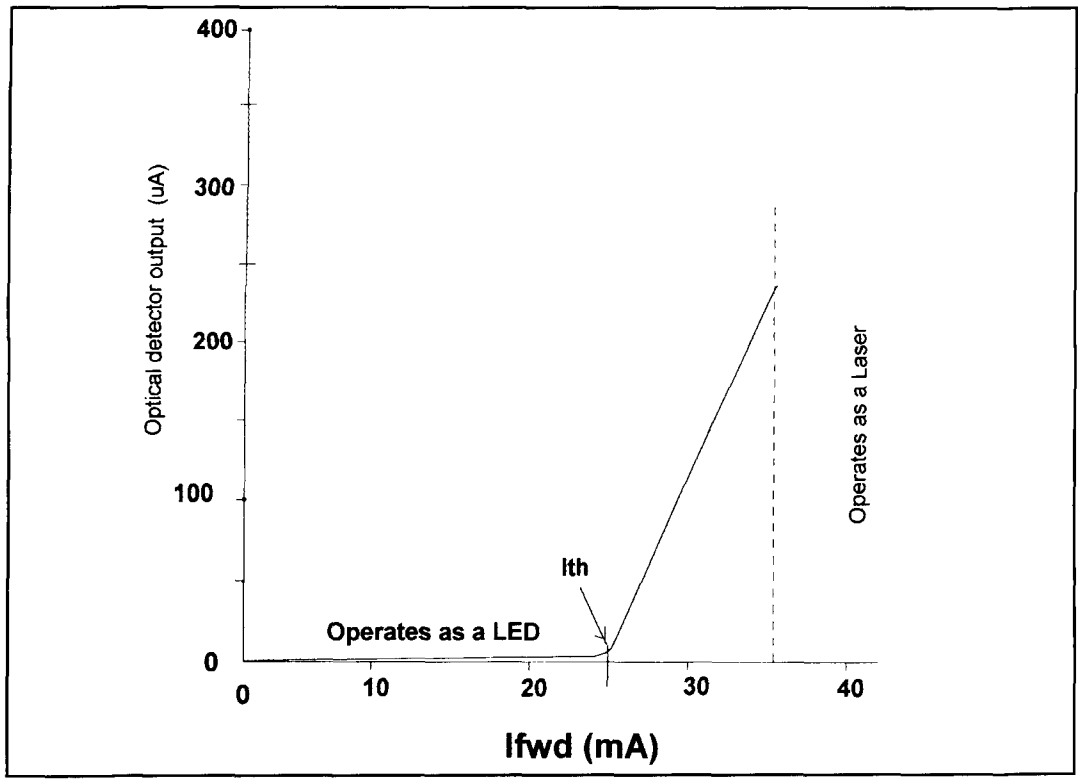

Figure 2. Laser optical output versus drive current.

be current-modulated to nearly 100 percent. However, diode lasers do have one drawback: The resonant optical cavities are very small, resulting in a fan-shaped optical output pattern. For an atmospheric link, a compound lens with a very short focal length must be placed close to the laser diode. The resulting aperture coupling loss reduces the useful optical output from the diode laser. Yet even with this drawback, these little devices are excellent candidates for optical transmitting systems.

Semiconductor LEDs versus diode lasers

The light emitting diode, or LED, and the semiconductor diode laser are both diodes that emit optical radiation. However, their methods of operation are quite different. The LED emits a broadband infrared or visible output through spontaneous emission when forward biased. While its spectral output is narrower than fluorescent or incandescent lamps, it's still very broad when compared to a diode laser output. The latter produces a very narrowband coherent optical output through stimulated emission. The LED's output is noncoherent and, while this is not a deterrent to using the device as the optical source in a transmitter, it places certain restrictions on the overall optical link performance.

For example, suppose we have two identical receivers, transmitters, and optical systems operating over the same propagation path. To optimize the signal-to-noise ratio, both receivers are equipped with narrowband interference filters preceding their detectors. Both transmitters have the same optical output power, except that one uses an LED and the other uses a diode laser as their respective transmitting sources.

When the received signal incident on the detectors in each receiver is compared, the signal from the transmitter using the diode laser will be larger than the signal from the transmitter using the LED source—even though both transmitters are operating at the same optical output power levels. Remember, the LED's output power is spread spectrally over a wide bandwidth. As the signal is propagated through the narrowband receiving filters, only a small part of the LED's signal reaches the detector where almost all of the diode laser signal incident onto the antenna reaches the detector. This makes the diode laser the logical choice as a transmitting source.

Heterostructure semiconductor diode lasers

There are two types of semiconductor diode lasers: the single heterostructure and the double heterostructure semiconductor laser. The single

heterostructure semiconductor diode laser was the first semiconductor laser developed for commercial and military applications. These lasers have large optical cavities, therefore their optical spectra is much wider than that of a double heterostructure semiconductor laser. They operate at an optical wavelength of 850 nm, in the near infrared region. Their current densities can range between 10000 to 50000 amps/cm^2. The peak current through the laser can vary between 10 and 80 amps, depending on the size of the laser chip.

These diode lasers would self-destruct at room temperature if operated in a continuous mode. They are normally operated in a pulsed mode with pulse widths between 100 and 200 nS and duty cycles between 0.01 to 0.2 percent. They require higher voltage power supplies operating from 40 to 600 VDC, depending on the type of pulser circuit used. When pulsed, a single diode laser is capable of generating 1 to 50 watts of peak pulsed infrared optical output power, depending on the size of the laser chip.

With high peak optical output power levels and radiation invisible to the eye, these devices can be dangerous without the proper eye protection. Infrared radiation from these lasers can be detected in a number of ways: (1) by the use of photosensitive screens that fluoresce from the incident infrared radiation after being exposed to visible light; (2) silicon semiconductor diodes, silicon FETs, and silicon photo transistors; and (3) vacuum photo diodes with an S-1 cathode surface. For those interested in experimenting with this type of diode laser, there are several books that describe the devices, their circuits and their applications.[1,2]

The double heterostructure diode laser is a more recent development. The main advantage of these lasers is their ability to operate continuously at room temperature. They can be fabricated to emit at infrared or a visible wavelength of 670 nm. They are found in optical scanners in supermarket checkout stations, laser pointers, card readers, compact disk readers, and as transmitters in fiber optic transmission systems.

These lasers are considerably more efficient than the typical HeNe gas laser for the same optical output. They are small and require low operating DC input power (approximately 2.4 VDC at 35 mA) for approximately 2 to 5 mW of coherent optical output. These lasers can be operated both in a pulsed mode or a continuous mode and are easy to current modulate. Typical modulation bandwidths are in excess of 200 MHz. Temperature compensation can be implemented by using the detected laser output from a photo diode packaged with the laser diode and using its detected signal to adjust the current through the laser. However, if adequate heatsinking is used, temperature compensation

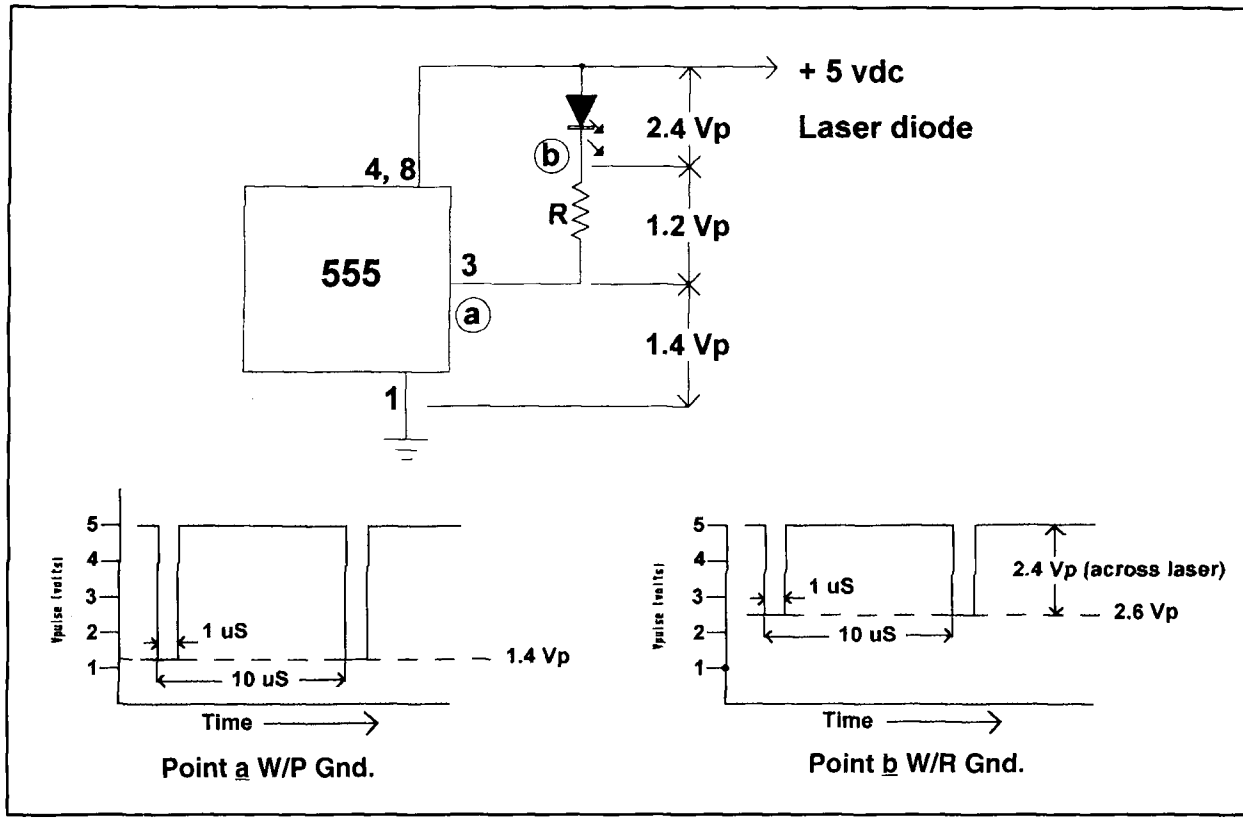

Figure 3. Pulsed diode laser output circuit.

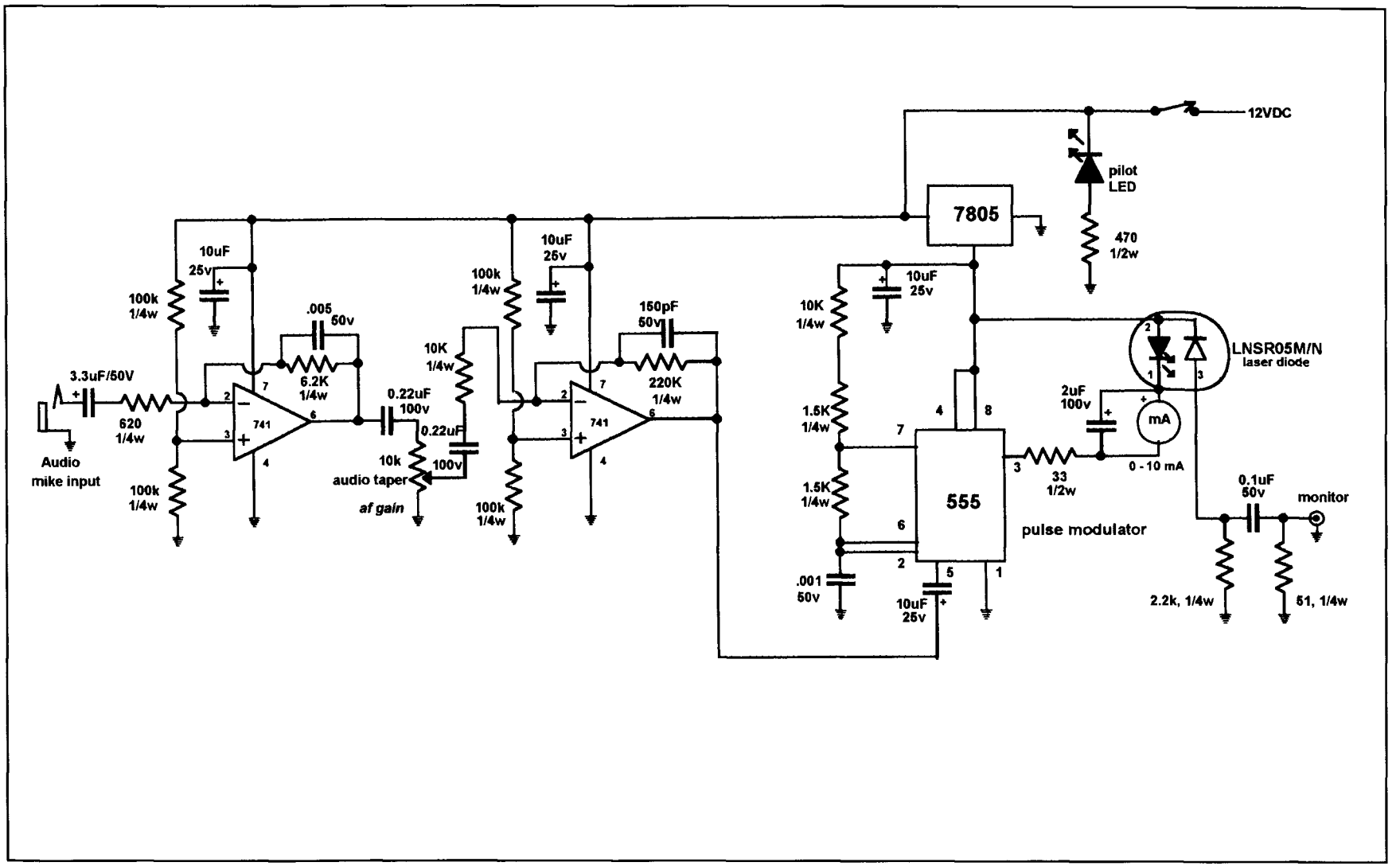

Figure 4. Schematic of PFM pulsed transmitter.

Table 1. Characteristics of a Matsushita model LN9R05M/N diode laser.

Output frequency	4.478 x 10^{14} Hz (447.8 THz)
Operating wavelength	670 nm
Typical operating voltage	2.5 volts DC
Typical operating current	35 mA
Typical optical output power	5 mW
Lasing threshold current	25 mA

isn't usually necessary, and this photodiode can be used as a transmit monitor.

Characterizing the double heterostructure laser diode

Before starting any optical transmitter design, it's important to know the characteristics of the laser diode. **Table 1** shows some of the characteristics of Matsushita model *LN9R05M/N diode laser I used from their* specification sheet.

Two pieces of additional information are required: the I-V characteristics and the diode laser current versus optical output. The former can be measured by connecting the diode laser in series with an adjustable resistance and measuring the voltage across the laser as a function of current, as shown in **Figure 1**. Using the same test setup, I focused the laser output into a photomultiplier tube (PMT). The PMT output current is linearly proportional to the detected optical input power (as long as the PMT isn't saturated). The current through the laser is measured as a function of PMT output current, as shown in **Figure 2**. The I-V information can now be used to establish the operating bias point of the laser diode, and the information in **Figure 2** is used to establish the laser modulation range.

Figure 1 shows that the diode laser doesn't begin to conduct current until the voltage drop across the laser has reached 1.7 V. However, lasing action doesn't start until the threshold current of 25 mA has been reached, as shown in **Figure 2**. This corresponds to a forward diode voltage drop of 2.25 VDC. As the current is increased through the laser, the diode acts as an LED with a noncoherent optical output. As the laser threshold current of 25 mA is reached, the laser diode output changes abruptly from a noncoherent to a coherent output. The diode laser can be operated between 25 to 35 mA (maximum current). The optical output intensity varies linearly with input diode current to achieve a linear modulation range between 30 to 300 µA out of a PMT, as shown graphically in **Figure 2**. The modulation percentage that can be achieved for this device is:

%Modulation = [(300-30)/(300+30)]*100 = 82%

The laser diode current can be varied between 30 mA +/-5mA to generate an 82 percent intensity modulated optical output that can be baseband or subcarrier frequency modulated. If the laser diode is to be pulsed, the diode current can be pulsed directly between 0 to 35 mA maximum. The pulse train can be pulse-frequency modulated.

Pulsed diode laser transmitter

Many types of laser diode pulser circuits can be used with the double heterostructure diode laser, but the most common uses a 555 timer IC operated off a regulated 5-VDC bus. **Figure 3** shows how the laser diode is connected to the 555. In this configuration, as the diode is pulsed, the internal voltage drop across the 555 output from pin 3 to ground is typically 1.4 V. A series resistor is used to develop an additional voltage drop so only the peak operating voltage appears across the laser. A negative-going pulse train appears at the output of pin 3 on the 555 as seen at "A" and "B" in **Figure 3**.

With the output of the 555 switched off, pin 3 is close to 5 V. As the 555 is pulsed on, current flows through the laser diode, the resistor, and the 555 timer for the width of the pulse. For our chosen laser diode, the full pulsed diode current is 35 mA, with the corresponding voltage drop across the laser of 2.4 Vpk. The laser diode will emit an output for the duration of the pulse. The drop across the resistor is:

E_R = 5.0-(1.4+2.4) = 1.2 Vpk

Therefore, the value for R is:

R = 1.2/0.035 = 34.3 ohms

Pd = 1.2*0.035 = 42 mW

A standard 33-ohm, 1/4-watt resistor can be used in the circuit.

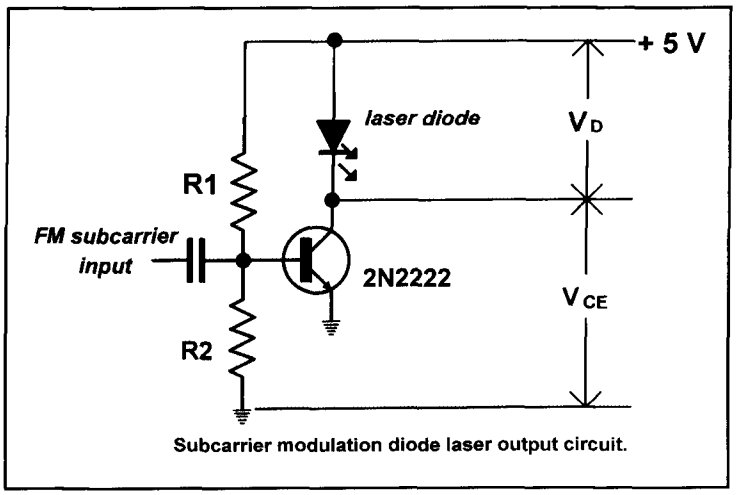

Figure 5. Subcarrier modulation diode laser output circuit.

Figure 4 shows the entire schematic circuit diagram for a pulse-frequency modulated laser diode transmitter. Almost all double heterostructure semiconductor diode lasers come with two diodes housed in the same package. One is the laser, the other is a photo diode. The latter is typically used to control the temperature of the laser via a feedback loop tying into the laser diode power supply. As I mentioned earlier, the laser diode doesn't get hot if heat sunk properly. As a result, the photo diode can be used for monitoring purposes. A meter ensures that the average current can be set and monitored.

The 555 is designed to operate as a free-running multivibrator powered off a regulated 5-VDC supply. The pulse repetition frequency of 100 kHz matches the VCO PLL frequency of my test receiver and is higher than five times the highest modulating frequency of 3 kHz. You can choose any pulse repetition frequency as long as it satisfies two conditions: (1) that the transmitted PRF is the same as the receiver PLL VCO frequency; and (2) that the PRF is five times greater than the highest modulating frequency. I chose the timing resistors in the 555 timer circuit so that with a 0.001 µF capacitor on pin 2, the pulse width is set at 1 µs and the period is set at 10 µs.

The laser transmitter uses a two-stage audio amplifier with a gain control between stages for setting the modulation rate of the output pulse train. The audio amplifier has a maximum gain of 220 with a 3-dB passband from 130 to 3500 Hz powered off the 12-VDC bus. The output of the audio driver is connected to pin 5 of the 555, which frequency modulates the pulse repetition frequency out of the 555 timer at an audio rate. The audio amplifier input impedance is approximately 600 ohms and is designed to match the 600-ohm impedance of most dynamic microphones. The photo diode in the laser package is used as a signal output monitor.

Upon the completion of the transmitter circuitry, I recommend that an LED be used in place of the laser diode to prevent damage to the laser during alignment and test (less expensive to replace than a diode laser in case of catastrophic problems). The LED also has a fairly linear optical output as a function of drive current, which makes it a good substitute for the laser during testing and alignment. The timing resistor values in the 555 timer circuit may have to be trimmed to obtain the desired PRF and duty cycle.

Once the circuit is being pulsed correctly, connect an audio generator set to a 1-kHz frequency at a 25-mVp-p output level into the audio input. This simulates the average level of a dynamic microphone. The optical receiver used for testing has been described in the literature.[3] It uses a PLL setup to operate at 100 kHz. With the LED shining into the photomultiplier detector, start advancing the audio gain until the demodulated 1-kHz signal is seen on the oscilloscope. Advance the transmitter audio gain until distortion is seen on the received signal and then back off a little. Once the transmitter alignment is complete, turn off the power, carefully remove the test LED, and insert the laser diode.

CAUTION

ESD can damage the laser. Make sure you are grounded properly when installing the laser diode, and make sure that laser diode leads are NOT **reversed** in the circuit. Turn the power back on and verify that the laser is working by holding a white paper up to the diode face. You should see a red specular glow indicating that the laser is working correctly. The 33-ohm resistor in series with the laser diode lead may have to be trimmed to maintain the proper voltage across the laser. Once this is done, the circuit can be mounted on the proper chassis and aligned with its lens system.

Subcarrier modulated diode laser transmitter

Another modulation method involves directly modulating the diode laser current with a high-frequency carrier and then frequency modulating the carrier at an audio rate. In this case, I again chose a 100-kHz carrier for compatibility with the test receiver. A voltage-controlled oscillator whose VCO is tuned to a center frequency of 100 kHz drives the laser diode through a transistor driver. **Figure 5** shows the driver arrangement. The laser diode is connected to the transistor collector. The transistor is biased so Vce plus Vdiode equal the supply

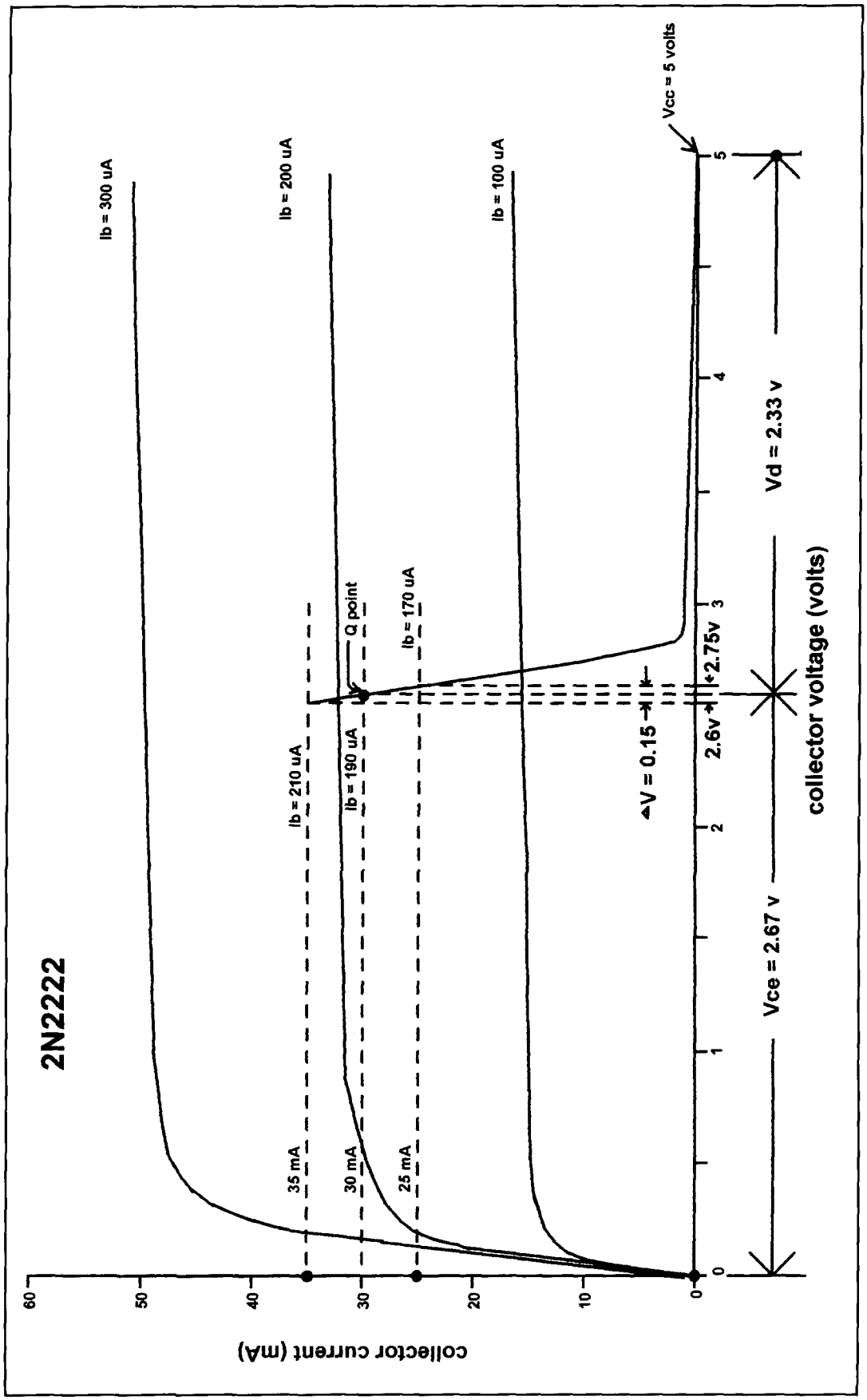

Figure 6. Graphical solution, subcarrier modulated diode laser driver.

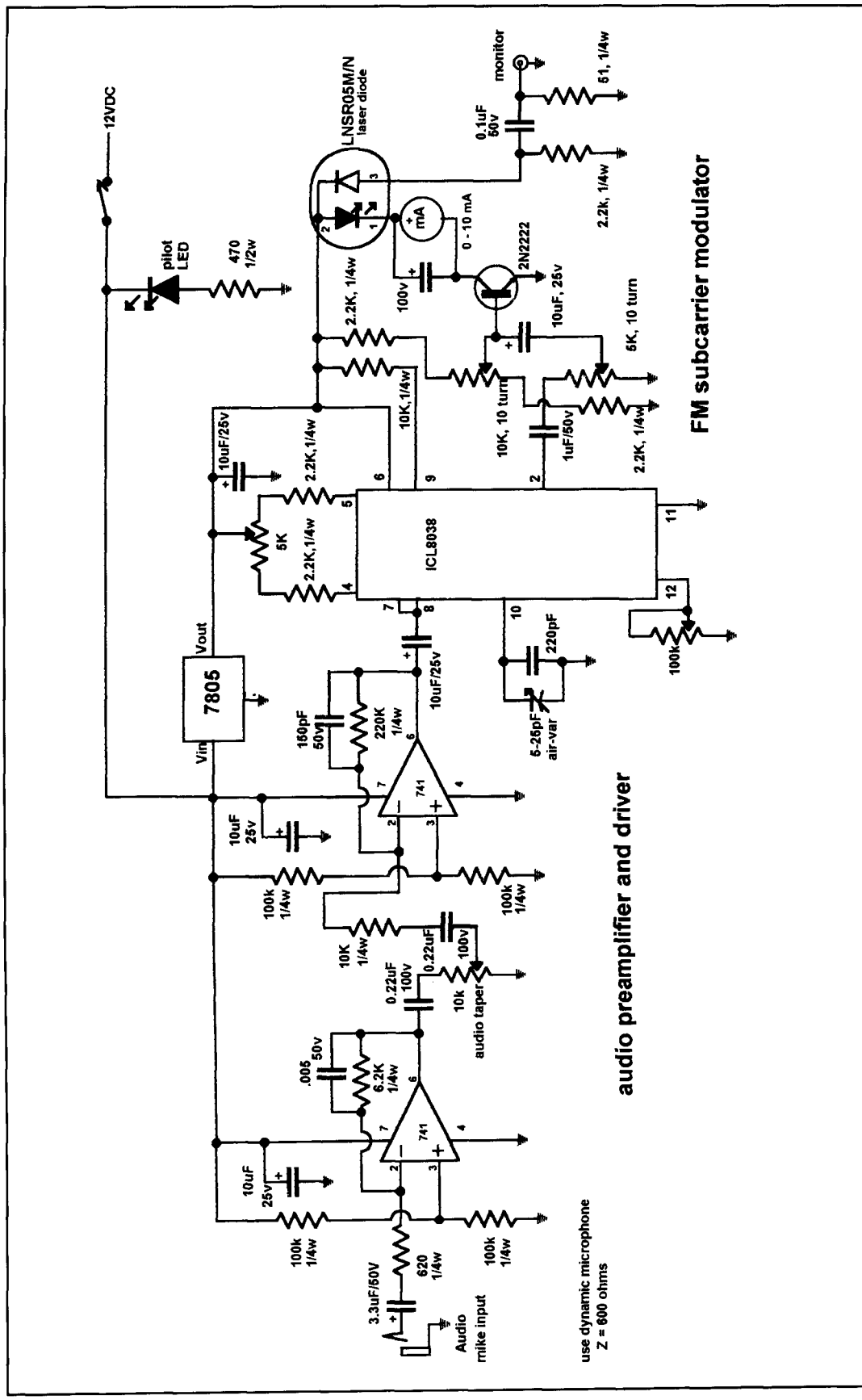

Figure 7. Schematic of subcarrier FM transmitter.

voltage. A regulated 5-VDC supply keeps the voltage values between transistor and laser diode at a reasonable level. Bias resistors R1 and R2 keep the voltage across the diode at 2.33 volts (the 30 mA-bias point) and Vce at 2.67 VDC based on a graphical solution.

Figure 6 illustrates the graphical solution. I measured and plotted the I-V curves of a 2N2222 transistor that will be used as a modulator. I then plotted the I-V inverse laser diode curve onto the same graph; this represents the laser as a load line with a negative slope of -$1/R_{diode}$. The diode line originates at 5 VDC. The laser is modulated by varying the current between 25 and 35 mA. Therefore, the quiescent (Q) point is set at 30 mA and 2.67 V. This voltage is the collector-to-emitter voltage drop (Vce) across the transistor. The difference between Vce and a Vcc of 5 VDC is the drop across the laser diode; i.e., 2.33 V at 30 mA. The graphical solution shows that a base current of +/-20 μA centered around the quiescent base current of 190 μA is required to drive the laser diode current +/-5 mA around 30 mA. The transistor beta was calculated to be 158. The measured values were in agreement with the calculated values. By modulating the diode laser current at 30 mA +/-5 mA, the diode laser is intensity modulated at 82 percent.

The schematic of a complete laser diode subcarrier FM optical transmitter is shown in **Figure 7**. The same audio amplifier/driver used in the pulse modulated version can also be used to drive the ICL8038 voltage-controlled oscillator (VCO). Rather than use fixed resistors for biasing the driver transistor, I chose a potentiometer to set the bias. The VCO subcarrier output has a gain control connected to pin 2 of the ICL8038 that is used to set the carrier modulation amplitude.

To adjust and test the circuit, I again suggest that you replace the diode laser with an LED. Set up an audio generator and connect it to the microphone input as was done for the pulsed version. With the power applied, adjust the 2N2222 bias potentiometer for 30 mA of collector current. With an oscilloscope and frequency meter connected to pin 2 of the ICL8083, adjust the sine wave symmetry of the 100-kHz output with the potentiometer connected between pins 4 and 5 of the VCO.

Next, connect the oscilloscope between the collector and the grounded emitter lead of the 2N2222. Increase the carrier gain potentiometer until signal distortion occurs, then back off slightly. As with the pulsed transmitter, shine the LED into the photomultiplier detector, and start advancing the audio gain until the demodulated signal is seen on the oscilloscope. Advance the transmitter audio gain until distortion is seen on the received signal and back off a little. This procedure sets up the proper deviation of the audio modulation signal onto the 100-kHz subcarrier. Once the transmitter alignment is complete, turn off the power, carefully remove the test LED, and insert the laser diode.

CAUTION

ESD can damage the laser. Make sure that you are grounded properly when installing the laser diode and that the laser diode leads are NOT **reversed** in the circuit. Turn the power back on. Verify that the laser is working by holding a white paper up to the diode face. You should see a red specular indicating that the laser is working correctly. You can now place the circuit board into a chassis and align the laser diode with the collimating optics.

Power supplies

Power supplies for injection diode laser systems needn't be elaborate. A typical power supply designed for a 12- to 14-VDC input must use a 5-VDC regulator for the laser diode and its driver circuitry. The laser diode and its current driver require a well-regulated and filtered supply; a standard 7805 three-terminal regulator is quite adequate for the job. The remaining audio amplifier and audio driver circuits aren't as critical and can operate off of the 12- to 14-VDC power bus directly, providing it's filtered adequately from external conducted susceptibility signals on the power line. If you use a car's 12-VDC system, the input to the power supply must be adequately filtered from any induced ignition electrical noise on the power supply input to the diode laser transmitter.

Conclusion

I have discussed the operation of semiconductor diodes lasers in optical transmitter applications along with the associated driver and audio circuitry. The pulse and subcarrier modulation methods employed use direct current modulation of the laser. The subcarrier modulation approach made use of the linear relationship between the diode laser's optical output and current drive. External optical modulators are available, however they are out of the financial reach of most amateur radio experimenters. Power to operate the lasers and their modulation circuits is simple and employs standard three-terminal regulators for maintaining stable supply voltages. ■

REFERENCES
1. R. Campbell and F. Mims, *Semiconductor Diode Lasers*, Howard Sams & Co., 1972.
2. F. Mims, *Light-Beam Communications*, Howard Sams & Co., 1975.
3. R. Bitzer, WB2ZKW, "Optical Communications," *Communications Quarterly*, Winter 1996, page 9.

Joseph J. Carr, *K4IPV*
P.O. Box 1099
Falls Church, VA 22041
E-mail: <carrjj@aol.com>

IS SALT WATER TAFFY BEING DISTRIBUTED?

Ferreting out the truth in scientific studies

Junk science and revisionist history advocates usually want you to uncritically accept their point of view. Otherwise, you cannot be persuaded to their way of thinking. The tendency—and temptation—is for advocates to over-interpret favorable data and to either under-interpret or suppress unfavorable data. How do you separate trash from treasure? How do you detect whether the offered food is nutritious, or merely salt water taffy? Several tactics help shed light on the truth.

First, *ask who is supplying the information.* There are advocacy groups that put out information to support or refute a position. Whether you deal with environmental issues, health food, alternative medicine, or the claims made for novel and bizarre radio antennas, you must ferret out the truth. One of the issues at hand is who supplied the information. Or, more precisely, how do they benefit if the information is accepted as true?

The news media

Newspapers and magazines often misinterpret scientific studies. While some of them are guilty of blatant advocacy, they are also afflicted by three pressures that force distortion: deadlines, the need to "scoop" the competition, and the fact that startling results "sell" better than the truth. Add to that the fact that journalists are rarely competent to interpret scholarly work and the result is often bad information being presented to the public. No one should accept popular media articles on any subject without independent verification.

Verification doesn't mean seeing the same material in two or more different media sources. Journalists often pick up stories from other publications. Seeing the same material in three publications could mean that one reporter wrote it for his or her newspaper (and got it wrong), and the next day (or next week) two more cribbed it for their papers.

Attempts to gain credibility

Advocates attempt to gain credibility for their position by citing studies that support it. And, if the study is a "scientific" or "university" study, then all the better. They will bolster their point by citing, by name, the author of the study—especially if the person quoted is famous, a well-known expert on the subject, or has the requisite credentials ("Doctor M. Weldon Sclotz of the University of Frabbitzville stated recently...").

Some people cite a well-credentialed expert who's found not to be expert in the matter under consideration. Having a doctoral degree, winning a Nobel Prize, or being famous doesn't add credibility outside one's narrow field of expertise. Tom Clancy may be a real good military yarn spinner, but that does not qualify him as a military affairs expert.

When a study is cited by an ardent advocate, it's a good idea to look further. I often follow up on footnotes in order to judge the quality of research. In one case, an advocate's paper had plenty of footnotes, so, on the surface, it looked like pretty good science. Footnotes are a paper's *bona fides*; they tell readers that the author did her homework. In the case above, I found that a critically important footnote didn't even exist! The journal cited was real, but when I located the actual copy of the cited issue in a library, the article claimed in the footnote didn't exist. Checking the annual index for that year, and the two years either side of it, revealed no articles or letters by the author cited in the paper. Mistake? Possibly. Deceit? I'd bet on it!

Critical footnotes need to be examined carefully to see if...

a) the cited source actually exists,

b) the source is accurately quoted, and
c) the source is *fairly used.*

The last criterion—fairly used—is especially important. Very often one finds that cited sources are taken out of context, or the conclusions of the study are twisted beyond recognition. If the author of the study would be surprised at the conclusions drawn, then it's a good bet the study isn't fairly used. While it's possible that an advocate could fairly draw different conclusions from those of a study author, such a situation is always suspect until verified by the evidence. Junk science advocates often hitch their wagons to legitimate stars, but nearly everyone else finds their interpretation novel and bizarre.

A study can sometimes be verified by contacting its author. Ask the author if the published study is the latest information on the subject. Published academic studies tend to lag behind the state of knowledge. Some scholarly journals print the acceptance date of the paper, and that date is often a year or two earlier than the issue of the journal in which it appears.

Journals also frequently publish the study's funding information, so you can judge whether or not there may be any particular bias in the results. A typical citation might read "Funded under NIH grant XXX-XYZ-1230." If the funding organization is also an advocacy group or commercial entity, be especially skeptical of the reported results (regardless of how well the group fits your own biases).

When you call the author of the study, ask about the methodology used. A lot of studies are terribly sensitive to methodology. Responsible researchers recognize that fact and take it into account when reading the study, but journalists often don't. By understanding the methodology, it's possible to detect biases, flaws, or limitations to the study.

Also find out whether the journal in which a published study appears is peer reviewed or merely editor reviewed. A peer-reviewed publication sends out every manuscript to one or more disinterested reviewers. They ask hard questions, provide critiques, and serve as general quality control. They point out weaknesses and suggest areas for improvement.

Another factor often left out of popular expositions of scholarly research is critical qualifying factors. Studies are often tightly controlled as to the conditions being examined, and they may not be valid in situations that depart from the controlled situation. It's often the case that studies will look at very narrow populations, and the results are not applicable to the population at large.

It may also be true that the interpretation of a study is different because critical information is left out of the report. Berkman[1] tells of a report that the U.S. population grew by 22 million people in the 1980s. On the surface, that figure looks horrific: *22 million new mouths to feed, with new jobs required to support them!* But a critical bit of information was missing: That growth *rate* for the decade was 9.8 percent, and it was the second lowest on record.

Even the multi-hundred billion dollar U.S. budget deficits of recent years don't look too awful when viewed as a percentage of gross national product (GNP). At least one paper in *Harvard Business Review*[2] argued that the deficit isn't as horrible as people believe, and may actually stimulate the economy if the debt were incurred for the right things.

Another thing that distorts the interpretation of otherwise valid studies is the improper combination of the results of two or more studies. This mistake is the "apples and oranges fallacy." Advocates cite two or more studies on the same subject to bolster their position in a manner that suggests the studies are somehow mutually reinforcing or complementary. A conclusion drawn as a synthesis from the results of two or more nonrelated studies is always suspect, and may be quite meaningless.

Studies almost always have some constraints, a basic methodology, and some (hopefully not hidden) basic assumptions. If the two studies cited don't have those factors in common, then drawing any conclusion that depends on combining them is invalid. The synthesized result is meaningless unless there's some means for compensating for the fundamental differences in the studies. Unless one is counting the category "fruit," one cannot fairly compare apples and oranges. It's very difficult for a layperson to make valid comparisons in such cases, so be wary when it's done without a good reason.

Scientific studies

Scientific studies seem to be particularly subject to abuse when presented to a lay audience. Few people outside science understand that the results of studies are always considered tentative. They also don't understand that very few issues can be definitively proven by a single study. The public is often understandably confused when two or more studies seem to contradict each other. "Is vitamin-C good for the common cold or not?" "Does eating bran lower cholesterol or not?"

Science makes progress by repetitively examining issues, and then holding up new data to public, and often very brutal, examination. As a result, each new study should build on earlier work and refine its focus to overcome objections to the earlier studies. After this is done a number of times, some good approximation of the truth should emerge. But if one takes

a "snapshot" view of the research by looking at only one study at a single point in time, then an erroneous picture may be seen.

Scientists understand this problem, and account for it in their thinking, but laypersons rarely know how to look at studies. All that disagreement between studies may indicate is that scientists haven't refined their knowledge of a subject well enough to ask Nature the right question...yet.

Some General Advice

From sets developed by Cohn[3] and Berkman[1], supplemented by some of my own criteria, we can list several questions that should be asked of the author of any article or study:

- How do you know that what you say is true?
- Is the published data preliminary or final?
- Do other experts in the field concur?
- Is their concurrence general or highly specific?
- What is the information based on?
- Have the assertions been validated in a formal study or experiment?
- Was the study designed according to generally accepted scientific standards?
- Who funded the work?
- What stake do you have in the outcome (reputation, money, promotion potential)?
- Who disagrees with the conclusions and why?
- How sure are you of the conclusions?
- Are the conclusions backed up by statistical evidence?
- Have the studies been replicated by others? What were the results?
- Were the results reasonably consistent from one study to the next?
- Are other explanations for the observations possible?
- Who else in field has seen the work?
- Was it peer reviewed?
- What methodology was employed?
- What are study's weak points?
- What criticism has been received and from whom?
- Do you agree with the advocate's conclusions drawn from your study? Was the work fairly used?
- Would competent experts in the field be surprised by the result? If so, would they find the interpretation novel and bizarre?

When evaluating researchers, look for agendas, hidden and otherwise, the backgrounds and qualifications of the researchers, their normal job function, their self-proclaimed mission (if any), and their source of support or funding to detect possible biases in the study. Ask a very pertinent question: "Why is this person interested, and how does it affect the results?" Use the word "interested" to mean "has a stake in" rather than "curious about."

It's also relevant to know what peer recognition the researcher enjoys (or is afflicted by). It may also be pertinent to note who referred you to that researcher. Was it someone you respect? Was it a self-nominated advocate? Does this person have a general reputation for reliability and integrity?

So Why Bother?

So why should you care that salt water taffy is being distributed by those trying to persuade you of their point of view? Because it pulls out your dental fillings, rips off your crowns, rots your teeth, raises your blood sugar level, is hard to chew, is generally unhealthy, and doesn't provide any form of intellectual nourishment in return for all its evils. It's icky stuff, so shun it. Better yet, stick the taffy maker to the wall with his own goo. ■

References

1. Robert Berkman, "But Is It The Whole Truth?", *Writer's Digest*, September 1993, page 42.
2. Robert Eisner, "Sense and Nonsense About Budget Deficits," *Harvard Business Review*, Vol. 7, No. 3, May–June 1993, page 99.
3. Victor Cohn, *News & Numbers*, Iowa State University Press, Ames, Iowa, 1989.

Bibliography

1. Russell L. Ackoff and Fred E. Emery, *On Purposeful Systems*,, 1972, Intersystems Publications (1981 reprint edition), Seaside, California.
2. Jerry Adler, "The Numbers Game," *Newsweek* Lifestyle Section, July 25, 1994, pages 56–59, New York.
3. Jonathan Baron, *Thinking and Deciding*, 2nd Edition, Cambridge University Press, New York, 1994.
4. Armin A. Brott, "Battered-Truth Syndrome: Hyped Stats on Wife Abuse Only Worsen the Problem," *The Washington Post*, Outlook Section, July 31, 1994, pages C1–C2.
5. John L. Casti, *Paradigms Lost: Images of Man in the Mirror of Science*, William Morrow & Co., Inc., New York, 1989.
6. Kenneth B.M. Crook, "Suggestions for Teaching the Scientific Method," *American Biology Teacher*, March 1961. Copyedited manuscript version supplied to the author by Dr. Crooks' family.
7. Cynthia Crossen, *Tainted Truth: The Manipulation of Numbers in America*, Simon & Schuster, 1994.
8. George Englebretsen, "Postmodernism and New Age Unreason," *Skeptical Inquirer*, May/June 1995, Vol. 19, No. 3, Amherst, New York, pages 52–53.
9. Antony Flew, *Thinking Straight*, Prometheus Books, Buffalo, New York, 1977.
10. Thomas Gilovitch, *How We Know What Isn't So: The Fallibility of Human Reason in Everyday Life*, Macmillan/Free Press, New York, 1991.
11. Morgan D. Jones, *The Thinker's Toolkit: Fourteen Skills for Making Smarter Decisions in Business and in Life*, Random House, New York,1995.
12. Daniel Kahneman, Paul Slovic, and Amos Tversky, *Judgement Under Uncertainty: Heuristics and Biases*, Cambridge University Press, New York, 1982.
13. Alfred C. Kinsey, Wardell B. Pomeroy, and Clyde E. Martin, *Sexual Behavior in the Human Male*, W.B. Saunders, Philadelphia, 1948.
14. C.I. Lewis, *Mind and the World Order*, Charles Scribner & Sons, 1929. Reprint edition: Dover Publications.
15. Kevin McKean, "Of Two Minds: Selling the Right Brain," *Discover*, April 1985, pages 30–38.
16. J.P. McLaughlin, "On Leaping and Looking and Critical Thinking," *Skeptical Inquirer*, May/June 1995, Vol.19, No.3, pages 6–7, Amherst, New York.
17. Richard Morin, "How to Lie With Statistics: Adultery," *The Washington Post*, March 6, 1994, page C5.
18. Richard Morin, "Racism on the Left and Right," *The Washington Post*, March 6 1994, page C5.
19. Richard E. Neustadt and Ernest R. May, *Thinking in Time: The Uses of History for Decision Makers*, The Free Press, New York, 1986.
20. Wardell B. Pomeroy, Dr. Kinsey and the Institute for Sexual Research, 1972, pages 292–293. Cited in Reisman 1990.
21. Judith A. Reisman and Edward W. Eichel, *Kinsey, Sex and Fraud*, Huntington House, Lafayette, Louisiana, 1990.
22. Michael Shermer, *Why People Believe Weird Things*, W.H. Freeman Co., 1997.
23. Theodore Schick, Jr. and Lewis Vaughn, *How to Think About Weird Things: Critical Thinking for a New Age*, Mountain View, Mayfield Publishing Co., Mountain View, California, 1995.
24. Christina Hoff Sommers, *Who Stole Feminism?: How Women Have Betrayed Women*, Simon & Schuster, New York, 1994.

Thomas V. Cefalo, Jr., *WA1SPI*
51 Oak Street
Winchester, Massachusetts 01890

DIPLEXERS

Some practical applications

Advances in technology have made the existence of dualband radios a common item in many ham shacks. The 2-meter/70-centimeter transceiver is one very popular dualbander. At these higher frequencies, feedline considerations now become an important issue. Using low-loss feedline for each antenna can be very expensive and impractical. It's possible to solve this problem by installing a diplexer in the antenna system, permitting the use of a single feedline.

I will present a review of diplexers, along with a computer program you can use to synthesize them. I'll also provide some practical diplexer applications.

Diplexer theory

In some applications, it becomes necessary to separate or combine a given frequency spectrum into specific bands. This can be done by connecting more than one filter in various configurations, a process known as multiplexing. Multiplexing is actually a general term, as an actual filter configuration hasn't been defined. Some defined examples of multiplexers are diplexers, triplexers, duplexers, absorption filters, and combiners. The type of multiplexer described here is a diplexer because it uses two filters.

When describing multiplexers it's important to remember the terms contiguous and noncontiguous. Contiguous means each filter has the same 3-dB point where power splits equally between the two filters. This is commonly known as the 3-dB crossover frequency. The term noncontiguous means the crossover point is any level of attenuation greater than 3 dB. Note that multiplexers with passive filters cannot cross over at levels less than 3 dB because more than half the power at that frequency would be present at the output ports or, to put it simply, power can't be in two places at the same time. Diplexers are generally designed to be contiguous.

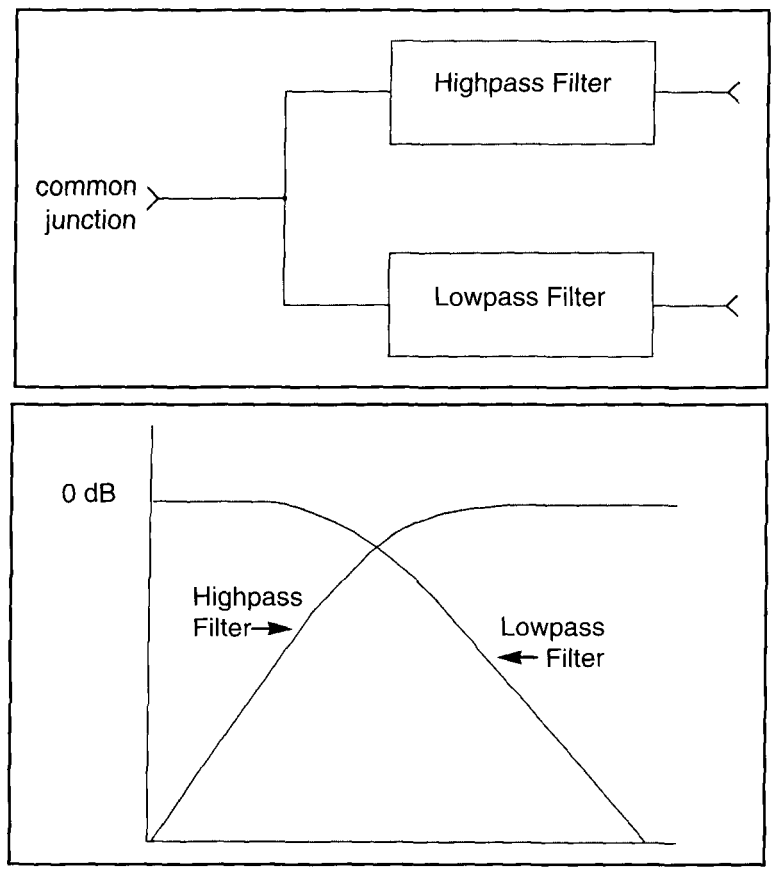

Figure 1. (A) Diplexer and (B) frequency response.

Figures 1A and **B** show a diplexer and its frequency response. The diplexer consists of a low-pass and high-pass filter joined together at the filter inputs. The graph shows the frequency response of the low-pass and high-pass filter, and the 3-dB crossover frequency. The frequency response of the diplexer clearly indicates

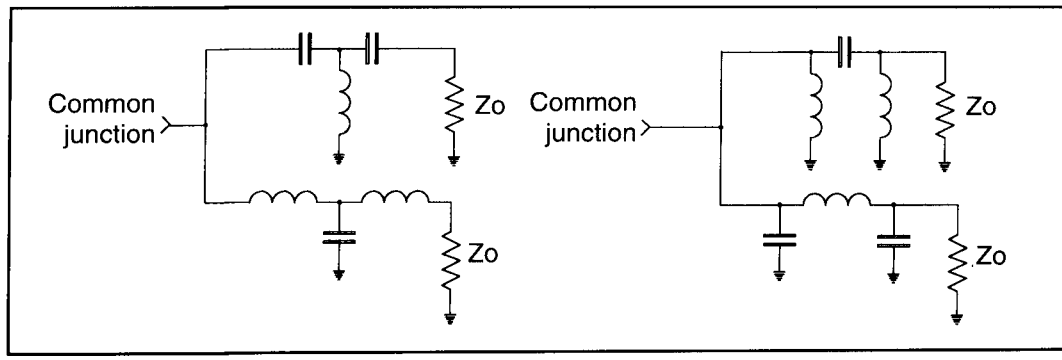

Figure 2. (A) Parallel-connected diplexer and (B) its dual version.

how the frequency spectrum has been separated into two individual bands, one below the crossover frequency and the other above.

A diplexer or multiplexer requires a special design to achieve good performance. A basic rule to remember when designing multiplexers is that the joined ends of the filters must present a very high impedance to each other, or each filter must present a complex conjugate to each other, so the sum is equal to the system's characteristic impedance. Connecting a doubly terminated filter—that is, a filter normally designed to operate into the same value of source and load impedance in a diplexer configuration—would produce undesirable consequences. A high VSWR would be introduced, causing the filters to exhibit a completely different response because they would no longer be operating at the impedance for which they were designed.

To meet the stipulations required to realize a complex conjugate, diplexers are designed with singly terminated filters. A singly terminated filter is designed so one end of the filter is terminated into the system's characteristic impedance, while the other end is terminated into a short or open circuit. This is a basic foundation for designing diplexers. Tables of normalized filter elements for singly terminated filters are available in a number of filter textbooks. Theoretically, one can achieve perfect diplexing with singly terminated Butterworth or maximally flat filters. The common junction of the high and low-pass filter produces a complementary impedance or admittance at all frequencies, including the crossover.

In **Figure 2A** the input admittance at the diplexer's common junction is equal to 1+j0 at all frequencies. The dual version of that diplexer is shown in **Figure 2B**, and its input impedance is 1+j0 at all frequencies.

Because a Butterworth filter makes a moderate descent into the stopband, it's sometimes advantageous to incorporate a Chebyshev filter response into a design. Compared to a Butterworth, a Chebyshev filter has a much

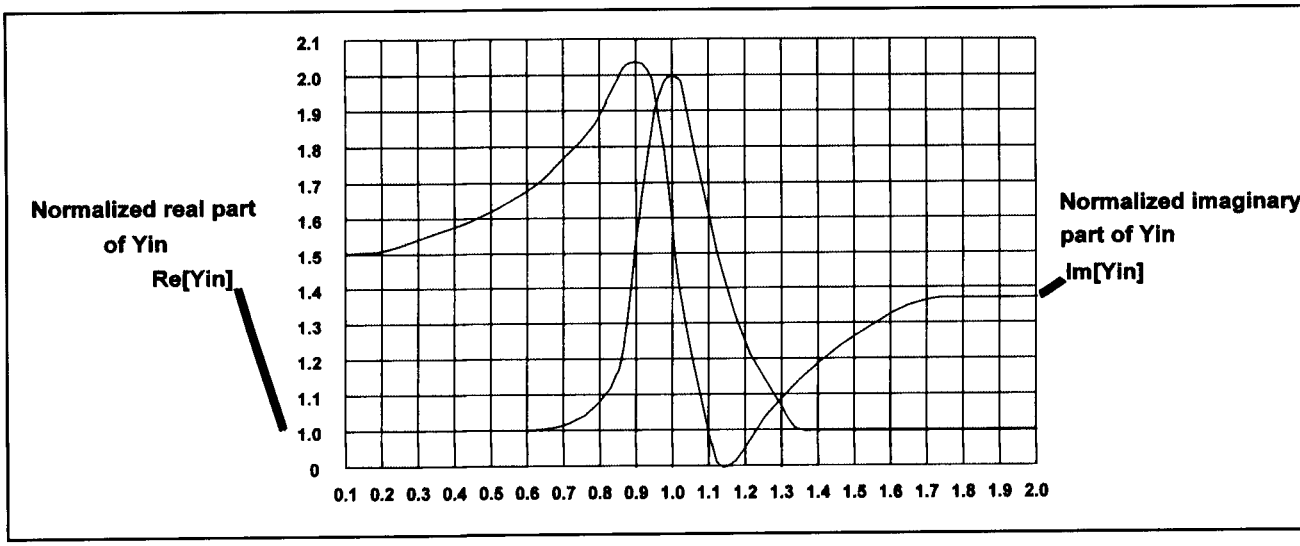

Figure 3. Common junction input admittance.

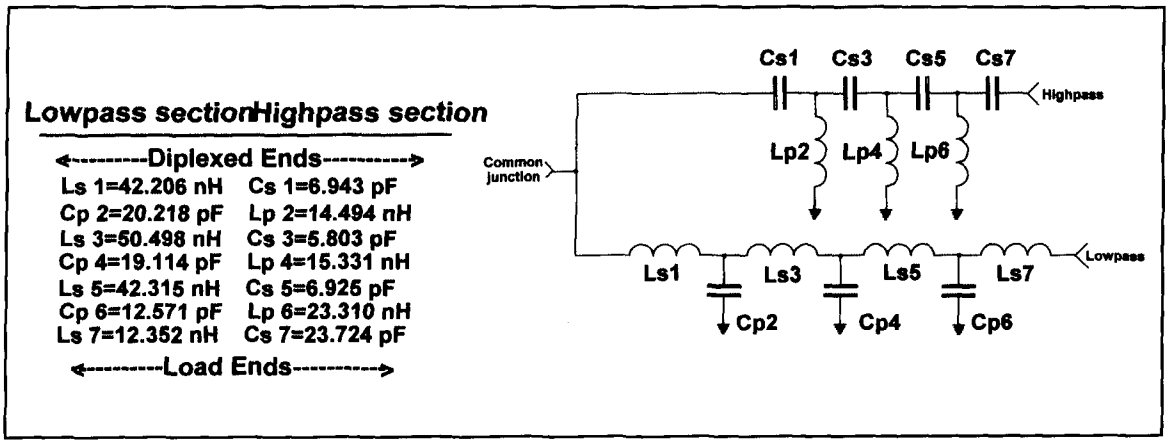

Figure 4. Computer printout of 294-MHz diplexer design.

greater initial descent into the stopband. Unlike the Butterworth, the Chebyshev filter doesn't yield a complementary admittance or impedance at the common junction. The common junction admittance is no longer equal to 1+j0 at all frequencies. To prove this, a plot of the normalized admittance at the common junction for a five-pole, 0.1-dB ripple Chebyshev diplexer is shown in **Figure 3**.

The performance of this diplexer is acceptable, except in the area of the crossover frequency. From the plot, one can see that the sum of the conductance increases to 2 at the crossover frequency. The sum of the susceptance for the most part is 0, except for a small residue on each side of the crossover frequency.

Because the sum of the conductances at the crossover frequency is equal to 2, the diplexer must be modified to preserve a normalized conductance of 1. This would require the conductance of the low and high-pass filters to be equal to 0.5 at the crossover frequency. This is done by shifting the crossover frequency of the low-pass filter down and the high-pass filter up by some predetermined factor. This will allow the common junction conductance to be equal to 1 over the entire bandwidth of the diplexer. The modification will also shift the susceptance characteristics to produce a more effective cancellation over the diplexer's bandwidth.

A general modification factor (**Equations 1** and **2**) to shift the crossover points has been developed by Matthaie.[1] These equations are a function of the normalized input conductance and take into account the filter's passband ripple and number of poles. This means the modi-

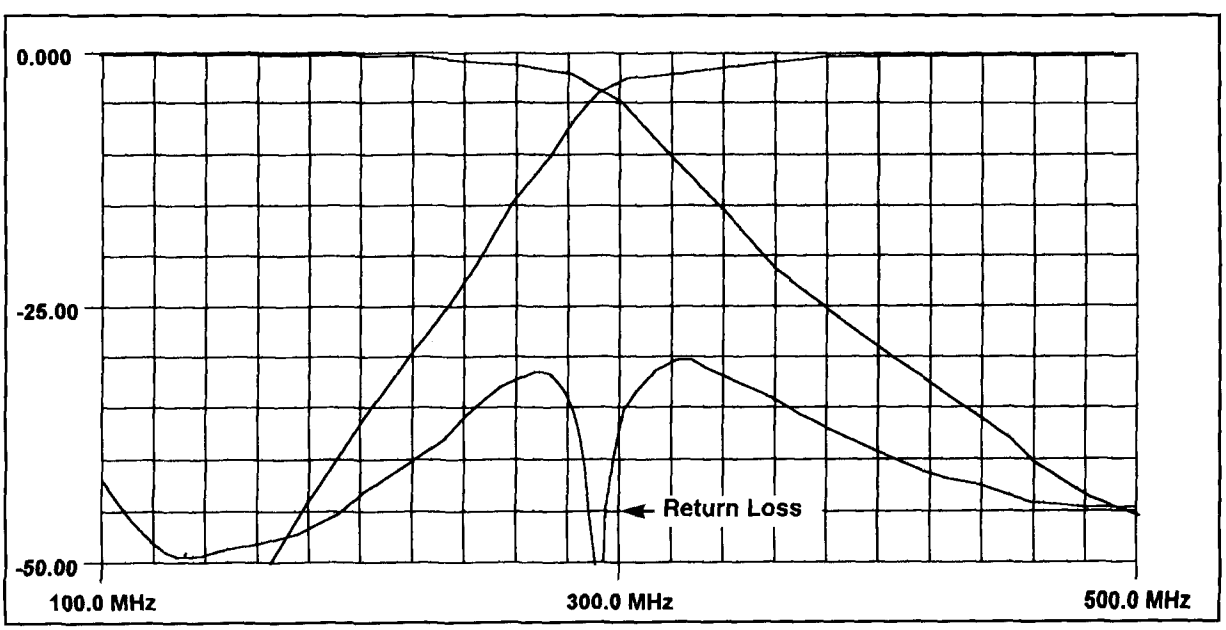

Figure 5. Plot of insertion and return loss of 294-MHz diplexer.

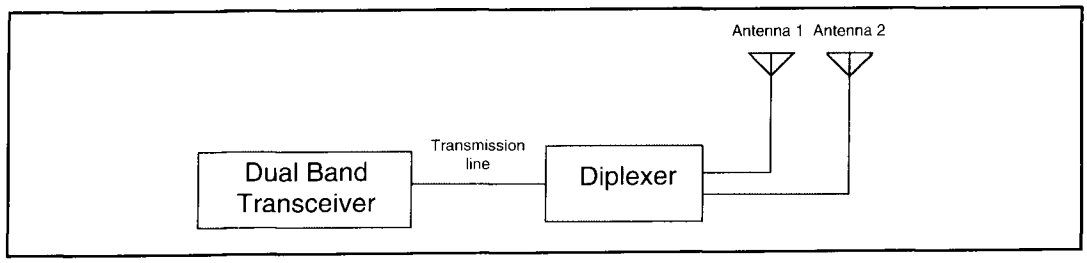

Figure 6. Dualband transceiver configuration.

fication must be applied to each case of ripple and number of poles.

$$N_{even} \quad \omega\,'3dB = \cosh\left[\frac{1}{N}\cosh^{-1}\left(\frac{1+2\varepsilon}{\varepsilon}\right)^{1/2}\right] \quad (1)$$

$$N_{odd} \quad \omega'3dB = \cosh\left[\frac{1}{N}\cosh^{-1}\left(\frac{1}{\varepsilon}\right)^{1/2}\right] \quad (2)$$

$$\varepsilon = \left(10^{\frac{\text{Ripple dB}}{10}}\right) - 1 \qquad N = \text{number of poles}$$

The diplexer computer program

The diplexer program was written with Microsoft's QuickBasic, Version 4.5 and is compatible with other versions of BASIC. A listing of the program's basic code is provided in **Appendix 1**. The user inputs the 3-dB crossover frequency, number of poles, passband ripple, and the system's impedance. Entering 0 dB for the passband ripple will generate a Butterworth response, otherwise the response is a Chebyshev. The diplexer is derived from a low-pass prototype filter function. The normalized G-elements (normalized to 1 rad/sec and 1 ohm) for each low-pass filter element are calculated using the equations given in **Table 1**. If the response is a Chebyshev, each element is modified with **Equations 1** and **2**. High-pass filter elements are generated by replacing each filter element in the low-pass prototype with its opposite and inverting it. For example, $C_{hp} = 1/L_{Lp}$ and $L_{hp} = 1/C_{Lp}$. Each G-value is then frequency and impedance scaled using the crossover frequency and the system's impedance.

As an example of the program's functionality, let's design a diplexer for the 2-meter/70-centimeter band. The diplexer is designed for seven poles, 0.01-dB ripple, a crossover frequency of 294 MHz (this is the center between the two bands), and a 50-ohm system. **Figure 4** contains the calculated component values of the diplexer design (less the schematic, which is only shown for clarity).

Figure 5 is a plot of the insertion and return loss of the 294-MHz diplexer using the component values calculated from the program. The analysis was performed using a computer-aided microwave simulation program called Touchstone. The frequency characteristics of the low and high-pass filters, as well as the 3-dB crossover frequency, are distinctly defined in the plot. More importantly, notice from the return loss that a low VSWR of 1.1 or better is maintained—indicating the impedance is constant across the frequency range.

Diplexer applications

Figures 6, **7**, and **8** show some specific applications that use diplexers. **Figure 6** is the familiar dualband configuration, where a single dualband transceiver is connected to two anten-

Singly Terminated Butterworth	Singly Terminated Chebyshev	
$a_K = \sin\frac{\pi}{2}\left(\frac{2K-1}{N}\right)$ K = 1,2,...,n	$B = \ell n\left[\coth\left(\frac{\text{Ripple dB}}{17.37}\right)\right]$	$\gamma = \sinh\left(\frac{B}{2N}\right)$
$C_K = \cos^2\left(\frac{\pi K}{2N}\right)$ K = 1,2,...,n	$a_K = \sin\left(\frac{\pi(2K-1)}{2N}\right)$	K = 1,2,...,n
$g_1 = a_1 \quad g_K = \frac{(a_K)(a_K-1)}{(C_K-1)(g_K-1)}$	$d_K\left[\gamma^2 + \sin^2\left(\frac{\pi K}{2N}\right)\right]\cos^2\left(\frac{\pi K}{2N}\right)$	K = 1,2,...,n
	$g_1 = \frac{a_1}{\gamma} \quad g_K = \frac{(g_K)(a_{K-1})}{(C_{K-1})(g_{K-1})}$	K = 2,3,...,n

Table 1. Equations to calculate normalized G,-elements for each low-pass filter.

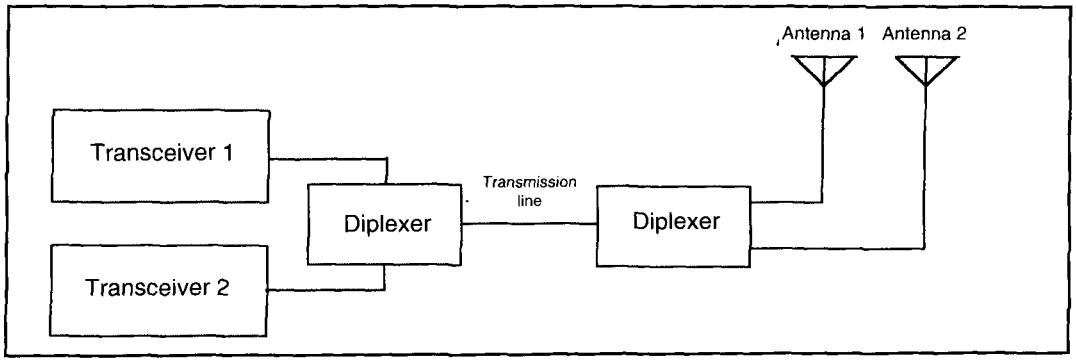

Figure 7. Dual transceiver configuration.

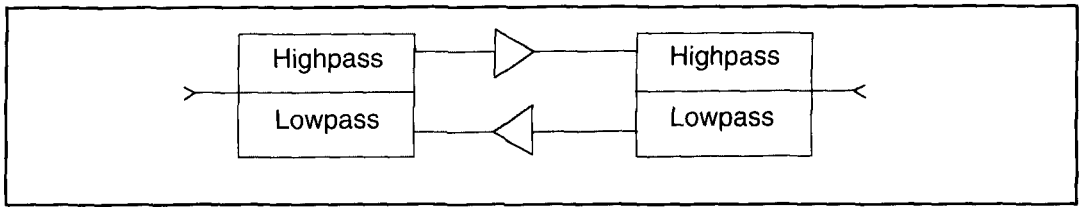

Figure 8. Bidirectional amplifier system.

nas via a single transmission line. Sometimes two separate transceivers are used. In **Figure 7**, a diplexer is placed at the transceiver output and at the antenna site. The radios are then connected to the antennas via a single transmission line. Other applications include a bi-directional amplifier system. By placing diplexers at each end of the system as shown in **Figure 8**, greater isolation beyond the limitation of the amplifiers can be achieved.

The IF port of a mixer is comprised of both the sum and difference frequency, and other unwanted frequencies, such as image and LO leakage. In most cases, the difference frequency is selected and the other unwanted frequencies are eliminated with a filter. However, the impedance of the filter outside the passband is no longer matched to the impedance of the IF port (usually 50 ohms). This mismatch causes the unwanted frequencies to reflect back to the IF port and recombine in the mixer, producing additional spurious frequencies. As shown in **Figure 9**, a diplexer now allows the IF port to be terminated in the same impedance at all the frequencies. The sum frequency and higher order products now pass through the highpass filter and are dissipated in the terminating resistor, eliminating spurious frequencies.

Conclusion

In this article, I've tried to show how singly-terminated low-pass and high-pass filters can be modified to produce a diplexer. I also introduced a computer program that may be used to synthesize diplexer component values. Finally, I've presented a number of common applications that use diplexers. ■

References

1. G. Matthaei, L. Young, and E.M.T. Jones, *Microwave Filters, Impedance-Matching Networks, and Coupling Structures*, Arttech House, Inc., 1980.

Bibliography

1. R.G. Veltrop and R.B. Wilds, "Modified Tables for Design of Optimum Diplexers," *The Microwave Journal*, 1964.
2. J. Porter, "Chebyshev Filters with Arbitrary Source and Load Resistances," *RF Design*, August 1989.
3. *Microwave Engineers Handbook*, Volume 1, Horizon House-Microwave, Inc., 1971.

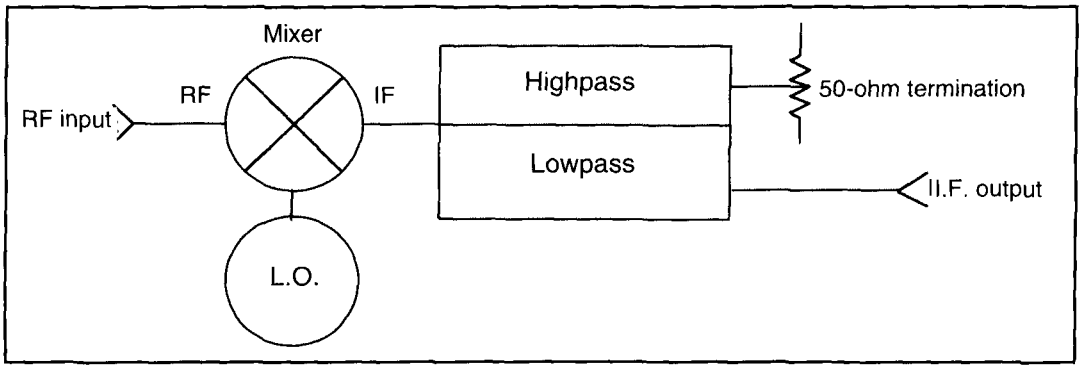

Figure 9. Mixer impedance matching with a diplexer.

APPENDIX 1

```
'*************************************************************************
'*******DIPLEXER DESIGN PROGRAM WRITTEN BY T. CEFALO Jr WA1SPI @1996***
'*************************************************************************
CLEAR : COLOR 7, 0: CLS : COLOR 14, 12
PRINT "T. CEFALO Jr            DIPLEXER DESIGN PROGRAM                    WA1SPI"
COLOR 7, 0: DEFDBL A-Z: OPTION BASE 1: PI = 3.1415926#: PRINT
DEF FNSinh (X) = (EXP(X) - EXP(-X)) / 2
DEF FNCosh (X) = (EXP(X) + EXP(-X)) / 2
DEF FNACosh (X) = LOG(X + SQR((X ^ 2) - 1))
DEF FNEvenOdd (X) = (X / 2) - INT(X / 2)'Test for even or odd N even=0 odd=.5
INPUT "Enter 3 dB Crossover Frequency (MHz)"; Fc: Fc = Fc * 1000000!
INPUT "Enter Number of Poles "; N
INPUT "Enter Passband Ripple in dB (0 for Butterworth)"; Am
INPUT "Enter External System Impedance Zo (ohms)"; Zo
DIM Ak(N), Ck(N), Dk(N), G(N)
IF Am = 0 THEN  'CALCULATE G-VALUES FOR BUTTERWORTH RESPONSE
FOR K = 1 TO N
Ak(K) = SIN(PI * (2 * K - 1) / (2 * N))
Ck(K) = (COS((PI * K) / (2 * N))) ^ 2: NEXT K: G(1) = Ak(1)
FOR K = 2 TO N
G(K) = (Ak(K) * Ak(K - 1)) / (Ck(K - 1) * G(K - 1)): NEXT K
ELSE          'CALCULATE G-VALUES FOR TCHEBYCHEV RESPONSE
X = Am / 17.37: e = 10 ^ (Am / 10) - 1
Beta = LOG(FNCosh(X) / FNSinh(X)): X = Beta / (2 * N): Gama = FNSinh(X)
FOR K = 1 TO N
Ak(K) = SIN(PI * (2 * K - 1) / (2 * N)): X = (PI * K) / (2 * N)
Dk(K) = (Gama ^ 2 + (SIN(X) ^ 2)) * (COS(X)) ^ 2: NEXT K: G(1) = Ak(1) / Gama
FOR K = 2 TO N
G(K) = (Ak(K) * Ak(K - 1)) / (Dk(K - 1) * G(K - 1)): NEXT K
FOR K = 1 TO N  'Modify the Tchebychev G(k) values
IF FNEvenOdd(K) = 0 THEN
G(K) = G(K) * FNCosh((FNACosh(SQR((1 + (2 * e)) / e)) / N))
ELSE
G(K) = G(K) * FNCosh((FNACosh(SQR(1 / e)) / N))
END IF: NEXT K
END IF
CLS : COLOR 7, 9: PRINT "T. CEFALO Jr            DIPLEXER COMPONENT VALUES
WA1SPI"
COLOR 7, 0: IF Am = 0 THEN A$ = "Butterworth" ELSE A$ = "Tchebychev"
PRINT "Filter Response is " + A$
PRINT "3 dB Crossover Frequency="; Fc / 1000000!; "MHz"; "    Ripple="; Am; "dB"
PRINT "Number of Poles="; N; "          System Impedance="; Zo; "ohms": PRINT
PRINT "LOWPASS SECTION          HIGHPASS SECTION"
PRINT "-------------------------------------------------------": COLOR 12, 0
PRINT "      <----------Diplexed End---------->": COLOR 15, 0
FOR K = N TO 1 STEP -1: I = (N + 1) - K: A$ = STR$(I)
IF FNEvenOdd(I) <> 0 THEN 'Lowpass and Highpass filter series components
Llp = (Zo * G(K)) / (2 * PI * Fc): Chp = 1 / (G(K) * (2 * PI * Zo * Fc))
PRINT "Ls" + A$ + "="; CSNG(Llp) / 1E-09; "nH", "Cs" + A$ + "="; CSNG(Chp) / 1E-12; "pF"
ELSE                'Lowpass and Highpass filter parallel components
Lhp = (Zo / G(K)) / (2 * PI * Fc): CLp = G(K) / (2 * PI * Zo * Fc)
PRINT "Cp" + A$ + "="; CSNG(CLp) / 1E-12; "pF", "Lp" + A$ + "="; CSNG(Lhp) / 1E-09;
"nH"
END IF: NEXT K: COLOR 12, 0: PRINT "      <----------Load Ends---------->"
COLOR 15, 0
```

John S. (Jack) Belrose, *VE2CV*
17 Tadoussac Drive
Aylmer, QC J9J 1G1;
Walter Maxwell, *W2DU*
243 Cranor Avenue
DeLand, Florida 32720-3914; and
Charles T. (Tom) Rauch, *W8JI*
3455 Monica Lane, SW
Conyers, Georgia 30208

SOURCE IMPEDANCE OF HF TUNED POWER AMPLIFIERS AND THE CONJUGATE MATCH

Understanding basic concepts and clarifying misunderstandings

The determination of optimum operating conditions for HF-tuned power amplifiers (HFTPAs) is a topic that spans more than 60 years of analytical, numerical, and experimental research. This study began with the pioneering work of Terman,[1] Mouromtseff, and Kozanowski,[2] along with many others, and continues today. Analytic methods based on static characteristics for the active device, using Fourier analysis, enable the determination of closed form expressions for the output power in terms of input voltage and current.

Heyboer and Zijlstra,[3] in perhaps the most detailed analytical methods developed to date, devised graphical/numerical procedures for pentodes, tetrodes, and triodes. Zivkovic-Dzunja[4] designed software for her analysis methods. The application of the "PSpice" program, a model that uses voltage and current-dependent sources with arbitrary nonlinear transfer characteristics, is a subject of current study (see Kostic et al.[5]).

All of these methods, including the simplest one (which involves looking at the manufacturers' specifications for the tube), allow the determination of the optimum load impedance Z_L (here in accord with usual nomenclature R_L, since $Z_L = R_L$ because the tank circuit is resonant), so the amplifier under specified operating conditions (plate voltage, plate current, and drive power) will deliver its design power to a selected load impedance (Z_{load}) at as high an efficiency as possible.

It's common to calculate optimum load impedance R_L—the impedance the plate of the tube "sees" looking toward the external load—but uncommon (yet necessary) to think of the dynamic output impedance of the source Z_S. The term "source resistance," as is often (mis)used in referring to the source of RF power delivered by Class B, C, and D power amplifiers, reveals a prevalent misconception that the real part of the source impedance in this class of amplifiers is a dissipative resistance. Clearly, plate resistance R_p of the active element (tube, transistor, etc.) is a dissipative resistance that converts electrical energy into heat. However,

the source impedance of the amplifier seen by loads connected to the output port of the amplifier is established by the impedance transformation characteristics and the Q of the tank circuit operating on the complex and nonlinear parallel impedances presented to its input side from both the active device and the power supply (including the RF choke and coupling capacitor). Thus, R_p contributes to, but does not establish, the output impedance of the amplifier.

Resistance is also defined as the real part of an impedance (from the *IEEE Dictionary*). Because the impedance of a network deals with energy transfer, it has nothing to do with where the energy came from, or what became of it. *The real part of the impedance of a network, therefore, does not dissipate energy of itself.* Only that portion of the real part of an impedance that is, in fact, a dissipative resistance will dissipate energy. Similarly, the characteristic impedance of a lossless transmission line, Z_o, say $Z_o = 50$ ohms, does not correspond to a dissipative resistance; nor does the intrinsic impedance of a medium such as free space, where $\eta_o = 377$ ohms. The effective source impedance—the dynamic output impedance of the power amplifier Z_s—may, therefore, be completely (ideal case) or largely (typical practical case) nondissipative, as by conjugate matching all (ideal case) or most (typical practical case) of the available power generated is transferred to the external load.

An understanding of this concept, which is probably one of the most serious misunderstandings in electrical engineering today (private communications with John Fakan, KB8MU, 1996), provides the basis for understanding why an RF power amplifier can deliver its design output power into a conjugately matched load while achieving efficiencies significantly greater than 50 percent. This understanding is important, because the ability of HFTPAs to be conjugately matched has been unjustly disputed—largely on the argument that conjugate matching establishes an upper limit of 50 percent efficiency.

Antenna-network theorems

In circuit theory, three network and antenna theorems have proven useful in simplifying a solution for this misconception, and also in understanding many problems. The theorems that are most useful for antenna and antenna matching problems are:

1. Thévenin's Theorem. "If an impedance Z_R be connected between any two terminals of a *linear* network containing a generator, the current which flows through Z_R will be the same as it would be if Z_R were connected to a simple generator whose generated voltage is the open circuit voltage that appeared at the terminals in question and whose impedance is the impedance of the network looking back from the terminals."

2. Maximum Power Transfer Theorem. "An impedance connected to two terminals of a network will absorb maximum power from the network when the impedance is equal to the complex conjugate of the impedance looking back into the network from the two terminals."

3. Compensation Theorem. "Any impedance in a network may be replaced by a generator of zero internal impedance, whose generated voltage at every instant of time is equal to the instantaneous potential difference that existed across the impedance because of current flowing through it."

Thévenin's Theorem strictly applies to linear networks and circuits with a well-defined source impedance; whereas, the current and voltage of an active device can be quite nonlinear, in spite of the fact that the amplifier itself may be linear. Notwithstanding, numerical methods based on Thévenin/Norton models are currently used to analyze the transient response of networks consisting of the interconnection of linear and nonlinear lumped or distributed networks (transmission lines), for arbitrary sources, using stepwise time delay methods, where the steps in time are so small that the current and voltage change during the step can be considered linear.[6,7]

The Compensation Theorem avoids this difficulty, as it is based on instantaneous values. Therefore this theorem does apply to power amplifiers, instant by instant. In the authors' view, the Compensation Theorem gives one look (an important one) at the nature of the output impedance of an RF power amplifier. Insofar as power generation is concerned, and transfer of power to the input terminals of the π-network tank circuit network, the tube can be replaced by a generator of *zero* internal impedance, whose generated voltage at every instant of time is equal to the instantaneous potential that exists across the load impedance R_L due to current flowing through it. And, since the instantaneous values of V/I at every instant of time correspond to instantaneous values of an impedance, the average dynamic output impedance of the source, Z_s, must equal the load impedance R_L, for all practical purposes.

When analyzing the match between an active device, which may be nonlinear, and its load, the concept of conjugate match must be carefully considered. One effective approach is to use the definition of conjugate match as one that provides for maximum power transfer (the Maximum Power Transfer Theorem). This is essentially an energy equation which is an

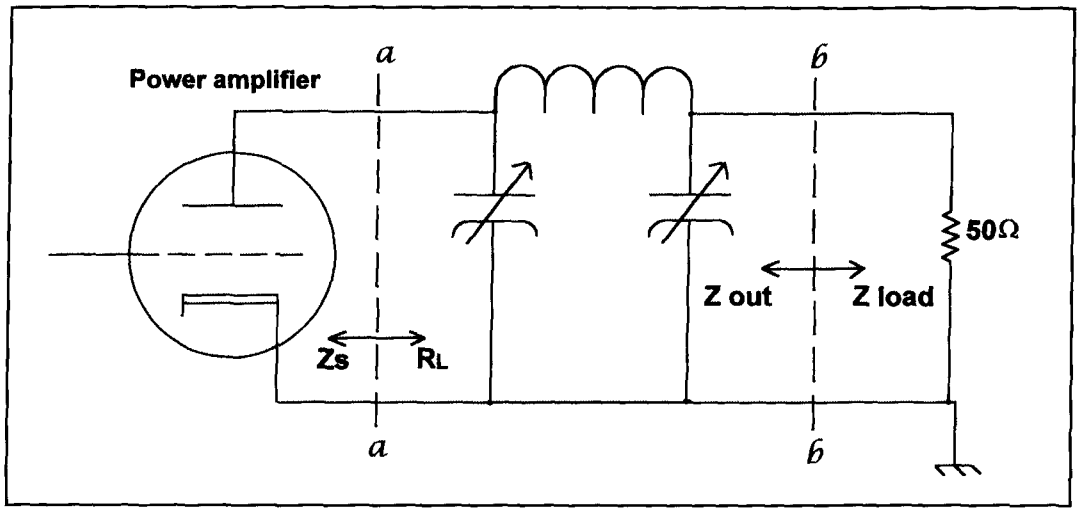

Figure 1. Sketch of an RF power amplifier tube and its π-network tank circuit, initially tuned to provide maximum available design power to its design load impedance (R_{load} = 50 ohms).

extremely powerful tool of physics used to avoid the pitfalls of nonlinear phenomena. Conservation of energy transcends all bounds. It is true for linear, nonlinear, periodic, nonperiodic systems, and so on. Simply stated, when the matching network presents a load that provides for the maximum transfer of available design power from the active device, the device is conjugately matched.

PA output (source) impedance, Z_S

A constant plate current flows in Class A amplifiers, even in the absence of a signal on the grid. The output source impedance, a resistance, is therefore easy to identify and measure. The generator may be considered a current generator that is impedance matched when the load resistance is equal to the dynamic output resistance of the source. See, for example, Sabin.[8] In Class B and C amplifiers, the output impedance isn't so easily measured or defined. We can measure the output impedance of source Z_S only when the amplifier is being driven to the input and output levels at which it is supposed to operate.

In the case of the Class A amplifier, the energy dissipated within the generator is equal to the energy delivered to the load, at best. This occurs at the conjugate match point. In the case of Class B and C amplifiers, the efficiency is markedly greater than 50 percent. This is because the vacuum tube or transistor isn't a linear device. An RF power amplifier is, in effect, a converter that converts DC energy (provided by the power supply) into RF energy at the highest possible efficiency. The DC source voltage supplies current to the load, and the transmitting tube connected in the circuit perturbs the current under the influence of the grid excitation.

If the plate current is analyzed by a Fourier expression, one learns that the output comprises not only a DC component, but also RF components of various frequencies. In a conventional power amplifier the desired component is the alternating grid voltage frequency. The transmitter's tank circuit, conventionally a π- or π-L network, which provides the required matching of impedances in the circuit (see **Figure 1**), must be arranged so the desired frequency can pass through, while other components, including the DC component, are blocked or bypassed. The energy delivered to the external load at the desired frequency can be calculated on the basis of Joule's law.

The tank circuit is *fundamental* in typical (non-Class A) RF power amplifiers. ***Any equivalent circuit for the amplifier, that doesn't include the tank circuit, is incomplete.*** The tank circuit flywheels, smoothing or averaging the time-varying impedance corresponding to the fluctuations of the fundamental alternating tank voltage to tank current at the input terminals of the π-network circuit, and transforming the value of this impedance. The smoothed power passed on by the flywheel to its load can't be different from the average, over time, of the power being delivered to it (regardless of the nature of the source impedance). With power amplifiers, the time-averaged value of the dramatically varying impedance of the tube, in parallel with the impedance of the power supply and other components (which includes the highly reactive RF choke), is equal to the transformed value of the amplifier's output impedance (Z_{out}).

From a practical standpoint, the output impedance of an RF power amplifier is almost entirely established by the characteristics of the

tank circuit. The dissipative losses in the active element simply represent collateral power loss that must be considered in efficiency calculations. The tube's conductance mechanism doesn't store and forward energy, so that particular power never makes it to the amplifier's output terminals. In fact, in all but Class A amplifiers, the power generated and transferred from the power supply to the output terminals isn't even transported through the active device. The active device simply perturbs the supply voltage, synchronously with the signal on the grid, at the junction of the plate choke and blocking capacitor. The shorter the dissipative resistive cycle, the closer the active device emulates a perfect switch, and the lower the losses will be.

The optimum load impedance, R_L, is the impedance the tube "sees" looking toward the load. The effective source impedance Z_s is the impedance associated with the generation, or conversion of power. As noted at the outset, methods to calculate R_L have been with us for more than 60 years. As an example only, we use nomenclature and equations given by Terman's approximate method of calculation. The power output:

$$P_{out} = \frac{(E_p - E_{min})\, I_1}{2} \text{ watts} \qquad \textbf{(1)}$$

And, the required load impedance is:

$$R_L = \frac{E_p - E_{min}}{I_1} \text{ ohms} \qquad \textbf{(2)}$$

Where E_p is the anode or plate voltage, E_{min} is the minimum value of the alternating voltage developed across the load, and I_1 is the fundamental AC plate current.

What does this tell us? Optimum load impedance R_L is a real, measurable, impedance. We can tune the tank circuit and any associated network needed for matching the antenna, with a load that has an antenna connected, so when looking into the input terminals of the tank circuit with the power on we see R_L. The power source is the current and voltage available at the input terminals of the π-network tank circuit. However, current and voltage define an impedance; therefore, the effective dynamic output impedance of the transmitting tube is

$$Z_s = \frac{E_p - E_{min}}{I_1}$$

This is exactly what our technical literature has been calling R_L. So, while the literature describes methods for calculating the optimum load impedance of the amplifier, *we have actually been calculating the optimum time-averaged dynamic output impedance of the tube.*

Following Fakan's lead in clarifying one of the most misunderstood concepts in electrical engineering, the issue of a nondissipative PA source impedance, Z_s, it will be helpful to examine this concept in greater depth. As was stated earlier, resistance is also defined in the *IEEE Dictionary* as the real part (Re) of an impedance. In a lossless network, or transmission line, Re represents the transfer of energy through the network with no dissipation until it reaches a terminating load, resistance R, where it is then dissipated.

Let's illustrate this concept with an example using a lossless transmission line terminated with a resistance, R, equal to its characteristic impedance Z_o.The impedance appearing at the input of the line is Z_o = Re, where Re is established by voltage-current ratio V/I appearing at the line input. Because the line is terminated in its characteristic impedance, there are no reflections. Therefore voltage-current ratio Re is constant everywhere along the line; thus the line impedance is also constant everywhere. However, note that *no energy has been dissipated in the line.* This means the real part, Re, of the line impedance everywhere along the line is derived wholly from the line voltage-current ratio—not from any dissipative element.

To be certain we really understand this very important concept, let's take one further step to examine the case where the transmission line is terminated in a mismatch, resulting in reflected waves of voltage and current along the line. We know that the addition of the forward and reflected voltage phasors, and the forward and reflected current phasors, respectively, results in a variation of the line impedance along the line, in contrast to the constant line impedance Z_o where the line termination is matched. Let's assume that at a point on the line where the angles of the phasor resultants are 0 degrees and 180 degrees, or vice versa (yielding a zero reactance), the voltage and current are 100 volts and 0.5 amp, respectively. This results in an Re of 200 ohms at that point, while *transferring* 50 watts of power toward the load.

At another nonreactive point on the line the voltage and current are 20 volts and 2.5 amps, resulting in Re = 8 ohms, still *transferring* 50 watts of power, although through a different value of the real part of the line impedance. From these examples, it is clearly evident that *no dissipation occurs* as the energy is transferred along the line while travelling through different values of Re.

This concept of a dissipationless impedance also applies directly in establishing the PA source impedance Z_s. Here the voltage and cur-

rent appearing at the input terminals of the π-network tank circuit are the time-averaged fundamental AC plate voltage and current, where the AC voltage is $(E_p - E_{min})$ and the current is I_1, as in **Equation 2**. Consequently, this voltage-current relationship at the tank input alone establishes the real part, Re, of the source impedance, where:

$$Z_S = \frac{V}{I} = \frac{(E_p - E_{min})}{I_1}$$

Clearly this expression contains no dissipative element. Thus, PA source impedance Z_S is also *nondissipative*, as in the transmission-line example above. In addition, comparing the above expression with **Equation 2** provides further evidence that $Z_S = R_L$, the condition required for delivery of all the available power in accordance with the Maximum Power Transfer and Conjugate Match Theorems.

Optimum load impedance R_L is nondissipative, as is the dynamic output impedance of the tube Z_S. Z_S is the only impedance in the circuit that accounts for the available power. And, because all available power generated is delivered to the load by conjugate matching, $Z_S = R_L$. In some textbook analyses, R_L is considered a real resistance because, from the point of view of amplifier design, it doesn't matter whether power is totally dissipated in the tank circuit, or whether power is generated there for transfer to the load—the antenna. The vacuum tube "couldn't care less." But this is the fundamental point we're trying to make by introducing the concept of a nondissipative impedance. We are concerned here with the generation or conversion of power, and with matching between the output impedance of the power amplifier and the antenna system for the purpose of transfer of maximum available power.

The dynamic internal output or source impedance Z_S of an operating non-Class A amplifier is not a constant fixed value, as is the internal impedance of a passive classic generator, because this impedance varies over the RF cycle. The average value of this impedance depends on how the amplifier is loaded, tuned, and operated. In amplifiers with conduction angles of less than 360 degrees, the tank circuit flywheels for a portion of the RF cycle. During this time, when the tube is cut off, the tank circuit delivers stored energy to the load. Yet, from the outside, it appears that the amplifier behaves as if its effective internal dynamic output impedance were equal to its optimum load impedance, as this is the condition for maximum power output for a given amount of drive power.

When correctly tuned to provide maximum power for a given operating condition, operating into the design optimum load impedance (R_L), the plate voltage and current vary over the RF cycle in such a way that the amplifier appears to have an average impedance Z_S equal to the design load impedance R_L, referenced to the plate of the tube. The π- (or π-L) tank circuit transforms this impedance to Z_{out}, the output impedance referenced to the output terminals of the amplifier. Typically $Z_{out} = 50$ ohms.

Because the internal dynamic output impedance of an HFTPA depends on the average fundamental AC voltage and current over an RF cycle, this impedance will change when the amplifier is mistuned or if, without retuning, the π- (or π-L) tank circuit is operated into a mismatched load. The dynamic output impedance also changes if the drive power is changed. The concept of conjugate match and maximum design power transfer strictly applies to a band of frequencies that are centered on the frequency to which the amplifier is tuned and matched, and only for a mismatch load impedance less than some value that depends on the amplifier design.

Output impedance Z_S can reduce the selectivity of the matching networks, and the antenna system itself, in the neighborhood of the resonant frequency. This is not because the output impedance is a dissipater of RF power, but because when the amplifier is correctly matched, it tends to maintain a more constant output power as the frequency departs from center. Whether the bandwidth of the amplifier and its antenna system is increased, and by what factor, is a subject beyond the scope of this article.

Establishing the conjugate match with the π-network

Before proceeding further, it will be instructive to examine the procedure used for adjusting the π-network in establishing the conjugate match. As stated earlier, a conjugate match is established when the load resistance R_L and the source impedance Z_S, are equal. This is the condition for delivery of maximum available power, which establishes this value of R_L as the *optimum* load resistance. With plate voltage and drive power set to obtain design output power, Z_S and R_L of the commonly used pair of 6146 tubes in parallel are around 2000 ohms resistive. We'll initially terminate the output of the π-network with a 50-ohm resistive load. To observe operating conditions while adjusting the network to obtain the optimum load impedance, we can use either an RF ammeter in series with the load, or the *relative* power indicator usually found on the transceiver. On most commercial rigs this indicator is simply an RF

voltmeter connected across the output terminals of the π-network tank circuit. Using conventional tuning and loading procedure, we begin with minimum loading, where load resistance R_L is substantially higher than the optimum resistance, resulting in delivery of minimum output power. We now increase the loading, which decreases R_L, and increases output power, while we simultaneously adjust the plate-tuning capacitor to maintain resonance in the tank circuit.

As R_L continues to decrease with further increase in loading, a point of maximum output power is reached, after which the power then *decreases* with further increase in loading. This indicates that R_L has passed the optimum value, and has decreased to a value *lower* than the optimum load resistance. The plate current dip will also have become broad and shallow. Before reaching maximum output, the tubes were *underloaded*, because load impedance R_L at the input of the π-network was *higher* than the source impedance Z_S, and the plate current was also lower than normal for delivery of all available power for the given drive level. After passing the point of maximum output, the tubes were *overloaded*, because R_L was then *lower* than Z_S, and the plate current at the dip minimum was higher than normal—possibly exceeding the rated value. However, the correct, or *optimum* load impedance, where $R_L = Z_S$, is obtained when the loading is adjusted to deliver the *maximum available power* with the given plate voltage and drive power. If the amplifier is properly neutralized, the minimum plate current dip (indicating network resonance) will occur simultaneously with delivery of maximum output power. When adjustments made during this procedure have resulted in delivering all available power, $R_L = Z_S$, and ***the load impedance R_L is conjugately matched to the source impedance Z_S.***

While we have shown how a conjugate match is established when the terminating load is a pure resistance, it will also be instructive to examine the condition when the terminating load is a *complex* impedance. As an example, we'll now replace the 50-ohm terminating resistance with a 30-ohm resistor in series with 40-ohm capacitor, for an impedance Z = 30 - j40 ohms. (This is a *50-ohm complex impedance*, at angle -36.9 degrees.) This impedance presents a 3:1 mismatch at the output of the amplifier, relative to the 50-ohm resistive termination, to which it was previously adjusted for a conjugate match. The π-network now transforms this new complex output load impedance to $Z_L = R_L + jX$ at the input of the π-network, which now presents a 3:1 mismatch to the source impedance Z_S. Thus the conjugate match is destroyed, the previous straight, resistive load line is changed to a reactive, elliptical load line, and the output power and efficiency are reduced. However, the conjugate match can be re-established by readjustment of the tuning and loading controls.

First, decreasing the capacitive reactance of the plate-tuning capacitor by 40 ohms causes the tank circuit to have a net *inductive* reactance of +j40 ohms, which cancels the -j40-ohm *capacitive* reactance in the load and restores the system to resonance. Second, readjustment of the loading control changes the impedance-transformation ratio of the π-network to transform the 30-ohm resistance of the load to again equal the required optimum value of R_L at the input of the network. The conjugate match between the tubes and the reactive output load is thus re-established, because the resistive R_L now appearing at the input of the π-network again equals the source impedance Z_S, and since the *net reactance is zero* the system is again resonant.

PA dynamic plate resistance, Rp

In the discussion above, we described a HFTPA as a power converter. The DC source voltage supplies current to the load, and the transmitting valve connected in the circuit makes and breaks the current under the influence of the excitation on the grid. Maximum power is delivered to the tank circuit when the plate current is a maximum, no power is delivered to the tank circuit during half or more than half of the RF cycle. Yet during this time, power is still delivered to the load, because the tank circuit flywheels.

One can attribute power dissipated over the RF cycle to an "averaged plate resistance," R_p, corresponding to an average value of DC plate current and voltage, averaged over the period during which the tube is conducting. The efficiency of the amplifier (output RF power divided by input DC power) corresponds to a power loss—power dissipated as heat in the vacuum tube. This power loss can be attributed to a plate resistance, the value of which is always less than Z_S when the efficiency is greater than 50 percent.

The energy per cycle dissipated in the vacuum tube is given by:

$$\text{Energy} = \int_0^{1/f} i^2(t)\ \ R_p(i)\ dt \qquad \textbf{(3)}$$

where $R_p(i)$ is a dynamic resistance, which is a function of the DC plate current, i.

This dynamic plate resistance, $R_P(i)$, is not a resistance having a single value to place in an equivalent circuit. During much of the RF cycle

in a typical Class B, C, and D power amplifier, no dissipation resistance is present, and efficiency can easily be more than 50 percent with a conjugate match. The value of $R_P(i)$ is low (a few hundred ohms) during the interval that power is delivered to the input terminals of the tank circuit; the value of $R_P(i)$ is very large (tens of kilohms) when no power is delivered to the tank circuit; while the load impedance, R_L, is a few thousands of ohms. Thus from **Equation 3**, it is evident that the value of plate resistance R_P can be determined by dividing the dissipated power P_d by the square of the DC plate current i^2.

Clearly, plate resistance R_p of the active element (tube, transistor, etc.) is a dissipative resistance that converts electrical energy into heat. However, the source impedance of the amplifier seen by loads connected to the output port of the amplifier is established by the impedance transformation characteristics and the Q of the tank circuit operating on the complex and nonlinear parallel impedances presented to its input side from both the active device and the power supply (including the RF choke and coupling capacitor). Thus, R_P contributes to, but does not establish, the output impedance of the amplifier.

Experiments that measure load impedance, output impedance, and provide support for the concept of a conjugate match

The applicability of the concepts of maximum power transfer and conjugate match to RF power amplifiers has been questioned and debated since November 1991. It was then that Warren Bruene, W5OLY, published his position that conjugate matching does not, in general, occur with RF power amplifiers.[9] Bruene has expressed the opinion that Walter Maxwell, W2DU's writings in the *ARRL Handbook*, the *ARRL Antenna Book*, and his book *Reflections—Transmission Lines and Antennas* are incorrect.

There is general agreement that these concepts apply to linear time-invariant systems, such as an antenna system fed by a Class A amplifier. The controversy broadens for a linear time-varying system, such as an antenna system fed by a Class B amplifier. The Class B amplifier is linear in the sense that the output voltage is proportional to the input voltage, even though the active component in the amplifier conducts only over a part of the RF cycle. On the other hand, if the antenna system is driven by a Class C amplifier, the situation is even more complex. The Class C amplifier is clearly a nonlinear time-varying system, because input/output linearity is not present. We believe this doesn't matter. The Maximum Power Transfer Theorem applies to this class of amplifiers because this theorem is essentially an energy equation used to avoid the pitfalls of nonlinear phenomena.

Those who do not believe that HFTPAs are, or could be, conjugately matched are just as firmly entrenched in their belief as those who do. As things stand now, it is unlikely that either side will change its stance. However, here are some experiments, including the test setup used initially by Warren Bruene, which we feel provide insight concerning the load impedance, the output impedance, and the concept of conjugate match.

Measuring load impedance

Our first experiment shows that load impedance R_L can be measured easily. First, using the setup in **Figure 1** and a bi-directional coupler in the line to the load, adjust operating conditions by tuning the π-network and adjusting the drive power so the HFTPA delivers its maximum available design power to the selected load—for example, 50 ohms. If the plug is then pulled on the power amplifier after tuning it correctly, an RF impedance meter can be connected from the anode to ground, with the external load—the selected load impedance—still connected, and the load impedance R_L can be measured. John Belrose, VE2CV, and Walter Maxwell, W2DU, have conducted this experiment on numerous occasions.

What does this tell us? If you're a believer in the conjugate match, then the measured impedance must equal Z_s because R_L must equal Z_s for maximum power transfer. When the plate sees its optimum load impedance, R_L, all the available power will be delivered to the load. That is a conjugate match. If you don't believe that HFTPAs are tuned correctly when conjugately matched, or if you believe as Bruene does, that conjugate matching is not achieved with HFTPAs when tuned and loaded in the conventional manner, continue reading. What's clear is that we can calculate and measure the optimum load impedance R_L.

Belrose has also carried out the above sequence of measurements and tuning in reverse order. Before turning on the power amplifier, he tuned the matching networks (in this case the antenna, its matching circuit, and the tank circuit) with the antenna connected, to provide a measured impedance at the anode equal to the design load impedance. There was a practical reason behind this reversal. Belrose was tuning and matching a very high power (1000 kW) HF pulse transmitter he'd designed,

and it wasn't possible to tune the transmitter in the conventional way, using current meter readings. The pulse rate would have had to be so high that the power supply couldn't provide the current, and the plate dissipation would have been excessive. The transmitter used a pair of the largest air-cooled tubes in the world (Philips TBL 12/1000 or 6078 tubes). When tuned in this manner, all that was required was to gradually increase the drive power until the amplifier delivered design power to the antenna system. No further "tuning" was required.

Measuring/calculating complex conjugate impedances

Our second experiment is designed to show that when a low-loss antenna system tuning unit (ASTU) is tuned for a match between the power amplifier and the antenna system, the antenna system is conjugately matched, and by inference the power amplifier is conjugately matched. It is necessary to have a mismatched antenna system for this experiment. Belrose has performed this experiment on many occasions. In fact, he has used a variation of this method to measure (though perhaps not very accurately) the impedance of an antenna system in the field, when all he had was a portable transmitter and an ASTU.

Carefully tune the power amplifier to deliver maximum available design power to the reference load impedance of 50 ohms. Next, using the setup shown in **Figure 2**, carefully tune the ASTU for maximum power delivered to the mismatched load using an in-line bi-directional coupler on the short length of coax connecting the ASTU to the power amplifier. This tuning maximizes the forward directed power and minimizes the reflected power. Next, disconnect the ASTU from the power amplifier and measure the impedance with an impedance bridge or impedance analyzer, looking into the input port of the ASTU with the antenna system connected. The input impedance will be 50 ohms. Now, connect a 50-ohm load to the input port of the ASTU, and measure the impedance looking back into the output port of the ASTU and then the impedance looking forward into the transmission line. These impedances will be almost exactly complex conjugate impedances. We would expect this under conjugate matched conditions, because this is how an ASTU works.

What have we learned? Those who don't hold our view on the conjugate match would say that this experiment tells us nothing about source impedance and, consequently, nothing about conjugately matching the amplifier. Their criticism rests on the fact that the SWR on a transmission line (or in one view forward and reflected power) depends only on the terminating load impedance and the impedance of the transmission line.[10] Certainly, devices like the MFJ-249 and the Autek RF-1 impedance analyzers measure SWR without reference to the impedance of the signal source. By their very design, these devices measure SWR with reference to 50 ohms. We could certainly use an instrument of this type to tune the ASTU for a 50-ohm match. It would be possible to connect the tuned antenna system to our HFTPA, which had been previously tuned using a 50-ohm load. As a result, we would find that, because the PA sees its design load, it will deliver design power. Thus, where's the reference to source impedance?

What one concludes from the experiment likely depends upon his point of view. We are not measuring SWR per se, we are matching for maximum power transfer. The fact that the directional coupler power meter we use for the experiment may have a built-in reference impedance is coincidental concerning our interpretation of this experiment. Bill Sabin, WØIYH, offers a bit of perspective regarding forward and reflected power in his article concerning an analysis of directional couplers.[11] We paraphrase it here, in accordance with our view: "If a classical generator (in our case we have a RF power amplifier) with output impedance Z_{out} 'sees' a load that is not equal to Z_{out}, a mismatch occurs, meaning that the maximum available power is not transferred from the generator to the load." Therefore, when we tune our ASTU for a maximum forward power out, and zero reflected power looking into the input of the ASTU, we are in effect conjugately matching the power amplifier to the load. The reason there is no reflected power at the ASTU input is because the load (the antenna system) is also conjugately matched.

Again, from Sabin: "In the directed power wave point of view, we say that the forward wave is what the generator 'tries' to send to the load. The mismatch loss is the fraction of available power that is not accepted by the load but is returned (reflected) from the load back to the source. The difference between forward and reflected wave power is equal to the power that is actually accepted by the load. It is also equal to the power that is actually delivered by the generator (the amplifier in our case). These two different points of view are numerically identical; they are two different ways of saying the same thing."

It doesn't matter whether we tune the ASTU so we see 50 ohms looking into the input port of the ASTU with an SWR analyzer; whether we tune for maximum forward power, which corresponds to a minimum reflected power,

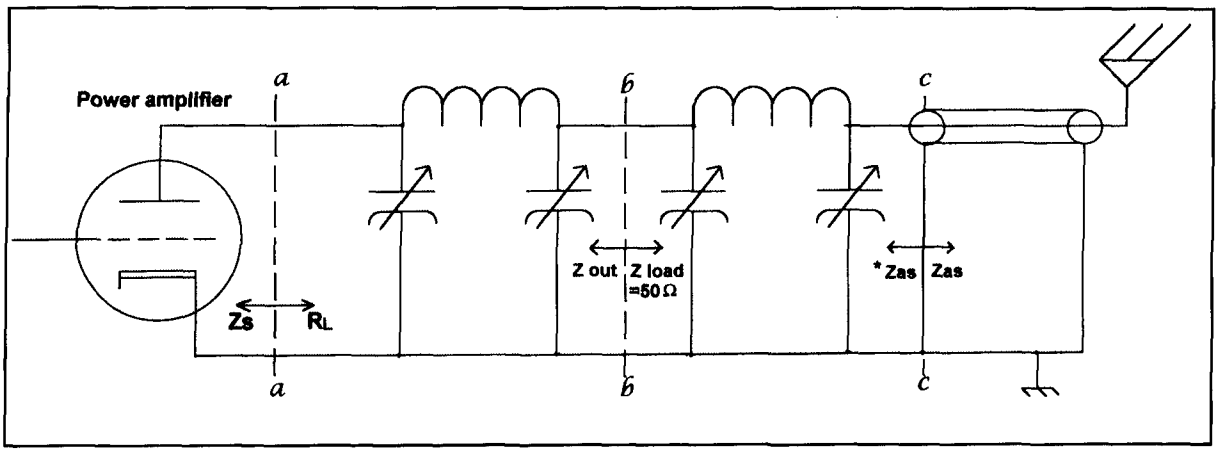

Figure 2. Sketch of an RF power amplifier used with an antenna system tuning unit to match a mismatched antenna system.

using an in-line, bi-directional coupler; or whether we tune for maximum power delivered to the load using a RF current meter connected anywhere on the antenna system. We will find that we have tuned for a 50-ohm match in each case. Why? Where is the 50-ohm reference in this latter case? The 50-ohm reference is the 50-ohm load sitting on the work bench, and the power amplifier. The HFTPA was first tuned to deliver its maximum available power using this reference load. Where is the 50-ohm reference in the power amplifier? We have tuned the HFTPA so when it sees a 50-ohm load it sees its optimum load impedance. Hence, when connected to the antenna system, and when the antenna system is correctly tuned so the HFTPA delivers its maximum available design power, it is looking into a 50-ohm matched antenna system. The instantaneous values of the fundamental RF plate current and voltage over the RF cycle are then identical to what they were when we tuned the amplifier looking into the reference 50-ohm load. The HFTPA sees its design load impedance, and its output impedance is therefore 50 ohms.

There's nothing special about 50 ohms. We could have tuned the π-network tank circuit of our PA to deliver maximum available design power into a 25- or a 100-ohm, or any other reasonable reference load. When we tuned our ASTU for maximum power delivered to the load, we would find we had tuned the ASTU so, looking into its input port, we would see 25- or 100 ohms. Those who say that the output impedance of the power amplifier doesn't matter are wrong. The output impedance is of *fundamental* importance, as this is the impedance to which we conjugately match for achieving maximum available power transfer to the load.

In our opinion, it follows from the above experiment that, because the antenna system is conjugately matched at the output port of the ASTU as we observed, there is a conjugate match at the input port of the ASTU. In fact, there's a conjugate match everywhere in the system. Therefore, when the ASTU has been adjusted for maximum forward power, because the HFTPA has been adjusted to deliver all its available power into a 50-ohm load, the amplifier "sees" a 50-ohm load looking into the antenna system. And, because the power amplifier is a part of the conjugately matched system, it too is conjugately matched. Consequently, there is a conjugate match at the output terminals of the power amplifier, so there must be a conjugate match at the input to the tank circuit. Why? Because these terminals are also a part of the totally conjugately matched system.

Let's digress for a moment to consider a relevant issue—transmission line losses. The matching network transforms the source impedance to the complex conjugate of the load impedance and visa versa. Thus a conjugate match exists at the input to the antenna system, and for a lossless transmission line, a conjugate match exists at any point on the transmission line. Consequently, a conjugate match is found at the antenna end of the transmission line.

Those who like using modern computer analysis programs, can try the following exercise. Calculate the input impedance of a nonresonant dipole antenna using the electromagnetic antenna analysis program NEC-2 (EZNEC or NEC-Wires versions). Next, connect an open wire lossless transmission line to the antenna, and calculate the antenna system input impedance (Z_{as}) using, for example, the ARRL transmission line program TL.EXE. Now, connect a load Z_{as}* that is the complex conjugate of Z_{as} to the input terminals (transmitter end) of the transmission line, and calculate the impedance at the antenna end of the transmission line. You'll find this impedance is exactly the complex conjugate of the dipole's impedance, Z_D.

Now introduce a bit of loss; that is, suppose

the transmission line is made of #12 copper wire, and repeat the exercise. This will provide a new value of Z_{as}, say Z_{as}'. The impedance calculated at the antenna end of the transmission line terminated in the complex conjugate of Z_{as}' will be now be approximately the complex conjugate of the dipole's impedance. Specifically, the real part of the impedance looking back into the transmission line terminated in the complex conjugate of Z_{as}' will be greater than the real part of the dipole's impedance because, in effect, we have translated impedances twice through a transmission line with loss—albeit a small loss. And, the power loss on the transmission line will be greater than it would be if the ASTU had been installed at the antenna end of the transmission line.

Measuring mismatch loss

Our third experiment was performed by W2DU, who recently made accurate measurements of mismatch loss on PAs. Before we discuss his findings, let's review what textbooks tell us about mismatch loss. Chipman[12] and Smith[13] have discussed reflection loss in numerical detail. Consider an HFTPA that's tuned and conjugately matched to work with its design load. The amplifier is connected to the load through a length of transmission line, but the length of the line is unimportant.

If only the load impedance is changed, so a mismatch occurs between the transmission line's characteristic impedance and the load, there will be a reduction of power delivered to the load. The reduction in load power as the load impedance changes is a measure of the reflection loss. Under a mismatched load condition, the PA will deliver less power to the transmission line. The reduction of power introduced to the transmission line at the HFTPA end is the same as the reflection loss in the load. In other words, the reflection loss at the load can be referred back along the transmission line to HFTPA terminals. Reflection loss

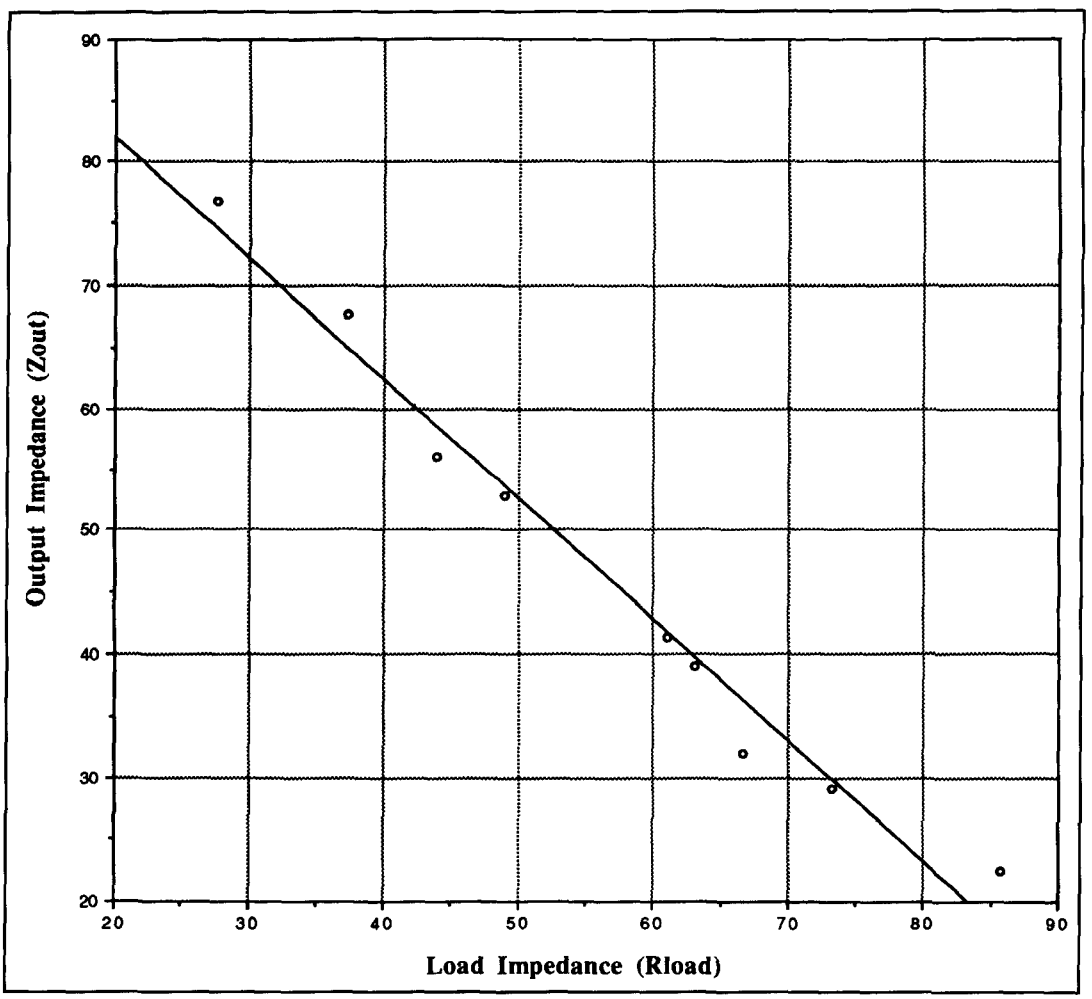

Figure 3. Measured output impedance Z_{out} of an operating Class B amplifier versus load impedance (R_{load} a non-inductive load). See text for detail on how Z_{out} was measured.

is a nondissipative type of loss representing only the unavailability of power to the line due to the mismatch of impedances, in this case between the HFTPA and the transmission line, resulting from the load mismatch being referred back along the line to the source.

Although the power delivered by the source to the transmission line is reduced by the amount of the reflected power returning to the input terminals of the source (in agreement with the principle of energy conservation to the multiply reflected wave model of the system), the implication that the reflected wave power is entirely absorbed in the source impedance without affecting the total output of the signal source generator is incorrect. If a matching network is placed at any point between the generator and the load to provide a conjugate match of impedances, as seen in either direction at the point of its insertion, then the reflection loss may be canceled by a negative reflection loss, also known as reflection gain,[13] which is introduced by the matching network. Now let's see how this applies to W2DU's measurements with a HFTPA.

Maxwell used a power amplifier under test (PAUT), an HP-8405 Vector Voltmeter and the HP-778D Dual Directional coupler, an HP-4815A RF Vector Impedance meter, a 50-ohm, 1500-watt Bird Termaline load, a Bird 43 Wattmeter, and a variable load impedance. The variable load impedance was an ASTU terminated with the 50-ohm load. By tuning the ASTU, it was possible to obtain any impedance looking into the input port.

The measurement reference was first set by adjusting the ASTU input for exactly 50 + j 0 ohms. With the Vector Voltmeter, the ASTU could be adjusted so the reflected wave was more than 40 dB below the direct wave. Maxwell then adjusted the drive level of the PAUT to deliver 100 watts into this load, with the tuning and loading controls of the PA adjusted for delivery of the maximum available power of 100 watts, as predetermined by that drive level. Next, he readjusted the ASTU to provide a range of impedance mismatch loads for the PAUT at the input of the ASTU. These (complex) impedances were obtained by adjusting the ASTU so the magnitude of the respective reflection coefficients caused the Vector Voltmeter to indicate their respective values of magnitude relative to the impedance mismatch. Before measuring the power absorbed at each value of mismatch, he measured the input impedance of the ASTU with the Vector Impedance Meter, and then by calculator determined that each impedance correctly agreed with the desired mismatch. All measurements of absorbed power, with the impedance mismatches measured in the experiment Maxwell conducted, agreed exactly with the theoretical values expected within the range of measurement error one would expect from Hewlett-Packard measuring equipment. That is, the decrease of absorbed power resulting from a given condition of mismatch in the loading on the RF power amplifier, relative to that absorbed with matched condition, agreed exactly with the decrease in power resulting from a similar mismatch relative to a conjugate match in which all available power is delivered and absorbed. It follows that the RF power amplifier is conjugately matched to its load when delivering all of its available power.

Direct measurements of output impedance

The following experiments provide a direct measure of the output impedance of an operating amplifier.

First, Bill Sabin, WØIYH, has derived an expression that he believes provides a direct measure of the true value of Z_{out} of an operating amplifier (refer to **Reference 8**, his **Equation 8**). In Sabin's model, the circuit analyzed is an impedance, Z_s, and is in series with the load impedance, R_L. Thus, by changing the load impedance and measuring the change in voltage across R_L and the change in current through R_L, for the two values of R_L, one can determine the source impedance Z_s from the expression:

$$Zs \approx \frac{V_{out}(2) - V_{out}(1)}{\frac{V_{out}(1)}{R_L(1)} - \frac{V_{out}(2)}{R_L(2)}} \quad (4)$$

$$= \frac{V_{out}(2) - V_{out}(1)}{I_{out}(1) - I_{out}(2)} \quad (5)$$

In Sabin's model, V_{out} would be measured across load impedance R_L, and I_{out} is the current through R_L.

In our fourth experiment, using Sabin's model, Maxwell measured the RMS voltage across an external load impedance R_{load} for various values of R_{load}, corresponding to impedance mismatches of < 2:1. The tank circuit for the power source (a Kenwood TS-830S with a pair of 6146s and a π-network tank circuit) was tuned and loaded with a drive level set to deliver the maximum available power of 100 watts into the matched load—a Bird Termaline 1500-watt load, with an impedance of 53.1 + j 0 ohms. No further adjustment of the Kenwood was made during measurements with various values of R_{load}. All values of R_{load}

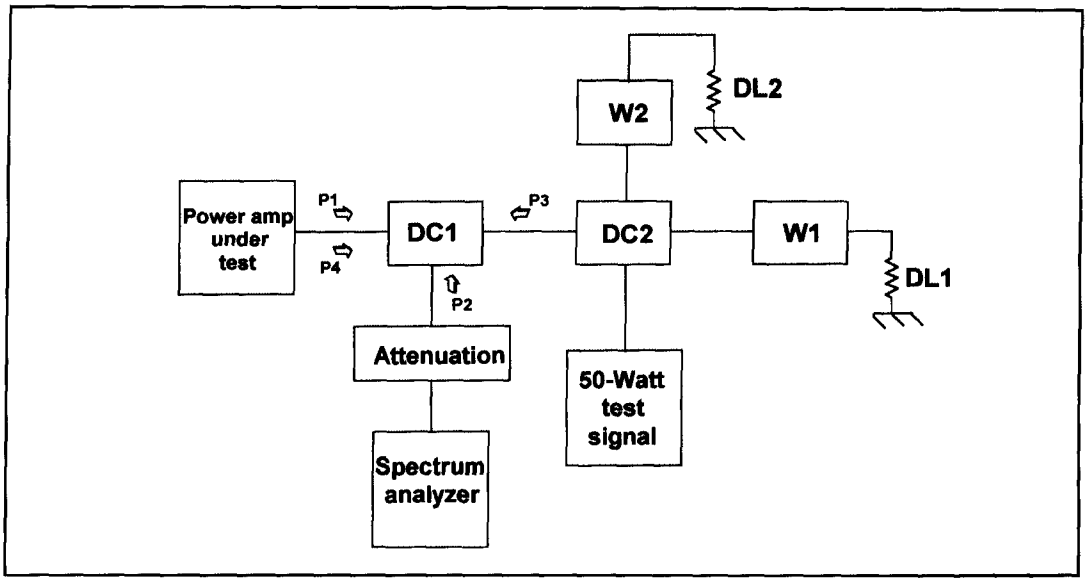

Figure 4. Test setup for measuring the output impedance of an operating RF power amplifier devised by Bruene.[13]

were noninductive resistances, R + j 0. Values of R_{load} were measured with an HP-8405A Vector Voltmeter and HP-778D Dual Directional coupler. Values of V_{load}, the RMS voltage across the load, were measured with an HP-410B RF Voltmeter and an HP-455A Coaxial Adapter. The results of this experiment are shown in **Figure 3**. Note that $Z_{out} = R_{load} = 51.3$ ohms. For R_{load} values less than this value, Z_{out} increases; for R_{load} values greater than this value, Z_{out} decreases.

The plate current, I_P, with the matched load was 260 mA. Plate current I_P with the lowest value of R_{load} was 280 mA; and I_p with the highest value of R_{load} was 210 mA. With equal mismatches of 1.66:1, the power delivered was the same for R_{load} high and R_{load} low. However, the plate current I_P for R_{load} high was lower than with matched conditions, and I_P for R_{load} low was higher than with matched conditions. Consequently, the efficiency was greater for higher R_{load} than for lower R_{load}. More on this later.

Note that application of Sabin's equation to determine the source impedance was intended for small changes in load impedance with respect to the matched value that permits delivery of all available power. Small differences in voltage and current at the load require high-accuracy measurements. To obtain the required accuracy, Maxwell modified the HP-410B RF Voltmeter to provide digital readout. Continuing the experiment with digital accuracy, he measured the RMS voltage across noninductive resistances. The values were only slightly different from the 53.1-ohm reference load, into which the amplifier was first adjusted to deliver 100 watts of maximum available power. In each case, again using Sabin's model, the source impedance of the amplifier was determined to be 53 ohms within measurement accuracy.

Maxwell repeated the experiment with reference loads of 25 and 75 ohms, respectively. With the above measurement accuracy, in each of these cases, the source impedance of the amplifier was determined to be 25 ohms when adjusted to deliver the available power into the 25-ohm reference load, and 75 ohms when adjusted to deliver available power into the 75-ohm reference load. However, large changes in load impedance (mismatches up to 2:1) show a systematic change (see **Figure 3**) providing further assurance that the source impedance for matched conditions can be measured very accurately. It is interesting to note that (R_{load} x Z_{out})1/2 was constant for all loads, for an average value 48.1 ohms.

At this point, we feel we have proven that the output impedance and load impedance are equal under matched conditions, at least for one amplifier. But the clincher is yet to come. Our fifth, and more direct, experiment, was performed by Tom Rauch, W8JI. He repeated Bruene's experiment (see **Figure 4**). Using Bruene's method, Rauch obtained reflected power measurements similar to Bruene's. However, when Rauch tuned and loaded his PAs in the conventional manner to obtain *maximum output power with any given, fixed amount of drive,* there was a significant difference. Under Rauch's test conditions, the standing wave ratio of the signal from the reverse-power generator (RPG) was approximately 1:1, compared to Bruene's 5:1 mismatch. Thus Rauch's experiment indicates that, when the

amplifier is tuned and loaded for operation in the conventional manner, *the output impedance, Z_{out}, is close to 50 ohms, and not a value five times greater.*

So why the difference between Bruene's initial measurements and ours? Were the directional couplers causing the discrepancy? To resolve this concern, Rauch devised a simple technique—our sixth experiment—that required less equipment and yielded a more direct result (see **Figure 5**). This test method uses the well-known properties of voltage distribution along a transmission line operating with standing waves. Unlike the directional coupler experiment, Rauch's new method allowed measurement of the *direction* of resistance change, as well as the *amount* of change. It was also totally free from the power limitations and potential inaccuracies that sometimes accompany ferrite cores when used in impedance and linearity critical high power system applications.

Rauch's improved test procedure involved feeding a small reverse generator signal into an operating amplifier via a high power attenuator, and measuring the reverse generator's voltage level along a 50-ohm transmission line. This test once again agreed with the results W8JI obtained using the test setup identical to that of Bruene's, but the new test's ability to determine the direction of change resulted in conclusions very much contrary to Bruene's earlier measurements.[9]

To measure standing waves, Rauch series-connected 1/16, 1/8, and 3/16 wavelength line sections. Tee connector access points were installed at each line section, the power amplifier under test port, and the 30-dB, 5 kW, 50-ohm attenuator. By connecting a bridging pad (an "L" pad with a 50-ohm output and 10,000-ohm source resistor) to any of the tee connectors, a sample of the voltage on the 50-ohm transmission line could be measured. Either a frequency-selective level meter or a spectrum analyzer was used to measure the voltages on the line. If the 200-watt Class-A RPG (attenuated by 30 dB, as it was feeding power in the reverse direction through the attenuator/load) was looking into 50 ohms (the output impedance of the PAUT), there would be no RPG voltage differences anywhere along the 50-ohm line. If there were voltage differences between the tee connectors, the effective output impedance of the PAUT wouldn't have been 50 ohms. If the voltage was higher at the PAUT output port, this would absolutely indicate the PAUT's output impedance was higher than 50 ohms—a conclusion impossible to verify with Bruene's directional coupler measurements.

Rauch's measurements revealed that, for some 14 amplifiers of widely varying types, maximum efficiency could be obtained by "tuning" the output network by solely observing the reverse mismatch change. As the tank network was adjusted to present a 50-ohm load to the reverse power generator (reverse generator voltage equal at every point along the 50 ohm line), maximum efficiency and output power was obtained. As a matter of record, Rauch noted it was much more difficult to obtain optimum efficiency using the meters on the amplifier and the power output indicator than it was by watching the mismatch for the reverse power generator (RPG).

When the reverse generator method was used to "look back" into any of the amplifiers tested at the power where they were peaked (tuned for maximum output power with a fixed amount of drive), all amplifiers exhibited an output impedance very close to 50 ohms (mismatch for the RPG a minimum). When the drive was reduced, the effective output impedance for the amplifier changed—except for Class A amplifiers, where there was no change at all. Class C amplifiers changed the most, and Class B amplifiers were somewhere in between. In all cases, the output port impedance increased (as indicated by higher RPG voltage at the PA out-

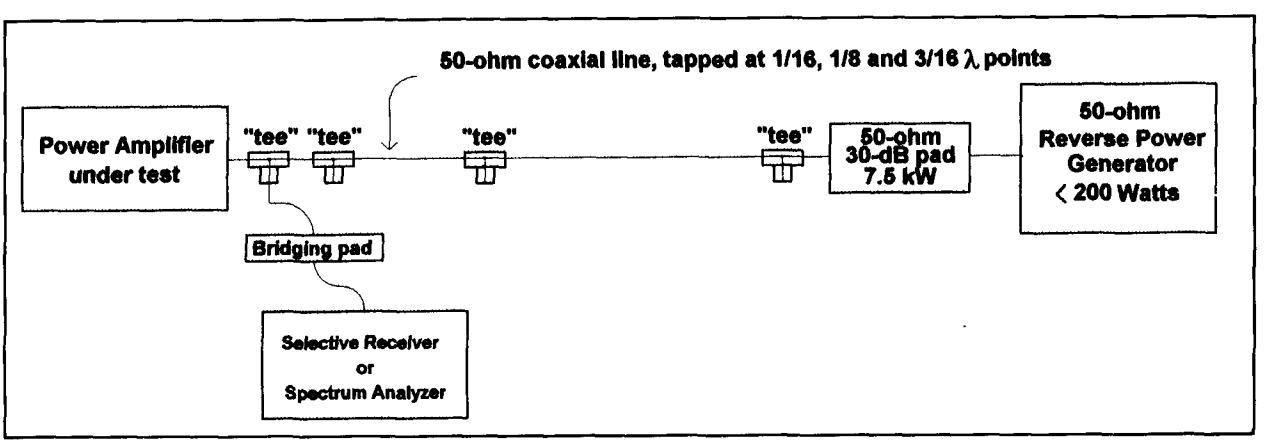

Figure 5. Test setup to measure the output impedance of an operating RF power amplifier, devised by W8JI.

put port, and lowest voltage 1/4 π closer to the RPG) as drive power was reduced. This held true for solid-state and vacuum tube PAs, with the exception of a KWM-2. The KWM-2 followed the same pattern in the "tune" position, but in the lock position it remained relatively stable in impedance and was very close to 50 ohms when properly adjusted.

With reduced drive, efficiency normally dropped. However, the amplifiers could be retuned with minor readjustment to minimize reflected power for the RPG, and efficiency was restored to the highest value possible for that particular drive level. Rauch also found plate efficiency rolled off faster if R_L was less than the conjugate value of the operating impedance (the plate current goes up), than it did when R_L was greater than the conjugate value of the operating impedance. Class C amplifiers had the largest non-symmetry in roll off, while Class A amplifiers appeared very symmetrical. In fact, Rauch noted that minimizing the reflected power for the RPG proved a perfect way to adjust every amplifier he tested for maximum efficiency and output power at a given grid drive level.

In one example, a pair of 6146Bs were operated with -150 volts of control grid bias, with third harmonic resonators in the anode and grid circuits to square the tube's anode current and voltage. In this configuration, the 6146s provided 83 percent efficiency with careful tank adjustment while comparing output power and plate input power. Unfortunately, using the output power meter and anode power measurements to obtain peak efficiency was both laborious and time consuming.

The same efficiency was obtained without complex input power-to-output power comparisons by simply measuring and adjusting the tank in order to provide a dynamic source impedance (looking back into the PA output port) of 50 ohms. There is little doubt that this proves that the dynamic operating source impedance is the conjugate of load impedance whenever the tank is tuned for maximum power transfer and efficiency with a fixed amount of control grid drive.

This second method confirmed earlier measurements down to the smallest detail. When the PAUT was tuned and operated at or near the optimum point for plate efficiency and output power, its output impedance, as seen by looking back into all the various power amplifiers tested, was very close to 50 ohms.

More on a measure of complex conjugate impedances

In a seventh experiment, Rauch tuned the Class C power amplifier using two 6146 tubes for maximum power into a 50 + j 50 ohm load. The load was the 30-dB attenuator (the setup was as in **Figure 5**) with a small inductor pruned to be + j 50 ohms at 7 MHz, connected in series at the junction of the attenuator and the tapped line. For this experiment, maximum output power and efficiency occurred with reverse generator standing waves on the line.

Next, after tuning the amplifier for maximum power output into a 50-ohm load, the impedance looking into the output port of the now "cold" amplifier was measured. At the same time, anode load components (a small variable capacitor and a series variable resistance) were adjusted to find the value of the anode termination impedance required to make the RF output port appear as 50 ohms, when measured using a network analyzer. The anode load components were then put aside, while the experiment continued.

Finally, the 50-ohm reactance inductor was re-connected in series with the output port of the amplifier. The amplifier was again readjusted for maximum power output (once again indicating some standing waves on the RPG. Upon removing all connections from the amplifier output port and reinstalling the untouched anode load, the measured impedance with a network analyzer looking back into the output port was indeed 50 - j 50 ohms—a complex conjugate match. When a 50 - j 50 ohm load replaced the PAUT, the RPG voltages along the line were exactly the same values measured with the real operating PAUT.

This final test indicates maximum power transfer and efficiency are obtained when the PA dynamic impedance and load impedances are complex conjugates of each other.

Discussion

Let's examine the basis for Bruene's position that RF power amplifiers are not conjugately matched to their loads. First, we need to clarify differences in terminology. We use Z_s to represent the source, or output, *impedance* of the amplifier. Bruene uses R_s to represent what he calls the source "resistance," a term we find inappropriate to represent a source of power. Load impedance R_L has been universally accepted as the correct means to obtain the proper loading provided by the input of the tank circuit. And, as we explained earlier, $Z_s = R_L$. However, according to Bruene, the nature of the source resistance is determined from an entirely different expression, one which we believe to be associated with the determination of the plate resistance of *Class A* amplifiers. In **Reference 14**, he says the tube "output resistance" is determined by the effective plate resistance R_{PE} over the RF cycle and by feed-

back. R_{PE} can be determined from the anode-current characteristic curves with constant grid voltage for the tube:

$$R_{PE} = 2\frac{\Delta E}{\Delta I} \quad (6)$$

Bruene also states that, although R_s is typically at least five times the normal plate load impedance R_L,[14,15] the actual tube output (source) "resistance" (his terminology) R_s is $< R_{PE}$ after being modified by feedback. Consequently, in typical power amplifiers that use no feedback, $R_s = R_{PE}$. Although Bruene's R_s is a dynamic resistance, we believe it is unrelated to the dynamic (operating) output impedance he should have been measuring in the experiment initially described[9].

We consider an output source resistance (Bruene's terminology) five times the value of R_L fundamentally unacceptable as the source impedance for delivering power to load R_L. It seems that, if the mismatch (SWR using Bruene's language) between the source and load impedance is 5:1, there can be no efficient transfer of power. But, in his November 1991 QST article,[9] Bruene states that, for a conjugate match to exist, R_L must equal R_s. This isn't true because Z_s is the source impedance, not (his) R_s. However, there is a conjugate match whenever the actual load is equal to the optimum load impedance R_L, because all available power is delivered when the load resistance equals the source impedance Z_s.

In our opinion, Bruene's R_s has no relation to the true source impedance, Z_s. *Consequently, we believe the basis for his position claiming there can be no conjugate match of impedances between an RF power amplifier and its load is invalid.* In addition, as we discussed earlier, any equivalent circuit for the amplifier that doesn't include the tank circuit is incomplete, because the true source impedance of an RF power amplifier is fundamentally dependent on the flywheel action of the tank circuit and the resulting fundamental RF AC voltage and current associated with the tank. But Bruene's expression for the source impedance fails to address or include the tank circuit, or the fundamental RF AC voltage and current associated with it, and his expression more closely resembles the method for determining the plate resistance of a Class A amplifier.

We have problems with what Bruene thought he measured, and with his different parameter measurement techniques. In **Reference 9**, he described an experiment that permits one to "look back" into an operating amplifier. In **Reference 15**, he states that "if we look back into the output network from the coax output terminals (with the amplifier turned on but no RF drive power applied), we would measure a high SWR, as previously reported." But the previously reported experiment[9] involved an ***operating amplifier***.

In our opinion, looking back into an operating amplifier, one measures the output impedance of the amplifier—the impedance attributable to the conversion of power from the DC of the power supply to the AC RF delivered to the load.

Finally, there are some who say that the conjugate match may be possible, but not always advisable. We don't claim a conjugate match is mandatory. Amplifiers that aren't conjugately matched can be adjusted to deliver required power to the load, but at the expense of efficiency. There are various special-purpose amplifiers, like broadband amplifiers—untuned amplifiers where the only tuning is the antenna system, and the amplifier is designed to provide a fixed current into the antenna system regardless of the mismatch, determined only by the KVA-to-output power ratio for the amplifier.

VLF/LF transmitters, which are normally operated into narrow band antenna systems, are designed with bandwidth as a most important consideration. Methods have been devised by amplifier design to realize this, as well as to measure the operating dynamic bandwidth of VLF systems.[16] But this topic, and a consideration of special purpose amplifier designs, is beyond the scope of this paper. We are concerned with typical HF tuned power amplifiers commonly used by the radio amateur and by HF communicators.

In conclusion

This article has been drafted and redrafted more times then we care to remember, and discussion has continued to the present time. However, in our opinion, the only conclusion we can reach from the above information concerning the applicability of the concepts of maximum power transfer and conjugate match, is that if the amplifier looks like it is conjugately matched, and if it behaves as if it is conjugately matched, then it is conjugately matched. All HF tuned power amplifiers used by radio amateurs, and some commercial amplifiers as well (we tested more than 17 in all), behaved as if they were conjugately matched when tuned and loaded to deliver all of their available power with plate voltage and drive level within the manufacturer's recommended ratings.

For the radio amateur, we match to the output impedance of the power amplifier, typically $Z_{out} = 50$ ohms. And, when we correctly load the amplifier with the antenna system connected, we are, in effect, tuning the output networks for a conjugate match. The concepts of maxi-

mum power transfer and conjugate match are particularly useful because this point of view provides an insight into how power amplifiers work, into the tuning of the amplifier's tank circuit, and into how an antenna system tuning unit functions in order to match a mismatched antenna system to the design load impedance for the power amplifier.

We therefore conclude that material written by Walter Maxwell, W2DU, that appeared in the *1986-1994 ARRL Handbook* and *ARRL Antenna Book*, and in the ARRL book by Maxwell[17] relating to complex conjugate match *is not in error, contrary to Bruene's statements.*[9] We further conclude that statements made by Jon Bloom, KE3Z, in his QEX article,[18] which contradict the principles of wave mechanics in relation to impedance matching, as explained in Maxwell's book, are in error.

The history of the RF power amplifier design and the concept of maximum power transfer and conjugate matching was first addressed more than 60 years ago (reference, for example, the classic texts/papers by Everitt and Anner[19] and more recently by Beatty[20]). It's interesting to read in the introduction to Beatty's 1964 paper: "...certain other concepts connected with insertion loss such as attenuation and mismatch loss are in need of clarification." Clearly the concept of RF amplifiers and conjugate match is also one that needs clarification. We hope that we have done so.

Acknowledgment

Thanks in particular to Dr. John Fakan, KB8MU, and Professors Dr. Albert Helfrick, K2BLA, Réal Gagné, and Zdenka Zivovic-Dzunja (now deceased); and to Peder Hansen, Fred Telewski, WA7TZY, Steve Katz, WB2WIK/6, Bob Haviland, W4MB, Wes Stewart, N7WS, Warren Amfahr, WØWL, Peter Onnigian, W6QEU; and Professor's Tony Ferraro, K3CJ, and Dennis Roddy; and others, who provided cogent comment and/or encouragement during the preparation of this article.

I also wish to thank co-authors Dr. John (Jack) Belrose, VE2CV, and Tom Rauch, W8JI, for their extraordinary support and assistance in bringing out the truth concerning conjugate matching, re-establishing the validity of my previous writings. To Tom, especially for performing the experiments that supplied the proofs, and to Jack, especially for the laborious and futile task of communicating and corresponding endlessly with our opponents.

The views expressed here are those of the authors.—W2DU

REFERENCES

1. F.E. Terman and W.C. Roake, "Calculation and Design of Class-C Amplifiers," *Proceedings of the IRE*, 24, April 1936, pages 620-632. See also Terman's *Radio Engineers' Handbook*, McGraw Hill, 1943, pages 444–454.

2. I.E. Mouromtseff and H.N. Kozanowski, "Analysis of the Operation of Vacuum Tubes as Class C Amplifiers," *Proceedings of the IRE*, 23, July 1935, pages 752–778.

3. J.P. Heyboer and P. Zijlstra, "Transmitting Valves: The Use of Pentodes, Tetrodes and Triodes in Transmitting Circuits," Phillips Technical Library, 1951.

4. Z. Zivkovic-Dzunja, "Software Program "DOKT" for Analyzing a High Power Tuned Amplifier," *IEEE Transactions on BC*, 40, September 1994, pages 190–198.

5. S. Kostic, V. Dragan, and Z. Zivkovic-Dzunja, "PSpice Analysis of High Power Tuned Amplifier and Comparison with Related Methods," *IEEE Transactions on BC*, 41, December 1995, pages 153–157.

6. M. Silverberg and O. Wing, "Time Domain Solutions for Networks Containing Lumped Nonlinear Networks," *IEEE Transactions on Circuit Theory*, September 1968, pages 292–294.

7. P. Bouchard and R.R.J. Gagne, "Transient Analysis of Lossy Parabolic Transmission Lines with Nonlinear Loads," *IEEE Transactions on Microwave Theory and Techniques*, 43, June 1995, pages 1330–1334.

8. W.E. Sabin, "Dynamic Resistance in RF Design," *QEX*, September 1995, pages 13–18.

9. W. Bruene, "RF Power Amplifiers and the Conjugate Match," *QST*, November 1991, pages 31–33. See also "Rs and the Conjugate Match," *QST*, "Technical Correspondence," May 1992, page 95

10. W.E. Sabin, "Computer Modeling of Coax Cable Circuits," *QEX*, August 1996, pages 3–10 (esp. 8).

11. W.E. Sabin, "The Lumped-Element Directional Coupler," *QEX*, March 1995, pages 3–11.

12. R.A. Chipman, "Theory and Problems of Transmission Lines," *Schaum's Outline Series*, McGraw-Hill, Section 9.10, pages 202–205 (especially 204 and 205).

13. P.H. Smith, *Electronic Applications of the Smith Chart*, McGraw-Hill, Section 4.1.3: Reflection Loss, page 37.

14. W. Bruene, Chapter 14, "High-Power Linear Amplifiers," *Single Sideband Systems and Circuits*, 2nd edition, W.E. Sabin, and E.O. Schoenike, editors, McGraw-Hill, 1995, pages 573–581.

15. W. Bruene, "Inside the Grounded-Grid Linear Amplifier," *QST*, October 1993, pages 28–30.

16. M.H. Harrington, "A dynamic bandwidth and phase linearity measurement technique for 4-channel MSK VLF antenna systems," AGARD Conference Proceedings 529, ELF/VLF/LF Radio Propagation and Systems Aspects, May 1993, pages 20-1–20-8.

17. W. Maxwell, *Reflections-Transmission Lines and Antennas*, American Radio Relay League, 1990.

18. J. Bloom, "Where Does the Power Go?," *QEX*, December 1995, pages 17–20.

19. W.L. Everitt and G.E. Anner, *Communications Engineering*," 3rd edition, McGraw Hill Book Co., New York, 1956, p. 408. Note that the same text appears in the 2nd edition (W.L. Everitt is the sole author), published in 1937, pages 243–244.

20. R.W. Beatty, "Insertion Loss," *Proceedings of the IEEE, 52*, June 1964, pages 663–671; and by the same author, "Microwave Mismatch Analysis," Hewlett-Packard Application Note 56, October 1967.

Parker R. Cope, *W2GOM/7*
8040 E. Tranquil Blvd.
Prescott Valley, Arizona 86314

JFET SIMPLIFIED

Demystifying JFET Self-Biasing

Biasing the Junction Field Effect Transistor (JFET) with a source resistor may seem like an exercise in "cut and try," but it needn't be. If you're familiar with vacuum tubes, it's just a small step to using JFETs. Some wag once said that a vacuum tube is just an n-channel depletion mode FET with a light in it to tell you when it's good. If you find tubes equally mystifying, don't despair. Help is on the way.

JFETs are voltage-operated devices: the output (drain) current is a function of the input (gate) voltage. Its input impedance is very high. A Bipolar Junction Transistor (BJT) is a current-operated device: the output (collector) current is a function of its input (base) current. The BJT's input impedance is low, but not zero. The input impedance of a JFET is many megohms at DC and can be realistically considered an open circuit. However, with AC signals, the input appears as a capacitor comprised of two parts: the gate-to-source capacitance, C_{iss}, typically under 10 pF; and the gate-to-drain capacitance, C_{rss}, typically about half of the gate-source capacitance. The gate-drain capacitance is multiplied by the "Miller effect," which is a function of the amplifier's gain. The input capacitance can be expressed as:

$$C_{in} = C_{iss} + C_{rss} \times (1 + A \times \text{Cos } B) \qquad (1)$$

where:

C_{iss} is the gate to source capacitance
C_{rss} is the gate to drain capacitance
A is the voltage gain of the amplifier
B is the phase angle between the input and output signals

The phase shift between the input and output of an untuned amplifier is nominally 180 degrees and the Cosine is -1. The input capacity then is:

$$C_{in} = C_{iss} + C_{rss} \times (1\text{-}A) \qquad (2)$$

The input impedance is very high for all JFETs and can be ignored when determining the DC operating point, the DC gate-source voltage V_{gs}, the drain current I_d, and drain source voltage V_d. The drain current for a particular V_{gs} and the change in output current for a change in input voltage (the forward transconductance, g_{fs}), is the chief electrical difference between devices. Some device data sheets give only the minimum g_{fs}, and the gate-source voltage needed to reduce the drain current to zero. V_{off}, is also very broadly provided, or just given as a maximum. But these values are critical to obtaining some desired performance from the devices. Even though the data sheets only indicate a ballpark figure for the parameter, simple tests in a following paragraph can determine the parameter values for a particular device.

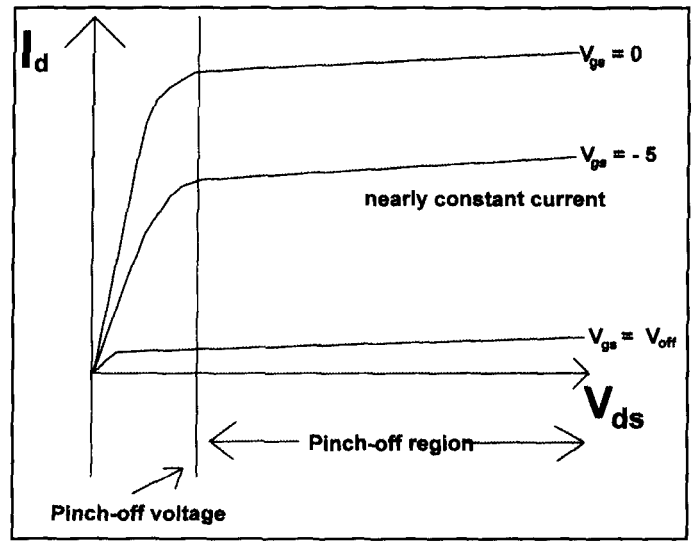

Figure 1. Output characteristics of a typical N-channel JFET.

In the design of an amplifier, the voltage gain is the feature of interest. Because the input impedance is essentially infinite, the input power is zero, and the power gain is infinite.

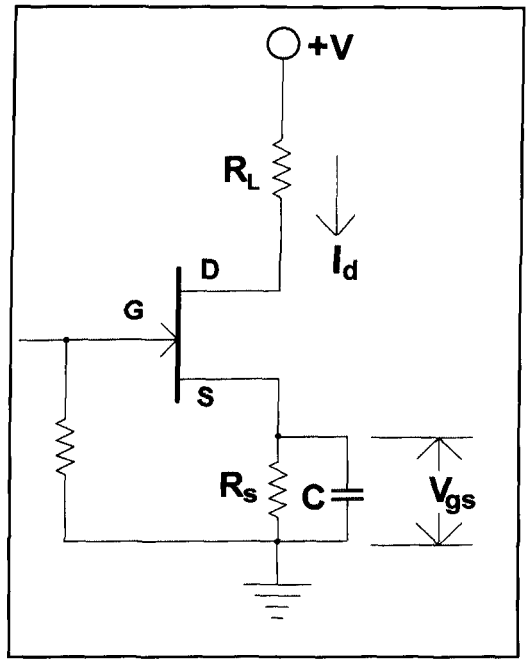

Figure 2. A JFET amplifier can be self-biased.

The voltage gain of a common-source amplifier man be expressed as:

$$VG = g_{fs} \times R_l \quad (3)$$

where:

R_l is the drain resistor in ohms
g_{fs} is the change in drain current for a change in gate voltage.

The voltage gain of a common-drain (source follower) can be expressed as:

$$VG = g_{fs} \times R_s / (g_{fs} \times R_s + 1) \quad (4)$$

where: R_s is the resistance in the source

The source follower is often said to have a gain of one, but that's only approximately true when $g_{fs} \times R_s$ is much greater than one. The source follower always has a voltage gain of less than one; however, the common-source amplifier can, and usually does, have a gain greater than one.

The gain of a JFET amplifier is dependent on g_{fs}, and g_{fs} is strongly dependent on drain current—g_{fs} is not a constant. Drain current specifications are usually quite wide, five or 10 to one is common, and are inadequate for detailed design. The relationship between gate voltage and drain current can be expressed as:

$$I_d = I_{dss} \times (1 - V_{gs}/V_{off})^{n} \quad (5)$$

where:

I_{dss} is the drain current when V_{gs} is zero
V_{gs} is the gate to source voltage for a particular I_d
V_{off} is the gate-source voltage necessary to reduce I_d to zero.
n = 2 for most JFET geometries, although some texts give values as low as 1.5

The forward transconductance g_{fs} can be expressed as:

$$g_{fs} = nxI_d/(V_{gs} - V_{off}) = 2 \times I_d]/(V_{gs} - V_{off}) \quad (6)$$

The values for I_{dss}, V_{off}, and g_{fs} can be easily determined empirically with simple test equipment: a DC supply, a current meter, and a resistor. To determine the critical parameter values for an n-channel JFET, the following procedures can be used:

(1) Connect the JFET to a suitable DC supply (e.g., 12 volts), with a source resistor of a few thousand ohms (e.g., 2.2 k), between the source and the negative side of the supply. Connect the gate to the negative side of the source.
(2) Measure the drain current, I_d.
(3) Measure the voltage across the resistor, V_{gs}.
(4) Short the resistor and measure drain current, I_{dss}. At the expense of some loss in accuracy, the current meter can act as the short across R and read I_{dss}. (Most multimeters have a resistance of less than 30 ohms on the 10-mA range, so they are a fair short.)

Equation 5 can be rearranged to compute the value of V_{off} or V_{gs}:

$$V_{off} = V_{gs}/[1 - (I_d/I_{dss})^{0.5}] \quad (7)$$

$$V_{gs} = V_{off} \times [1 - (I_d/I_{dss})^{0.5}] \quad (8)$$

The value of V_{gs} needed to produce a particular value of I_d can be calculated with the computed value of V_{off} and the measured value of Idss. The value of g_{fs} for a particular I_d can be calculated with **Equation 6**. For n-channel FETs, I_{dss} is positive and V_{off} is negative; for p-channel FETs, I_{dss} is negative and V_{off} is positive; g_{fs} is a positive quantity for both n- and p- channel FETs.

These equations allow you to establish the parameter values of a JFET and determine the operating point and low frequency gain of an amplifier with a chosen value of Rl. The gain of a common-source amplifier can be found by substituting **Equation 5** into **Equation 2**:

$$VG = 2 \times R_l \times I_d/(V_{gs} - V_{off}) \quad (9)$$

The DC drain voltage then is:

$$V_d = V_{supply} - I_d \times R_l \quad (10)$$

The drain-source voltage should not drop below pinch-off at the peak input voltage (peak drain current). That is, the drain should stay in the constant current region where drain current is essentially independent of drain voltage (**Figure 1**). When the drain voltage is below the

pinch-off, the drain current varies with drain voltage and the dynamic drain resistance falls to a value in the range of 500 or 1000 ohms for small low-current JFETS. Pinch-off is not always given in the data sheets but it is about 2 x V_{off}.

To illustrate the process, let's determine the operating point of a 2N5458 audio amplifier operating with a 12-volt power supply. **Figure 2** shows an amplifier with self bias provided by R_s. The effects of bypassing Rs will be discussed in following paragraphs.

The device data sheets show:

V_{off} = -1.0 to -7.0
I_{dss} (mA) = 2.0 9.0, with 6.0 typical
g_{fs} (µmhos) = 1500 to 5500

Measured data:	Calculated data:
R_s = 2.3k,	V_{off} = 3.8V
V_{gs} = 2.1V	g_{fs} = 0.00105
I_{dss} = 5mA	
I_d = 0.9mA	

The JFET can be biased with a source resistance or with a fixed DC voltage on the gate. Self bias offers the advantage of a more stable operating point because of the negative DC feedback produced by the source resistance. The source resistor needed to produce a particular drain current is:

$$R_s = V_{gs}/I_d$$

which after manipulation of **Equations 5** and **6** resolves to:

$$R_s = [1 - (I_d/I_{dss})\ 0.5] \times V_{off}/I_d \qquad \textbf{(11)}$$

A bypassed source resistor has no effect on AC gain, but an unbypassed source resistor produces negative feedback for both DC and AC and reduces the amplifier gain. The gain of an amplifier with an unbypassed source resistor can be expressed as:

$$VG = g_{fs} \times R_l/(g_{fs} \times R_s + 1) \qquad \textbf{(12)}$$

For a particular DC voltage drop across Rl,

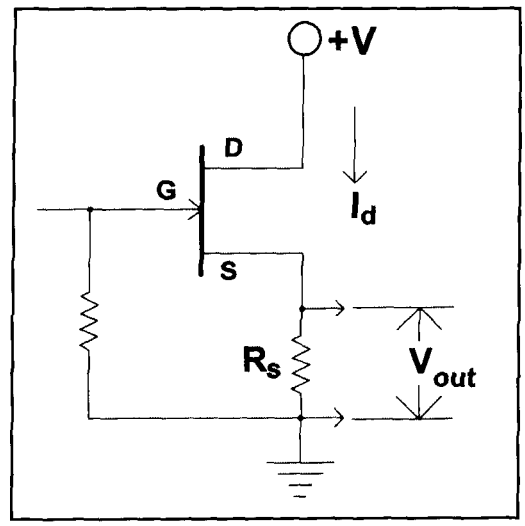

Figure 3. A source follower is self-biased.

there is a trade off between R_l and I_d. At first blush, it might seem that the lower g_{fs} resulting from low I_d would reduce the potential gain, but the higher possible R_l that can be used with lower I_d more than compensates for the reduced g_{fs}. For example, if a 5-volt drop can be tolerated across R_l, R_l can be 2, 5 k with 2 mA of drain current and g_{fs} is 0.00166 and the gain is about 4. If I_d is reduced to 0.1 mA, g_{fs} falls to 0.000370, but R_l can be increased to 50 k and the gain is about 18.

Predicting the operating point of a source-follower with a given value of Rs is a bit cumbersome (**Figure 3**), but it yields readily to a graphical solution as shown in **Figure 4A–C**. Plot the curve of the calculated values of V_{sg} and I_d and the curve of $I_d \times R_s$ for the chosen source resistance. The intersection of the two curves is the operating point. **Table 1** below shows the calculated values of I_d and V_{gs} and the corresponding values of R_s, g_{fs}, and voltage gain.

From a table similar to **Table 1**, the region to

Table I. Calculated Values of I_d and V_{gs} and Corresponding Values of R_s, g_{fs}, and Voltage Gain

Id (mA)	Vgs	Rs (ohms)	gfs	VG
4.50	0.20	43	0.00250	0.11
4.00	0.40	100	0.00235	0.20
3.50	0.62	177		
3.00	0.86	285		
2.50	1.11	445	0.00186	0.42
2.00	1.40	698	0.00166	0.54
1.50	1.72	1146		
1.00	2.10	2100		
0.5	2.60	5200		
0.1	3.26	32600	0.000370	0.92

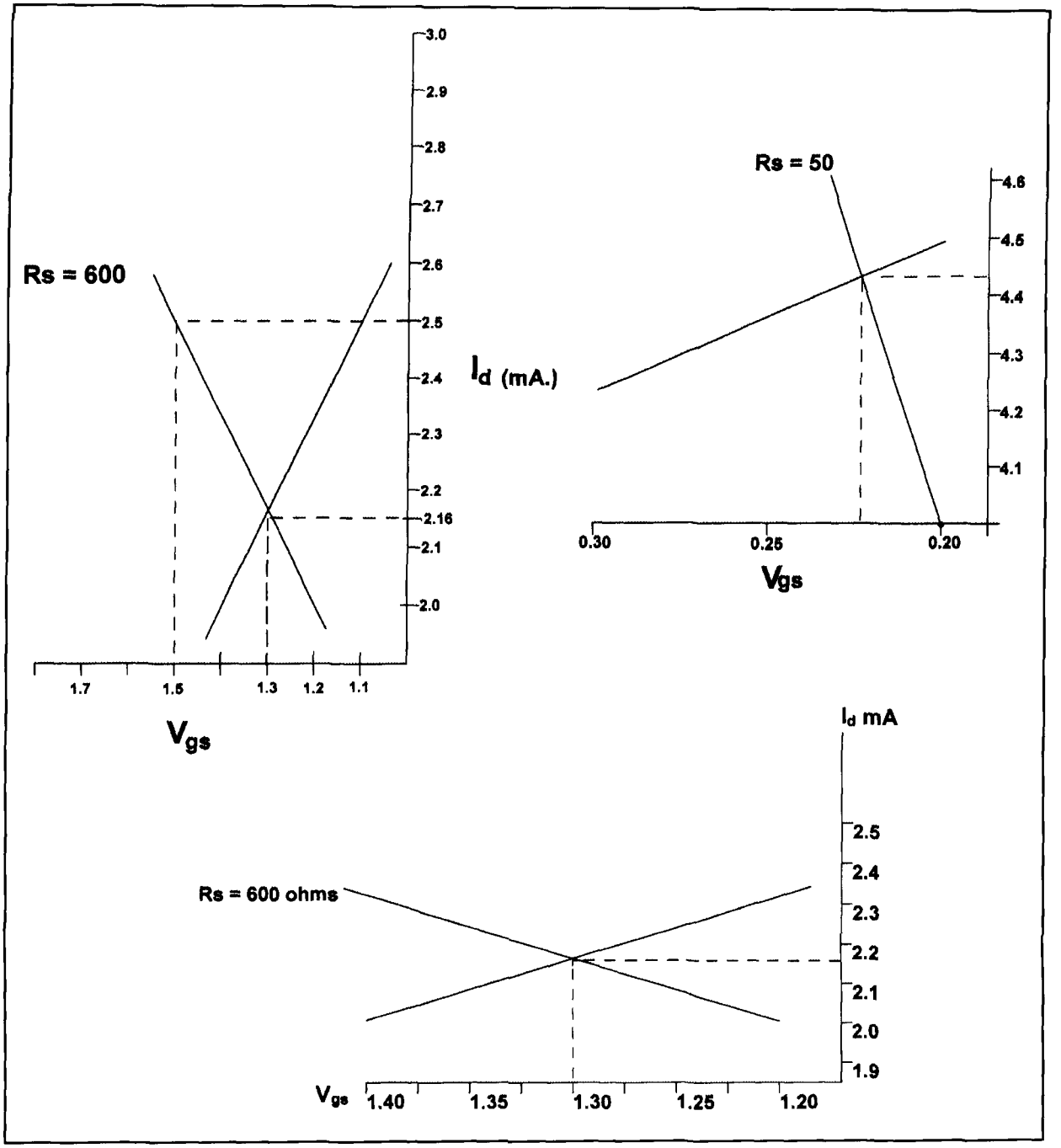

Figure 4. (A) A JFET's operating point can be established graphically. (B) 50-ohm intercepts I_d V_s V_{gs} at 4.49 mA and 0.225 volts. (C) 600-ohm intercepts I_d versus V_{gs} at 2.16 mA and 1.30 volts.

be investigated narrows quickly. If R_s is 600 ohms, I_d will be between 2.0 and 2.5 mA and the gain between 0.42 and 0.54; or, if R_s is 50 ohms, I_d will be between 4.0 and 4.5 mA and the gain between 0.11 and 0.20.

The capacitor needed to bypass the biasing resistor R_s in a common-source amplifier depends on the lowest frequency to be bypassed, the impedance seen looking into the source, $1/g_{fs}$, and the value of R_s. The reactance of the bypass capacitor must be less than the parallel combination of $1/g_{fs}$ and R_s at the lowest frequency of interest. For example, if I_d is 0.1 mA, then R_s is 33 k and $1/g_{fs}$ is 2.7 k and the capacitor must have a reactance less than 2.5 k at the lowest frequency to the bypassed. At 300 Hz, C would be greater than 0.2 µF.

The equations presented here give insight as to how and why a particular operating point is established. These equations take the mystery out of determining the JFET's operating point and will eliminate the cut and try. With no cut and try, there is just the danger of burning yourself on a hot pencil or calculator. ■

Robert R. Brown, *NM7M*
504 Channel View Drive
Anacortes, Washington 98221

HEARD ISLAND

The low-band logs of VKØIR

The 1997 Heard Island Antarctica DXpedition proved to be one of great interest to amateur radio operators—so much so, that a record number of over 80,000 contacts were made, worldwide, during the period of operations from January 14 to 27. The radio logs of the VKØIR DXpedition are interesting in that they not only show aspects from the intense competition for DX contacts and the demographic distribution of amateur radio operators, but also important features of the ionosphere itself, from the state of the solar/terrestrial environment and the geographic location of stations relative to Heard Island.

It is ionospheric aspects of the last two points that will form the major part of the present discussion; but the first two, the competitive air of the time and demography, are also considered as they bear on the interpretation of the results.

Initial conditions

To begin the discussion, it should be noted that the trip to Heard Island (53.2S, 73.6E) was

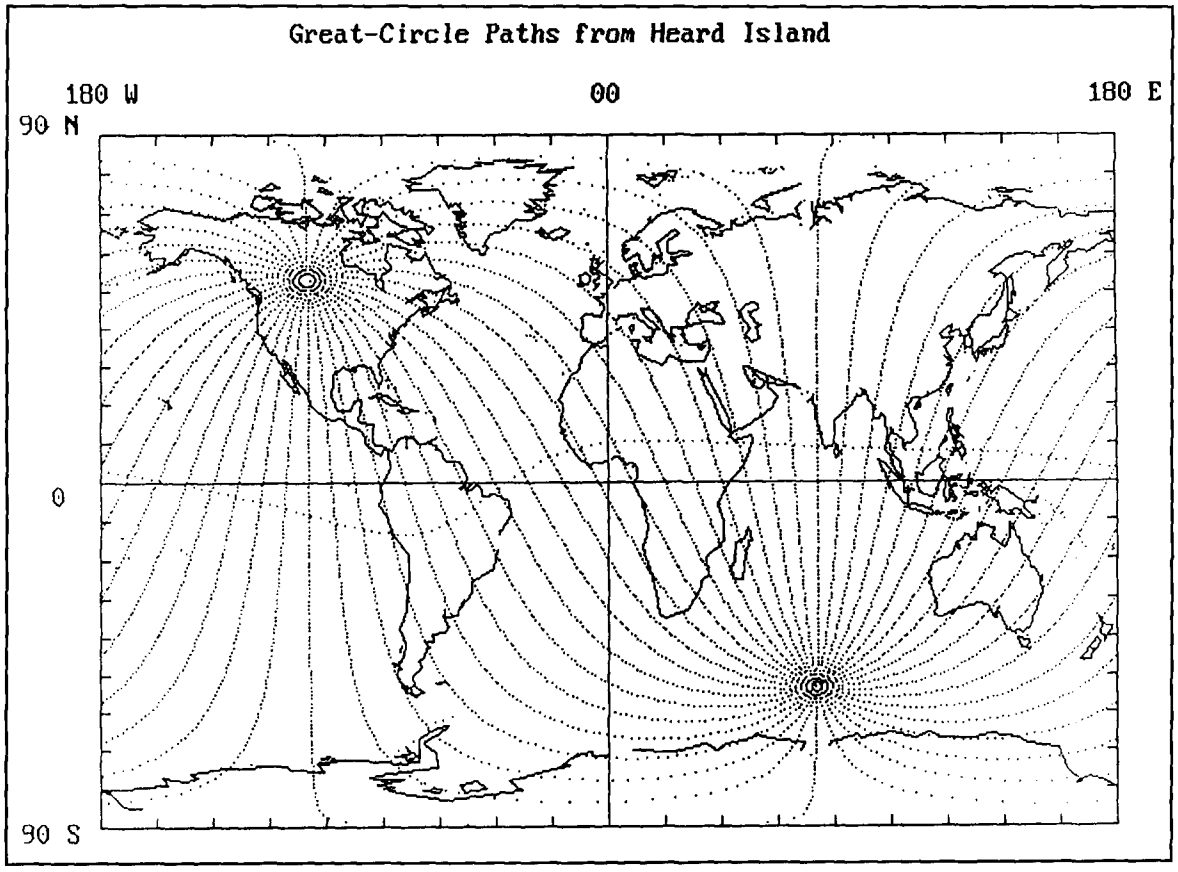

Figure 1. Great-circle paths from Heard Island, in 10-degree intervals of heading.

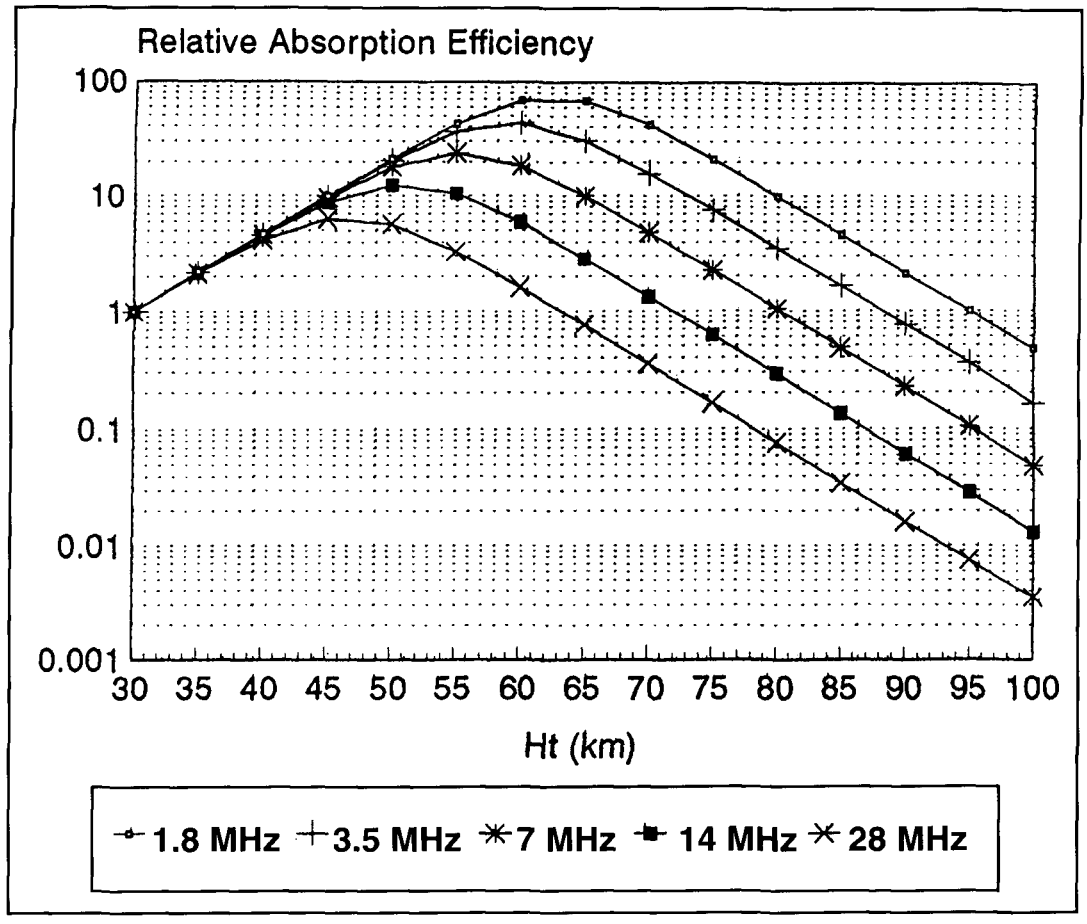

Figure 2. Relative ionospheric absorption efficiency per electron as a function of frequency and height.

made during the austral summer at a time close to the minimum of solar cycle 23. The location of Heard Island in the South Indian Ocean and those other two points determined a good deal of what followed when the DXpedition became active on the amateur bands. The operating period, being close to solar minimum, meant that critical frequencies in the ionosphere were not sufficient to permit operation on the highest HF bands, say 28 MHz, at least not without outbursts of solar activity. But there was sufficient ionization for the lower bands, 7 MHz and below, to be open on a global basis, and those will be the focus of attention in this article.

The principal amateur radio populations were at varying distances from Heard Island. South Africa was the closest at about 4,000 to 5,000 kilometers, followed by Australia at 4,000 to 6,000 kilometers, South America and Japan at 11,000 to 12,000 kilometers, Europe at 11,000 to 14,000 kilometers, and North America at 17,000 to 18,000 kilometers. From Heard Island, radio transmissions to those locations on the lower bands were carried out using directive arrays like a two-element Yagi on 7 MHz, Four-Square antennas on 3.5 and 7 MHz, and just simple vertical radiators that radiate equally in azimuthal directions.

Yagi radiation patterns are well known and need not be discussed here. As for the Four-Square Array, it has a 5.5-dB gain over a single vertical radiator, 3 dB or greater forward gain over a 90-degree angle, 20 dB or better front/back ratio over a 130-degree angle, and can have directional switching in 90-degree increments, according to the *ARRL Antenna Book*.

As for signals radiated from Heard Island, **Figure 1** shows great-circle paths to its antipode at 53.2N, 106.4W; the paths are given for every 10 degrees of heading relative to north. For North America, the interesting feature of **Figure 1** is that it shows that the paths from Heard Island to North America were divided at Heard Island, with paths to the east of Heard Island heading off toward the western part of North America and those to the west heading off toward the eastern part of North America. Beyond that, the dates of the DXpedition were such that the southern polar cap was in sunlight, pole ward from 68.4S on January 14 to 71.6S on January 27. As a result, paths crossing those parts of the polar cap were

subject to absorption, depending on signal frequency, in the *D*-region of the ionosphere.

Ionospheric absorption and ray paths

The frequency dependence of absorption (in dB) is shown in **Figure 2**, where the relative absorption efficiency per electron is shown for *D*-region heights and signals in the harmonically related bands of the amateur spectrum. To calculate signal absorption on a path, those results must be converted to absolute absorption per electron and then weighted by the number of electrons per square meter as encountered along the length of a path. For that purpose, the path and propagation mode must be specified as well as the electron density profile and its variations along the path.

For the frequencies of interest in the present discussion, 1.8, 3.5, and 7 MHz, there are a number of modes possible, depending on the radiation angle from the antenna and the state of the ionosphere at the time in question. Normally, propagation is discussed in terms of earth-ionosphere hops, say *E*- or *F*-hops, depending on the degree of penetration of the path into the ionosphere. But the properties of the ionosphere vary, more at *F*-region than *E*-region heights, so there are electron density gradients along, or transverse to, a path that must be considered.

Ray-tracing of paths shows that there are also complex propagation modes. These are in addition to the simple *E*-or *F*-hops where a ray normally is returned to ground from an ionospheric region at distances of, say, 1,500 kilometers for an *E*-hop or 3,000 kilometers for an *F*-hop. If the electron density varies along a path, it is possible to have chordal hops or chordal ducting where paths go to much greater distances before returning to ground. Those situations would be found at the lower frequencies con-

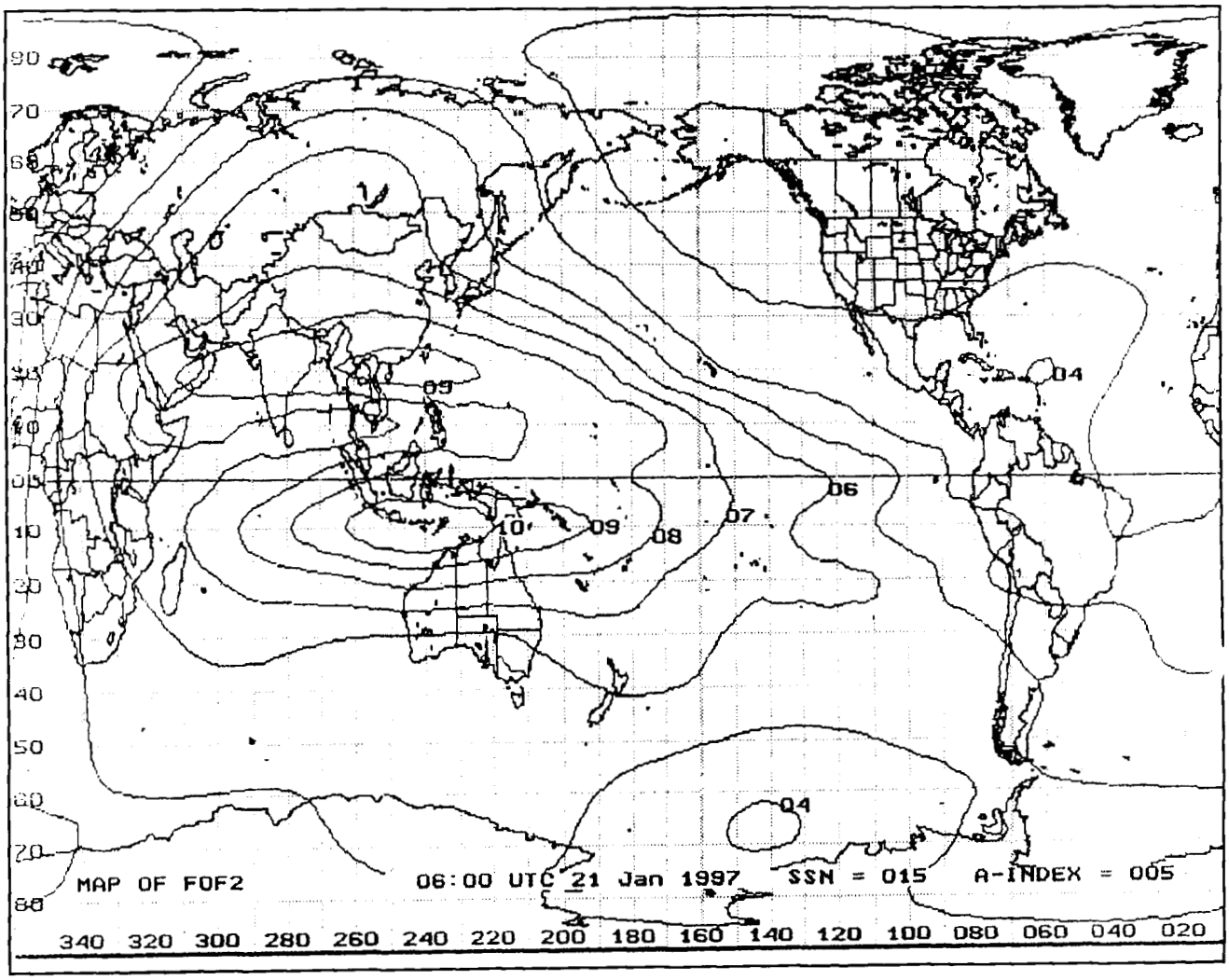

Figure 3. Global foF_2 map for January 21, 1997.

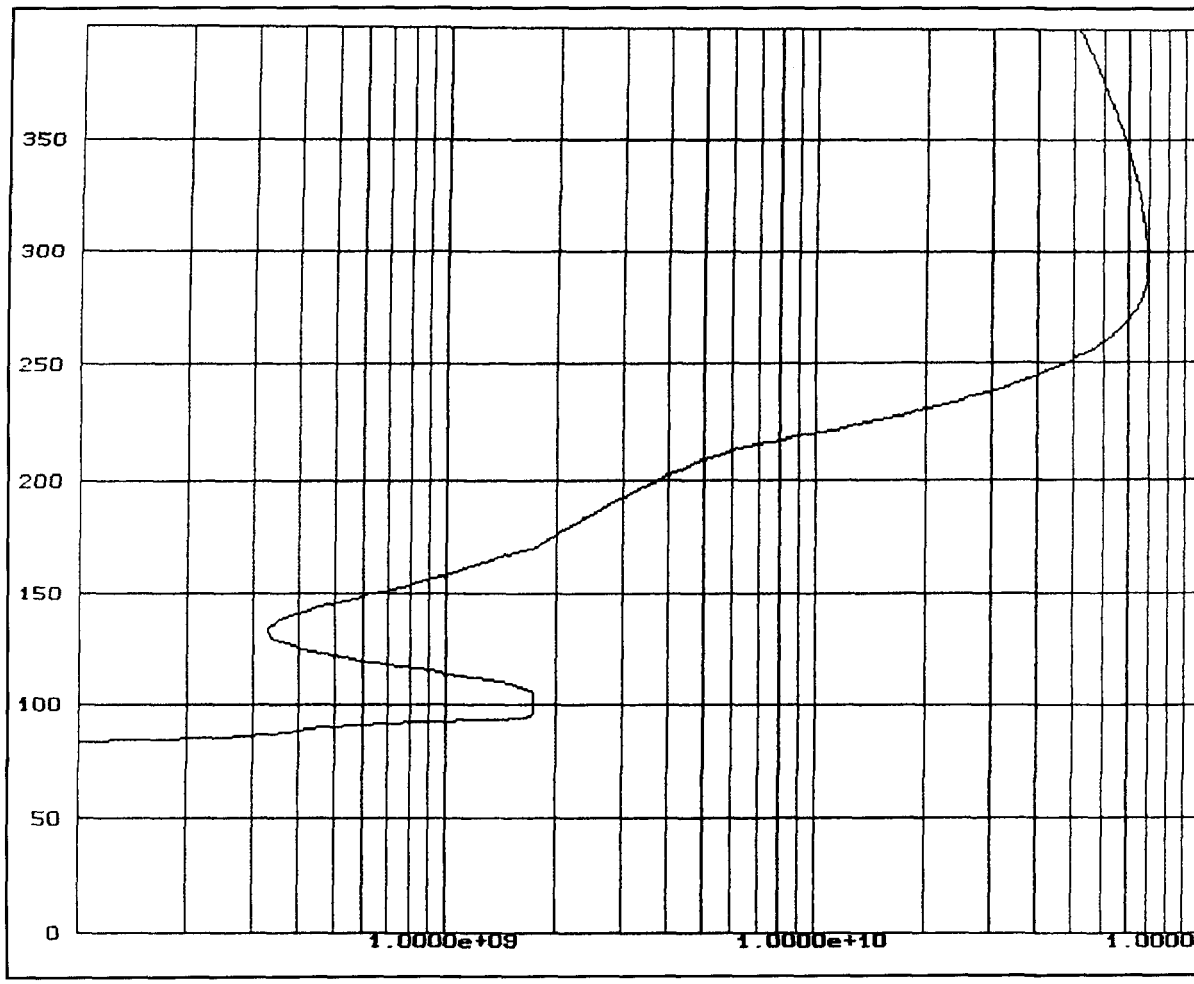

Figure 4. Night-time electron density profile, with a valley above the *E*-peak. (Altitude in kilometers and density in electrons/cubic meter).

sidered here, in the 80- and 40-meter bands. In addition, if the electron density varies significantly in the direction transverse to a path, refraction could skew the path away from regions of higher ionization.

The types of electron density variations spoken of above are found as regular features on ionospheric maps, as seen in **Figure 3** for the foF_2 critical frequency of the *F*-region. As the electron density at a point on a global map is proportional to the square of the critical frequency there, one can evaluate longitudinal or transverse gradients along a path by placing its great-circle on an foF_2 map and simply examining the variation of foF_2 in those directions and doing the arithmetic. The magnitude of the effects for a given gradient vary with the inverse-square of the frequency, so 1.8-MHz signals would be affected far more than on 3.5- or 7-MHz signals.

Propagation of 1.8-MHz signals

It is important to note that the lowest frequency of interest in the present discussion, 1.8 MHz, not only would suffer the greatest refraction effects from ionospheric gradients, but also the most severe absorption in the *D*-region. As a result, it can be used effectively only if the path is in darkness and when the electron density profile is not disturbed. For times of darkness, the electron density in the *D*-region is greatly reduced but some ionization still remains, the result of ionization by scattered sunlight from the geocorona, UV and x-rays from starlight, and the flux of galactic cosmic rays through the atmosphere.

Beyond that, there is another important feature of the night-time ionosphere: the electron density valley that develops above *E*-region heights after sunset. A typical electron density profile for a night-time ionosphere is shown in **Figure 4**. Such circumstances have been regarded as a possible means for ducting of signals over great distances as well as efficient propagation of signals by reflections between the upper *E*- and the lower *F*-regions, with few reflections of rays off the earth's surface, whether ground or salt water.

In any event, the effective propagation of

1.8-MHz signals requires darkness along the path, as communication during daytime hours is limited to ground-wave coverage. In darkness, all the various modes of propagation can and will be in effect after rays are launched from a transmitting antenna; then, the question that remains has to do with which mode is responsible for the signal that reaches the receiver. It cannot be expected that successful modes will not, at one time or another, have rays which go down into the *D*-region. Hence, it stands to reason that, whatever the path, the physics of the *D*-region requires darkness along the path for the DX propagation.

Sunrise and sunset terminators

Obviously, darkness along propagation paths from Heard Island would require that Heard Island itself be in darkness. For paths to North America, darkness was in common at times; first, when Heard Island was already in darkness and North America went into darkness in the evening hours. As an example, during the DXpedition, the time of common darkness along paths to the Eastern U.S. began when the sunset terminator started to sweep across the Atlantic coastline, say after sunset at Calais, Maine. That was about 2106 UTC at the start of the DXpedition. Then common darkness ended when the sun rose at Heard Island, at 2310 UTC on January 14.

Those circumstances apply to signals heading westward from Heard Island. For signals heading eastward, common darkness along propagation paths from Heard Island to North America was found when Heard Island went into darkness, while North America was already in darkness during the hours before sunrise.

Thus, darkness along paths to the Western U.S. began with sunset on Heard Island; that was at about 1520 UTC at the start of the DXpedition. Then common darkness ended at locations along paths to the Western U.S. as the sunrise terminator swept westward toward the west coast.

The idea of "common darkness" points to limitations on the times for receiving signals from Heard Island that depended on location. For example, for the Eastern U.S., signals were received from about local sunset until sunrise at Heard Island while for the Western U.S., signals were heard in hours of morning darkness after the sun set at Heard Island and until local sunrise. But between those two times, sunrise and sunset at Heard Island, it is clear that the paths for all signals or transmissions from

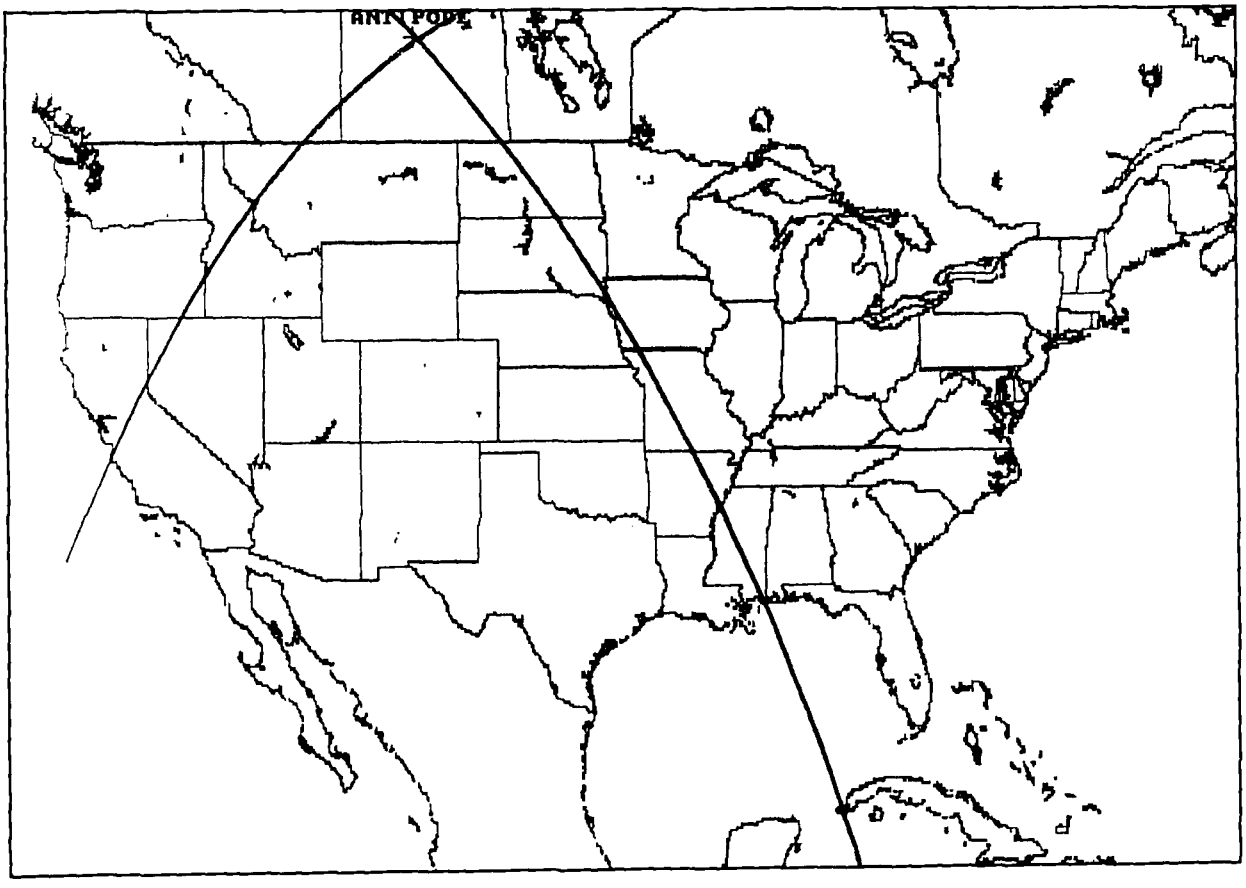

Figure 5. Map of U.S. with sunset (right) and sunrise (left) terminators for January 14.

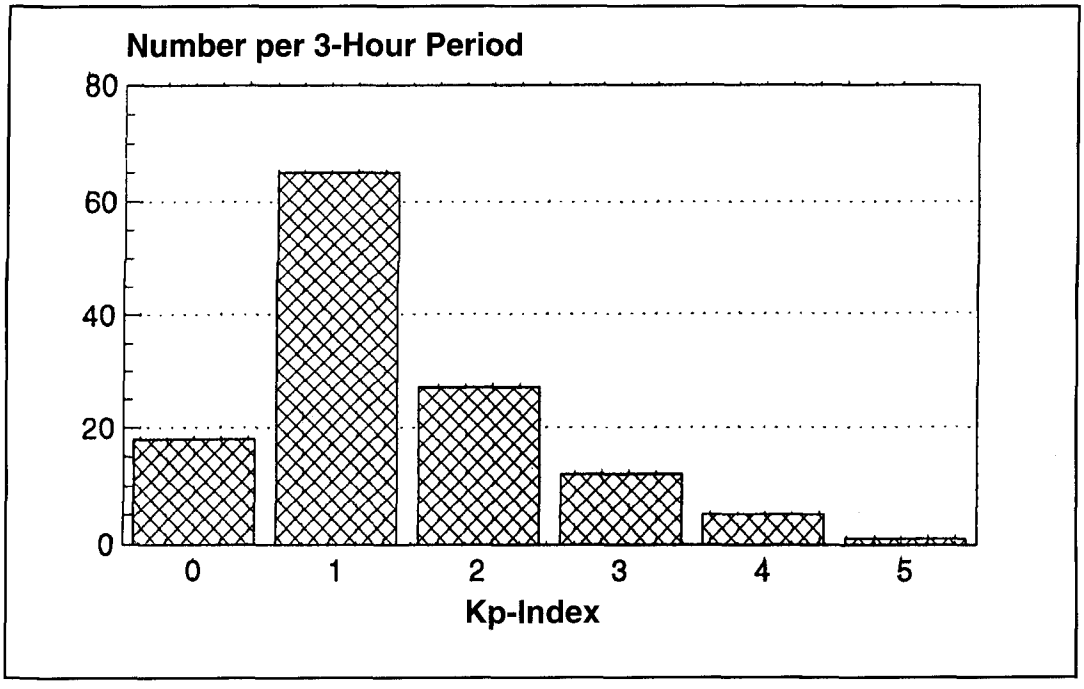

Figure 6. Distribution of Kp-values for January 14-27, 1997.

Heard Island were in sunlight to some degree. With the 1.8-MHz signals suffering severe absorption, the corresponding terminators gave the boundaries of the region within which 1.8-MHz signals from Heard Island would not be received, as shown in **Figure 5**.

Of course, for the other frequencies of interest, 3.5 and 7 MHz, the ionospheric absorption (in dB) would be lower by factors of about 4 and 16, respectively. The log data for contacts with Heard Island on those frequencies show the extent to which ionospheric absorption limited access to that region in the time between sunrise and sunset at the Heard Island end of the path. In addition, the log data show the extent to which signal propagation continued on those frequencies at times before sunrise or after sunset, when Heard Island was still in darkness, and the distant ends of the paths over the U.S. were in sunlight.

Magnetic and auroral considerations

In addition to ionization in the lower ionosphere, which is released by energetic photons in the UV and x-ray range, ionization may be produced with the incidence of auroral electrons on the atmosphere. Ionospheric currents flow at auroral altitudes during those displays and K- and A-indices from high-latitude magnetic observatories give a measure of the auroral activity by the levels of simultaneous magnetic disturbance.

The K-indices are given for three-hour intervals of UTC and standardized across observatories so as to range from K=0 (magnetic quiet) to K=9 (severe magnetic storm). The A-index, on the other hand, represents a measure of magnetic activity for a 24-hour period. Both indices are sampled on a global basis and planetary values, Kp and Ap, are published for the days of each month.

During the period of interest, January 14 to 27, the Ap-index ranged from a low value of 2 on January 17 to a high value of 18 on January 26, while the Kp-index ranged from a low value of Kp=0 during 18 three-hour periods and a high value of Kp=5 at the end of the day on January 26. The average of the Ap-index was 6.4, making the period one of low magnetic activity, far short of major storm levels which begin at Ap=40. This distribution of Kp-values for the period is shown in **Figure 6**.

Because a number of the great-circle paths to North America head south from Heard Island toward the southern auroral zone, it is of interest to show its position relative to the paths and its extent at times during the DXpedition. This is of particular importance for the case of 1.8-MHz operations, as those signals would suffer the greatest ionospheric absorption from auroral ionization, as well as skewing away from great-circle paths.

To illustrate the matter, **Figure 7** provides a view of the southern auroral zone on an azimuthal equidistant map centered on Heard Island for 1508 UTC on January 24, when Kp=1 and the Ap-value was 4. North American

locations, west of the terminator and toward the target at Seattle were in darkness, and it is seen that those paths would pass through a significant portion of the auroral zone.

Another map is shown in **Figure 8**, now for January 22 and 2324 UTC, when Kp=2 and the Ap-value was 6. The time chosen for **Figure 8** corresponds to sunrise at Heard Island on that date. North American locations east of the terminator, say to the target at Boston, were in darkness, and it is seen that those paths only pass tangentially through the auroral zone.

1.8-MHz contacts with Heard Island

Of the 80,673 contacts in the VKØIR logs, there were only 225 contacts made on 1.8 MHz. Of those, some 194 were with stations in Eastern North America, 15 with Central North America, and 16 with Western North America. What might seem like an imbalance in the distribution of contacts was due in part to demography, the competitive circumstance, weather on Heard Island, and propagation, most notably the effects of ionospheric absorption. That last factor, absorption, was the one that determined the final shape of the geographical distribution of contacts on 1.8 MHz.

As noted earlier, the world was divided into halves as far as signals from VKØIR were concerned. Those going off to their east would, hopefully, reach Western North America, and signals going to their west would reach Eastern North America. The dividing line here in the U.S. was the line along 106.4 W longitude, between Aspen and Leadville, Colorado, and running north, close to Saskatoon, Saskatchewan.

It is clear from **Figure 1** that stations close to that longitude would have a difficult, if not impossible, time even hearing VKØIR as their short-path signals would have to go across the southern polar cap, in full daylight, and come up to the U.S. from the south. As a result, there were no contacts with VKØIR made by stations in the W5 district and only a few contacts made in states from the W6, W7, and W0 districts, as suggested by the limiting sunrise and sunset terminators in **Figure 5**.

On 1.8 MHz, the region between the limiting terminators could be considered a "dead zone" for signals from Heard Island. When examined, this zone turns out to cover an area about five times as large as the state of Texas—all of

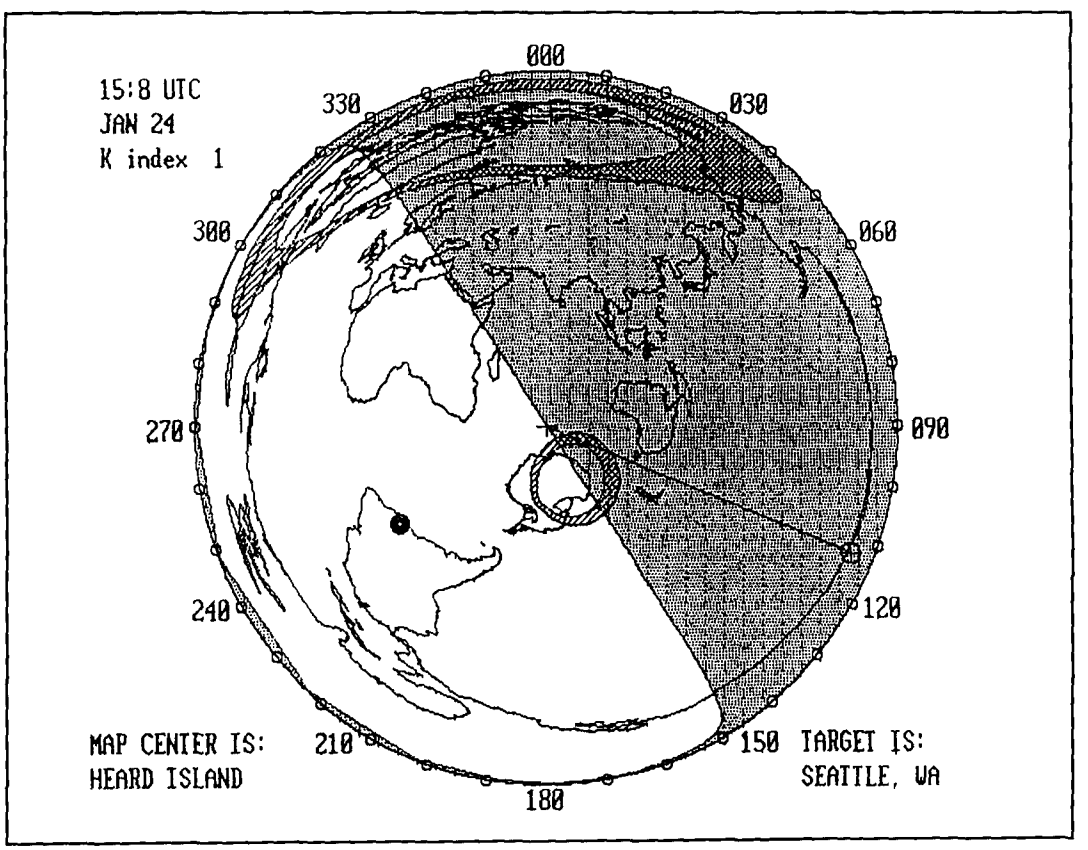

Figure 7. Azimuthal equidistant map centered on Heard Island for 1508 UTC, January 24, 1997, and when Kp=1.

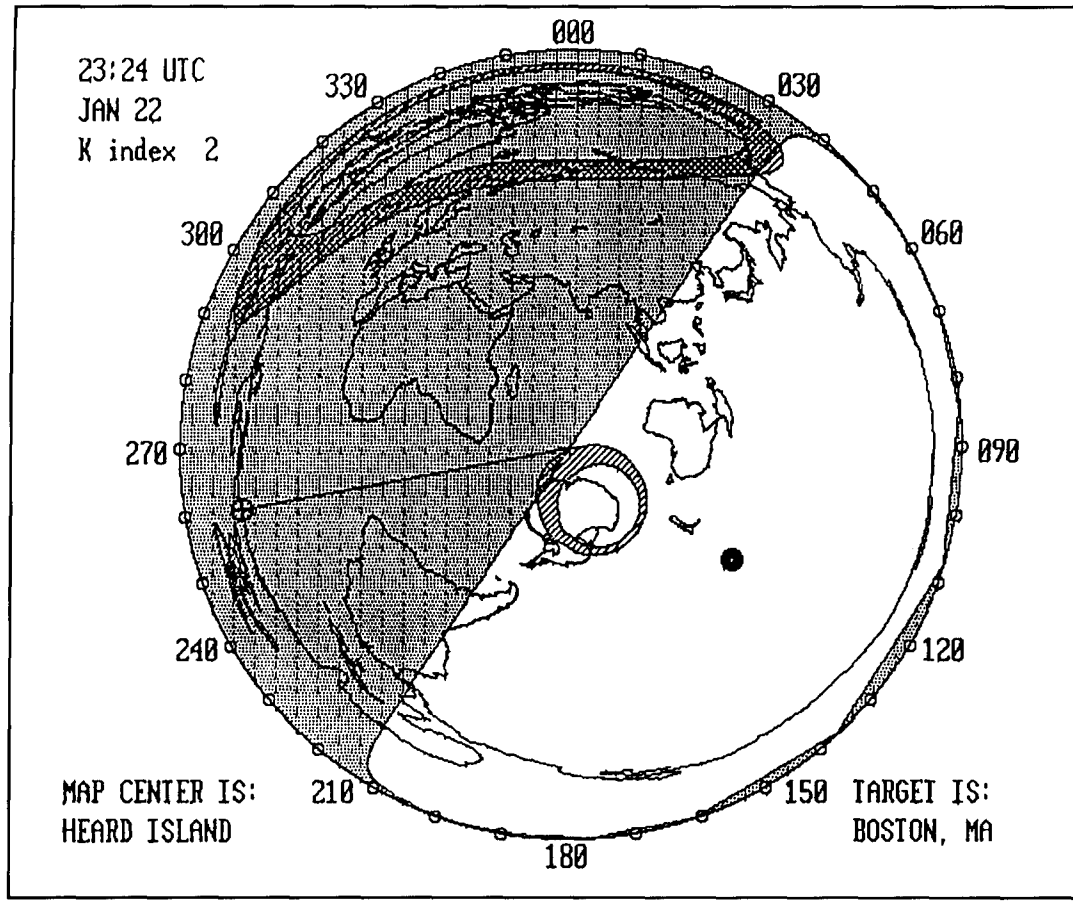

Figure 8. Azimuthal equidistant map centered on Heard Island for 2324 UTC, January 22, 1997, and when Kp=2.

Arizona, New Mexico, Texas, Louisiana, Oklahoma, Utah, Colorado, Wyoming, Kansas, Nebraska, as well as most of Arkansas and Nevada, half of Idaho, Eastern Montana, and western portions of North and South Dakota. While the statistical sample is small, VKØIR logs confirm the effects of ionospheric absorption, giving rise to that division. As of the 225 contacts on 1.8 MHz, there were no contacts with any station between eastern Washington and eastern Kansas, by the Missouri River.

Earlier, mention was made of the absorption effects which would result from the addition of ionization along a path from Heard Island that might cross the southern auroral zone. In that regard, **Figures 7** and **8** show the locations and extent of the auroral zones and limiting terminators for the sunrise and sunset dates and times when the Kp values were 1 and 2, respectively. The geometrical aspects of the auroral zone in those figures were derived from NOAA/TIROS satellite data, but it should be noted that nothing of the intensity or spatial distribution of auroral ionization is represented in those figures.

That sort of information was provided in two forms by means of particle detectors aboard the NOAA/TIROS satellites. The first form is an estimate of the power input (in Gigawatts) to the entire southern hemisphere from auroral electrons on each satellite pass, and the second is a color print that shows the energy input along a pass and the average energies of the electron influx at each location. The detectors were sensitive to particle energies from 0.3 keV to 17.5 keV, and the color code for energy inputs ranges from white (0.1) to red (10.0) in units of ergs/sq-cm/sec or, equivalently, as milliwatts/sq-mtr, and a blue background (0.0) for no particle influx.

For those interested in the details of the NOAA satellite observations, the Space Environment Center of NOAA has a Web page at <http://www.sec.noaa.gov/index.html>. When the page comes up, click on the button labeled Auroral Activity. More direct access is available via http://www.sec.noaa.gov/hempower/ index.html. Presently, auroral activity is updated once a day at about 15 UTC, but an improved system is in development and will update data about three hours after taken from the satellite.

The hemispheric power input measurements range from less than 2.5 GW for quiet condi-

tions (Kp=<1) to more than 500 GW for severe storm conditions (Kp=8-9). For satellite passes over the southern polar cap at times close to those used in making **Figures 7** and **8**, the particle detectors showed the hemispheric power inputs to be 5.4 GW and 14.7 GW when K=1 and K=2, respectively.

For the period of the DXpedition, NOAA/TIROS satellite data show that the daily average of hemispheric power input ranged from a low of 7.1 GW on January 16 to a high of 33.3 GW on January 21, with an average of 16.8 GW for the entire period. Given the ranges of power inputs mentioned in the previous paragraph, it is clear that the time of the VKØIR DXpedition was one not only one of geomagnetic quiet, with an average Ap of 6.4, but also minimal auroral disturbance, with only an average of 16.8 GW for the power input by auroral electrons.

Beyond the energy input features, the satellite data show that auroral energy input always minimizes at about the noon meridian and maximizes around midnight. In that regard, it should be noted that the 1.8-MHz entries in the VKØIR log were for a few hours before and after sunset, indicating that the auroral ionization encountered on a path was far less than the maximum value on any given day.

Given the data cited above showing a weak auroral energy input during the DXpedition, the complete lack of 1.8-MHz contacts in the dead zone is attributed to ionospheric absorption of VKØIR signals at times between sunrise and sunset on Heard Island, with little in the way of effects from auroral ionization.

3.5-MHz contacts with Heard Island

The VKØIR logs show that on the 80-meter band, there were 977 contacts with Eastern North America, 195 contacts with Central North America, and 347 contacts with Western North America. Of those 1,519 contacts, 45 percent were on CW and 55 percent on SSB, but none were made on RTTY. The logs showed contacts made over a total of 28 hours, with about 21 hours around sunrise at Heard Island and seven hours at sunset. The operating times, as well as the times for sunrise and sunset, are shown in **Figures 9** and **10**.

In contrast to the 1.8-MHz operations, where there were no contacts with the W5 call district, there were 14 contacts in the 80-meter logs. But only one contact was in the dead zone, in East Texas; the other 13 contacts were with states outside the region, like Arkansas, Louisiana, and Mississippi, but none with the other states, such as New Mexico and Oklahoma.

The contact with Texas was made 30 minutes

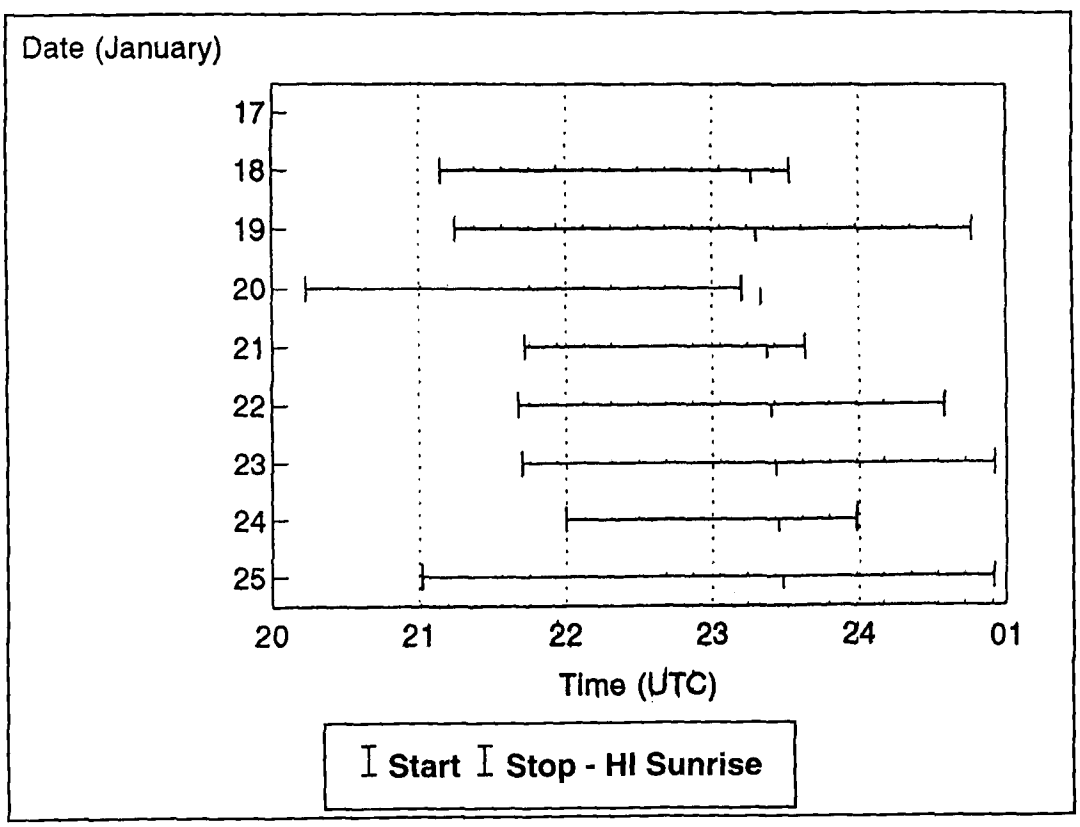

Figure 9. Eighty-meter operating times around Heard Island sunrise.

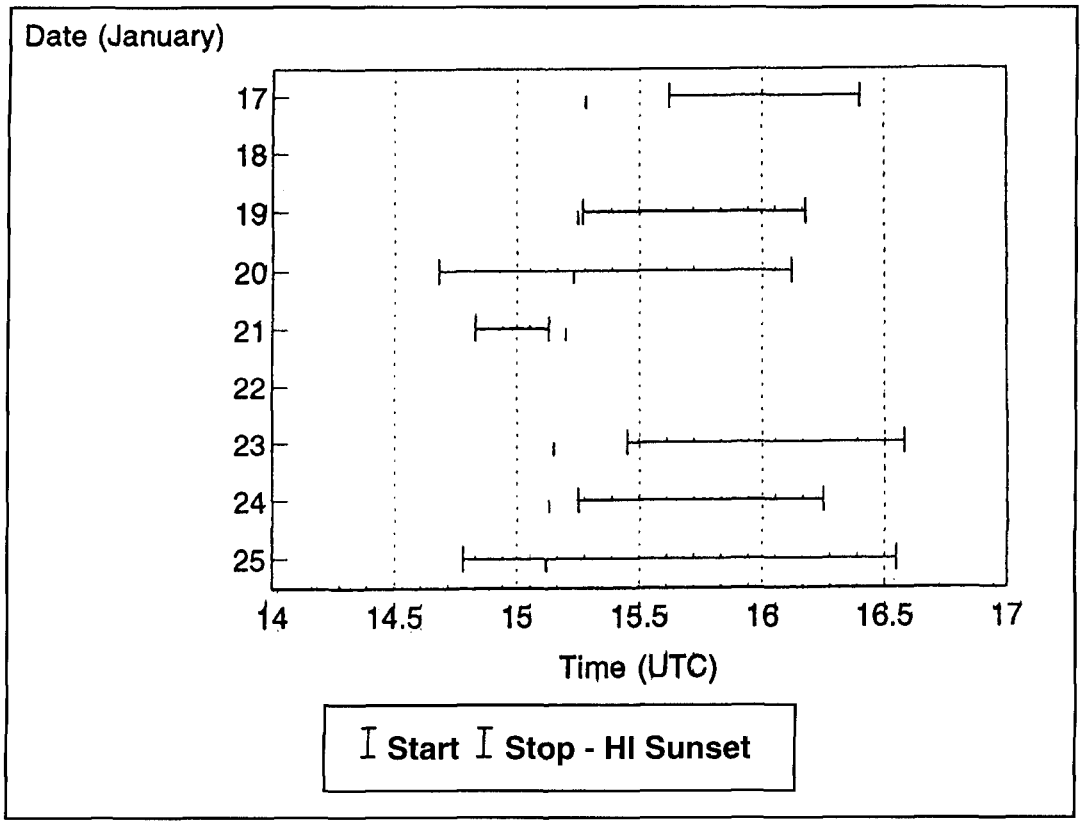

Figure 10. Eighty-meter operating times around Heard Island sunset.

after Heard Island sunrise on January 25 and 10 minutes after local sunset in Texas. A review of the short-path from Heard Island showed that of the 17,300-kilometer length of the path, 11,300 kilometers were in sunlight and 6,000 kilometers in darkness. On the other hand, a review of the long-path from Heard Island showed that only 5,000 kilometers were in weak sunlight, similar to a gray-line situation, and 15,700 kilometers of the path were in complete darkness. Given those results, it was concluded that the East Texas contact was via long-path and the 80 logs were searched for other long-path contacts that might enter the dead zone from the north.

A total of 33 other long-path contacts were found in the 80-meter logs, and a number of them entered the region shown in **Figure 5** from the north, reaching Saskatchewan and states such as Montana, Wyoming, Utah, Colorado, and Arizona. Most of those long-path contacts were made shortly after sunrise or before sunset at Heard Island and were only weakly illuminated in that region, but essentially in darkness over the remainder of the paths.

An example of a post-sunrise path from Heard Island is shown in **Figure 11** and a pre-sunset path is shown in **Figure 12**. The post-sunrise example has about 1,400 kilometers of its length in weak illumination before local sunset at the end in California and less illumination at the Heard Island end after sunrise there. Similarly, the pre-sunset case has about 1,500 kilometers of weak illumination on the path in the half-hour before sunset at Heard Island and much less than that length of path illuminated just after dawn in Arizona. It should be noted that the corresponding short-paths, more than 17,500 kilometers in length, for those contacts were in full sunlight and, given the degree of absorption on 80-meter signals, were not viable as paths for successful communication with Heard Island.

A few other long-path contacts were made after sunset at Heard Island. All in all, states outside the dead zone reached by that means included Illinois, Michigan, Minnesota, and North Dakota, notable for their northern latitudes. By way of summary, the range and mode of 80-meter contacts in the vicinity of the dead zone are shown in **Figure 13,** along with the sunrise and sunset terminators for the last day of 80-meter operations (January 25).

As for short-path contacts up to sunrise and after sunset on Heard Island, the openings differed in duration, with 130 to 150 minutes for the former and 30 to 45 minutes for the latter. The openings to Eastern and Central North America show more of the competitive dynamics than those to Western North America. That

difference was the result of the longer duration of the opening as well as the greater concentration of amateur radio operators in the W1 to W3 call districts.

In spite of the brief duration of the short-path openings in Western North America, log data for those times are interesting in that they clearly show how ionospheric absorption affects contacts made during an opening. Thus, even with a competitive situation, the dawn terminator cut off paths rapidly in succession—southern California, central California, then Oregon—all because the terminator and great-circle paths coming up from the southwest were at small angles with respect to each other and significant lengths of the paths were quickly illuminated as the terminator moved westward. At the end of those openings, the logs closed with contacts to the Seattle-Vancouver area...all that in less than an hour's time.

To the east, openings before Heard Island sunrise were much longer and just the opposite case, with openings developing slowly as the local sunset terminator swept westward. Thus, early in an opening, the log was dominated by stations along the East Coast until the sunset terminator moved west of Pennsylvania and New York. At this time, stations in the Midwest started to make contact with Heard Island while those to the East continued, as before. In short, there was no sharp cut-off of paths, only new ones added until finally the sun rose at Heard Island.

Examples of paths before sunset and after sunrise are given in **Figures 11** and **12**. Those involved some illumination at the Heard Island end of the path and possibly at the far end, too. The operating times before sunset were quite limited, less than 90 minutes total, but were rich in long-path contacts into the dead zone. At the same time, the operating times after sunrise amounted to almost seven hours, with a few long-path contacts beyond 106.4 W longitude, but were otherwise rich in contacts with the eastern states of the U.S. and provinces of Canada. Generally speaking, both those circumstances showed illumination on paths which, in total, mounted to about 1,500 kilometers or the length of an *E*-hop in daylight.

7-MHz contacts with Heard Island

On the 40-meter band, the VKØIR logs show there were 3,021 contacts with Eastern North America, 1,158 contacts with Central North America, and 1,337 contacts with Western

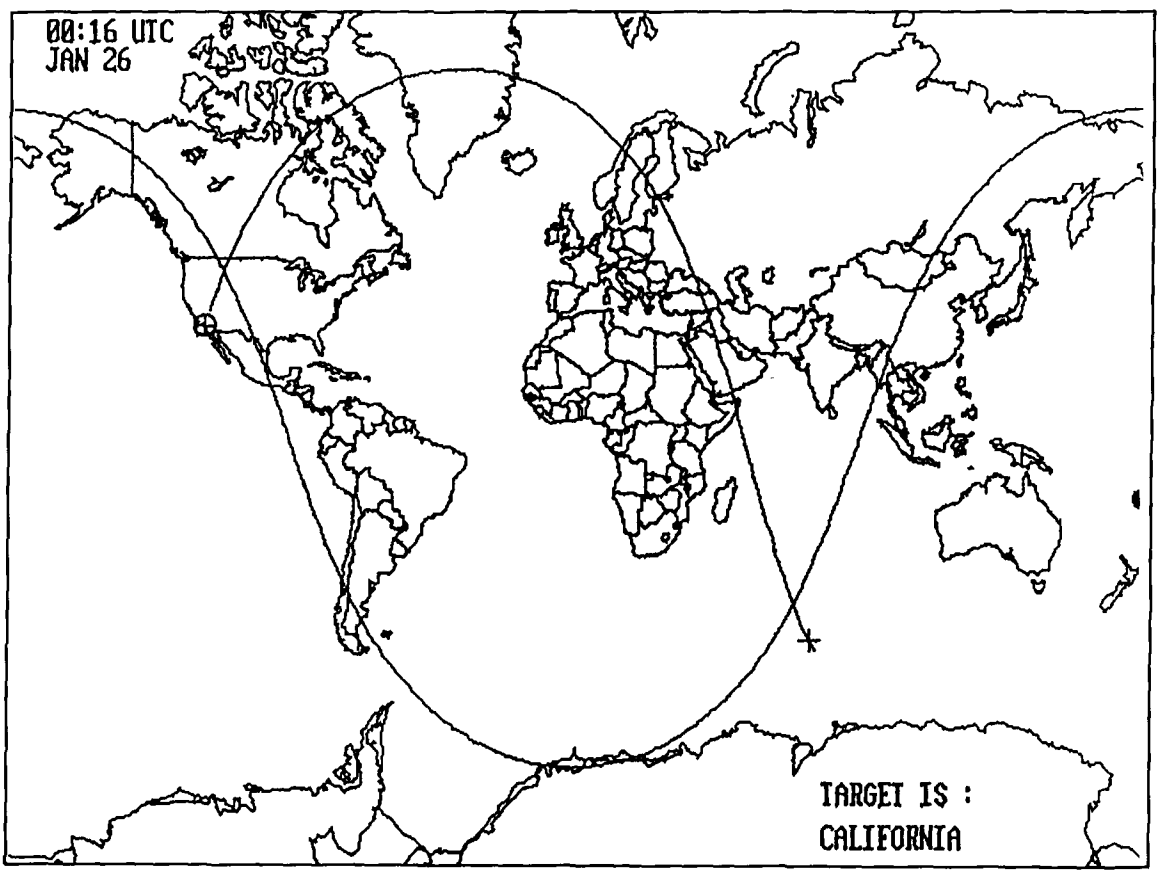

Figure 11. Mercator map showing a path from Heard Island to California at 0016 UTC on January 26, 1997.

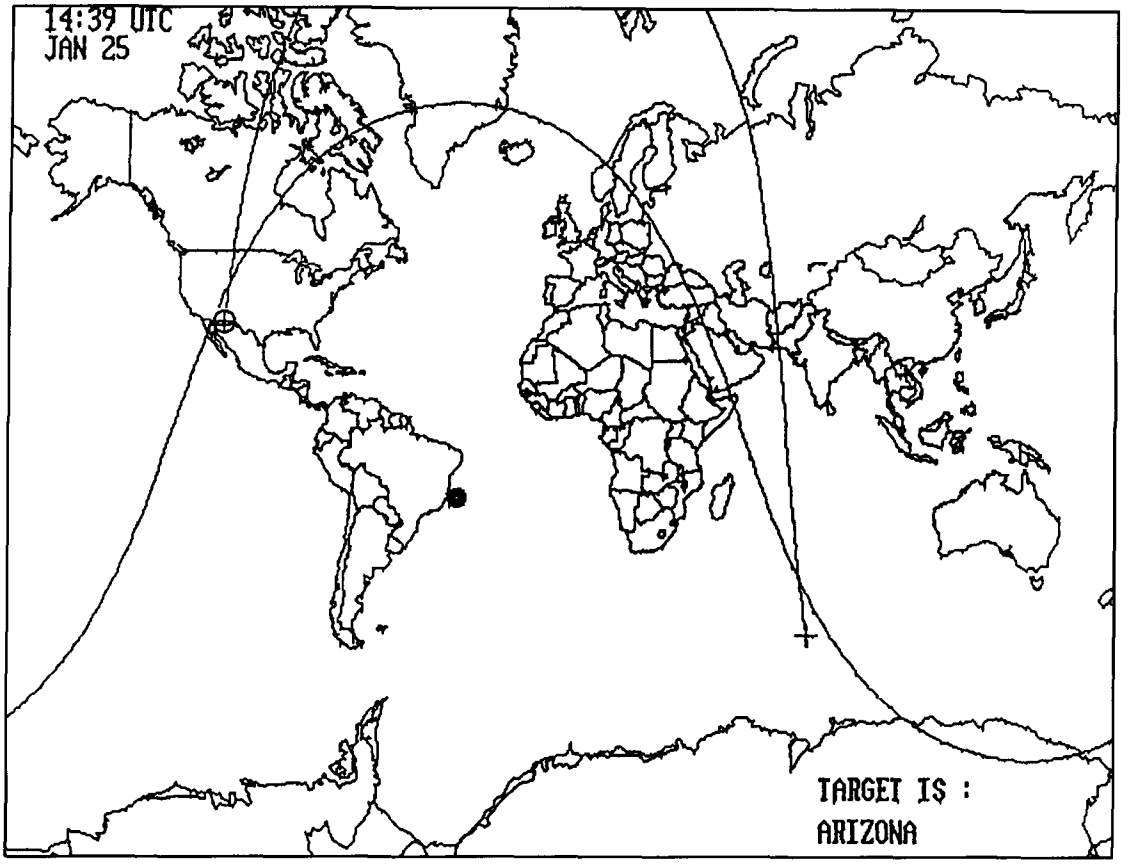

Figure 12. Mercator map showing a path from Heard Island to Arizona at 1439 UTC on January 25, 1997.

North America. Of those 5,516 contacts, 76 percent were on CW and 24 percent were on SSB, but none were made on RTTY. The logs showed contacts made over a total of about 78 hours, with about 41 hours around sunrise at Heard Island and almost 37 hours at sunset. The operating times, as well as the times for sunrise and sunset, are shown in **Figures 13** and **14**.

On the 40-meter band, ionospheric absorption (in dB) is about a factor of 4 lower than on 80 meters. As a result, there were contacts with all the states in the dead zone. However, the locations in the lower states of the W5 call district—say in New Mexico and near longitude 106.4W in Colorado, Wyoming, and Montana—were still only accessible via long-path because of intense absorption on short-paths across the southern polar cap in full daylight.

Beyond the states in the dead zone and the special problem they posed for propagation, all the other states in the U.S. were reached on short-path, say before sunrise or after sunset at Heard Island. In addition, during the sunrise period around 2300 UTC, stations in all the states beyond the dead zone made contacts with Heard Island via long-path (California, Oregon, and Washington, as well the western portions of Idaho and Nevada). Furthermore, during the sunset period around 1500 UTC, stations in all the states east of the dead zone made contacts with Heard Island via long-path.

While illumination on paths for successful long-path contacts on 80 meters could be as much as 1,500 kilometers, or about the length of an *E*-hop, the distance on 40 meters was as long as 3,000 kilometers—now about the length of an *F*-hop. As a result, long-path propagation played a significant role on 40 meters, and it is estimated that approximately 15 percent of the 5,500 contacts on 40 meters were via that mode.

One other point, again showing how significant a role long-path propagation played with less ionospheric absorption, the Heard Island openings were longer, and, on more than one occasion, long-path contacts were made at a rate of more than 20 per hour.

Discussion

Trying for a contact with a rare, isolated location would be a challenge for any amateur radio operator under most conditions, but now, at solar minimum, it is even more difficult. In

the case of Heard Island, amateur operators in North America faced greater challenges than the rest of the world because the continent is located almost half an earth away from Heard Island. And while one contact would be interesting by itself, it would not add very much to our understanding of propagation.

The Heard Island DXpedition proved quite different. It offered not only the possibility of a rare contact, but also attracted the interest of tens of thousands of amateur operators. All the contacts they made in two weeks time provided a fine opportunity to observe propagation effects, particularly on the lower bands.

While the log of contacts by VKØIR cannot be considered, in the classic sense, as data from an experiment, the log does provide a clear, even separable, demonstration of how ionospheric absorption can affect propagation. In that regard, the contacts of interest were those made on the lower frequencies, during relative magnetic quiet and on bands where critical frequencies (MUFs) were never an issue. Thus, the logs showed effects of the intense absorption on 1.8 MHz, which ordinarily limits propagation in daytime hours to just ground-wave distances. Such absorption resulted in a dead zone here in the U.S. that was south of Heard Island's antipode, a large area where signals from VKØIR could not be received between sunrise and sunset on Heard Island.

That was the unique aspect of the Heard Island DXpedition, the location of its antipodal point in Saskatchewan, Canada. It brought the role of absorption effects to a focus, as it were, in a bounded region within the U.S. Of course, the location and size of the absorption region were determined by the location of the terminators in the U.S. at the times of sunrise and sunset at Heard Island. Those depended on the time of year, and, had the DXpedition been a month earlier, at the solstice, the region would have been larger than shown in **Figure 5**, with the terminators crossing coastlines around Tallahassee, Florida, and San Francisco, California. On the other hand, if the DXpedition had been a month later, the region would have been smaller, crossing coastlines around Brownsville, Texas, and at the head of the Gulf of California in Mexico.

For successful communication on 1.8 MHz, a path must be in darkness, without significant ionospheric absorption. In that regard, the westward movement of the sunset terminator over

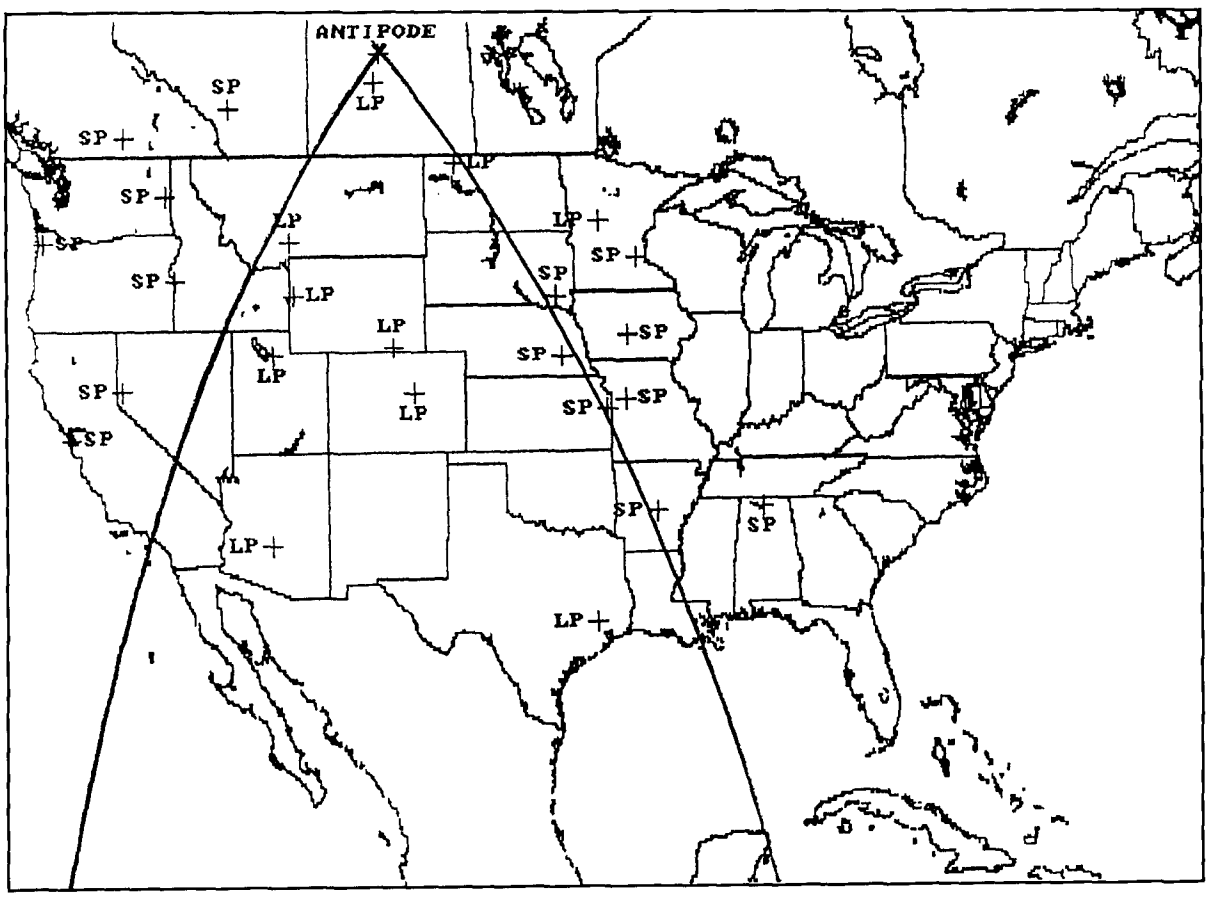

***Figure 13. Map of* U.S. showing sunset and sunrise terminators on January 25, 1997, with designations of types of paths to locations in the U.S. from Heard Island on 80 meters.**

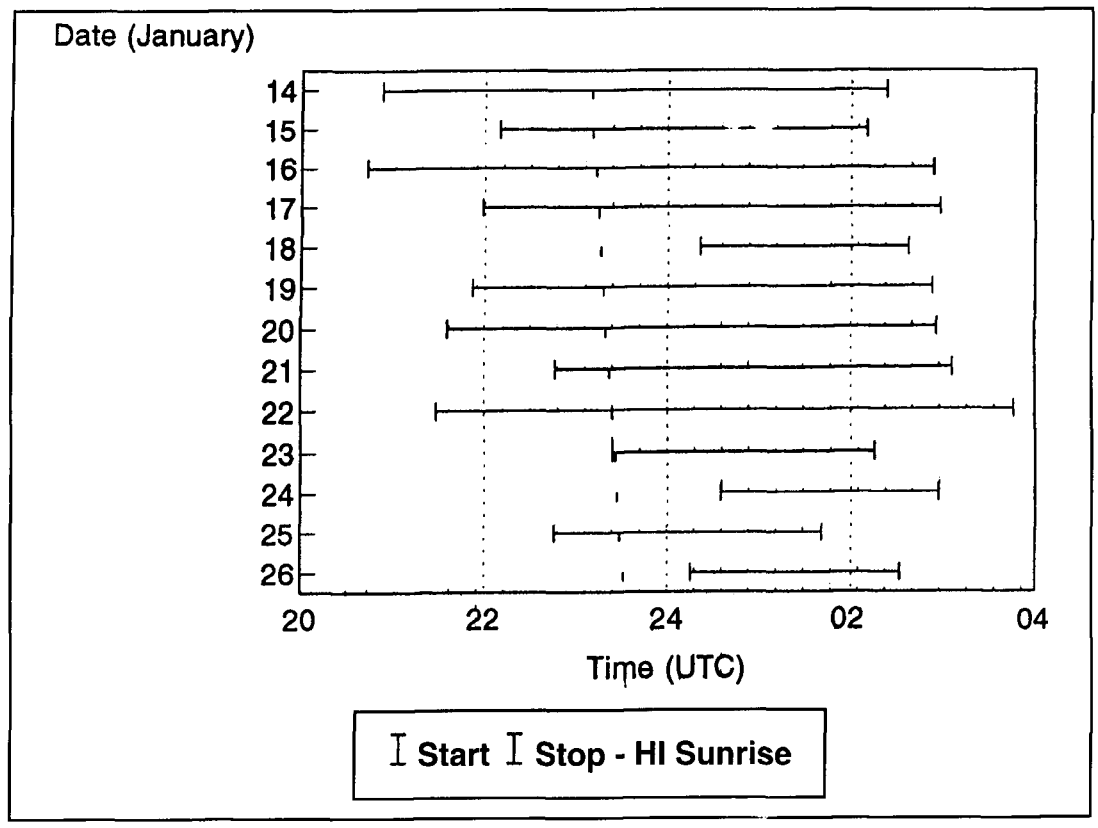

Figure 14. Forty-meter operating times around Heard Island sunrise.

the eastern part of North America translated into a moving boundary that enlarged the area where signals could be exchanged with Heard Island, then also in darkness. But when the dawn terminator reached Heard Island, that expansion of the coverage stopped and the addition of paths of two-way propagation on 1.8 MHz came to a halt because signals were absorbed at the Heard Island end.

For the western portion of North America, propagation on 1.8 MHz was possible later in the day, as soon as Heard Island went into darkness. That condition set the boundary of the greatest eastern penetration of signals from Heard Island, and as the dawn terminator moved westward, the region that was accessible grew smaller in area and finally vanished as the terminator crossed the coastline in the northwest part of Washington.

Between the location of those two terminators in North America, corresponding to the times for sunrise and sunset on Heard Island, propagation was impossible on 1.8 MHz. But the number of 1.8-MHz contacts during the Heard Island DXpedition was not sufficient to show those limits in detail. And, of course, the limiting positions of the terminators are only mathematical constructs and fail to deal with the twilights that exist around sunset and dawn. That lack of precision in width along the length of the boundaries is a small matter when one notes that the dead zone itself covers an area about five times as large as the state of Texas.

On the 80-meter band, the higher frequency meant that ionospheric absorption (in dB) was smaller by about a factor of four. That being the case, it was not surprising to find that contacts in the VKØIR log showed paths with some sunlight on them, after dawn or before sunset at Heard Island. As before, the westward-moving sunset terminator in the U.S. slowly increased the area in eastern North America from which contacts were possible with VKØIR; but, with less absorption, the increase in area on 3.5 MHz was greater than on 1.8 MHz, as it continued somewhat after sunrise at Heard Island.

Again, with less absorption, the area in Western North America was greater on 3.5 MHz than on 1.8 MHz as the paths opened somewhat before sunset on Heard Island. But once the sun set on Heard Island, the small area that was accessible initially was reduced rapidly by the westward-moving dawn terminator.

Perhaps most important was the fact that the angle between the paths into the region and the dawn terminator was small, quickly ending propagation by bringing the effect of ionos-

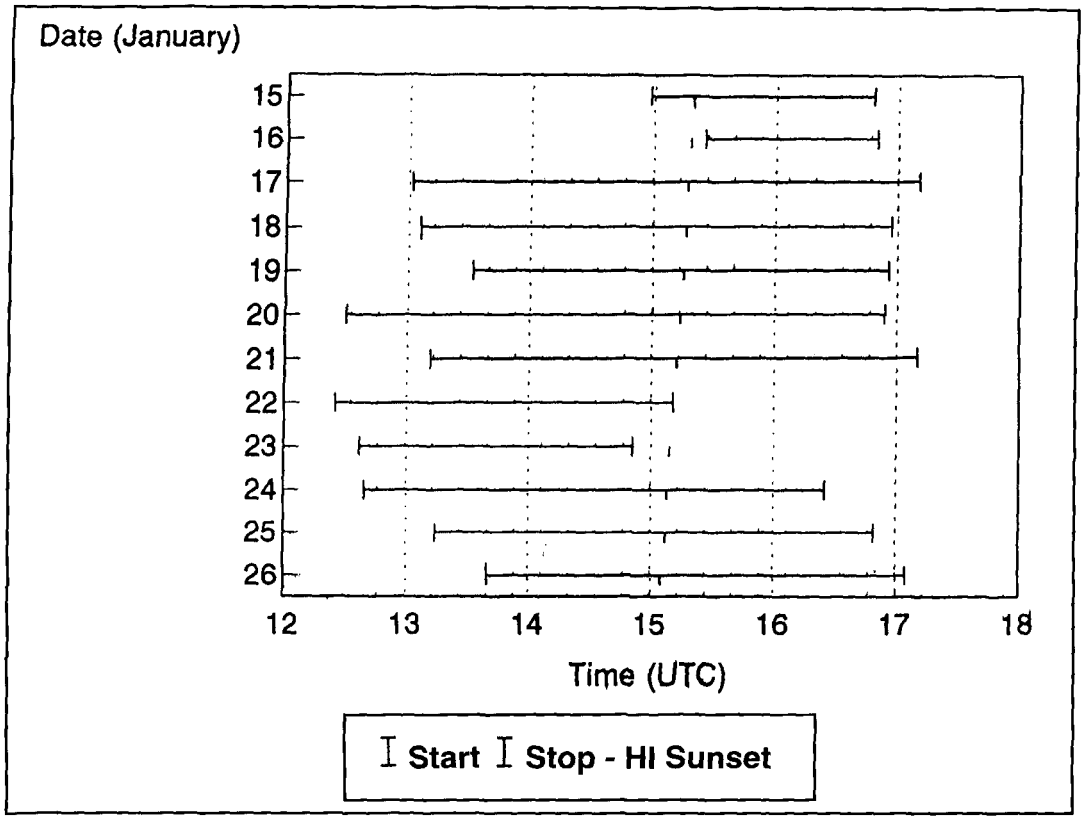

Figure 15. Forty-meter operating times around Heard Island sunset.

pheric absorption to a large portion of a path all at once.

Conclusions

The presence of a dead zone for low-band propagation results from the combination of the location of the antipodal point for a transmitter site falling on a land mass and the terminators at the times of sunrise and sunset at the transmitter. The area of a dead zone is the greatest at the time of the solstice and decreases toward zero as the equinox approaches.

In addition to Heard Island, discussed in this article, the other French sub-Antarctic islands, Crozet, Kerguelen, and Amsterdam, have antipodal points that are close to or within the Continental U.S. The dead zone for Crozet Island only includes a small portion of the Pacific Northwest during December, while Kerguelen Island's is similar to that for Heard Island, as the antipodal point is about 4 degrees further south but still within Canada. For Amsterdam Island, the antipodal point falls at 38N, 102.4W, close to the Colorado-Kansas border; as a result, the area of its dead zone is much smaller than that of Heard Island's at any given date.

There is the possibility of dead zones without having the transmitter's antipodal point fall within a large land mass. Australia is a case in point for low-band operations during DXpeditions in the austral summer. With a transmitter located well to the west of Australia, say Bouvet Island (55.4S, 3.3E), it is possible to have a large fraction of the continent in a dead zone, to the east of where the local terminator falls at the time of sunset on Bouvet Island. The large difference in longitude, just over 110 degrees in this case, is the determining factor; no such problems would occur for the French sub-Antarctic island.

Finally, except for invoking the power of ionospheric absorption on low-frequency signals, the present discussion has been largely of a geometrical nature: i.e., the location of terminators and great-circle paths. There is little further discussion needed for terminators, except to recognize their inherent fuzziness for ionospheric applications due to the nature of twilight. Great-circle paths, in the first instance, are geometrical in nature—but for radio propagation. It is understood that Ionospheric refraction along a path may result in deviations from the geometry of a great-circle calculation. The sideward deviation of signals is the result of electron density gradients perpendicular to the

advance of a ray path, the path refracted away from the regions of greater ionization.

There are always such gradients in the *F*-region, as illustrated in **Figure 3**, and they will result in a certain amount of skewing of paths during quiet conditions. Those are not normally noted; only unusual path directions come to our attention. That skewing is usually due to intense, concentrated gradients of ionization at auroral latitudes. In that regard, such auroral disturbances are always accompanied by geomagnetic activity and are found in the records of high-latitude magnetometers. They are readily identified by high K-values in the published records of A- and K-indices from the magnetometers.

For the Heard Island DXpedition, it was a time of relative quiet at auroral latitudes, shown by the Kp-values in **Figure 6** along with K-indices from the nearby Kerguelen magnetometer and the auroral energy input, as obtained from satellite-borne particle detectors. On the days of the 1.8-MHz operations, the Kp index was 2+ or lower; while for the days of 3.5-MHz operations, the Kp was 30 or lower for all but two three-hour periods. Higher levels of geomagnetic activity, Kp=4 and 5, were encountered only after the 1.8-MHz and 3.5-MHz operations had ended. Because those frequencies are the most sensitive to any auroral effects, one can conclude that there was little in the way of skewing or other absorption that would affect the discussion of great-circle paths relative to geometry of the dead zone.

Acknowledgments

I am indebted to Robert Schmieder, KK6EK, for permission to analyze the logs of the Heard Island Antarctica DXpedition and to Robert Fabry, N6EK, for providing them in a timely manner. In addition, through the efforts of Carl Luetzelschwab, K9LA, I was able to obtain the magnetometer data from the French Antarctic Islands. Dr. David S. Evans of the Space Environment Laboratory at NOAA provided the NOAA/TIROS satellite data on auroral energy deposition and Kp/Ap data for the times of interest.

Beyond those special acknowledgments, I must express my debt to the operators who manned VKØIR during difficult circumstances; without their efforts, this study would not have been possible. ■

L.B. Cebik, *W4RNL*
1434 High Mesa Drive
Knoxville, Tennessee 37938-4443
e-mail: <cebik@.utk.edu>

MODELING AND UNDERSTANDING SMALL BEAMS: PART 8

Capacity hats and Yagis

For horizontal antennas, capacity hats seem to have gone out of style. However, we may be overlooking a useful means of shortening Yagi antennas by neglecting what some call "capacity loading." In fact, by using hats, we can construct quite a useful two-element Yagi and gain something over inductive loading.

The elements for the proposed Yagi were just under 75 percent of full size, so I calculated the anticipated hat size using the usual means for antennas down to about 2/3 normal length. The results were far off the dimensions modeled on NEC-2. The shortened capacity-hat two-element Yagi for 10-meters built as a test prototype answered closely to the NEC results. The success of the antenna suggested that the traditional methods for calculating hats might need some revision to calibrate them to NEC models. Both the calibration and the antenna are worth noting, if for no other reason than to restore capacity hats to the repertoire of techniques for building shortened Yagi beams.

Modeled antennas with hats

A hat is a "loading" assembly attached to the end(s) of an antenna element. It has two very significant properties. First, it is used to bring a shortened antenna to resonance or some other specific set of characteristics. An example of the use of a hat for other than feedpoint resonance is the shortening of a parasitic element in a Yagi. Second, the hat does not contribute to the radiation of the overall antenna element.

In these two characteristics, the hat performs like a lumped constant load inserted at the feedpoint (center-loading for a dipole, base-loading for a vertical) or along the antenna element (mid-loading for a dipole, center-loading for a vertical). For a given antenna length down to about 60 degrees (for a vertical or for each side of a dipole), a hat generally provides greater efficiency than other forms of loading.

A hat performs its function as a significant physical structure rather than as a lumped component. To programs like NEC and MININEC, an antenna is just a physical structure along which currents flow. Inductive and capacitive loads are treated as lumped constants. Hats, however, are parts of the structure and modeled as such. Models may thus provide some insight into hat operation.

Related to the hat is the bent antenna, one with the element beginning in one direction and, at a certain point, taking off in a direction 90 degrees different. The bent vertical over perfect ground, modeled in **Figure 1**, illustrates the current flow along the antenna. Notice that the current in the bent portion contributes significantly to the overall antenna pattern, as illustrated in the far field pattern modeled in **Figure 2**.

By way of contrast, a hat is a symmetrical structure. Although **Figure 3** shows a Tee configuration, any number of symmetrical structures achieve the same goal. Among the more

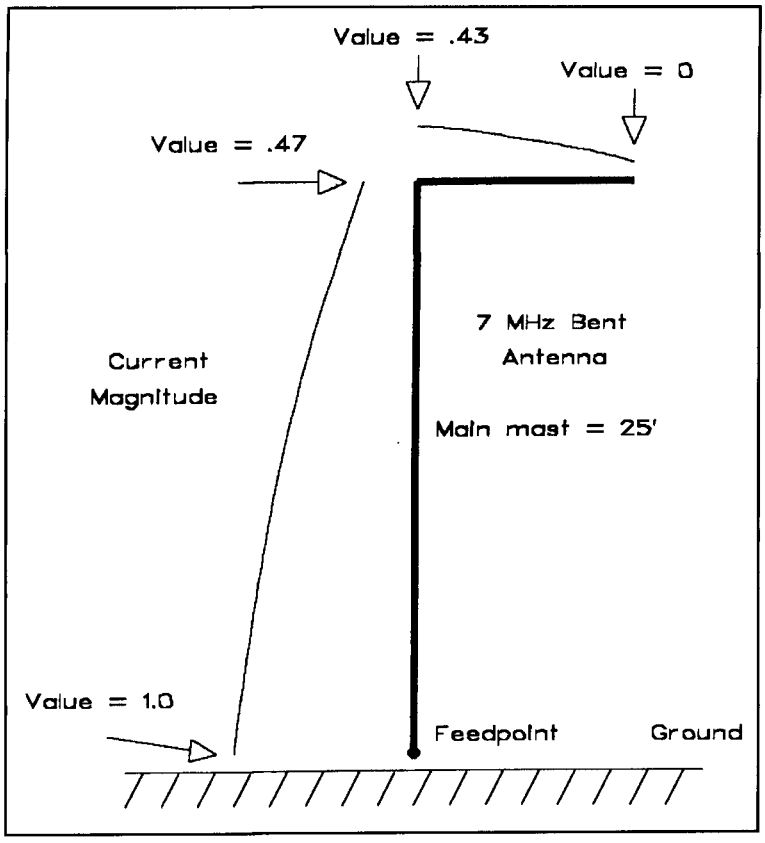

Figure 1. The current flow along a "bent" vertical antenna.

common forms are spokes, circular disks, and other open-frame structures with perimeters, including squares, hexagons, and octagons. Even triangles or simple opposed wires will work well, so long as symmetry is maintained. **Figure 4** shows a few examples of hat structures.

At corresponding points outward from the element end to which the hat is attached, currents are equal but flowing in opposite directions. The result is (if perfect) no resultant field or (within construction limits) a negligible field. **Figure 5** models the far field for an antenna of the same vertical dimension as the antenna in **Figure 2**, but with a hat instead of a bent top. There is no horizontal far field component to the antenna's radiation pattern.

The antenna's current distributes itself at the hub of the hat and flows equally, but at decreasing values, along the hat spokes. If the structure has a perimeter wire, the current then proceeds from the spoke tip in two directions, reaching minimum value at the mid-perimeter points of the framework. Assuming a vertical antenna portion of fixed length, the current level at the hat hub will be somewhat higher than the current level at the bend of an antenna like that in **Figure 1**. The lower level for the bent vertical is occasioned by the interaction of fields at and near the bend point.

Well-modeled antennas with hats provide a close correlation to constructed antennas. The models I have used generally provide enough wire segments in the main element so each segment length is similar to the segment lengths in the hat. The results have been as accurate as my modest shop equipment will allow me to reproduce.

However, hat models tend to drive both NEC-2 and MININEC toward their limits of accuracy, but in different ways. Some hat models in NEC can easily exceed recommended limits for multi-wire junctions and for minimum angles between adjoining wires. If the hat material is of a different diameter than the main antenna element, NEC-2 can respond to some combinations with scarcely credible values for gain and source impedance. Although MININEC handles such junctions as a matter of course, it is sensitive to the acute angles between hat spokes. Moreover, complex hat structures can quickly exceed the allowable number of segments permitted by the program.

Both programs are sensitive to other limitations as well. Nonetheless, models of closed hats structures (with spokes and a perimeter wire) showed a close correlation between programs, while the deviation between the programs with hats composed of spokes alone was usually within 2 percent, or so. I suspect that the antenna current cancellation within the hat assemblies has much to do with the better than anticipated modeling results.

Modeling capacity hats also requires careful attention to detail, depending upon the data one seeks from the model. As suggested in **Figure 6, part A**, the most casual technique in modeling would be to create a dipole and then add outward pointing spokes at each end. Finally, connect the spoke tips with a perimeter wire. Although this model will return correct values for gain and feedpoint impedance, the currents along the spokes will be incorrect with respect to phase at the left (or starting) end of the model. For example, in one 10-meter model, the current phase along the spoke is approximately -4.6 degrees, instead of the figure of 175.3 degrees that the casual model returns.

Reversing the spokes at the initial end to model them from point to hub (main element) will correct this error, as shown in **Figure 6, part B**. However, using single wires to connect the spokes will return an erroneous phase reversal at the midpoints of the wires on both ends. Current is least at the midpoints of the perimeter wires: this is the point at which the model should begin on one end and end on the other. For most accurate modeling of antenna current, each perimeter segment should be split in the

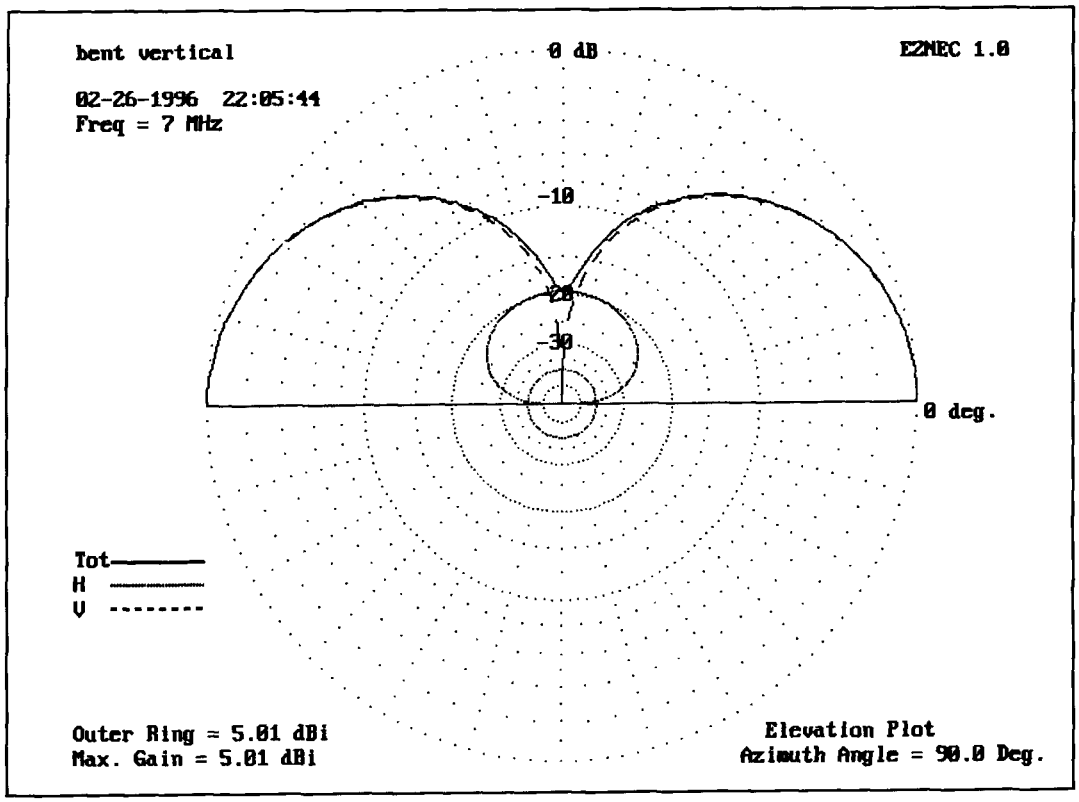

Figure 2. The far-field pattern of the bent vertical, showing both vertical and horizontally polarized components.

middle into two wires, as shown in **Figure 6, part C**. On the initial end, begin from the midpoint and extend the wire to the spoke point. On the finishing end, model the last wires from the spoke points to the perimeter midpoints.

If you only require a little data from your model of a capacity-hat vertical, dipole, or Yagi, quicker casual models will do. However, if you wish to derive the maximum understanding of antenna performance and properties, model with great care. Even with the greatest care in model construction, there remain limits to what method-of-moment models can calculate, especially within the boundaries of non-engineering versions of the programs.

So far, we have a shortened antenna with a symmetrical physical end structure called a hat. However, looking at the antenna this way alone does not yet justify calling the assembly a capacity hat.

Capacity hats

According to the classical transmission-line analogy for antennas, we may view an antenna as a single open-wire transmission line. The usual sorts of antennas investigated from this perspective are either equal to or shorter than quarter-wavelength verticals or half wavelength dipoles. If not resonant, these antennas will exhibit capacitive reactance. Hence, lumped

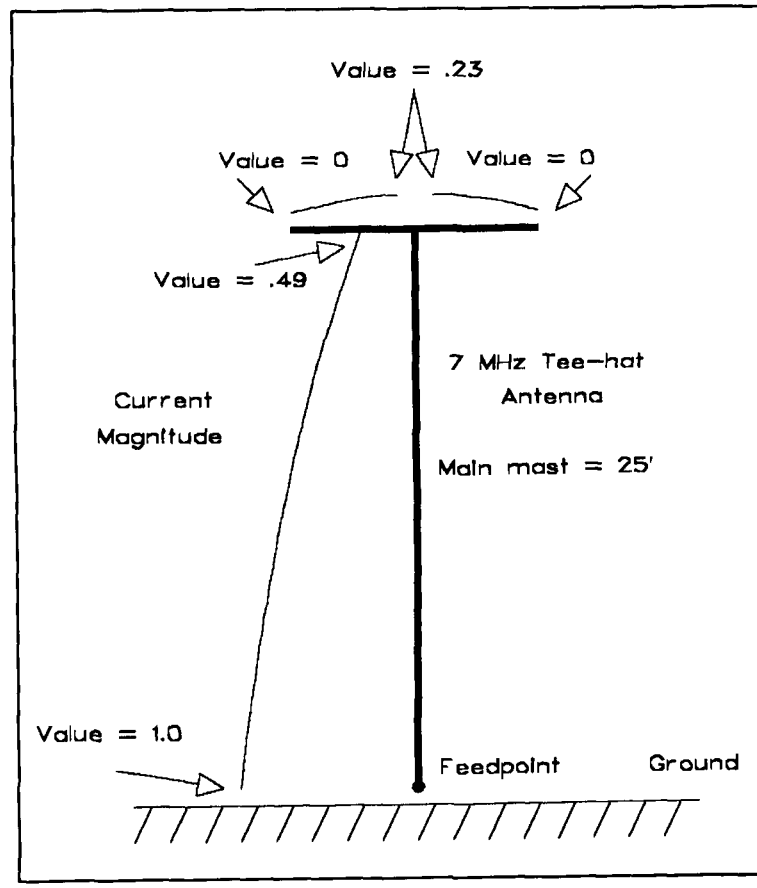

Figure 3. The current flow along the elements of a hat structure.

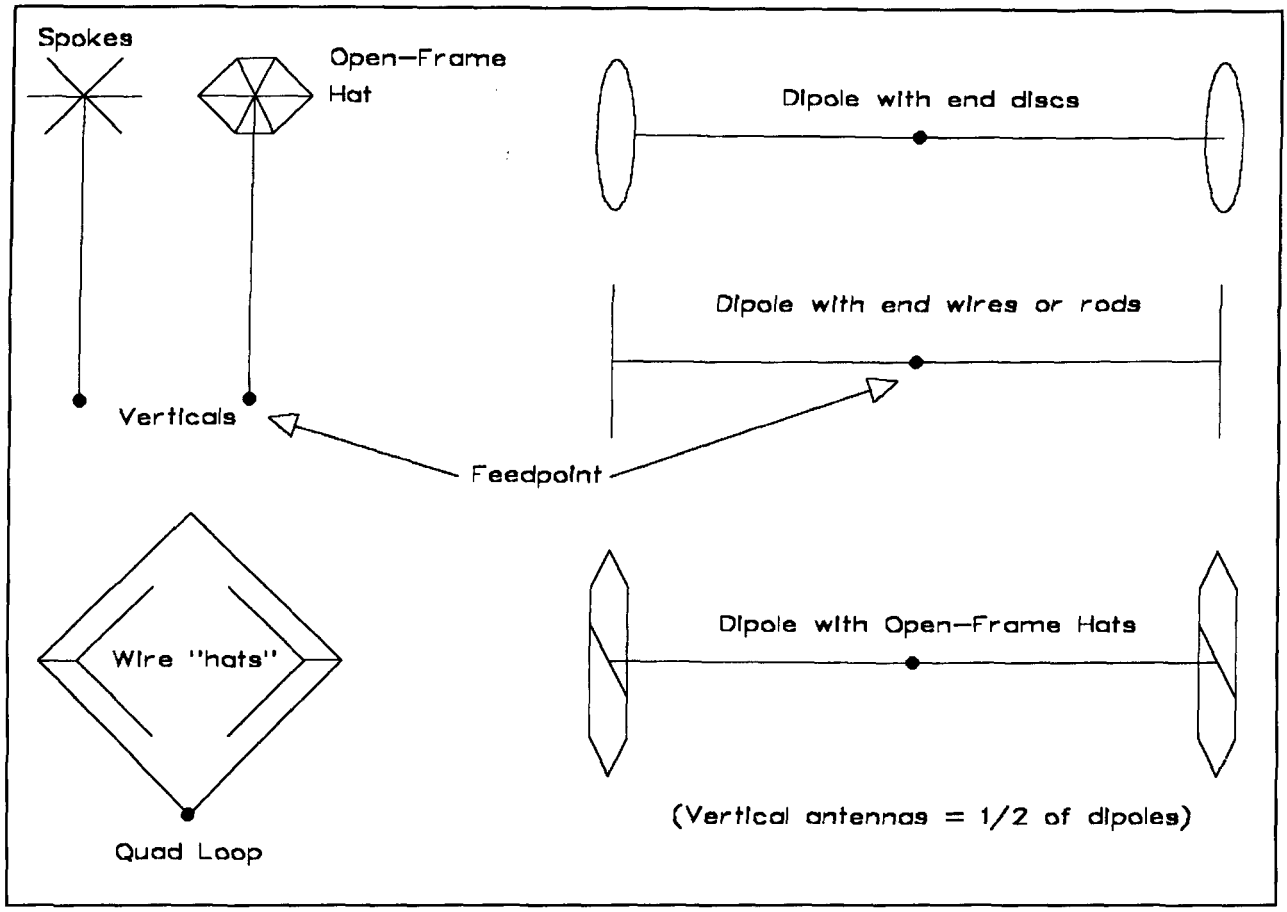

Figure 4. Some examples of *hat structures*.

component inductive loads may be used to increase their electrical length.

Alternatively, one may calculate the amount by which an antenna is shorter than resonant in electrical degrees. If we know the characteristic impedance of the antenna-transmission line, we can use this figure in the same way we do for parallel line capacitive stubs to calculate the necessary size of a corresponding single-wire "stub" for the end of the antenna.

A stub for a single wire transmission line will have a different construction from parallel line stubs. It will appear as a symmetrical surface or framework of a size providing the necessary capacitive reactance called for by the calculation of the missing antenna segment. This is the capacity hat.

Thinking of the hat as a capacitor "plate" can lead to many misleading conceptions about hats. Although real-world antennas capacitively couple to many conductive objects and surfaces, the capacity of a capacity hat is not a function of coupling to anything. For example, the capacitance between capacity hat "plates" for a free space dipole at 3 MHz and 2/3 resonant length is under 0.05 pF. Hat "capacity" is a function of the capacitive reactance necessary to bring a shortened antenna to resonance (or some other specification) under the transmission-line analogy calculation. The value of calculating it is to convert the electrical property of reactance into a physical property: area. The standard model surface for a hat has long been the circular disk with no thickness in isolated free space. Standard references correlate its diameter to a certain capacitance.

$$C = 0.8992d \text{ or } d = 1.1121C \quad (1)$$

where C is the capacitance in pF and d is the diameter of the disk in inches.[1]

The capacitance of open-frame capacity hats made up of spokes and (optionally) a perimeter wire is not the same as that of a flat disk. Open-frame capacity hats have a finite thickness. Moreover, the capacity of the hat will vary with the number of spokes in a complex manner. Therefore, the simple correlation between disk diameter and capacitance will not work for these types of hats.

As an exercise, I constructed models of hats at 3 MHz for a 60-degree long, 1-inch diameter antenna using increasing numbers of spokes for

both spoke-only and perimeter-wire configurations. The hats in the models used #28 wire to approach a condition where the thickness was insignificant relative to the surface area. The exercise ceased at 32 spokes, which approaches or exceeds the NEC-2 recommended number of wire junctions at any given point on an antenna. The data points included 3, 4, 6, 8, 12, 16, 24, and 32 spokes, which were then resolved into curves fitting the following equations:

$$L_T = L_S + [(.4225 \ln \frac{N_H}{N_X})^{EE} \cdot (L_L - L_S)] \quad (2)$$

where L_T is the spoke length, L_S is the shortest spoke length (at 32 spokes), L_L is the longest spoke length (at 3 spokes), N_H is the highest number of spokes considered (32), and N_X is the number of spokes presently in question. The exponent, EE, is given by:

$$EE = 2.2 - [.03(N_X - N_L)] \quad (3)$$

where N_L is the lowest number of spokes considered (3). This simple curve-fitting exercise made it possible to generate graphs on a linear baseline, as shown in **Figure 7**.

The significance of the curves is that they indicate a convergence in the vicinity of about 60 inches. This value would approximate a solid disk, because adding more spokes would not significantly further reduce the length of each spoke. A disk with a diameter of 120 inches would have a capacitance of approximately 108 pF. This value is from 30 to 60 percent distant from values generated by any of the transmission-line analogy equations. Nonetheless, one can correlate open-frame hats to antenna element loading requirements and to modeled hats in a rough but systematic manner. See **Appendix A** for further notes on calibrating transmission-analogy calculations to NEC-modeled hats.

Whatever the correlation may be between capacity hats and loading requirements, it will work equally well for a vertical over perfect ground and for each end of a dipole in free space with no ground reference of any sort. The same holds true of open-frame hat structures. In short, the hat should be thought of in the same way we think of parallel transmission-line capacitive stubs: both provide requisite amounts of reactance where it is needed. Like stubs, capacitive hats are thrown off their prescribed task by being too closely coupled to external objects.

Calculating capacity hats

Modeling a capacity hat is a matter of trial and error without some guiding approximation of the proper hat size. However, without exten-

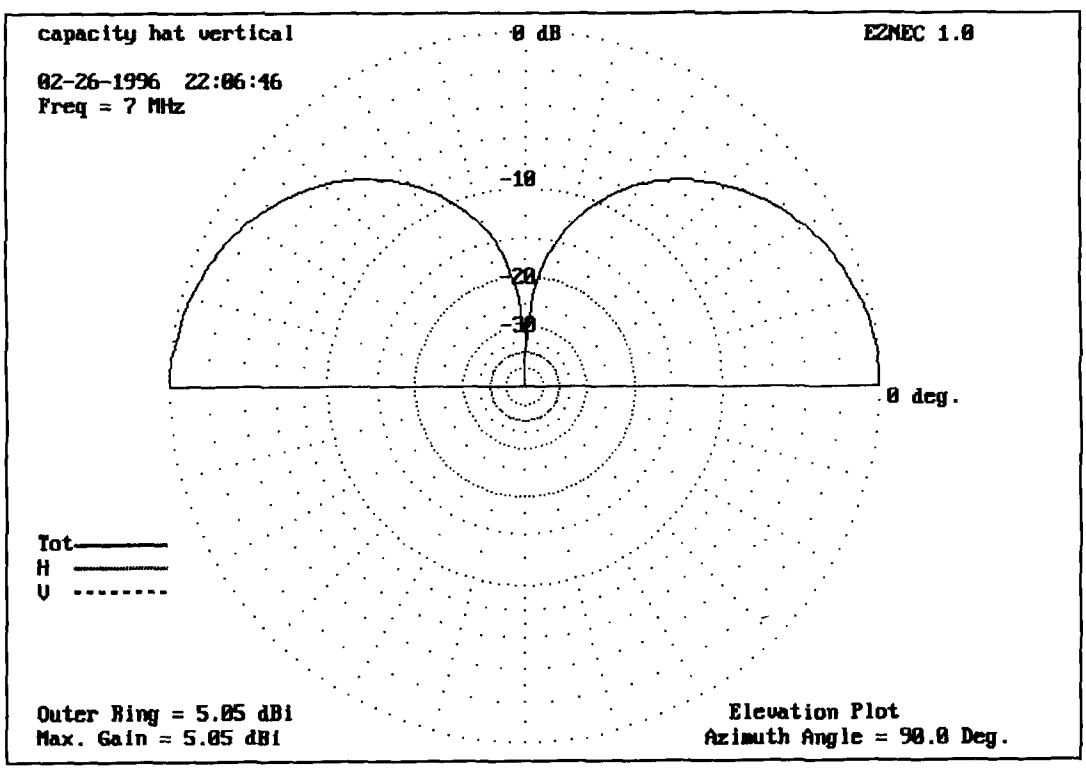

Figure 5. The far-field pattern of a hatted vertical. Note the absence of a horizontal component.

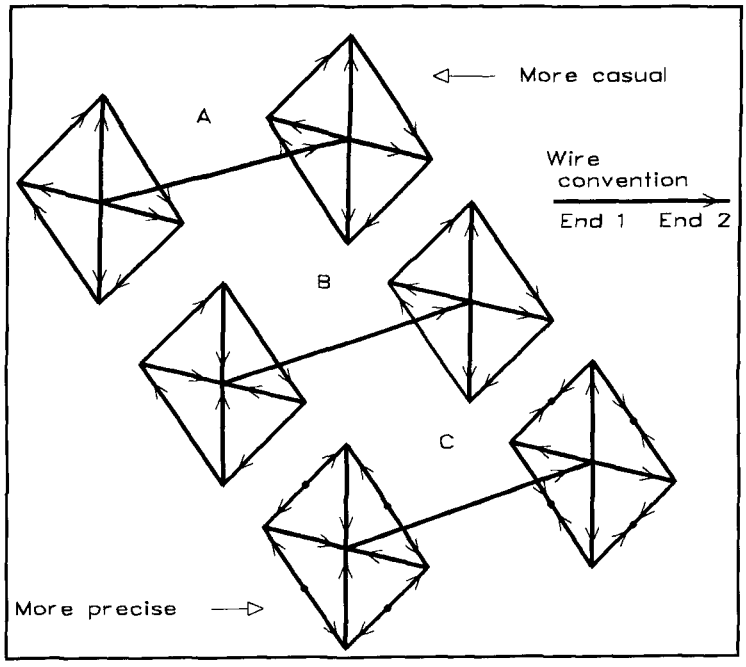

Figure 6. Moving from very casual to more precise methods of modeling. The arrows indicate directions of wires from End 1 to End 2 in NEC wire table conventions. The sample dipole consists of a 10.6-foot 1-inch aluminum element with 1-inch material also used in the hat, which has 0.8-inch spokes.

sive modification, classical VLF calculations of hat size provide confusing guidance, if any at all. (See **Appendix A** for further notes on this subject.) Here we shall briefly look at the traditional transmission-line analogy.

Figure 8 shows the essential elements of two antennas: a conical dipole and a wire dipole. For the conical dipole or bi-conical transmission line, the ratio of voltage to current will be the same everywhere along the length of the dipole (ignoring the ends). Hence, the antenna-transmission line has a constant or characteristic impedance, Z_0. Thin wire antennas only approximate this condition: the impedance varies along the wire and is greatest at the ends. However, it is useful to derive the average impedance of the antenna and to use that figure as if it were the characteristic impedance.

As Belrose has noted in his review of resolutions to the integrals that describe the average characteristic impedance (Z_0) of antennas, there are at least four different formulations: Shelkunoff, Laport, Howe, and Labus (as modified by Jordan and Balmain). All were developed for low frequency applications.[2] The methods all give different values for Z_0 and consequently for the requisite loading capaci-

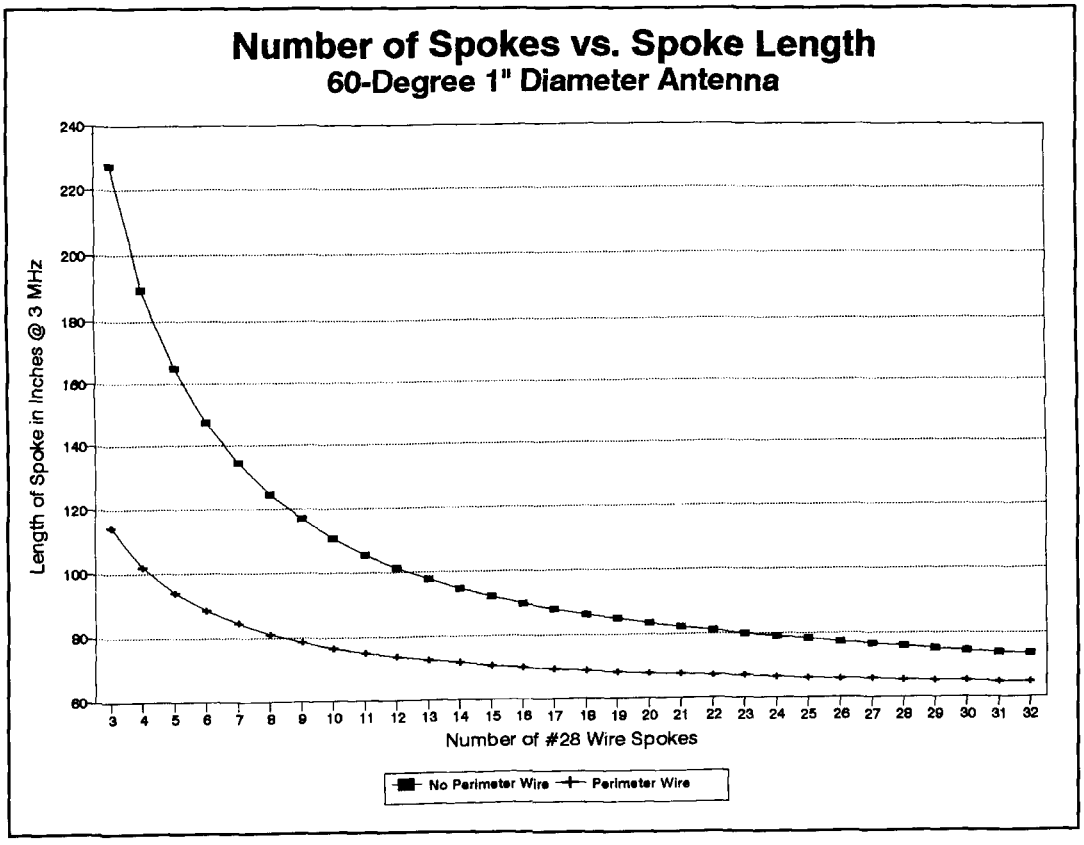

Figure 7. The required length of spokes versus the number of spokes in spoke-only and in spoke-plus-perimeter-wire capacity hats (from 3 to 32 spokes) at 3 MHz for a 60-degree-long, 1-inch diameter aluminum antenna.

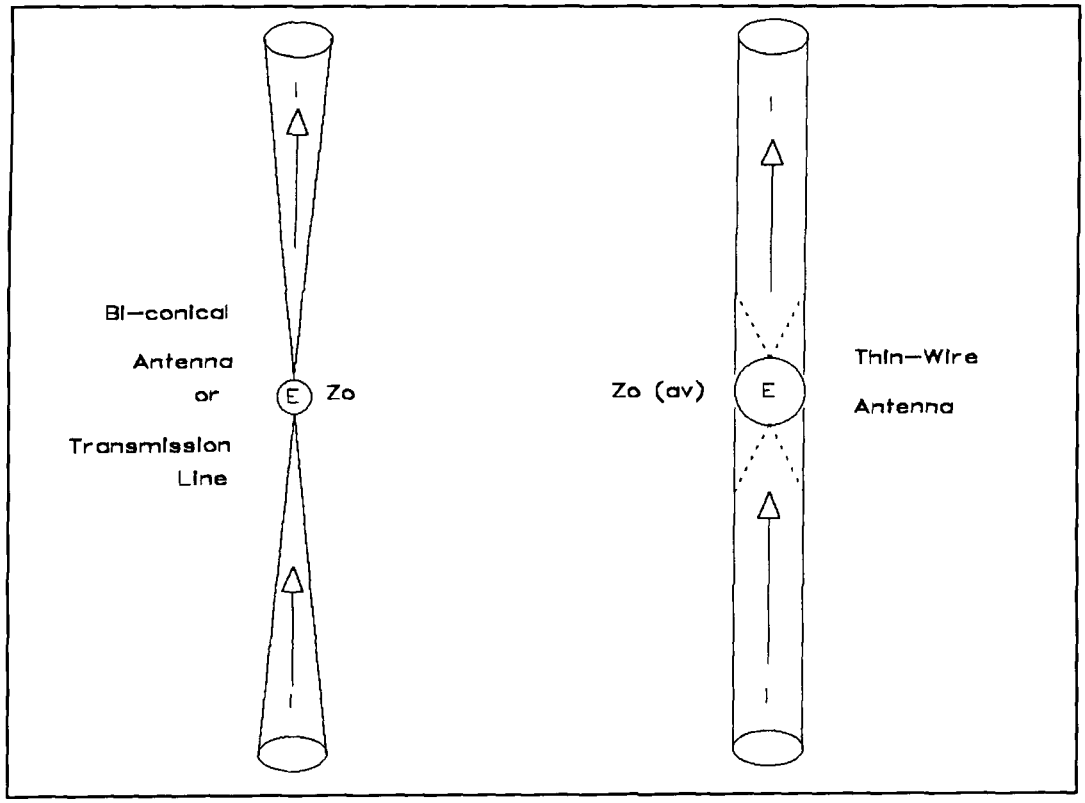

Figure 8. A bi-conical antenna transmission line and a thin-wire antenna.

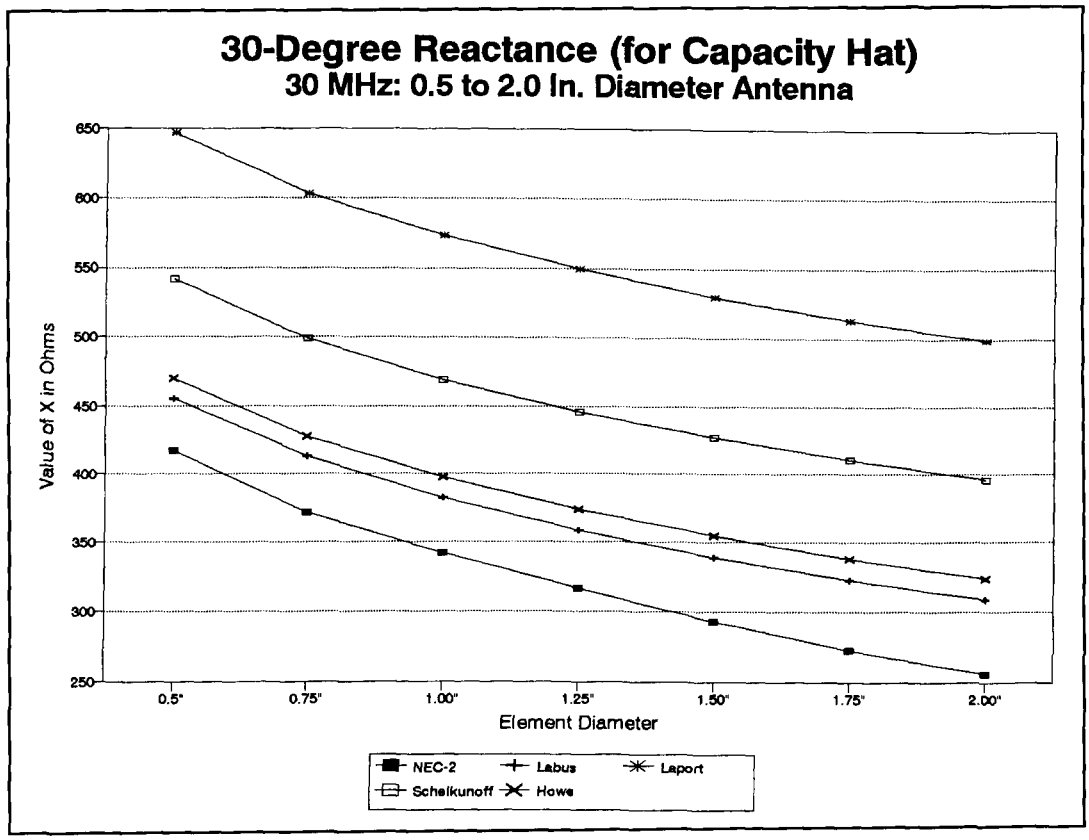

Figure 9. A comparison of calculated "loading" (compensating) reactances derived from several formulations of the characteristic impedance equation. The line labeled "NEC" is the curve of values derived from the feedpoint reactance of 30-degree-long verticals over perfect ground and 60-degree-long dipoles in free space.

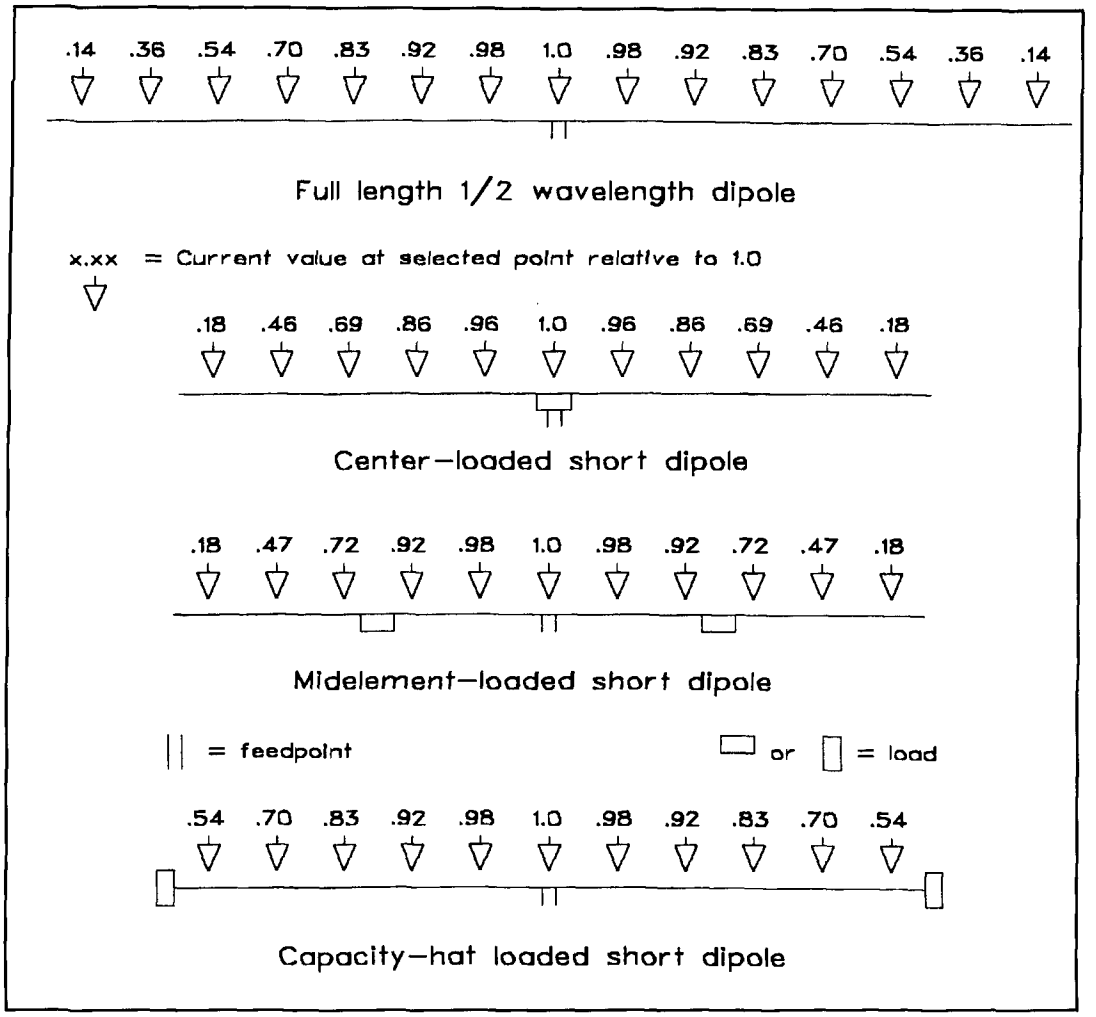

Figure 10. Simplified portrait of current levels along a full-size, center-loaded, mid-element loaded, and capacity-hat loaded dipole.

tive reactance and its associated capacitance at the frequency of interest. **Figure 9** demonstrates the differences at 30 MHz, using capacitive reactance as the comparative figure for a 30-degree compensating hat. None closely approaches the reference curve of reactances derived from NEC models of 30-degree long antennas, which most closely approximate the values of capacitance indicated by exercises illustrated earlier in **Figure 7**.

Belrose adopts Howe's equation as yielding results for feedpoint impedances that agree most closely with measured results. For purposes explained in **Appendix A**, I shall note the Shelkunoff equation to illustrate the calculation technique. This is also the version used by Schulz and appears in ARRL publications.[3] For dipole antennas less than a half wavelength long,

$$Z_0\,(\text{av}) = 120[\ln(2h/a) - 1] \qquad \textbf{(4)}$$

where Z_0(av) is the "average" characteristic impedance of the antenna, h is the overall height or length of the antenna element, and a is its radius (with h and a in the same units and where h is much greater than a). For a vertical antenna, a quarter wavelength or less in height, the multiplier is halved:

$$Z_0\,(\text{av}) - 60[\ln(2h/a) - 1] \qquad \textbf{(5)}$$

For clarity, the following discussion will be limited to shortened vertical antennas at least 60 electrical degrees long; that is, at least 2/3 full size. To apply the discussion to dipoles in free space, think of the dipole as two verticals base-to-base.

Neither **Equation 5** nor any of the other versions noted above provides a basis for correlating open-frame capacity hats to antenna element lengths of varying diameter throughout the HF frequency range (3 to 30 MHz). Because the antenna diameter is a significant

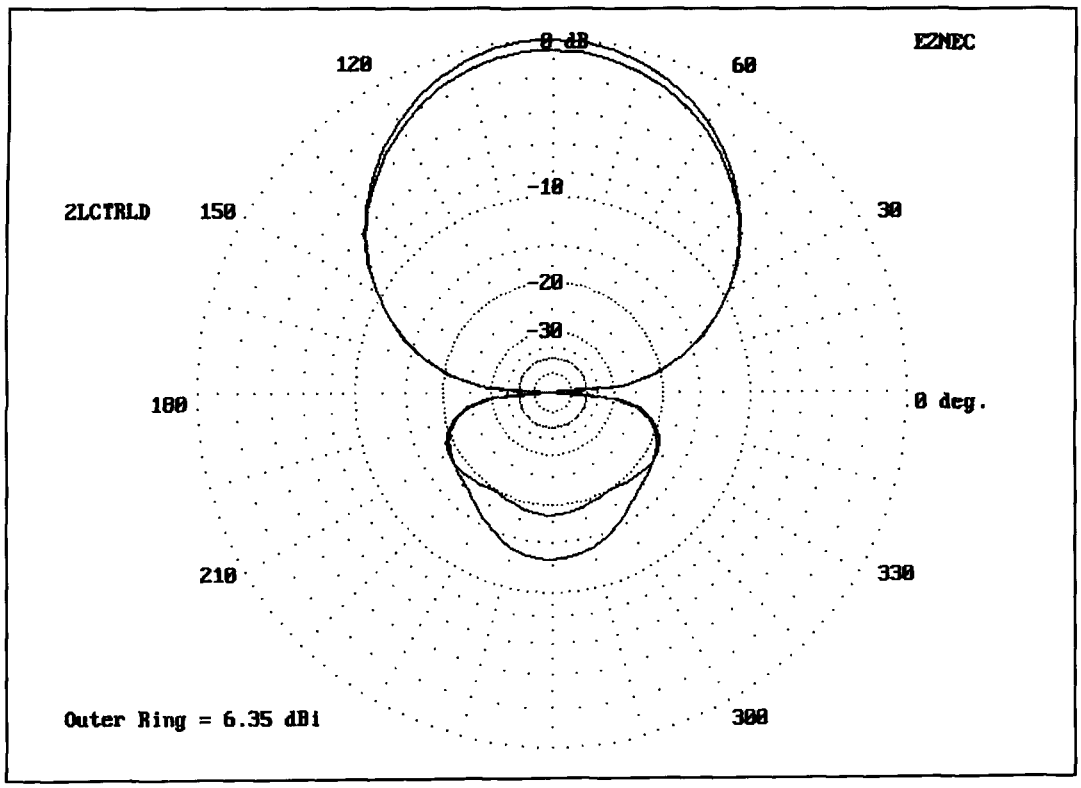

Figure 11. Free space azimuth patterns for two-element center-loaded and capacity-hat loaded Yagis using identical element lengths.

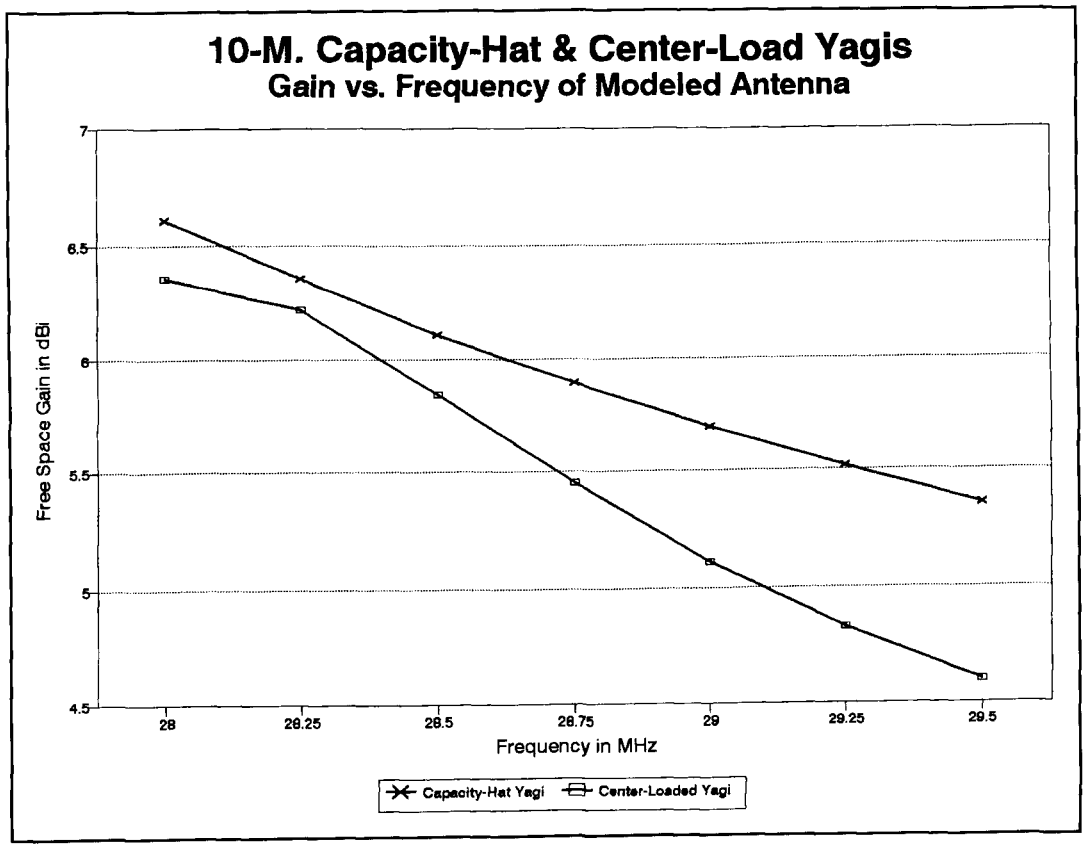

Figure 12. Comparative gain from 28 to 29.5 MHz of center-loaded and capacity-hat loaded two-element Yagis.

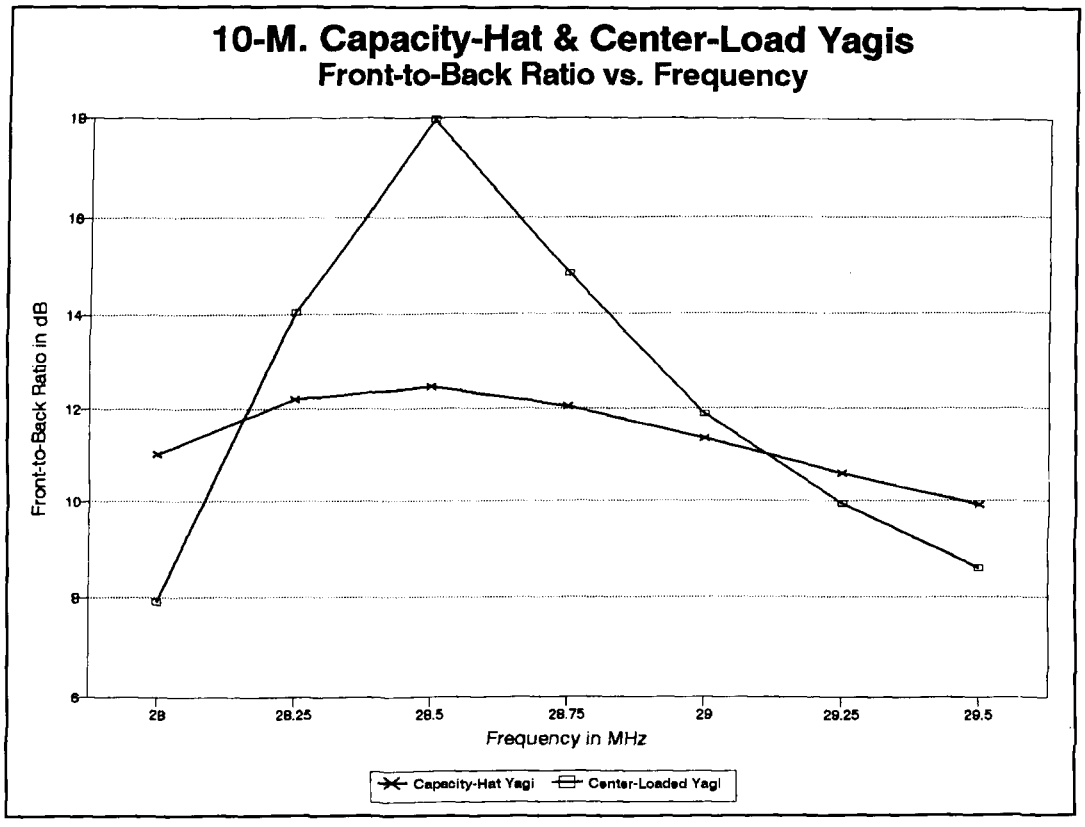

Figure 13. Comparative front-to-back ratios from 28 to 29.5 MHz of center-loaded and capacity-hat loaded two-element Yagis.

percentage of antenna length at HF, and a varying one as the frequency increases, we must introduce a corrective based upon the ratio of diameter (or radius) to length. The diameter corrective will yield consistent results as the main element is varied in diameter at any given frequency, but the correlation varies as the frequency is raised. Hence, an additional frequency corrective is needed.

The remainder of the required calculation is provided by most recent editions of *The ARRL Antenna Book*. The difference (in electrical degrees) between the shortened antenna and the full-size antenna represents the number of degrees of capacitive reactance to be supplied by the capacity hat. The required capacitive loading can be found in two simple equations:

$$X_C = -j\cot\theta Z_O \text{ or } X_C = -jZ_O/\tan\theta \qquad (6)$$

where Z_o is the average characteristic impedance just calculated, X_c is the required capacitive loading reactance in ohms, and θ is the required loading length in electrical degrees; that is, the missing part of a quarter wavelength. From the capacitive reactance, we move to the required capacitance:

$$C = 10^6/2\pi f X_C \qquad (7)$$

where f is the frequency in MHz and C is the capacitance in pF. Ostensibly, we need only move to **Equation 1** in order to convert this value into the diameter of a capacity hat. However, we have already seen that complex open-frame hat structures do not answer readily to this simple maneuver.

Capacity hat dipoles and Yagis

To construct a capacity hat dipole, simply construct two vertical antennas, base-to-base, and feed at the base junction. The capacity hat sizes for any given frequency and choice of materials will be virtually identical to those calculated for a vertical. Expect the feedpoint impedance of a 120-degree dipole to be about double that of a corresponding 60-degree vertical: about 59 ohms compared to 28 ohms.

Horizontal capacity-hat dipoles do not suffer the same type of ground loss as ground-mounted verticals. Assuming similar structural losses as a vertical due to the choice of antenna and hat materials, as well as construction methods, a capacity-hat dipole is subject to standard ground reflection losses that depend upon ground quality. Capacity-hat dipoles do not radically change their feedpoint impedance when modeled over ground, which makes them

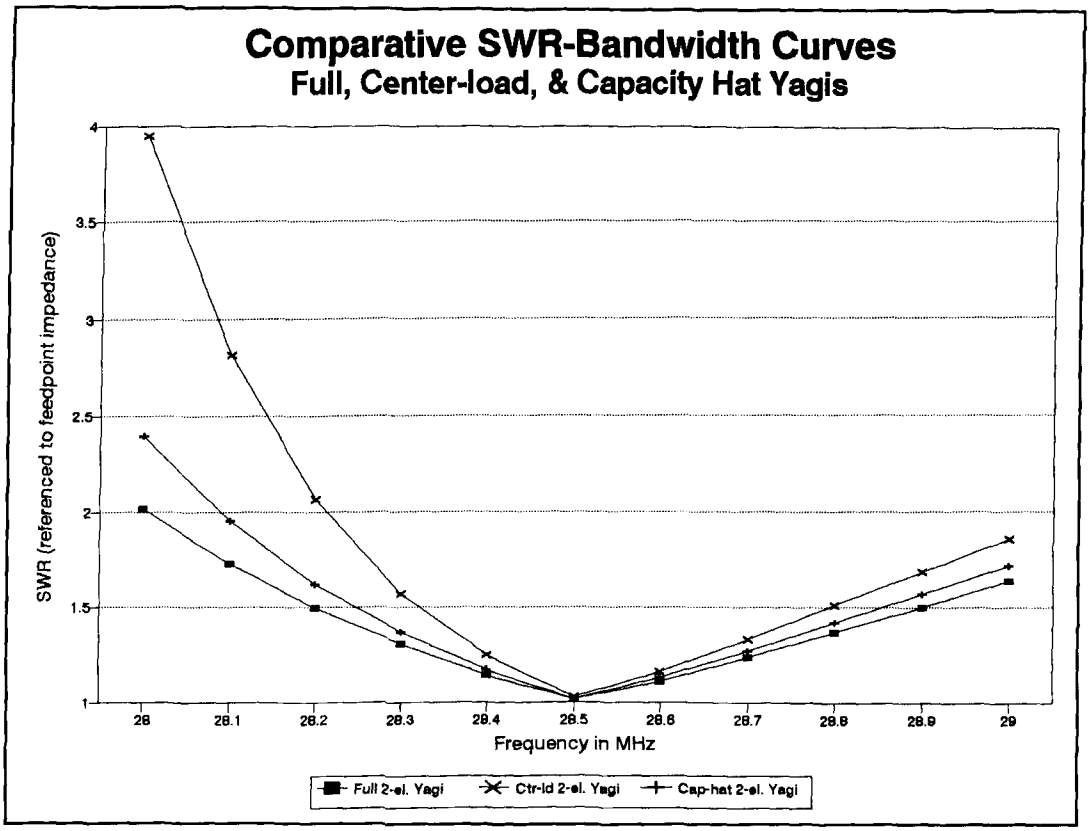

Figure 14. SWR bandwidth curves for full-size, center-loaded, and capacity- hat loaded two-element Yagis, referenced to the feedpoint impedance.

reasonably close matches for 50-ohm coax feedlines. Moreover, they do not suffer nearly the degree of narrowed SWR bandwidth experienced with center-loaded dipoles.

The comparative gains of 120-degree dipoles (twice the length of a 60-degree vertical) when center loaded with a 300-Q inductor (a generous value out of doors) and when capacity-hat loaded are approximately 1.85 dBi and 2.05 dBi, respectively. **Figure 10** demonstrates the reason for the difference: the capacity hat dipole maintains close to the same current levels—increment for increment—as a full-size dipole, whereas the center-loaded dipole shows lower current levels everywhere along the element. The gain differential for a dipole is small, perhaps small enough to be ignored in operation. However, when such dipoles are placed in a two-element Yagi configuration, they suffice to alter performance more significantly.

The center-loaded Yagi can attain a higher front-to-back ratio, which can be tailored to some degree by changing the reflector inductor Q. However, the increase comes at the expense of forward gain. The capacity-hat Yagi exhibits higher gain that approaches the value for a full-size Yagi of the same spacing. At the same time, its front-to-back ratio is limited essentially to the levels achieved by a full-size two-element Yagi. **Figure 11** provides comparative free-space azimuth patterns for the two types of Yagis using identical element lengths, diameters, and spacings. **Figure 12** shows in graphical form the gain across the 10-meter band of center-loaded and capacity-hat-loaded Yagis with elements of identical length, diameter, and spacing. **Figure 13** shows the front-to-back ratio across the band for the same antennas.

The weight one gives to the relative advantages of center-loaded and capacity-hat Yagis depends upon the requirements of the application. For general amateur work, the greatest advantage of the capacity-hat Yagi may lie in its broader SWR-bandwidth curve. **Figure 14** compares 10-meter two-element Yagis of comparable spacing. The capacity-hat model more closely approximates the performance of a full-size antenna than does the center-loaded model (set for a load Q of 300). Moreover, the capacity hat Yagi also maintains its other characteristics—gain and front-to-back ratio—over a wider bandwidth. The capacity-hat Yagi is at least a candidate for a small monoband Yagi—if one can build it.

Building a capacity-hat Yagi

The test antenna was a 10-meter two-element Yagi with the following dimensions: driven

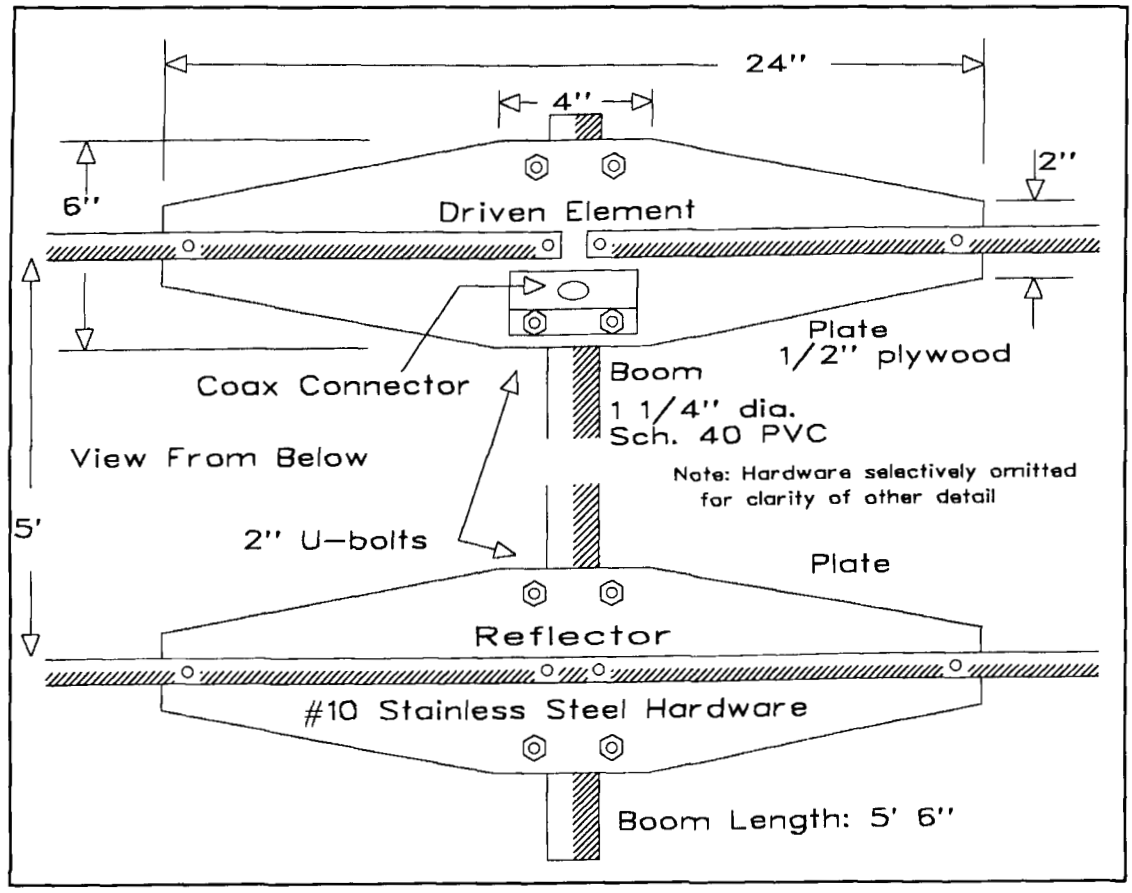

Figure 15. General construction of a two-element, 10-meter capacity-hat loaded Yagi.

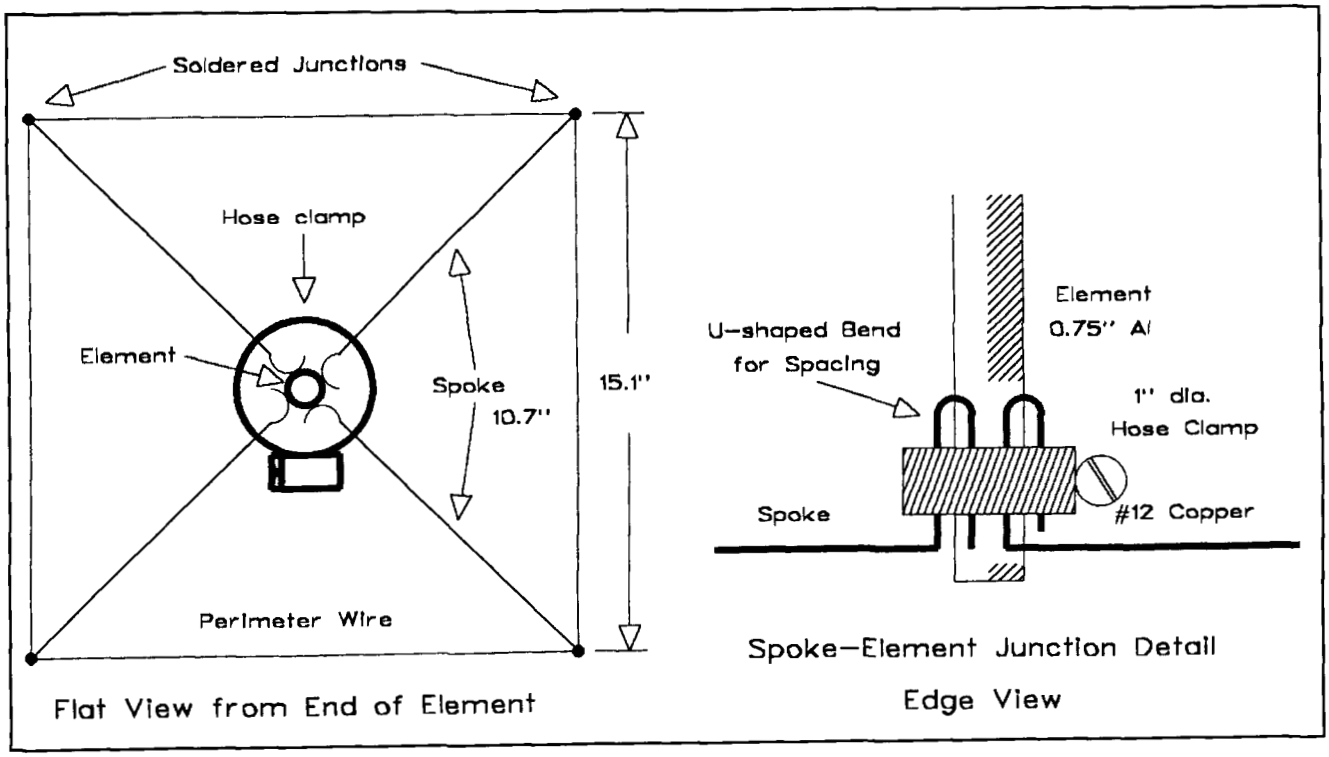

Figure 16. Simple hat construction for the 10-meter beam.

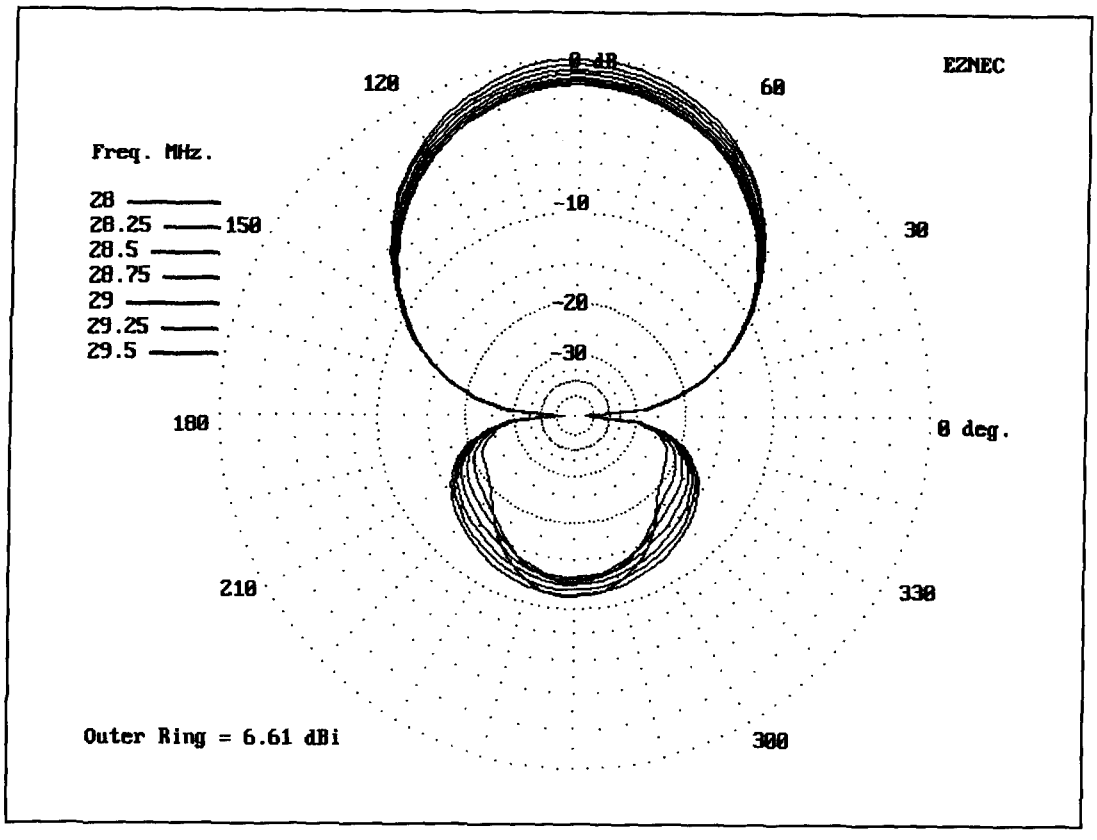

Figure 17. Free-space azimuth patterns for the 10-meter capacity-hat Yagi across the band.

element, 11 feet 7 inches; reflector, 12 feet 2 inches; spacing, 4 feet 3 inches; elements, 0.75-inch diameter hardware-store aluminum (0.05-inch wall thickness). These dimensions are the same as those for the linear-loaded antenna used as a test model. In fact, the capacity-hat antenna was created by removing the linear loads and adding capacity hats to the element ends. **Figure 15** reviews the general construction methods used for the PVC boom and half-inch plywood element plates.

Because the linear loads (or corresponding inductive loads) were of equal value for the driven element and for the reflector, I anticipated that I would need capacity hats of equal size for these elements. Models indicated that a #12 square hat with a perimeter wire would require spokes between 10.6 and 10.8 inches long for both elements. I constructed four "identical" hats from #12 house wire with the insulation removed. Using a scrap of plywood about 2 feet square, I drilled a 3/4-inch hole in the center and laid out the spoke and perimeter wire runs in pencil. I then placed a short scrap of 3/4-inch diameter aluminum tubing in the hole. The spoke wires were cut long with a 1.5-inch "U" at one end, bent 90 degrees to the spoke. The four spoke Us were placed against the aluminum tube and clamped with a stainless steel hose clamp. The Us spaced the spokes evenly around the outside of the tube. The excess of the U at the curved end was bent outward slightly to prevent the clamp from falling off when loosened. The spokes were temporarily stapled to the base-board along their inscribed paths. Each was about a 1/2 inch longer than the correct spoke length.

The assembly of the hat was a task for a heavy (100 watt) soldering iron or gun. Starting at one corner, I bent the spoke end around the perimeter wire and soldered the junction. Bending the perimeter wire 90 degrees, I proceeded to the next corner and repeated the process, finally ending back where I began. **Figure 16** shows the outlines of the hat on the jig. After construction, each hat was removed from the jig tube by loosening the hose clamp and moved to its element. Because copper met aluminum at the junction, both metals were coated with contact "butter" during assembly. For long-term outdoor installation, the junction should be sealed as much as possible to slow weathering and other dissimilar metal problems.

Models indicated that the individual elements of the Yagi, if fed as dipoles, should resonate at 28.25 MHz for the driven element and 27.3 MHz for the reflector. I pretuned each element by resonating it independently. The maximum

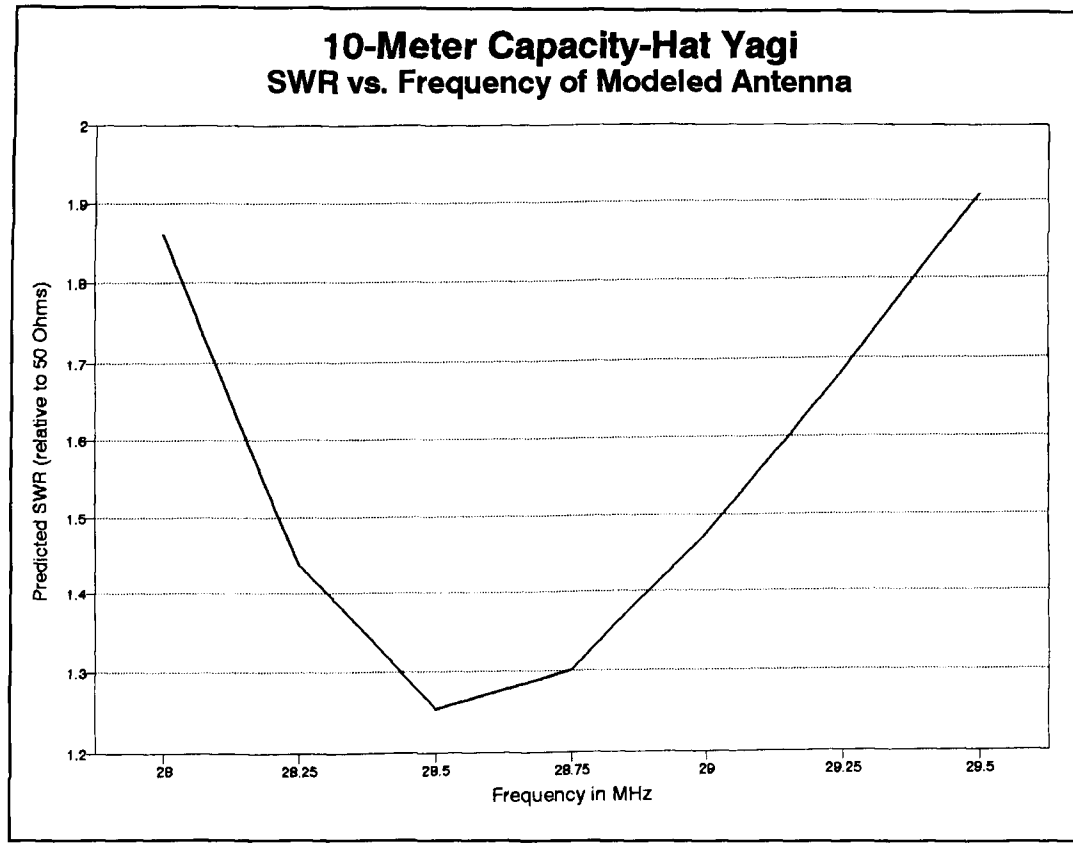

Figure 18. Calculated SWR of the compensated two-element capacity-hat Yagi across 10-meters.

hat placement adjustment required was about a 1/4 inch down the element length, a move likely created by the inexactness of my simple shop technique or by the flaring structure at the hat-element junction, or both. The models proved quite accurate, and each dipole resonated with a feedpoint impedance close to 60 ohms.

Combining elements into a Yagi required two steps beyond mounting the dipoles on the boom. First, the reflector-element feedpoint space was closed with a half-section of tubing across the former feedpoint opening. Second, the driven element feedpoint reactance was compensated by two 300-pF series capacitors, one from each side of the element center. This compensation provided a modeled SWR under 2:1 from 28 to 29.5 MHz without compromising antenna performance.

Figure 17 shows the modeled antenna performance across the 10-meter band. Although the figure does not permit one to sort the lines, the overall consistency of performance in terms of gain and front-to-back ratio is clear. **Figure 18** shows the modeled SWR across the band. Although both figures are for models in free space, at 20 feet above medium ground, the antenna showed no significant variations.

Pretuning the elements individually resulted in a Yagi requiring no further adjustments after final assembly. Band-edge SWR figures were slightly higher than those modeled, rising to about 2.2:1. Local point-to-point tests confirmed performance similar to my full-size two-element Yagi, allowing for a 15-foot height differential. Several months of use has also confirmed the ability of the simple hats to slip the wind and remain well-positioned, since no change of performance of SWR has been noted. However, the dissimilar metal junction should be inspected and renewed at least yearly.

Like its linear-loaded predecessor, the capacity-hat Yagi can be partially disassembled for transport to other operating sites. A 6-foot-long truck bed or van handles the 10-meter antenna with ease.

Conclusion

This exercise began with a simple question: Are capacity hats an apt candidate for short two-element Yagis? The initial model for the 10-meter beam was discovered by a trial-and-error process after handbook calculation procedures missed the mark by a good bit. That failure led to a more detailed investigation of the applicability of classical transmission-line anal-

ogy calculation procedures to HF antennas.

The capacity hat is a very reasonable way to obtain most closely full-size performance from a shortened-element Yagi. Although the hat structure is somewhat more ungainly than a feedpoint linear or inductive load, the capacity-hat Yagi exhibits a broader bandwidth for the essential performance properties of gain, front-to-back ratio, and feedpoint impedance. If these factors are important to a particular operational set-up, then building a capacity-hat Yagi is worth serious consideration.

The other artifact of the exercise, the simple GW BASIC program attached to this article, in conjunction with one of the MININEC or NEC-2 modeling programs, may get you started.* ■

REFERENCES

1. F.E. Terman, *Radio Engineers' Handbook*, McGraw-Hill, New York, 1943, page 113.

2. John S. Belrose, "VLF, LF, and MF Antennas," in Rudge, et al., editors, *The Handbook of Antenna Design*, Volume 2, Peregrinus, London, 1983, pages 562–565, 598–599. See also E.C. Jordan and K.G. Balmain, *Electromagnetic Waves and Radiating Systems*, 2nd Edition, Prentice-Hall, Englewood Cliffs, 1968, pages 390–396, for a treatment of the work of Siegel and Labus. Also recommended is E.A. Laport, *Radio Antenna Engineering*, McGraw-Hill, New York 1952, Chapter 1: "Low Frequency Antennas." Laport notes that even at these low frequencies, we must be "contented" with approximations (page 28). Finally, see S.A. Shelkunoff, *Electromagnetic Waves*, Van Nostrand, New York, 1943, page 290, as well as Jordan and Balmain, pages 384–388.

3. Walter Schulz, K3OQF, "Designing a Vertical Antenna," *QST*, September, 1978, pages 19–21. Schulz's graphs have been replaced by equations in recent editions of *The ARRL Antenna Book*, 17th edition, American Radio Relay League, Newington, 1994, page 2-40.

*All NEC-2 models were done on EZNEC 1.06, available from Roy Lewallen, W7EL.

Appendix A: Calibrating transmission-line analogy calculations to NEC models

The classic process of calculating the required size of a capacity hat to load a shortened vertical antenna to resonance presents a model of apparent simplicity in four steps. Using the height and radius of the main antenna element, one calculates the average characteristic impedance, treating the antenna as a one-wire transmission line. From the characteristic impedance and the "missing" length of antenna relative to a resonant quarter wavelength antenna, one calculates the required capacitive reactance to achieve resonance. That reactance, in turn, converts to a capacitance for the frequency in question. Finally, using a solid disk without thickness as a model, one calculates the diameter of the final capacitive hat.

Unfortunately, for amateur antennas in the HF range, the calculations and the theory underlying them are fraught with problems at every step. However, it seemed possible to at least correlate this independent means of calculating capacity hat size to modeled antenna-hat combinations in the HF frequency range. The attempt is summarized in the accompanying BASIC program (**Appendix B**). The goal was not to add anything significant to the fundamental theory underlying the transmission-line analogy on which the calculation scheme is based. A brief look at a number of the hurdles encountered along the way may be useful in understanding the application of that method to HF antennas in the 60-degree-length range, whether for verticals over perfect ground or dipoles in free space.

For the project at hand—correlating hat calculations to NEC-2 and MININEC models—the exact values of average characteristic impedance, reactance, and capacitance are unimportant except in the most derivative sense, because the feedpoint reactance can be determined by modeling. What the calculations required were values of Z_0, X_c, and C amenable to simple correlation to the spoke lengths of various configurations of open-frame capacity hats. The Shelkunoff equation proved to be best suited to serve as the basis of these correlations. The final form of the modified Schelkunoff equation for the calculation of Z_0 for the HF range became:

$$Z_0(av) = 60[\ln(4Mh/d) - (1 - NF/30)] \qquad (8)$$

where h is the antenna height, M is the inverse of K (the antenna end effect shortening factor), d is the main element diameter, F is the frequency of interest in MHz (and 30 is the highest frequency of interest in MHz), and N is a calculation constant. Because the correctives are only approximate, the selection of N will bias the equation for certain types of capacity hats in preference to others. Using N = 0.583 biases the equation toward square spoke-plus-perimeter-wire closed hats of small hat-wire diameters. The result will be errors up to 5 percent for some types of hats.

There are two separate modifications of the basic Shelkunoff equation to account for varying antenna element diameters and for variations of frequency in the HF range. First, of all the various techniques tried, placing the antenna shortening factor (K, or M in **Equation 1**) into the fundamental formulation

for antenna height yielded the most correct curve for the effect of antenna element diameter on the spread of open-frame capacity hats considered. The same goal might have been achieved using an external correction equation, but it would have added considerable complexity to the calculation.

The first step in the process of finding a usable figure for K is to derive from NEC models an adequate approximation. Resonating models of full-length quarter-wave verticals at the highest and lowest frequencies of interest—here 3 and 30 MHz—over perfect ground allows calculation of intermediate values for K. (Throughout, resonance of a model is defined as a feedpoint reactance of less than ±0.01 ohms.) One very good approximation is:

$$K = K_{hf} + [(\log \frac{F_H}{F})^{K_V} \cdot (K_{lf} - K_{hf})] \quad \textbf{(9)}$$

where K is the antenna shortening factor, K_{hf} is the K of a resonant quarter-wavelength antenna of a given diameter at its highest frequency, K_{lf} is the K of a resonant quarter-wavelength antenna of a given diameter at its lowest frequency, F_H is the highest frequency (for K_{hf}), and F represents any frequency in the range of interest. The exponent, K_V, also varies with frequency,

$$K_V = .033[(F/3) - 1] + .61 \quad \textbf{(10)}$$

for the frequency range 3 to 30 MHz.* The resulting values are those implicit in NEC-2 models and therefore most apt to fit the goal of correlating independent calculations to modeled structures.

The frequency correction factor was applied to the logarithm adjustment factor in **Equation 1** by decreasing the reduction in the logarithm of height versus radius from the standard value of 1. Again, this correction could have been introduced externally to the basic calculation of Z_o, but would have required a more complex formulation, the form of which would have resembled that of the calculation of K, but with a different progression of the exponent. Even the given form of the adjustment is an oversimplification, as letting N = 0.583 is accurate within 1 percent only for small diameter square hats with a perimeter wire of the same diameter as the spokes. Focusing other parts of the matrix of hat configurations considered could vary the value of N by as much as 10 percent.

The value of C, the requisite capacitance that translates into a set of physical dimensions for a capacitive hat, is somewhat arbitrary, even if useful in this exercise. The capacitance value given in the accompanying program is for calculational reference only and not to be construed as a reliable figure. The calculation of a value of C required for a hat provides a convenient number which, when multiplied by a constant for a common hat configuration, results in an approximation of the spoke length required for the hat. Low order hats commonly consist of 4, 6, or 8 open-ended spokes. Alternatively, they may consist of 4, 6, or 8 spokes connected by a perimeter wire. Both modeling and calculations here assume the perimeter wire is the same diameter as the spokes. This assumption may not be true in reality and result in further deviations from calculated sizes. Squares, hexagons, and octagons are perhaps the most common hat geometries hams will use at HF, and **Figure 19** illustrates the three. The key dimension is the spoke length, from which everything else can be hand calculated or laid out on the shop bench. Hams use a variety of element sizes ranging ordinarily from 0.5 to 2 inches in diameter. Hat material is likely to range from #12 wire (0.0808 inch in diameter) up to about 1-inch tubing.

Determining the final constant of correlation between the previously calculated value of capacitance and the spoke length for the various configurations requires modeled hats at the four corners of the matrix: 3 MHz and 0.5-inch antenna element, 3 MHz and 2.0-inch element, 30 MHz and 0.5-inch element, and 30 MHz and 2.0-inch element. For any size spoke material, the modeled length is divided by the capacitance to produce a constant. The four constants are then averaged. The process is repeated for each hat configuration and for each size of spoke material.

With the selection of the value of N given above, deviations from modeled antenna-hat combinations increase with the number of spokes and the increasing size of the hat spoke material. However, the method is accurate to within about 5 percent of the modeled hat size at the extremes of the matrix marked by the frequency range and the hat material range. Over much of the matrix, deviations from modeled antennas is in the 1 percent range.

Accuracy of the calculations can be improved by introducing further "curve-fitting" correctives to the final determination of spoke lengths. They are omitted here, because my purpose has been to provide only initial guid-

* For further notes on correlating the antenna shortening factor to NEC-2 models, see "Calibrating K to NEC," to appear in *QEX*.

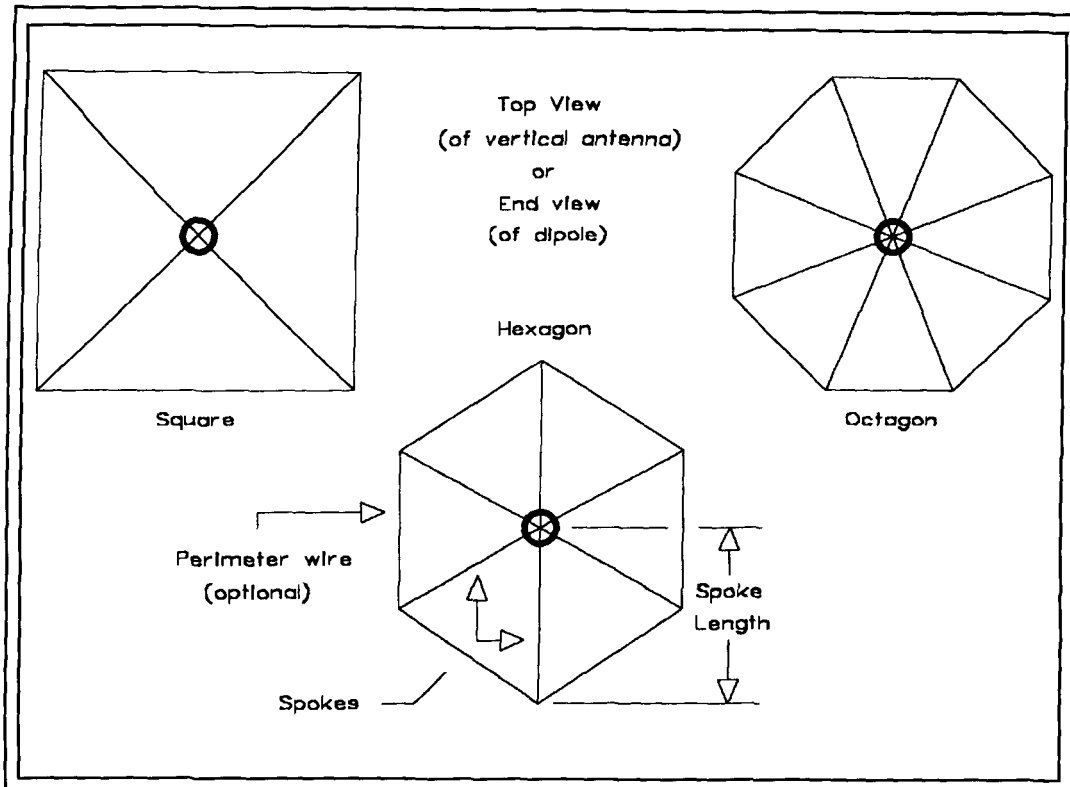

Figure 19. Outlines of square, hexagon, and octagon hats.

ance toward the development of detailed capacity-hat models.

Choice of NEC modeling parameters will, of course, vary the baseline of calibration. The models I used placed 25 segments in the main element so their length was reasonably close the length of segments in the spokes and perimeter. Spokes used three segments each. Square perimeter sides used five segments, while hexagon and octagon perimeter sides used three segments.

The hat size calculations are only as accurate as the models, plus or minus the inherent error factors in the equations and the care of calibration. The methods we have looked at are not so much designed for lab precision as they are a convenient starting point for other tasks. One of those tasks is modeling a capacity hat antenna at a new frequency. Another is constructing a hat in the home ham shop. When used with due caution, the calculation technique used here may be adequate for both tasks.

The attached GW BASIC listing (**Appendix B** provides a convenient utility program for starter calculations toward the construction of capacity hats of square, hexagon, and octagon configurations. Given the modifications of fundamental transmission-line analogy equations to produce the calibration, the values for characteristic impedance, capacitive reactance, capacitance, and standard disc size should be considered only as artifacts of the calculations, not as accurate values.

These investigations suggest that classic transmission-line analogy theory faces serious challenges if extended into the HF range, where the diameter of an antenna element is virtually always a quite significant percentage of the antenna height and the departure of the antenna shape from conical reduces the reliability of what careful theorists have always called an approximation, even at very low frequencies. The difficulty of calibrating classic calculations to method-of-moments models is a double hurdle, as neither method to this point provides a definitive baseline for the other. At best, the modifications to basic equations, gathered into the simple GW BASIC program accompanying these notes, can provide a rough guide to modeling efforts for capacity hat antennas in the 60 degree or longer range. The program returns results that are less than precise, but perhaps much better than a blind guess.**

**A more accurate (and longer) version of the program included here is part of the HAMCALC collection compiled by George Murphy, VE3ERP.

Appendix B: Program

```
10 '    file "CAPHAT.BAS" — Compensated calculation of capcity-hat Zo equation with aver-
        aged results used to calculate hat spoke lengths
20 COLOR 11,1,3
30 CLS:LOCATE 1,12:PRINT"Calculation of Capacitive Hats for Vertical Antennas":LOCATE
        2,28:PRINT"L. B. Cebik, W4RNL"
40 PRINT:PRINT" The information requested yields approximations for spokes of open-frame
        hats with 4, 6, and 8 sides for common materials used by hams in the HF bands from"
50 PRINT" 3 to 30 MHz. Spoke lengths are within about 5% of NEC-2 Models.":PRINT
60 '    Frequency selection
70 LOCATE 8,1:X$=STRING$(79,32):PRINT X$:LOCATE 8,1:INPUT" Enter the frequency of
        interest in MHz    ",F
80 FL=3:FH=30:IF F<FL OR F>FH THEN 70 ELSE 90
90 LOCATE 8,1:X$=STRING$(79,32):PRINT X$:LOCATE 8,1:PRINT" Selected frequency in
        MHz        ";F
100 '   Antenna element diameter selection
110 LOCATE 9,1:PRINT" Select the letter by the main element diameter (in inches) closest to
        yours.":PRINT" a. 0.50  b. 0.75  c. 1.00  d. 1.25  e. 1.50  f. 1.75  g. 2.00"
120 A$=INKEY$:IF A$="a" THEN 130 ELSE IF A$="b" THEN 140 ELSE IF A$="c" THEN
        150 ELSE IF A$="d" THEN 160 ELSE IF A$="e" THEN 170 ELSE IF A$="f" THEN
        180 ELSE IF A$="g" THEN 190 ELSE 120
130 KL=.9688:KH=.953:D=.5:GOTO 200
140 KL=.9669:KH=.9483:D=.75:GOTO 200
150 KL=.9654:KH=.9445:D=1:GOTO 200
160 KL=.9641:KH=.9412:D=1.25:GOTO 200
170 KL=.963:KH=.9383:D=1.5:GOTO 200
180 KL=.962:KH=.9358:D=1.75:GOTO 200
190 KL=.9611:KH=.9335:D=2:GOTO 200
200 KV=(((F/3)-1)*.0333333)+.61:KQ=KH+((.4342945*LOG(FH/F))^KV)*(KL-KH):
        LK=KQ*245.8928:MQ=1/KQ
210 LOCATE 9,1:X$=STRING$(79,32):PRINT X$:LOCATE 9,1:PRINT" Selected main element
        diameter in inches  ";D
220 '   Open-frame hat wire or tubing diameter selection: perimeter wire      assumed to have
        same diameter as spoke wire.
230 LOCATE 10,1:X$=STRING$(79,32):PRINT X$:LOCATE 10,1:PRINT" Select the letter by
        the material you plan to use for the capacity hat.":PRINT" a. #12=.0808 b.#10=.1019 c.
        #8=.1285 d. .25  e. .50  f. .75  g. 1.00"
240 A$=INKEY$:IF A$="a" THEN 260 ELSE IF A$="b" THEN 290 ELSE IF A$="c" THEN
        320 ELSE IF A$="d" THEN 350 ELSE IF A$="e" THEN 380 ELSE IF A$="f" THEN
        410 ELSE IF A$="g" THEN 440 ELSE 240
250 '   Calibration constants derived from models
260 KCL=1.2397:HKCL=1.1042:OKCL=1.0359
270 KCLS=2.1124:HKCLS=1.7032:OKCLS=1.483:KLC=.9745:KHC=.9664
280 DCAP=.0808:GOTO 470
290 KCL=1.2272:HKCL=1.0913:OKCL=1.0234
300 KCLS=2.0761:HKCLS=1.6726:OKCLS=1.4542:KLC=.974:KHC=.9652
310 DCAP=.1019:GOTO 470
320 KCL=1.2143:HKCL=1.078:OKCL=1.0106
330 KCLS=2.0385:HKCLS=1.6416:OKCLS=1.4312:KLC=.9732:KHC=.9639
340 DCAP=.1285:GOTO 470
350 KCL=1.1747:HKCL=1.0376:OKCL=.9723
360 KCLS=1.9122:HKCLS=1.5441:OKCLS=1.3508:KLC=.9713:KHC=.9593
370 DCAP=.25:GOTO 470
380 KCL=1.1276:HKCL=1.0037:OKCL=.9293
```

```
390 KCLS=1.7822:HKCLS=1.449:OKCLS=1.2625:KLC=.9688:KHC=.953
400 DCAP=.5:GOTO 470
410 KCL=1.096:HKCL=.9678:OKCL=.9028
420 KCLS=1.6889:HKCLS=1.3598:OKCLS=1.2007:KLC=.9669:KHC=.9483
430 DCAP=.75:GOTO 470
440 KCL=1.0707:HKCL=.9372:OKCL=.8831
450 KCLS=1.6244:HKCLS=1.3067:OKCLS=1.1576:KLC=.9654:KHC=.9445
460 DCAP=1!:GOTO 470
470 LOCATE 10,1:PRINT X$
480 LOCATE 10,1:PRINT" Selected hat material diameter in inches  ";DCAP
490 '    Antenna length selection between 60 and 85 electrical degrees
500 KV=(((F/3)-1)*.0333333)+.61:KR=KHC+((.4342945*LOG(FH/F))^KV)*(KLC-KHC)
510 KF=LK*12:KA=KF/90
520 HS=(KA*60)/F:HL=(KA*85)/F:HSF=HS/12:HLF=HL/12
530 LOCATE 11,1:PRINT X$:LOCATE 11,1:PRINT" For a frequency of";F;"MHz, a capacitive
        hat vertical should be between ":PRINT"  ";HSF;"feet long and";HLF;"feet long."
540 INPUT" Enter the desired antenna length in feet  ",HF:IF HF>HLF OR HF<HSF, THEN 550
        ELSE 560
550 PRINT" Length must be between";HSF;"and";HLF;"feet":GOTO 540
560 LOCATE 11,1:PRINT X$:LOCATE 12,1:PRINT X$:LOCATE 11,1:PRINT" The desired
        antenna length in feet    ";HF
570 '    Required hat capacitance calculation
580 HR=LK/F:H=HF*12
590 ZO=60*(LOG((4*(H*MQ))/D)-(1-((F/30)*.583)))
600 LA=(HF/HR)*90:LC=90-LA:LCR=(3.14159*LC)/180:X=ZO/TAN(LCR)
610 C=1000000!/((2*3.14159)*(F*X)):CHD=1.1121*C
620 PRINT:PRINT" The antenna length in degrees is    ";LA
630 PRINT" The loading length in degrees is    ";LC
640 PRINT" The required capacitive reactance in Ohms is ";X
650 PRINT" The required capacitance in pF is    ";C
660 PRINT" Solid disc radius in inches is    ";CHD/2
670 PRINT " Spoke Length (inches)    Spoke only    Spoke & Perimeter"
680 '    Square spoke calculation and calibration
690 SPT=(KCL*C)
700 SPTS=(KCLS*C)*KR
710 PRINT"  Square":LOCATE 19,34:PRINT SPTS:LOCATE 19,58:PRINT SPT
720 '    Hexagon spoke calculation and calibration
730 HSPT=(HKCL*C)
740 HSPTS=(HKCLS*C)*KR
750 PRINT"  Hexagon":LOCATE 20,34:PRINT HSPTS:LOCATE 20,58:PRINT HSPT
760 '    Octagon spoke calculation and calibration
770 OSPT=(OKCL*C)
780 OSPTS=(OKCLS*C)*KR
790 PRINT"  Octagon":LOCATE 21,34:PRINT OSPTS:LOCATE 21,58:PRINT OSPT
800 '    Closeout
810 PRINT:PRINT" <A>nother run or <Q>uit?"
820 A$=INKEY$:IF A$="A" OR A$="a" THEN 30 ELSE IF A$="Q" OR A$="q" THEN END
        ELSE 820
```

Because we were unable to obtain reproduction permission from the author, the following article does not appear in the *ARRL Communications Quarterly Collection*...

Nikola Tesla

By Wallace Edward Brand, Malcolm Watts and John Wagner, W8AHB

3890 Tubbs Rd
Ann Arbor, MI 48103

Summary: An article describing the achievements of Tesla in pioneering modern AC power systems as well as radio.

Fall 1997 issue, pages 80-86.

Please contact the author for additional information.

PRODUCT INFORMATION

HP Signal Analyzer Enhanced for Low Phase-Noise Floor

Hewlett-Packard's enhanced HP 4352B VCO/PLL (voltage control oscillator/phase-lock loop) signal analyzer (10 MHz to 3,000 MHz) offers a lower phase-noise floor to meet wireless VCO test requirements. The analyzer features 157 dBc/Hz at 1 MHz offset, typically. In addition, the HP-4352B with Option 001 now provides -15 to +35 volts control voltage drive. The HP 4352B VCO/PLL signal analyzer systems tests all types of voltage-controlled oscillators with embedded phase-lock loops from 10 to 3000 MHz (26.5 GHz optional). The unit has been customized to measure several important parameters including VCO tuning characteristics (frequency, sensitivity, RF power), phase noise, signal spectrum, FM deviation, RF transient (VCO tuning drift, PLL frequency transition), and DC power consumption. It also supplies DC power, ultra-low-noise, VCO test-control voltage and digital-control signals for the PLL.

Measurement speed has been optimized for high throughput, covering 100 Hz to 10 MHz frequency offset in 7.1 seconds/sweep in the phase-noise measurement mode. A carrier-tracking mode cancels carrier drift, speeding up the normally tedious phase-noise characterization. The system is programmable with HP IBASIC. Mail inquiries to: Hewlett Packard Company, Test and Measurement Organization, P.O. Box 50637, Palo Alto, California 94303-951.

Jay Jeffery, *WV8R*
26150 Village Lane, Apt. 209
Beachwood, Ohio 44122

KIRCHHOFF'S LAWS

The classic cube problem

There's a classic problem that illustrates how a simple arrangement of resistors can result in a complex puzzle that can't be solved using formulas for series and parallel resistors. Learning to solve this kind of problem can prepare you to solve other circuit problems that present the same difficulty.

The famous (or infamous) problem consists of a cube outlined by resistors; that is, each edge is a 1-ohm resistor (see **Figure 1**). Three resistors are connected at each corner of the cube, and there are 12 resistors in all. The problem asks you to determine the resistance of the cube from one corner (or vertex) to the opposite corner. In **Figure 1**, the arrows heading into and out of the cube indicate the current flow.

At this point, you may want to try to solve the problem on your own, before you get to the explanations. But, if you're like me, you may need a little review first. Or if this is new territory for you, some clarification will probably be helpful.

In **Figure 2**, the cube circuit is pretty much diagrammed in two dimensions. Looking at the figure, it's easy to see that simple formulas won't handle the problem. We need the more fundamental and, in some ways, more difficult approach based on Kirchhoff's Laws.

Kirchhoff's laws or rules seem deceptively simple and obvious: the trouble comes in the application. One law states that the same amount of current flows into a junction of conductors as flows out. The other states that the sum of the voltage drops across a closed path of a circuit is equal to the voltage applied to the circuit.

What does this mean? **Figure 3** illustrates the first law concerning current. If a current i flows in from the left, then the *total* of the currents coming out on the right must be i. Putting this into an equation, we get, $i = i_1 + i_2$. Using such an algebraic equation to describe an electrical situation brings a handy mathematical tool into the picture.

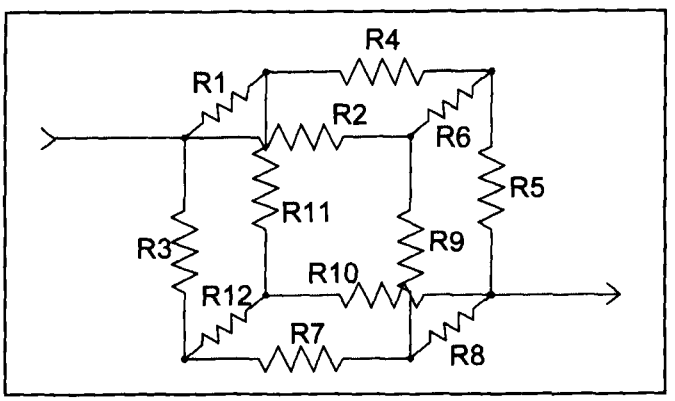

Figure 1. The resistor cube.

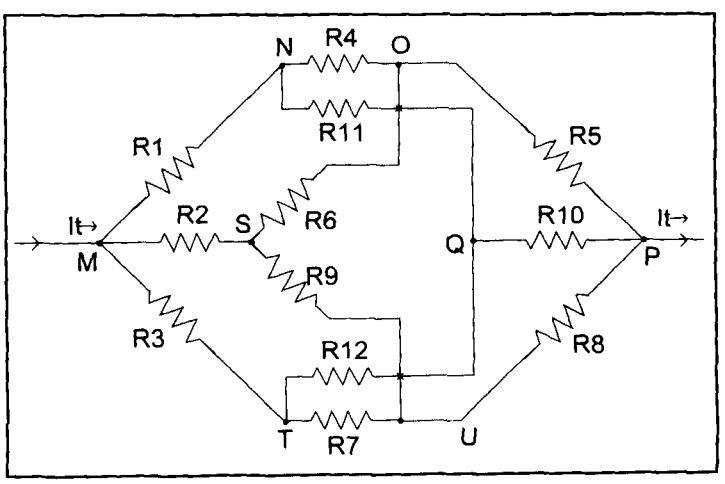

Figure 2. Two-dimensional diagram of the cube.

Figure 4 is an example of the voltage and current rules. The voltage from A to B to C is the battery voltage and is equal to the voltage

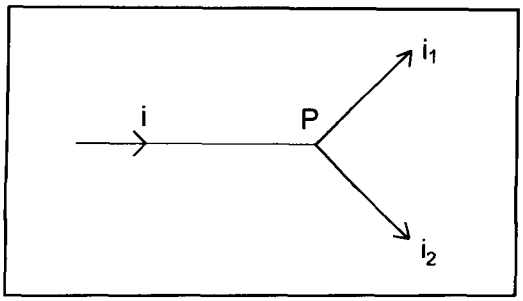

Figure 3. Kirchhoff's current rule.

from A to D to C. If the voltage from the battery is 3 volts, the total current flowing through the circuit is i and the resistors are r_1, r_2, r_3, and r_4, then we can choose i_1 as the current through the upper branch and i_2 as the current through the lower branch. This gives us the current equation $i = i_1 + i_2$, just as in **Figure 3**. (Note that $r_1 = 1$ ohm, $r_2 = 2$ ohms, $r_3 = 3$ ohms, and $r_4 = 4$ ohms.)

Because E = IR (Ohm's Law), the voltage from A to B is $i_1 r_1$ and the voltage from B to C is $i_1 r_2$. Similarly, from A to D it is $i_2 r_4$, and from D to C it is $i_2 r_3$. Using the voltage law, we can write the following equations:

$$3 = i_1(1) + i_1(2)$$
$$3 = i_2(3) + i_2(4)$$

Now we can determine the resistance from A to C using the equation derived from **Figure 4**:

$$3 = 3i_1 \qquad 3 = 7i_2$$
$$i = 1 \qquad i_2 = \frac{3}{7}$$

$$i = i_1 + i_2$$

$$i = 1 + \left(\frac{3}{7}\right)$$

$$i = \frac{10}{7}$$

$$E = IR$$

$$3 = \left(\frac{10}{7}\right) R$$

$$R = 3\left(\frac{7}{10}\right)$$

$$R = \frac{21}{10} = 2.1 \text{ ohms}$$

In the preceding example, we could have used series and parallel formulas to obtain our results. Instead, we illustrated the use of Kirchhoff's Laws, although use of these laws is not appropriate for such a simple problem.

In the final example, you'll note that the flow

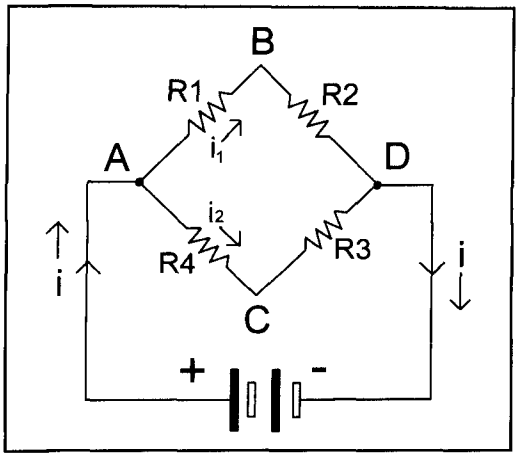

Figure 4. Kirchhoff's voltage and current rule.

of current must be assumed to follow certain paths in the network. Whether the current actually follows the directions you choose isn't important, but it is important to make your guess consistent with itself.

Little arrows in **Figure 2** indicate the assumed flow of current. In some problems the flow isn't obvious, but it's necessary to make a good, consistent guess. The important concept mentioned above has to do with the direction of this flow. If you're following the current path through a junction, one or more paths may show current in opposition to the direction you must go. If so, the term for that path is negative. If the current runs in the same direction, the term is positive. Because the terms are variables, the actual sign indicating the direction of the current flow will "come out in the wash" when the equations are solved.

Here's a specific example. In **Figure 2**, moving from point S through R_6 to point O, the current in R_6 (i.e., I_6) splits and goes to the left and right. The left branch through R_4 is in opposition to the assumed flow direction, so that term is negative. The part that goes to the right through R_5 runs with the current and is positive. This equation for current is $I_6 = I_5 - I_4$ or $I_6 + I_4 = I_5$.

Note that the current in each resistor has the same subscript as the resistor with which it's associated. Thus, I_4 is the current in R_4, and I_5 is the current in R_5. At this point, you can try to generate the voltage and current equations for the classic cube problem itself, or simply try to verify the equations that will be listed.

Assuming a logical pattern of current flow, and assuming that each resistance is 1 ohm, E = 10 volts, and Ij is the current in Rj, using E = IR, I obtained the following voltage equations:

1. $10 = I_1(1) + I_4(1) + I_5(1)$
2. $10 = I_1(1) + I_{11}(1) + I_{10}(1)$

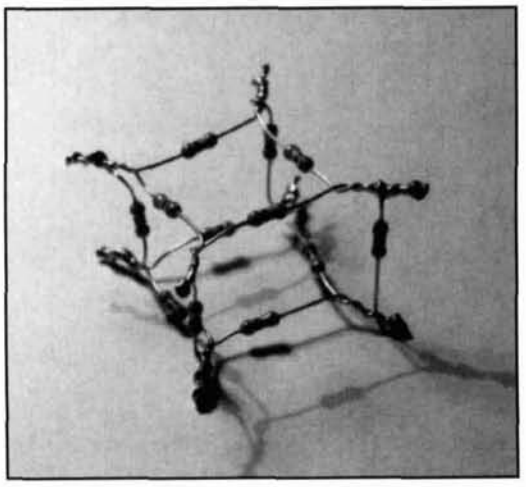

Photo A. Author's resistor cube.

3. $10 = I_2(1) + I_6(1) + I_5(1)$
4. $10 = I_2(1) + I_9(1) + I_8(1)$
5. $10 = I_3(1) + I_{12} + I_{10}(1)$
6. $10 = I_3(1) + I_7(1) + I_8(1)$

The current equations are as follows:

7. I_t (total current) $= I_1 + I_2 + I_3$
8. I_t (total current) $= I_5 + I_{10} + I_8$
9. $I_1 = I_4 + I_{11}$
10. $I_3 = I_{12} + I_7$
11. $I_2 = I_6 + I_9$
12. $I_6 = I_5 - I_4$ or $I_6 + I_4 = I_5$
13. $I_9 = I_8 - I_7$ or $I_9 + I_7 = I_8$
14. $I_{11} = I_{10} - I_{12}$ or $I_{11} + I_{12} = I_{10}$

The next step is to put the equations in some sort of order and then try to solve them by substitution and the elimination of variables. Because we need total current I_t to obtain total resistance, that's the variable we'll aim for. This can be done by adding up all the equations, except **7** and **8**, and then substituting from **7** through 14, where appropriate.

$$60 = (2I_1 + 2I_2 + 2I_3) + (2I_5 + 2I_{10} + 2I_8) + (I_4 + I_{11}) + (I_{12} + I_7) + (I_6 + I_9) + (I_5 + I_{10} + I_8) - (I_{11} + I_{12}) - (I_7 + I_9) - (I_6 + I_4)$$

$$60 = 2(I_1 + I_2 + I_3) + 2(I_5 + I_{10} + I_8) + (I_1 + I_3 + I_2) + (I_5 + I_{10} + I_8) - I_{10} - I_8 - I_5$$

$$60 = 3(I_1 + I_2 + I_3) + 2(I_5 + I_{10} + I_8)$$

$$60 = 3I_t + 2I_t$$

$$5I_t = 60$$

$$I_t = 12 \text{ amps}$$

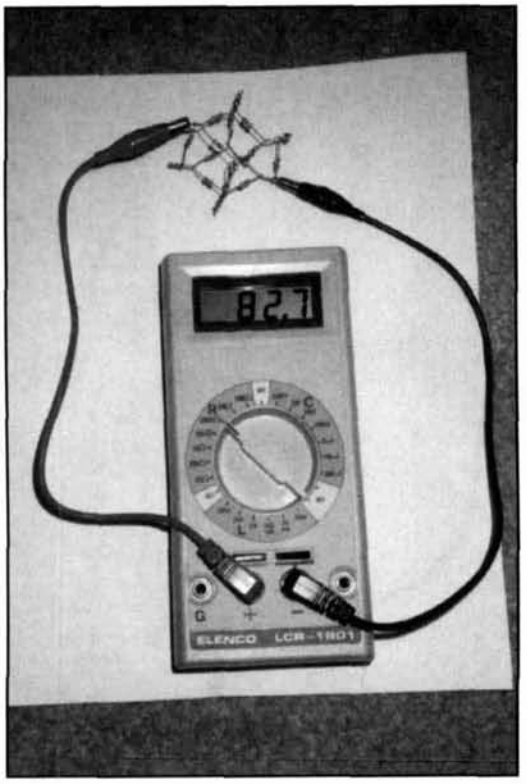

Photo B. Measuring the resistance of the cube.

We can also put the equations in order using zeros for the missing terms, add **Equations 7** and **8** together to cut the number of equations to 13 (the number of unknowns), and enter the coefficients into a computer or calculator program that solves n equations in n unknowns.

Finally, because we can obtain I_t we can use Ohm's Law to calculate the total resistance of the network from M to P this way, as well as all other I values.

$E = IR$
$10 = 12R$
$R = 5/6$ ohms

This method may or may not be clear to you now. It helps to try other problems until you get it right.

The experimental approach

Finally, it's possible to simply build a cube of resistors and make measurements with a meter. Try to pick resistors close to the correct value; don't go by the color code alone. To try this out, I used an ohmmeter to select twelve 100 kohm resistors. They weren't exactly right, but they were close (mostly under 100 k). The rounded result was 83 k (see **Photos A and B**). As this is about 5/6 of 100 k, perhaps the math is right! I'll leave it to you to check it out. ■

Edited by Peter Bertini, K1ZJH
Senior Technical Editor

A Reference Dipole for 2-Meters

Rick Littlefield, K1BQT

Just as user-friendly antenna software stimulates greater interest in designing and building experimental antennas, it is also responsible for spinning off a number of new, low-cost products to help users evaluate their creations.

Here are some examples. Palomar Engineers recently introduced the PFS-1 multiband field-strength meter. This handy device offers continuous coverage from 1.8 to 150 MHz with a 30-dB metering range, and up to 60-dB measurement range with a built-in attenuator. Another new product, the MFJ-224 2-Meter FM Analyzer, provides calibrated field-strength readings from -100 to -40 dBm at 1-dB resolution via a built-in tunable NBFM receiver. Also, the just-announced MFJ-232 precision attenuator converts any HF to UHF receiver with an S-meter into an accurate dB measurement tool. Products such as these make designing and testing new antennas easier than ever before for experimenters on a limited budget.

While affordable test-range equipment is a plus, seasoned antenna engineers are quick to point out that there are many important set-up skills to master—including how to correctly position the test antenna and signal source. And, you'll need to know how to root out false responses from multipath, cross polarization, impedance mismatches, and radiating feedlines. In the end, the *only* variable you want to measure is the performance of the antenna itself, and that's not always as simple as it sounds! Certainly, gathering the right tools is an excellent place to start. This tech note describes a particularly useful item for making 2-meter dBd comparisons: a "technically correct" 146-MHz reference dipole.

The dBd as a Comparison Measurement

The dBd measurement compares forward gain exhibited by a test antenna to the performance of an identically positioned 1/2-wave reference dipole. Not all dBd measurements are universally embraced by the technical community. Some will argue that dBd assessments made at HF are fairly meaningless because of the impact local ground conductivity may have on antenna performance.

At VHF and above, however, the dBd comparison becomes more widely accepted, mostly because it becomes practical to elevate the signal source and test antenna several wavelengths above ground, where the impact of soil conductivity on gain and TOA is less intrusive. Also, "on-the-horizon" radiation is of primary interest at VHF and above, and this is the parameter simple range experiments measure best. The dBd specification is often used as a figure of merit in competitive advertising, and remains an important—if occasionally abused—benchmark of antenna performance.

Any reference dipole used for making comparative dBd measurements must meet at least two fundamental criteria. First, it must present a 50-ohm source at the feedpoint in order to provide a fair and accurate voltage reading at the far end of the test cable. Above two wavelengths AGL, the characteristic impedance of a thin-wire dipole approaches 73 ohms, which represents a significant mismatch into a 50-ohm system. Any reference dipole must, therefore, be corrected for mismatch without introducing measurable loss into the system or significantly altering element gain.

Probably the simplest strategy for lowering element impedance is to increase effective element diameter by shaping the radiator as a batwing. This shaping not only lowers the feedpoint impedance in free space without introducing loss, but it also lowers element Q-increasing the antenna's usable bandwidth. An EZNEC model of the aluminum-wire batwing shape used for this antenna predicted a gain of 2.21 dBd at 146 MHz. This is within 0.1 dB of the accepted 2.14-dBi definition for dBd.

In addition to providing a good match, the reference antenna element must be totally isolated from the exterior surface of its feedline. This mandates the installation of a low-loss balun or wound coaxial choke. If the element is not isolated in this manner, pattern distortion and feedline pickup will almost certainly introduce significant response errors that invalidate results. To further ensure accuracy, the dipole element should also be electrically isolated from its mount, and the upper support mast should be made from a non-conductive material such as fiber glass to prevent any opportunity for pattern disruption.

Constructing a Reference Dipole

The element shape shown in **Figure 1** details a simple batwing 50-ohm element formed from two pieces of RadioShack solid-aluminum ground wire. When constructing the antenna, clamp each leg in place onto a 3-inch by 4-inch Plexiglas™ center block with #8 hardware and oversized washers. The dimensions shown should resonate at approximately 146 MHz, and present a source impedance of 50 ohms when mounted over two wavelengths above ground.

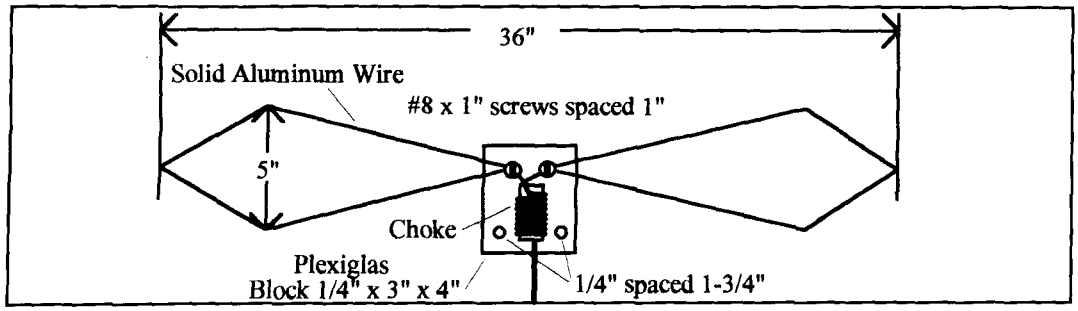

Figure 1. Two-meter, 50-ohm reference antenna.

The antenna's choke balun consists of 11 or 12 turns of RG-316 Teflon™ coax solenoid wound on a 2-inch length of 1/2-inch I.D. plastic water pipe. Secure windings in place with #6 nylon screws tapped into the form. Install solder lugs on short pigtails at one end of the choke for connection to the antenna's mounting studs, and install a standard 50-ohm female connector on the other end for feedline connection. (BNC or "N" connectors are recommended over SO-239 for VHF and UHF.) Finally, drill two 1/4-inch holes spaced at 1-3/4 inches at the bottom of the center block to permit mast mounting with a standard TV mast clamp.

Tuning

Careful adjustment for resonant frequency and feedpoint impedance is essential to ensure accurate results on the range. While a lab-grade network analyzer is ideal for this task, a less sophisticated VHF analyzer, such as the Autek RF-5 or MFJ-259, will also do the job. In addition to an analyzer, you'll need a 12- to15-foot insulated mast to elevate the antenna well above ground. Be sure to pick a test location clear of surrounding metallic objects or absorptive clutter that might alter element performance.

Because simple handheld analyzers lack the test-cable compensation circuitry found in more costly lab models, I recommend tuning your test cable to the frequency of interest (mid-band or 146 MHz for 2 meters). This will prevent unwanted impedance transformation in the line for sources other than 50 ohms and force the impedance-magnitude readings on your analyzer to jibe with what is actually happening at the antenna feedpoint.

To accomplish this, the total electrical feedline length, including any coax in the choke balun, must be an even multiple of 1/2 wave. Begin by cutting a piece of low-loss cable (RG-8/X or better) a couple feet longer than your test pole. Install a connector on one end of the coax and connect it to the choke balun. Now, short the pigtail leads on the other end of the choke balun firmly together and measure the impedance at the far end of the test coax. If it doesn't register Z-minimum (and odds are very good that it won't), prune the cable until minimum Z is obtained. By tuning the analyzer up and down in frequency, you can locate the point of minimum Z and then estimate how much to trim off. When this is done, install a connector on the analyzer end of the test cable.

This cable/choke balun combination may now be used with any 2-meter experimental antenna to ensure complete feedline isolation and accurate impedance measurements over a wide range of values.

Finally, if you have a precision 50-ohm load available, connect it to your analyzer and note the impedance value displayed on the screen or meter. If the display reads slightly higher or lower than 50 ohms, note the reading and adjust your reference antenna for *that value* rather than for the 50-ohm mark. This will correct for calibration errors in the analyzer's bridge or metering circuit.

Once your test setup is ready to go, connect the balun to the element and raise the antenna. If you followed **Figure 1** closely during construction, the antenna's resonant point—as indicated by minimum VSWR—should fall close to 146 MHz. If only a small adjustment is needed, try expanding or compressing the bat wing before resorting to cutting or lengthening the aluminum wire. Changing the element shape will affect both feedpoint impedance and resonant frequency, so be sure to monitor both parameters when making adjustments.

Again, the objective is to resonate the antenna at mid-band with a feedpoint impedance as close to 50-ohms as possible. You should be able to hit this within a couple-hundred kHz and 2 to 3 ohms without major effort.

Conclusion

With care, it's possible to make reasonably accurate dBd comparisons at VHF using very modest equipment. Needless to say, a good reference antenna is an important tool that will help you achieve optimal results. However, don't be too quick to rewrite antenna theory or announce a startling new breakthrough to the world if your first-round data exceeds theoretical convention or NEC projections. Whenever the data looks too good to be true, it probably is! All field-strength measurements are subject to innumerable sources of error, and nothing beats caution, repetition, careful cross-checking, and replication by other investigators to ensure bullet-proof results. ■

CORRECTIONS

Remove the dot

In **Figure 9** of "The Lazy-H Vertical" by Rudy Severns, N6LF (Spring 1997, page 31), there is a connection dot where the lead from the 140-pF capacitor crosses the 27-foot radial on its way to the 70-foot vertical wire. That dot should not be there.

Will the real Figure 15 stand up?

In Dick Weber, K5IU's article "Optimal Elevated Radial Vertical Antennas" (Spring 1997, page 9), the wrong graphs were used for **Figure 15**. **Figure 14**, which is correct, was repeated as **Figure 15**. The correct **Figure 15** is shown below.

Corrected tables

The last two columns of **Table 1** and the last column of **Table 2** in Jacques Audet, VE2AXZ's, article "Upgrading Boonton Models 92/42 RF Voltmeters" (Spring 1997, page 53) were a bit askew in their published version. Here are the corrected versions:

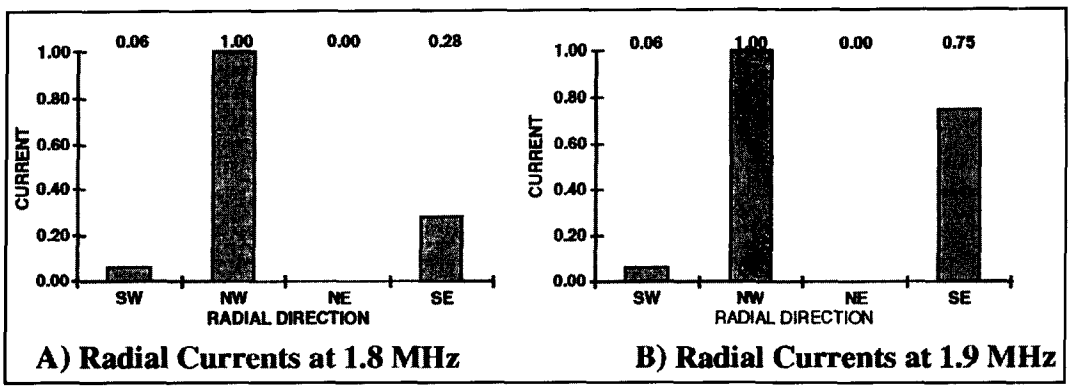

Figure 15. "Last Attempt" radio current measurements at two frequencies. (A) Radial currents at 1.8 MHz. (B) Radial currents at 1.9 MHz.

RANGE (mV)	ATTENUATOR GAIN	FIXED GAIN AMP	SECOND AMP GAIN	TOTAL GAIN	NOMINAL INPUT V AT F.S.	MEASURED INPUT V AT F.S.
1	1	100	1000	100000	3.10E-05	3.80E-05
3	1	100	100	10000	3.10E-04	3.76E-04
10	1	100	10	1000	3.10E-03	3.68E-03
30	1	100	1	100	3.10E-02	3.19E-02
100	0.18716	100	1	18.72	0.166	0.1844
300	0.04231	100	1	4.231	0.733	0.748
1000	0.013325	100	1	1.333	2.326	2.610
3000	0.004231	100	1	0.4231	7.327	8.660

Table 1. Boonton RF voltmeter gain distribution before modifications. Rightmost column data is for the author's voltmeter.

RANGE mV	PREAMP GAIN	PREAMP OUTPUT VOLTS	GAIN SECOND AMP	TOTAL GAIN	FULL SCALE INPUT VOLTS
1	100	0.0031	1000	100000	3.10E-05
3	100	0.031	100	10000	3.10E-04
10	100	0.31	10	1000	3.10E-03
30	100	3.1	1	100	3.10E-02
100	1	0.166	18.716	18.72	0.17
300	1	0.631	4.909	4.909	0.63
1000	1	2.326	1.333	1.333	2.33
3000	1	7.327	0.4231	0.4231	7.33

Table 2. Boonton RF voltmeter gain distribution after modification.

Three minor corrections

In Richard Formato, K1POO's, article "Loading Profiles for Wideband Antennas" (Summer 1997, page 27), a few small errors crept into the text. On page 30, the reactance term X^1 was missing from the first sentence of the last paragraph of the first column.

In **Equation 6**, a parenthesis was ommitted. The corrected equation appears below:

$$f(z) = 2\nu(h-|z|)^{\nu-2}\left\{1 - j\frac{\nu-1}{2k_o(h-|z|)}\right\} \quad (6)$$

Finally, there was an incorrect sign used in **Equation 7b**. Here is the corrected equation:

$$X^i(z) = 60\nu(h-|z|)^{\nu-2}\left\{\psi_I + \frac{(1-\nu)\psi_R}{2k_o(h-|z|)}\right\} \quad (7b)$$

Trouble with transmission line transformers

Donald McClure, KB2Z, requested that we make the following corrections to his article "Transmission Line Transformers" (Summer 1997, page 45)

On page 45, the caption for **Figure 1** should read: A simple 1/3 voltage ratio Guanella transformer example of **prior art**.

On page 47:

In **Equation 8** change V1 to V_1.

Equation 10 should read: $V_1 - I_1 K Z_o = 0$

Change **Equation 11**: $I_2 - V_2 K Y_o = 0$

Finally, down below in the "where" statements substitute capital I for the 1 in input current and load current.

On page 48, KB2Z has sent the revised copy of **Figure 4** below.

On **Table 1** on page 50–51, new information has been added between the values of 1/13 and 4/13 as shown below.

Voltage Ratio K	Connections	Minimum No. Lines
1/13	13P*	13
2/13	2S, 6P > P	8
3/13	4P, 3S > P	7
4/13	4S, 3P > P	7

Under the heading "Selection sample 2" on page 53, the 2/3 ratio should read:

2S, 1 > P

On page 58, **Reference 3** is for Part 1, not Part 2, of McClure's *RF Design* article "Broadband Transmission Line Family Matches a Wide Ranges of Impedances."

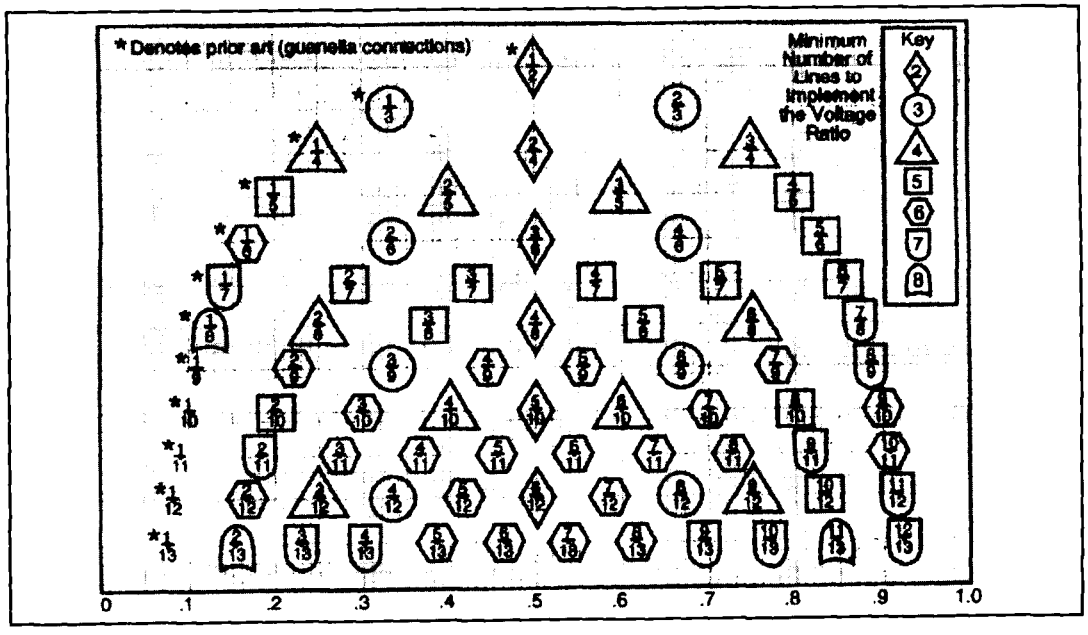

Figure 4.

COMMUNICATIONS QUARTERLY ARTICLE INDEX

FALL 1992–SUMMER 1997

AM

A Unique Approach to AM Synchronous Detection
Scott D. Prather, KB9Y
Fall 1994, page 13

AMPLIFIERS

Building a Wide Range RF Preamplifier
Joseph J. Carr, K4IPV
Spring 1995, page 85

HF MOSFET Linear Amplifier
Yoji Tozawa, Hiroyuki Sakaue, Ken-ichi Takada, Koji Furukawa, and Shinichiro Takemura
Summer 1993, page 53

Low-Noise AGC-Controlled IF Amplifier
From Pat Hawker's "Technical Topics" in *Radio Communication*
Winter 1996, page 93

Power on a Budget
Marv Gonsior, W6FR
Winter 1995, page 55

Simple and Inexpensive High-Efficiency Power Amplifier
Frederick H. Raab, Ph.D., WA1WLW
Winter 1996, page 57

Variable High-Power Biasing
Marv Gonsior, W6FR
Summer 1996, page 82

4CX400A Russian Tubes for the MLA-2500 Amplifier
B.N. "Bob" Alper, W4OIW/6
Summer 1996, page 29
Technical Conversations: W8JI, *Fall 1996, pages 4 and 5*; W4OIW/6, *Winter 1997, page 4*; W8JI, *Winter 1997, page 5*; AB6BO, *Winter 1997, page 5*; W4OIW/6, *Winter 1997 page 5*

ANTENNAS AND RELATED TOPICS

A Featherweight 6-Meter Beam
Rick Littlefield, K1BQT
Summer 1995, page 5

A Note on the Radiation Resistance of Loop Antennas with Short Circumferences
Peter Bertram, DJ2ZS
Summer 1997, page 99

A Practical Reversible Beverage
Tom Rauch, W8JI
Spring 1997, page 102

A Single Coil Z-Match Antenna Coupler
T.J. Seed, ZL3QQ
Technical Conversations: K6UPZ, Spring 1995, page 6

Aerodynamic Balancing: Part 1
Dick Weber, PE, K5IU
Summer 1994, page 61

Aerodynamic Balancing: Part 2
Dick Weber, PE, K5IU
Winter 1995, page 89

An "Ultralight" Center-Fed Vertical Antenna for 20 Meters
Rick Littlefield, K1BQT
Winter 1994, page 89

Anapoles
Yardley Beers, WØJF
Summer 1996, page 67

Antennae Exotica: Genetics Breeds Better Antennas
Nathan "Chip" Cohen, N1IR
Fall 1996, page 55

Antennae Exotica: The Arecibo Dish
Nathan "Chip" Cohen, N1IR
Summer 1996, page 17

Antennae Exotica: The Serpentine "Stealth" Vertical
Nathan "Chip" Cohen, N1IR
Spring 1996, page 79

Beyond the Z-Match: The IBZ Coupler
Charles A. Lofgren, W6JJZ
Winter 1995, page 27

Build a High-Performance, Low-Profile 20-Meter Beam
Cornell Drentea, WB3JZO
Spring 1993, page 85
Technical Conversations: N2WLG, *Fall 1996, page 6*; WB3JZO, *Fall 1996, page 6*

Build a Short-Stack for 2-Meter SSB
Rick Littlefield, K1BQT
Spring 1996, page 96

Build a 20-Meter DX-Pole Antenna
Rick Littlefield, K1BQT
Spring 1997, page 98

Design and Construction of Wire Yagi Antennas
Floyd A. Koontz, WA2WVL
Winter 1994, page 96

Determination of Yagi Wind Loads Using the "Cross-Flow Principle"
Dick Weber, K5IU, P.E.
Spring 1993, page 13
Letters: AA4NG, *Summer 1993, page 6*; W6QEU, *Summer 1993, page 6*; Darden, *Winter 1994, page 104*

Double Resonant Antennas With Loading Reactors
Yardley Beers, WØJF
Winter 1994, page 57

Fractal and Shaped Dipoles
Nathan "Chip" Cohen, N1IR
Spring 1996, page 25

Fractal Antennas: Part 1
Nathan "Chip" Cohen, N1IR
Summer 1995, page 7

Fractal Antennas: Part 2
Nathan "Chip" Cohen, N1IR
Summer 1996, page 53

Fractal Loops and the Small Loop Approximation
Nathan "Chip" Cohen, N1IR, and Robert G. Hohlfeld
Winter 1996, page 77

From a J to a Zepp
Gary O'Neil, N3GO
Fall 1996, page 61

Instruments for Antenna Development and Maintenance Part 1: Voltage and Current Measurements
R.P. Haviland, W4MB
Spring 1995, page 77

Instruments for Antenna Development and Maintenance Part 2: Signal Generators
R.P. Haviland, W4MB
Summer 1995, page 95

Instruments for Antenna Development and Maintenance Part 3: SWR and Other Precision Measurements
R.P. Haviland, W4MB
Fall 1995, page 79

Instruments for Antenna Development and Maintenance Part 4: Field Strength Meters, Grid Dip Oscillators, and Some Mechanical Devices
R.P. Haviland, W4MB
Winter 1996, page 73

Insulated Antennas
R.P. Haviland, W4MB
Winter 1993, page 75

Miniaturized Antennas
Mike Traffie, N1HXA
Spring 1996, page 99

Modeling and Understanding Small Beams Part 1: The X-beam
L.B. Cebik, W4RNL
Winter 1995, page 33

Modeling and Understanding Small Beams Part 2: VK2ABQ Squares and Moxon Rectangles
L.B. Cebik, W4RNL
Spring 1995, page 55

Modeling and Understanding Small Beams Part 3: The EDZ Family of Antennas
L.B. Cebik, W4RNL
Fall 1995, page 53

Modeling and Understanding Small Beams Part 4: Linear-Loaded Yagis
L.B. Cebik, W4RNL
Summer 1996, page 85

Modeling and Understanding Small Beams Part 5: The ZL Special
L.B. Cebik, W4RNL
Winter 1997, page 72

Modeling and Understanding Small Beams Part 6: Fans, Bowties, Butterflies, and Dragonflies
L.B. Cebik, W4RNL
Spring 1997, page 81

Modeling and Understanding Small Beams" Part 7: Shrunken Quads
L.B. Cebik, W4RNL
Summer 1997, page 71

Optimized Elevated Radial Vertical Antennas
Dick Weber, K5IU
Spring 1997, page 9

Practical Estimation of Electrically Small Antenna Resistance
Bob Vernall, ZL2CA
Spring 1993, page 81
Correction: *Summer 1993, page 106*
Letters: WD8KBW, *Summer 1993, page 6*

Small Loop Antennas: Part 1
Joseph J. Carr, K4IPV
Winter 1993, page 52

Small Loop Antennas: Part 2
Joseph J. Carr, K4IPV
Spring 1993, page 71

Supergain Antennas
R.P. Haviland, W4MB
Summer 1992, page 55
Letters: Hansen, *Fall 1992, page 8*

The Effects of Antenna Height on Other Antenna Properties
L.B. Cebik, W4RNL
Fall 1992, page 57

The EXJAY
Bob Rylatt, G3VXJ
Fall 1992, page 30

The G2AJV Antenna and Maxwell's Displacement Current
Roger C. Jennison, G2AJV
Summer 1995, page 23

The Lazy-H Vertical
Rudy Severns, N6LF
Spring 1997, page 31

The Uni-Directional Long Wire Antenna
R.P. Haviland, W4MB
Fall 1993, page 35

The 2-Meter Discpole Antenna
Rick Littlefield, K1BQT
Summer 1996, page 77

The 20-Meter PVC-EDZ Antenna
Rick Littlefield, K1BQT
Summer 1997, page 105

ANTENNA EXOTICA

BALUNS

COMPUTERS

CONSTRUCTION

DDS

DSP

EDITORIALS

FIBER OPTICS

FILTERS

HF

HISTORICAL

INTEGRATED CIRCUITS

LETTERS

MISCELLANEOUS

OPTICAL COMMUNICATIONS

PACKET

PROPAGATION AND METEOROLOGICAL EVENTS

QRP

Deluxe QRP Station
Jim Pepper, W6QIF
Winter 1994, page 25

QUARTERLY COMPUTING

Quarterly Computing: Building a PC Toolkit
Brad Thompson, AA1IP
Summer 1995, page 91
Quarterly Computing: HFx 1.1
L.B. Cebik, W4RNL
Summer 1997, page 93
Quarterly Computing: Introducing a New Column Exploring Computer Applications to Amateur Radio
Brad Thompson, AA1IP
Fall 1994, page 95
Quarterly Computing: NTE's WinBoard and WinDraft
Peter Bertini, K1ZJH
Fall 1996, page 76
Quarterly Computing: Software for Homebrewing Plus an Updated CD-ROM
Brad Thompson, AA1IP
Winter 1995, page 99
Quarterly Computing: Software Shortcuts
Brad Thompson, AA1IP
Spring 1996, page 84
Quarterly Computing: Software That's Good Enough to Use
Brad Thompson, AA1IP
Winter 1996, page 82
Quarterly Computing: Take a Dip in the Information River
Brad Thompson, AA1IP
Spring 1995, page 99

QUARTERLY DEVICES

Quarterly Devices: Build Dummy Loads and Resistive RF Networks with these Power-Film Resistors
Rick Littlefield, K1BQT
Summer 1995, page 73
Technical Conversations: W6TC, *Winter 1997, page 5*
Quarterly Devices: Low-Cost SMD Prototype Construction
Rick Littlefield, K1BQT, and Peter Bertini, K1ZJH
Spring 1996, page 49
Quarterly Devices: New Devices for Loops and Linears
Rick Littlefield, K1BQT
Summer 1993, page 89
Quarterly Devices: New Receiver Chips from Analog Devices
Rick Littlefield, K1BQT
Fall 1994, page 75
Quarterly Devices: PC Designer
Rick Littlefield, K1BQT
Fall 1996, page 18
Quarterly Devices: Pin Diodes
Rick Littlefield, K1BQT
Winter 1995, page 66
Quarterly Devices: Radios Without Knobs
Rick Littlefield, K1BQT
Spring 1993, page 65
Quarterly Devices: Solve RF Design Problems with Elegant Simplicity Using MMICs
Rick Littlefield, K1BQT
Fall 1992, page 87
Quarterly Devices: The Collins Mechanical Filter—"Back to the Future"
Rick Littlefield, K1BQT
Winter 1993, page 64
Quarterly Devices: The Den-On SC70007 Vacuum Desolder
Rick Littlefield, K1BQT
Summer 1997, page 96
Quarterly Devices: The Harris Semiconductor HFA3600 Low-Noise Amplifier/Mixer
Rick Littlefield, K1BQT
Spring 1994, page 94
Quarterly Devices: The Motorola MC13175/6 UHF FM/AM Transmitter
Rick Littlefield, K1BQT
Fall 1993, page 67
Quarterly Devices: The MRF-255 RF Power Field-Effect Transistor and Digi-Key's Panasonic Multilayer Ceramic Chip Capacitor Kits
Rick Littlefield, K1BQT, and Peter Bertini, K1ZJH
Winter 1996, page 64
Quarterly Devices: The NE577 Compandor
Rick Littlefield, K1BQT
Winter 1994, page 77
Technical Conversations: W6DJ, *Spring 1995, page 8*
Quarterly Devices: The Secrets of "High-Tech Scrounging"
Rick Littlefield, K1BQT
Spring 1995, page 37
Quarterly Devices: The Wiltron Site Master
Rick Littlefield, K1BQT
Summer 1996, page 72

RECEIVERS

A Gyrator Tuned VLF Receiver
Arthur J. Stokes, Sr., N8BN
Spring 1994, page 24
G3SBI's H-Mode Receiver
From Pat Hawker, G3VA's, "Technical Topics" in *Radio Communications*
Fall 1994, page 81
Technical Conversations: W7SX, *Spring 1995*

REVIEWS

SETI

SURFACE MOUNT TECHNOLOGY

TECH NOTES

TECHNICAL CONVERSATIONS

TEST EQUIPMENT

TEST PROCEDURES AND MEASUREMENT TECHNIQUES

THE FINAL TRANSMISSION

THE SOLAR SPECTRUM

The Solar Spectrum: Gamma Rays and Solar Flares
Peter O. Taylor
Fall 1992, page 54
The Solar Spectrum: New Organization Helps Amateurs Obtain Eclipse Data
Peter O. Taylor
Fall 1994, page 53
The Solar Spectrum: Sunspot Distribution
Peter O. Taylor
Winter 1993, page 80
The Solar Spectrum: The Hayden System for Recording Ionospheric Anomalies; Predictions for Sunspot Cycle 22
Peter O. Taylor
Winter 1994, page 83
The Solar Spectrum: The Realm of the Sun
Peter O. Taylor
Fall 1993, page 84
The Solar Spectrum: Ulysses Verifies the Shape of the Interplanetary Magentic Field
Peter O. Taylor
Winter 1996, page 20
The Solar Spectrum: Understanding the Total Solar Irradiance
Peter O. Taylor
Summer 1993, page 49
The Solar Spectrum: Update on the VLF Receiver
Peter O. Taylor
Spring 1993, page 51

TRANSCEIVERS

A Low-Power 20-Meter Transceiver
Clint Bowman, W9GLW
Winter 1995, page 69
An FT-990/1000 Interface Circuit
Phil Salas, AD5X
Summer 1996, page 14
Improving the Drake TR-7
Scott Prather, K9BY
Summer 1992, page 19

TRANSMITTERS

A Logarithmic Audio Speech Processor
William E. Sabin, WØIYH
Winter 1997, page 9
Technical Conversations: WØIYH, *Spring 1997, page 108*
A 1.8 to 30-MHz 100-Watt SSB Transmitter
Wayne Ryder, W6URH
Fall 1994, page 57

VHF/UHF

VHF/UHF Combiner for Mobile Use
Ian Keenan, VK3SYK
Winter 1995, page 86

VIRTUAL EQUIPMENT

Connecting Computers to Radios: A PC Interface for the Ramsey 2-Meter Transceiver
Howie Cahn, WB2CPU
Fall 1993, page 13
Connecting Computers to Radios: Adding DDS Frequency Control
Howie Cahn, WB2CPU
Winter 1995, page 9
Quarterly Devices: Radios Without Knobs
Rick Littlefield, K1BQT
Spring 1993, page 65

VLF OPERATION

Simple Very Low Frequency (VLF) Receivers
Joseph J. Carr, K4IPV
Winter 1994, page 69
The Solar Spectrum: A Portable VLF Receiver and Loop Antenna System
Peter O. Taylor
Spring 1995, page 67
The Solar Spectrum: Update on the VLF Receiver
Peter O. Taylor
Spring 1993, page 51

PRODUCT INFORMATION

WinCam.Live, a New Webcam System

StarDot Technologies, a California-based digital camera company, offers WinCam.Live— the first expandable and customized digital camera system designed specifically for webcam use. Webcams, or Internet cameras, snap live images which can then be viewed with any web browser. The update rate of these live cameras varies from once every few seconds to once a day.

WinCam.Live uses the flexible RS-232 protocol for multiple camera connections and remote camera placement, including dial-up and wireless connections. StarDot also offers interchangeable lenses and an outdoor enclosure for use with WinCam.Live cameras.

For information and to see WinCam.Live in action, visit the StarDot Technologies website at: <http://www.wincam.com>, or call (714) 528-9719.

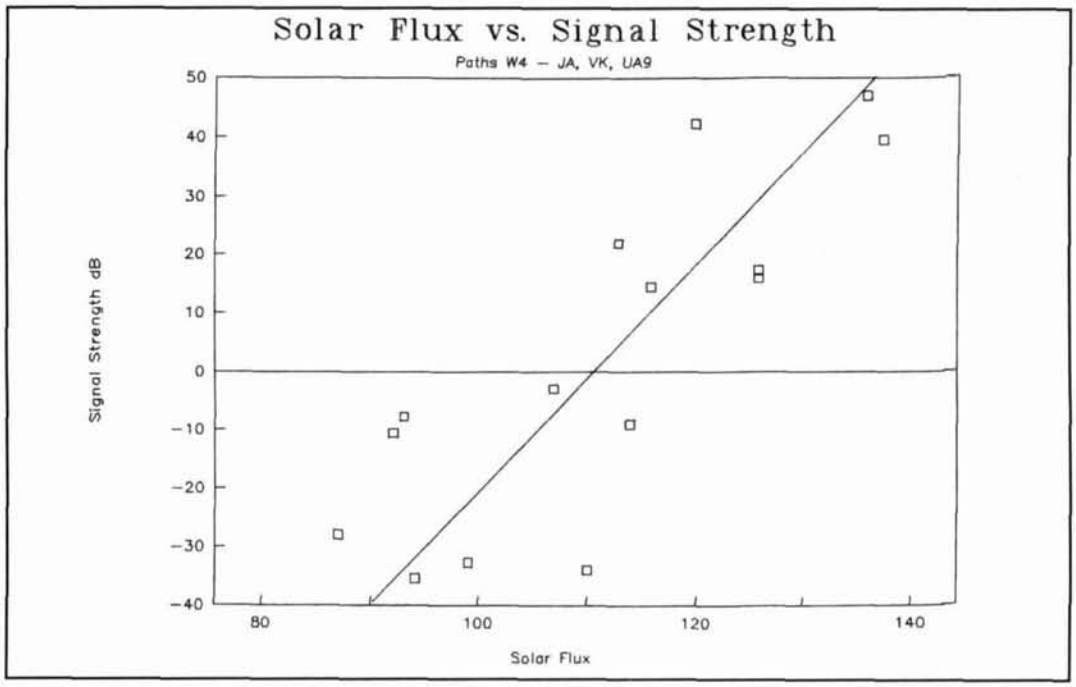

Figure 1. Solar flux versus signal strength. Paths W4 - JA, VK, UA9.

three minor corrections that I want to point out. *(See our "Corrections" page.—Ed.)*

I also want to mention that I'm making available, to anyone who is interested, free PC software for computing loading profiles. Any reader who would like a copy should send me a blank 3.5" diskette and a stamped, self-addressed return mailer.

Richard A. Formato, K1POO
Boylston, Massachusetts

Give the gift of great reading for the Holidays... or ask Santa for your very own gift of your favorite magazine!

BONUS Holiday Gift!

Subscribe for yourself or a friend and save lots of money and add one free issue with any full year subscription order as our FREE Holiday Gift!

CQ THE RADIO AMATEUR'S JOURNAL

If you enjoy Amateur Radio you'll love CQ! Fun to read, CQ is written for the active Ham.

1 year (~~12~~ 13 issues) $27.95
6 issues Only $13.95

CQ Contest

People • Analysis • Techniques • Reporting • Technology

In-depth coverage of contesting worldwide. Required reading if you're interested or involved in contesting

1 year (~~10~~ 11 issues) $30.00
5 issues Only $15.00

CQ VHF Ham Radio Above 50 MHz

It's the only publication covering the full spectrum of VHF/UHF Activities. The perfect gift for new hams and old hams alike:

1 year (~~12~~ 13 issues) $24.95
6 issues Only $12.49

COMMUNICATIONS QUARTERLY

The leading journal of communication technology in Amateur Radio. A must for the person who takes pride in being on the leading edge of technology

1 year (~~4~~ 5 issues) $33.00
3 issues Only $19.95

POPULAR COMMUNICATIONS

The world's most authoritative monthly for shortwave listeners and scanner monitors. Read by more active listeners than all other listening publications combined.

1 year (~~12~~ 13 issues) $25.95
6 issues Only $12.95

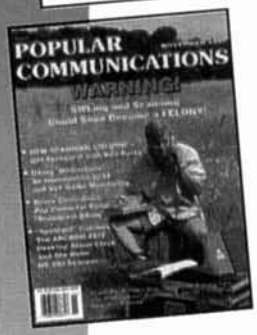

ELECTRONIC Servicing & Technology

The magazine for consumer electronic servicing professionals. There's nothing like it!

1 year (~~12~~ 13 issues) $26.95
6 issues Only $13.49

All subscriptions include a gift card sent in your name guaranteed to arrive in time for the holidays. (If received by December 15, 1997.)

Phone:800-853-9797 FAX:516-681-2926 MAIL

Please Send My Subscription To:

Name _____ Call Sign _____
Address _____
City _____ State _____ Zip _____
Country _____

*US Magazine Gift Pricing	13 Issues	6 Issues
CQ AMATEUR RADIO	☐ $27.95	☐ $13.95
CQ VHF	☐ $24.95	☐ $12.49
POPULAR COMMUNICATIONS	☐ $25.95	☐ $12.95
CQ CONTEST	☐ $30.00 (11 Issues)	☐ $15.00 (5 Issues)
COMMUNICATIONS QUARTERLY	☐ $33.00 (5 Issues)	☐ $19.95 (3 Issues)
ES&T	☐ $26.95 (13 Issues)	☐ $13.49 (6 Issues)

* Canada/Mexico and Foreign orders call for pricing!
Total Amount for this address $ _____

Send Gift Subscription To:

Name _____ Call Sign _____
Address _____
City _____ State _____ Zip _____
Country _____

*US Magazine Gift Pricing	13 Issues	
CQ AMATEUR RADIO	☐ $27.95	☐ $13.95
CQ VHF	☐ $24.95	☐ $12.49
POPULAR COMMUNICATIONS	☐ $25.95	☐ $12.95
CQ CONTEST	☐ $30.00 (11 Issues)	☐ $15.00 (5 Issues)
COMMUNICATIONS QUARTERLY	☐ $33.00 (5 Issues)	☐ $19.95 (3 Issues)
ES&T	☐ $26.95 (13 Issues)	☐ $13.49 (6 Issues)

* Canada/Mexico and Foreign orders call for pricing!
Total Amount for this address $ _____

GRAND TOTAL FOR THIS ORDER FORM $ _____

Method of payment: ☐ Check ☐ Money Order ☐ VISA ☐ Mastercard ☐ Discover ☐ American Express

Credit Card # _____ **Exp.Date** _____

CQ Communications, Inc. 76 North Broadway, Hicksville, NY 11801, Phone:516-681-2922/Fax: 516-681-2926

Antenna Software by W7EL

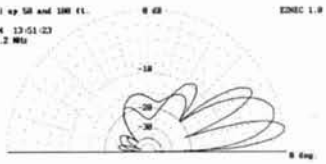

EZNEC ("Easy-NEC") captures the power of the NEC-2 calculating engine while offering the same friendly, easy-to-use operation that made ELNEC famous. **EZNEC** lets you analyze nearly any kind of antenna - including quads, long Yagis, and antennas within inches of the ground - *in its actual operating environment*. Press a key and see its pattern. Another, its gain, beamwidth, and front/back ratio. See the SWR, feedpoint impedance, a 3-D view of the antenna, and much, much more. With 500 segment capability, you can model extremely complex antennas and their surroundings. Includes true current source and transmission line models. Requires 80386 or higher **with coprocessor**, 486DX, or Pentium; 2Mb available extended RAM; and EGA/VGA/SVGA graphics.

ELNEC is a MININEC-based program with nearly all the features of EZNEC except transmission line models and 127 segment limitation (6-8 total wavelengths of wire). Not recommended for quads, long Yagis, or antennas with horizontal wires lower than 0.2 wavelength; excellent results with other types. Runs on any PC-compatible with 640k RAM, CGA/EGA/VGA/Hercules graphics. Specify coprocessor or non-coprocessor type.

Both programs support Epson-compatible dot-matrix, and HP-compatible laser and ink jet printers.

Prices - U.S. & Canada - EZNEC $89, ELNEC $49, postpaid. Other countries, add $3. VISA AND MASTERCARD ACCEPTED.

Roy Lewallen, W7EL *phone* **503-646-2885**
P.O. Box 6658 *fax* **503-671-9046**
Beaverton, OR 97007 *email* **w7el@teleport.com**

NEMAL Cable & Connectors for the Electronics Industry

CALL NEMAL FOR RF

- Connectors
- Adapters
- Cable Assemblies
- Coaxial Cable

Manufacturer Of Custom Electronic Wire And Cable.
• Low Minimums • Quick Delivery

CALL US AT 1-800-522-2253
OR FAX YOUR REQUIREMENTS TO
1-305-895-8178
EMAIL:info@nemal.com
Internet:http://www.nemal.com

Call for your copy of our new 48-page Cable & Connector Selection Guide. More than 2,500 commercial and QPL cable and connector products in stock.

12240 NE 14th Ave.
N. Miami, FL 33161
(305) 899-0900

NEMAL Cable & Connectors for the Electronics Industry

---

(602) 820.5411
FAX (800) 706.6789

TUBES - PARTS - BOOKS - SUPPLIES

FIND EVERYTHING YOU NEED AT A GREAT PRICE, AND THAT'S NO LINE.

6221 SOUTH MAPLE AVENUE
TEMPE, AZ U.S.A. 85283

VISIT OUR WEBSITE AT WWW.TUBESANDMORE.COM

Call or fax today for our new 60 page FREE catalog of vintage tubes, hard to find parts, books and supplies. We have everything you need to build new or repair classic audio equipment at prices you haven't seen in decades.

CALL TOLL FREE
(800) 292-7711 orders only
Se Habla Español

YOUR ONE STOP SOURCE FOR ALL YOUR TEST EQUIPMENT NEEDS

CALL OR WRITE FOR OUR NEW FREE 64 PAGE CATALOG!
(800) 445-3201

NEW **XK-700 Digital / Analog Trainer**
Elenco's newest advanced Digital / Analog Trainer is specially designed for school projects. It is built on a single PC board for maximum reliability. It includes 5 built-in power supplies, a function generator w/ continuously sine, triangular and square waveforms, 1,560 tie point breadboard area. Tools and meter shown optional. (Mounted in a professional tool case made of reinforced metal).

XK-700
Assembled and Tested
$189.95
XK-700-SEMI Kit
Assembled and Tested
$174.95
XK-700K - Kit
$159.95

Made in U.S.A.

Elenco Scopes
Free Dust Cover & Probes

S-1325	25MHz		$325
S-1330	25MHz	Delayed Sweep	$439
S-1340	40MHz		$475
S-1345	40MHz	Delayed Sweep	$569
S-1360	60MHz	Delayed Sweep	$749
S-1390	100MHz	Delayed Sweep	$995
DS-303	40MHz/20Ms/s	Analog/Digital	$995
DS-603	60MHz/20Ms/s	Analog/Digital	$1295

4 Functions in One
MX-9300
$459.95
Features
- One instrument w/ four test leads and measuring systems.
  - 1.3GHz Frequency Counter
  - 2MHz Sweep Function Generator
  - Digital Multimeter
  - Digital Triple Power Supply
- 0-30V @ 3A, 15V @ 1A, 5V @2A

NEW **Tektronix DMMs**
- 40,000 Count
- High Accuracy
- Tektronix Quality
- 3 Year Warranty

DMM 912	$189
DMM 914	$235
DMM 916	$275

20MHz Sweep/Function Generator with Frequency Counter
Model 4040
- 0.2Hz to 20MHz
- AM & FM Modulation
- Burst Operation
- External Frequency Counter to 30MHz.
- Linear and Log Sweep

$399

10MHz - Model 4017	$309
5MHz - Model 4011	$239

Fluke Scopemeters

123	NEW	$950
92B		$1445
96B		$1695
99B		$2095
105B	NEW	$2495

ALL FLUKE PRODUCTS ON SALE!!

Technician Tool Kit
TK-1500

28 tools plus a DMM contained in a large flexible tool case with a handle ideal for everyone on the go!
$49.95

Fluke Multimeters

Model 10	$63	Model 12	$84
Model 70II	$75	Model 83	$235
Model 73III	$97	Model 85	$269
Model 75III	$129	Model 87	$289
Model 77II	$154	Model 863E	$475
Model 79II	$175	Model 867BE	$650

B&K Precision Multimeters

Model 389	$109	Model 388A	$99
Model 390	$127	Model 2707	$75
Model 391	$143	Model 2860A	$79
Model 5360	$195	Model 5370	$219
Model 5380	$265	Model 5390	$295

DIGITAL LCR METER NEW
Model LCR-1810
- Capacitance 0.1pf to 20µF
- Inductance 1µH to 20H
- Resistance .01Ω to 20000MΩ
- Temperature -20°C to 750°C
- DC Volts 0-20V
- Frequency up to 15MHz
- Diode/Audible Continuity Test
- Signal Output Function
- 3 1/2 Digit Display

$99.95

B&K High Current DC Power Supply
- Variable 3-14VDC
- Thermal Function
- Current Limiting

Model 1686 12A
$159
Model 1688 28A
$239

B&K 13.8V Fixed DC Power Supplies

Model 1680 6A	$39
Model 1682 15A	$75

Quad Power Supply Model XP-4
Four Fully Regulated DC Power Supplies in One Unit
4 DC Voltages: 3 Fixed;
- 1 Variable 0-12V @ 500mA
- +12V @ 500mA
- +5V @ 20mA

$29.95

Digital Multimeter
Model M-1700
$39.95
11 functions including freq to 20MHz, cap to 20µF. Meets UL-1244 safety specs.

10% OFF ON ALL STANDARD AMATEUR RADIO PRODUCTS Including Accessories

Handheld Universal Counter

Model F-2850
10Hz - 2.8GHz
Dual Input
$149

NEW
F-2800
1MHz - 2.8GHz
$99

Features:
- Full range 10Hz - 2.8GHz (F-2850)
- 16 segment RF signal strength bargraph 1MHz - 2.8GHz (F-2800)
- Dual 50Ω/1MΩ inputs. (F-2850 only)
- 16 segment RF signal strength bargraph
- 10 digital LCD display with backlight. (F-2850 only)
- 6 hour NiCd battery operation.
- High speed 250MHz direct count for high resolution.
- Multifunctions: Frequency, Period and Auto Trigger & Hold. (F-2850).

Specifications
Input Sensitivity (Typical)

Amplifier	1MΩ (F-2850 only)	50Ω
Impedance	1MΩ (F-2850 only)	50Ω, VSWR<2:1
Range	10Hz - 50MHz (F-2850 only)	1MHz - 2.8GHz
Sensitivity	<10mV @ 10Hz - 10MHz <20mV @ 10MHz - 50MHz (F-2850 only)	<1.5mV @ 100MHz <5mV @ 250MHz <5mV @ 1GHz <100mV @ 2.4GHz
Maximum Input	100Vrms (F-2850 only)	15dBm

Model AR-2N6K
2 Meter / 6 Meter
Amateur Radio Kit

$34.95

Model AM/FM-108K
Transistor Radio Kit **$29.95**

35mm Camera Kit
Model AK-540 $14.95
Learn all about photography

No Soldering Required

Radio Control Car Kit
Model AK-870
- 7 Functions
- Radio Control Included

$24.95

No Soldering Required

Guaranteed Lowest Prices
UPS SHIPPING: 48 STATES 5%
OTHERS CALL FOR DETAILS
IL Residents add 8.25% Sales Tax

C&S SALES, INC.
150 W. CARPENTER AVENUE
WHEELING, IL 60090
FAX: (847) 541-9904 (847) 541-0710
http://www.elenco.com/cs_sales

VISA MasterCard

15 DAY MONEY BACK GUARANTEE
FULL FACTORY WARRANTY

PRICES SUBJECT TO CHANGE WITHOUT NOTICE

CQ Books & more...

NEW!

33 Simple Weekend Projects

by Dave Ingram, K4TWJ

A wide ranging collection of do-it-yourself electronics projects from the most basic to the fairly sophisticated. You'll find: station accessories for VHF FMing, working OSCAR satellites, joining the fun on HF, trying CW, building simple antennas, even a complete working HF station you can build for $100. Also included is a measure of practical tips and techniques on how to build electronic projects yourself.

Order No. 33PROJ.... $15.95

McCoy on Antennas

by Lew McCoy, W1ICP

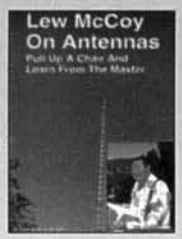

This is truly a unique antenna book that's a must read for every amateur. Unlike many technical publications, Lew presents his invaluable antenna information in a casual, non-intimidating way for anyone!

Order No. MCCOY $15.95

CQ Amateur Radio Almanac

by Doug Grant, K1DG

Filled with over 600 pages of ham radio facts, figures and information. 1997 edition, next volume won't be published until 1999.

Order No. BALM97 $19.95

The NEW Shortwave Propagation Handbook

by W3ASK, N4XX & K6GKU

The most comprehensive source of information on HF propagation is available from CQ! Read about propagation principles, sunspots, ionospheric predictions, with photography, charts and tables galore—it's all in this unique reference volume!

Order No. SWP..... $19.95

Where Do We Go Next?

by Martti Laine, OH2BH

Ever dream about what it's like to go on a DXpedition? Have you ever imagined thousands of stations calling only you? Whether it's from the windmills of Penguin Island or the volcanoes of Revillagigedo each chapter conveys a unique story that you won't be able to put down.

Order No. WGN..... $9.95

The Quad Antenna

by Bob Haviland, W4MB

Second Printing

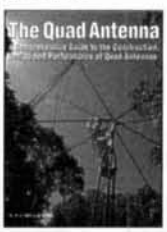

You'll enjoy this authoritative book on the design, construction, characteristics and applications of quad antennas.

Order No. QUAD..... $15.95

The Vertical Antenna Handbook

by *Paul Lee, N6PL*

Learn basic theory and practice of the vertical antenna. Discover easy-to-build construction projects for anyone!

Order No. VAH..... $9.95

The VHF "How-To" Book

by Joe Lynch, N6CL

This book is the perfect operating guide for the new and experienced VHF enthusiast.

Order No. BVHF..... $15.95

Keys, Keys, Keys

by Dave Ingram, K4TWJ

You'll enjoy nostalgia with this visual celebration of amateur radio's favorite accessory. This book is full of pictures and historical insight. If you've ever wondered about the old days of Morse, this book's for you.

Order No. KEYS $9.95

The Packet Radio Operator's Manual

by Buck Rogers, K4ABT

CQ has published an excellent introduction and guide to packet operation. It's the perfect single source, whether you're an advanced user or just starting out.

Order No. PROM..... $15.95

W6SAI HF Antenna Handbook

by Bill Orr, W6SAI

Nearly 200 pages filled with dozens of inexpensive, practical antenna projects that work! This invaluable resource will guide you through the construction of wire, loop, yagi and vertical antennas.

Order No. HFANT..... $19.95

Building and Using Baluns and Ununs

by Jerry Sevick, W2FMI

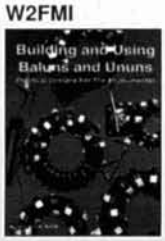

This volume is the source for the latest information and designs on transmission line transformer theory. Discover new applications for dipoles, yagis, log periodics, beverages, antenna tuners, and countless other examples.

Order No. BALUN . . . $19.95

SPECIAL!

Ham Radio Horizons: The Book

by Peter O'Dell, WB2D

Written by Peter O'Dell, WB2D, this is a book about ham radio that every beginner can enjoy! If you want to get in on the fun and excitement of Amateur Radio, Ham Radio Horizons is the perfect way to get started. HRH is full of tips from expert hams in: DXing, Contesting, Serving the Public, Ham Radio in Space, Experimenting, Digital Communications — you name it! This exciting book is an excellent gift to a prospective ham or for use in your club's licensing classes and library.

Order No. BHOR..... ~~$12.95~~ $8.95

CQ Videos, Calendars & more...

T-Shirt Blowout Sale

Videos

These videos are filled with easy to understand advice and tips that can't be found anywhere else. **ONLY $19.95 EACH!**

Ham Radio Horizons: The Video.....Order No. VHOR
Getting Started in VHF.....Order No. VVHF
Getting Started in Ham Radio.....Order No. VHR
Getting Started in DXing.....Order No. VDX
Getting Started In Packet Radio.....Order No. VPAC
Getting Started in Amateur Satellites.....Order No. VSAT
Getting Started in Contesting.....Order No. VCON

Hats

A Must for Every Ham

Poplin cap with adjustable strap has 5 panels with fused buckram backing

Order No. : 97G (Green), 97B (Black).....**$12.00**

Backpacks

Go Ahead! Load it up!

This useful and rugged backpack will be your greatest asset when carrying around your ham accessories. Embroidered design, 2 front pockets.

Order No.: 96N (Navy), 96G (Green),96B (Black) ...**$12.00**

Playing Cards

Top quality, plastic coated playing cards.
ONLY $9.95 per deck

Glass Steins

This glass stein holds 19 oz. and has CQ's logo etched into the glass.

Order No. 91....**$9.95**

CQ Award Pins

If you've earned any of CQ's Awards, you can also display the corresponding CQ Award pin. Available for WAZ, 5 Band WAZ, 160 Meter WAZ, CQ DX, CQ DX Honor Roll, WPX, WPX Honor Roll, and USA-CA awards. ONLY $5.00 EACH.

1998/99 Calendars

Fifteen month calendars - January '98 through March '99

Please specify Amateur Radio or Classic Radio Calendar

Buy One T-Shirt at Regular Price of $17.95* + $4 S&H**
Get Second T-Shirt at
HALF-PRICE
*XX-Large $19.95
** Orders over $50 receive FREE S&H

Here's what we have ↓

T 1	Life's Too Short For QRP	(L,XL,XXL)
T3	CQWW The Contest	(L)
T7	TVI...What TVI	(L,XL,XXL)
T8	QCAO	(XXL)
T9	DX IS	(XL)
T 1 1	Just Work It	(L,XL,XXL)
T12	No Waves Like Shortwaves	(XL,XXL)
T13	Radioman	(L,XL,XXL)
T14	How's DX	(XL)
T16	Viking	(XL,XXL)
T17	Hammus Sapien	(XL,XXL)
T18	Real Radios Glow	(XL)

Phone: 800-853-9797 **FAX: 516-681-2926** **MAIL**

YES! Rush me my book(s), calendar(s), video(s) right away!

Qty	Item #	Description	Price	Total Price
			Shipping/Handling	
			Total	

U.S. and possessions - add $4 shipping/handling. FREE S/H on orders $50 and over. Foreign - shipping/handling charges are calculated by order weight & destination. A $4 credit will be applied for Foreign orders over $50.

Name _____

Callsign _____ Phone/Fax No. _____

Street Address _____

City _____ State _____ Zip _____

MasterCard VISA DISCOVER AMERICAN EXPRESS

CQ Communications, Inc.
76 North Broadway, Hicksville, NY 11801
Phone: 516-681-2922/Fax: 516-681-2926

ADVERTISER'S INDEX

Reach this dynamic audience with your advertising message, contact Don Allen, W9CW at 217-344-8653, FAX 217-344-8656, or e-mail: QtrlyAds@aol.com

QuickCheck

The Xplorer Test Receiver. The professional choice when speed, performance, and reliability are an issue !

For Commercial and Mobile Radio testing, the **Optoelectronics Xplorer** stands alone. Let the Xplorer perform all your quick radio checks, instantly determining the radio's frequency, **CTCSS, DCS, DTMF**, deviation or signal strength. The Xplorer automatically locks on to any nearfield signal from **30MHz - 2GHz** in less than a second.

There is **no setup necessary**-Whether you're in the field or in the shop, the Xplorer is the portable, compact and **economical solution** for any two-way communications business.

Patent No. 5,471,408

FEATURES

- Nearfield receiver, sweeps 30MHz-2GHz in <1 second (Cellular bands are blocked on all U.S. versions)
- Decodes CTCSS, DCS, and DTMF. Manually record tones into memory
- Lockout up to 1000 frequencies
- Store 500 frequencies in memory with time & date stamp, as well as number of hits per frequency
- NMEA-0183 GPS interface for recording Latitude & Longitude coordinates (GPS Required)
- VFO mode for tuning to specific frequencies
- PC interface for downloading data from memory
- FM demodulation / Built-in speaker
- Auto or manual frequency hold
- Maximum nearfield reception / Up to 1/4 mile away

$899

Summer Special Includes: Spectrum CD & CC30 Case

Xplorer includes: TA100S antenna, NiCads, Charger, PC Download cable and software

SPECIFICATIONS	
Freq. Range	30MHz - 2GHz
Modulation	FM Deviation
Freq. Response	50 - 3000Hz
Auto Sweep Time	<1 second
Input 50 Ohm	-59dBm @100MHz -25dBm @1GHz
Display	2 line LCD
Power	Internal NiCad

CTCSS Decode

DCS Decode

DTMF Decode

FACTORY DIRECT ORDER LINE: 800•327•5912

OPTOELECTRONICS®

5821 NE 14th Avenue • Ft. Lauderdale, FL • 33334
Telephone: 954•771•2050 Fax: 954•771•2052 EMail: sales@optoelectronics.com
Prices and specifications are subject to change without notice or obligation.
Payment terms are Visa, MasterCard or C.O.D. (Cash or MoneyOrder)

Check out our Web Site
www.optoelectronics.com

MADE IN U.S.A.

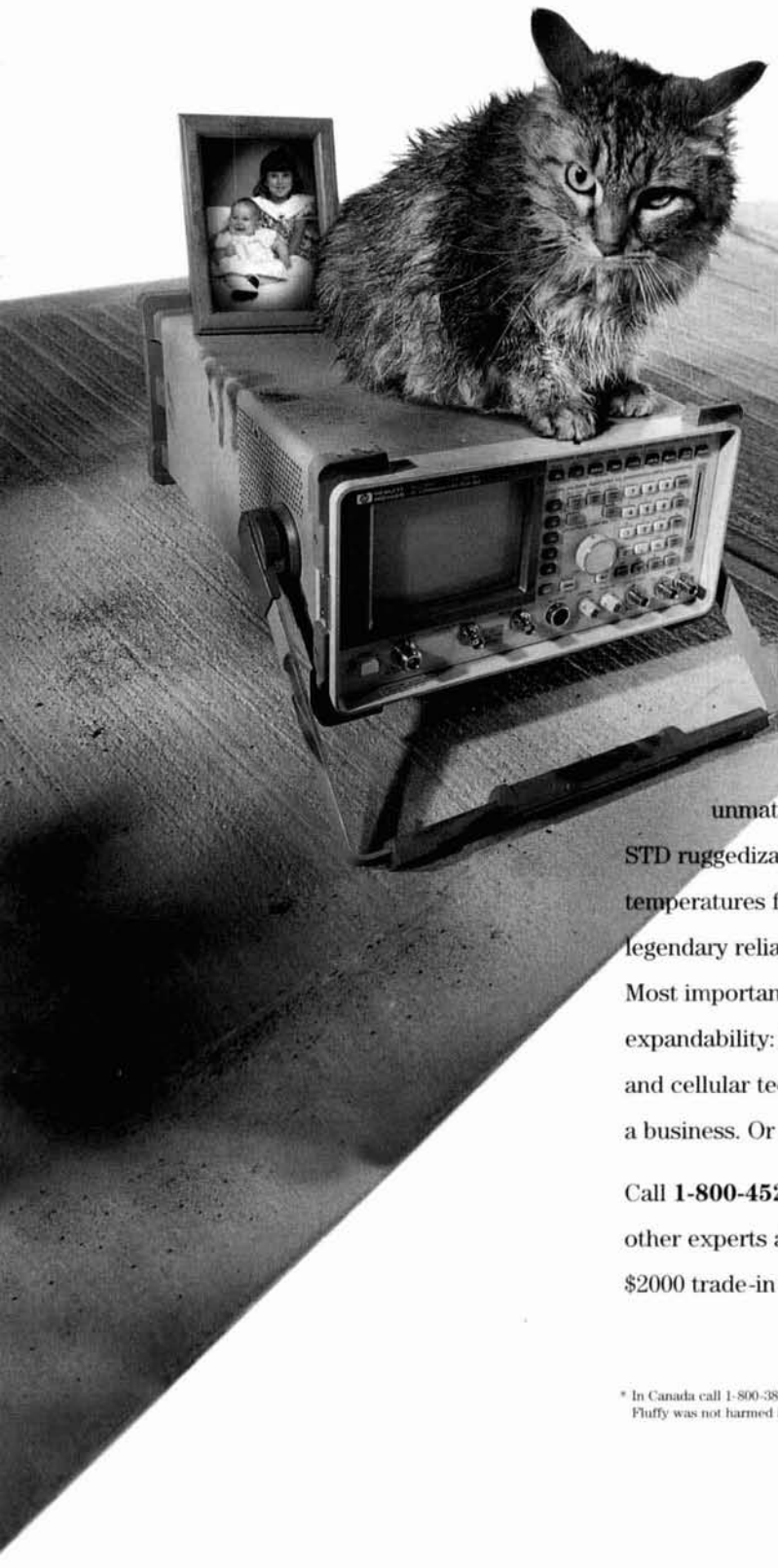

October 2, 1996.

Bob Jensen had
a fire at his mobile
radio repair shop.

He had only a
few seconds to
save things.

Thanks for the vote of
confidence, Bob.

No offense, Fluffy, but the HP 8920A is irreplaceable, too. Because the HP 8920A service monitor provides the edge you need to survive in today's tough business environment. It offers unmatched accuracy (frequency to within .1 ppm). MIL-STD ruggedization means it can withstand shock forces up to 30 g's, temperatures from 0 to 50 °C, and humidity from 0 to 95%. With the legendary reliability of HP (20,000 hrs mean time between failures). Most importantly, the 8920A service monitor offers superior expandability: it can test everything from two-way radios to pagers and cellular technologies. Which is important when you're building a business. Or rebuilding one, as the case may be.

Call **1-800-452-4844,* Ext. 5308**. Talk to Charlie or one of our other experts about the HP 8920A and find out how you can get a $2000 trade-in value for your old service monitor.

* In Canada call 1-800-387-3154, program number TMU310.
Fluffy was not harmed in the making of this ad. She's as rambunctious as ever, and enjoying Bob's new location.

HEWLETT® PACKARD